# UC Irvine

## UC Irvine Electronic Theses and Dissertations

### Title

Aerosol Liquid Water: Sources and Partitioning

### Permalink

https://escholarship.org/uc/item/7q3102x3

### Author

Burns, Alyssa Marie

### Publication Date

2024

### Copyright Information

This work is made available under the terms of a Creative Commons Attribution License, available at https://creativecommons.org/licenses/by/4.0/

Peer reviewed|Thesis/dissertation

eScholarship.org Powered by the California Digital Library
University of California

UNIVERSITY OF CALIFORNIA,
IRVINE

# Aerosol Liquid Water: Sources and Partitioning

DISSERTATION

submitted in partial satisfaction of the requirements
for the degree of

DOCTOR OF PHILOSOPHY

in Chemistry

by

Alyssa Marie Burns

Dissertation Committee:
Professor Ann Marie Carlton, Chair
Professor Sergey Nizkorodov
Professor James N. Smith

2024

© 2024 Alyssa Marie Burns

# TABLE OF CONTENTS

Page

**LIST OF FIGURES** **v**

**LIST OF TABLES** **viii**

**ACKNOWLEDGMENTS** **ix**

**VITA** **xii**

**ABSTRACT OF THE DISSERTATION** **xvi**

**1 Introduction** **1**
- 1.1 Background . . . 1
  - 1.1.1 Atmospheric Aerosol . . . 1
  - 1.1.2 Aerosol Composition and Sources . . . 2
  - 1.1.3 Measurements and Estimates of Ambient Aerosol . . . 6
- 1.2 Motivation . . . 12
  - 1.2.1 Public Health and Environmental Justice . . . 12
  - 1.2.2 Radiative Forcing . . . 13
  - 1.2.3 Informed and Effective Action . . . 14
- 1.3 Key Knowledge Gaps . . . 16
- 1.4 Research Questions and Specific Aims . . . 17
- 1.5 Structure of Dissertation . . . 18

**2 Data Gap: Surface Air Quality Networks Miss Air Pollution from Concentrated Animal Feeding Operations** **20**
- 2.1 Abstract . . . 21
- 2.2 Introduction . . . 21
- 2.3 Materials and Methods . . . 24
  - 2.3.1 County-Level Animal Unit Density Maps and CAFO Trends . . . 24
  - 2.3.2 Satellite Retrievals . . . 25
  - 2.3.3 Surface Air Quality Data and Data Set Synthesis . . . 26
- 2.4 Results and Discussion . . . 27

**3 Aerosol Liquid Water Predictions: Sensitivities and Application towards Aerosol Optical Properties, Radiative Forcing, and Ambient Chemistry 36**
3.1 Abstract . . . 37
3.2 Introduction . . . 38
3.3 Methods . . . 42
3.3.1 Data Sources . . . 42
3.3.2 ALW Observational Estimates . . . 47
3.4 Results and Discussion . . . 50
3.4.1 ALW Sensitivities . . . 50
3.4.2 Trends in ALW Mass Concentrations . . . 57
3.4.3 Application 1: Explaining Clear and Cloudy Sky Differences in Aerosol Optical Depth and Size in Bondville, IL . . . 58
3.4.4 Application 2: Elucidating Aerosol Radiative Impacts on Surface Air Temperature Modulation in the Southeast US . . . 61
3.5 Conclusions . . . 67

**4 Gas-Phase Water Soluble Organic Carbon in the South Coast Air Basin: $NO_x$ and VOC solubility 70**
4.1 Abstract . . . 71
4.2 Introduction . . . 72
4.3 Methods . . . 74
4.3.1 Sampling Locations . . . 74
4.3.2 Ambient Measurements and Chemical Analysis . . . 76
4.3.3 Modeling . . . 78
4.4 Results . . . 79
4.4.1 $WSOC_g$ Mass Concentrations in Irvine and Pasadena . . . 79
4.4.2 Associations among $WSOC_g$, $O_x$, and $NO_x$ . . . 82
4.4.3 Discussion . . . 85
4.5 Conclusions and Future Directions . . . 87

**5 Summary and Future Directions 89**
5.1 Summary . . . 89
5.1.1 Data Gap: Air Quality Networks Miss Air Pollution from Concentrated Animal Feeding Operations . . . 89
5.1.2 Aerosol Liquid Water Predictions: Sensitivities and Application towards Aerosol Optical Properties, Radiative Forcing, and Ambient Chemistry . . . 90
5.1.3 Gas-Phase Water Soluble Organic Carbon in the South Coast Air Basin: $NO_x$ Influence on VOC Solubility . . . 91
5.2 Future Directions . . . 92
5.2.1 Bridging Data Sources and Emission Discrepancies . . . 92
5.2.2 Aerosol Molality: Effects towards Partitioning and other Physicochemical Properties . . . 94
5.2.3 Chemical Education: Active and Inclusive Practices in Upper-Division Chemistry Courses . . . 98

**References** **100**

**Appendix A Supporting Information for Chapter 2** **138**

**Appendix B Supporting Information for Chapter 3** **148**

**Appendix C Supporting Information for Chapter 4** **158**

**Appendix D A Specifications-Graded, Spice-Themed, General Chemistry Laboratory Course Using an Argument-Driven Inquiry Approach** **169**

# LIST OF FIGURES

Page

2.1 Spatial distributions and trends of animal unit density and ammonia over the CONUS. (A) Animal units (1000 lb. of live weight) at medium- and large-sized CAFOs normalized by county area for the year 2017. (B) Average summertime 2017 $NH_3$ mixing ratios from the ESA IASI product. (C) Change in county-level AU density at medium- and large-sized CAFOs from 2002 to 2017. (D) Change in summertime $NH_3$ mixing ratio from NASA AIRS product from 2002 to 2017. . . . . 29

2.2 Relationship between remotely detected $NH_3$ and EPA surface $PM_{2.5}$ monitor coverage within the "hotspot" region of highest animal unit density. . . . . 30

2.3 Trends in EPA measured $PM_{2.5}$. Each point represents an EPA $PM_{2.5}$ monitor active over the study period (2002–2017), and is color-coded according to the quartiles of the overall trend distribution, where black points represent trends within the interquartile range, blue points represent trends above the third quartile (less decrease than average), and green points represent trends below the first quartile (greater decrease than average). . . . . 32

2.4 Trends in $PM_{2.5}$ mass and speciation across U.S. EPA climate regions (A) and USDA Farm production regions (B). OV refers to the Ohio Valley, UM refers to the Upper Midwest, SE refers to the Southeast, NE refers to the Northeast, W refers to the West, NW refers to the Northwest, S refers to the South, NR+P refers to the Northern Rockies and Plains, and SW refers to the Southwest. Each column represents a different EPA- or USDA-defined region, mapped in row 1. Row 2 represents average concentrations for each region in 2002, and row 3 shows the same for 2017. Purple circles display the average $PM_{2.5}$ mass for each year and are sized accordingly. Bar charts show annual average concentrations of ammonium (orange), nitrate (blue), organic matter (green), and sulfate (red), measured through EPA CSN. . . . . 34

3.1 Regions and sites used for ALW sensitivity analysis and applications. The four IMPROVE/CSN colocated sites (square markers) are used for ammonium sensitivities. The Bondville location (green marker) is used for Application 1. The four SEUS sites (light and dark blue markers) are used for meteorology and dust sensitivities, as well as Application 2. Due to data limitations with urban sites in this region, just the rural SEUS sites (light blue markers) are considered for some analyses, including Application 2. The GB region (pink markers) is used for meteorology and dust sensitivities. . . . . 43
3.2 Comparison between reanalysis datasets for surface-level monthly average ALW and AWP for the rural SEUS region (2000-2014). NARR significantly overestimates both ALW and AWP in comparison to ERA5 (p-values $< 0.05$ via Mann-Whitney U test). Only sulfate and nitrate were used as chemical inputs for water calculations. . . . . 51
3.3 Comparison (percent difference) between ERA5 and NARR derived average surface-level ALW for the year 2010. Only sulfate and nitrate were used as chemical inputs for water calculations. . . . . 52
3.4 Comparison between daily surface-level ALW calculated with and without ammonium ion ($NH_4$) at EPA CSN sites. ERA5 meteorology is used for both calculations. Temporal resolution is limited to just 2016-19 due to analytical lab uncertainties. . . . . 53
3.5 Comparison of meteorological and dust sensitivities in monthly average surface-level ALW predictions for a humid region (total SEUS, left) and an arid region (Great Basin, right). All available measurement days are used (1988-2014). 54
3.6 Comparison (percent difference) of dust sensitivities (Dust - No Dust) in yearly average surface-level ALW predictions across CONUS IMPROVE sites for 2005 (A) and 2019 (B). ERA5 meteorology is used for both calculations. . . 56
3.7 Trends (percent $yr^{-1}$) in predicted ALW mass concentrations at CONUS IMPROVE sites with different data products. Panels A and C show trends from 2005 with and without dust ions respectively, both using ERA5 meteorology. Panels B and D show trends from 2005-2014 with ERA5 and NARR meteorology respectively. . . . . 57
3.8 Seasonal distributions from 2010 to 2019 of AOD at 440 nm (A) and AE for the 440–870 nm (B) wavelength range on clear sky (gold) and cloudy (blue) days as binned by the AERONET quality assurance algorithm method. Vertical gold (clear sky) and blue (cloudy) bars represent the $25^{th}$ to $75^{th}$ quartile of each distribution, with the black horizontal line as the median. Black numbers are p-values from two-sided Mann-Whitney U tests, with bold italicized font indicating statistical significance between distributions where a p value $< 0.05$ indicates the two populations are not equal. . . . . 60
3.9 Stacked bars of median total $PM_{2.5}$ chemical composition and ALW observation-based estimates during clear sky (left bars, gold numbers) and cloudy (right bars, blue numbers) days as binned using the AERONET QA algorithm for 2010-2019. Crustal species include calcium, potassium, magnesium, and sea salt species of sodium and chloride. Table B.3 identifies statistical significance for individual chemical constituents. . . . . 61

3.10 Long-term trend of annual averaged surface air temperature anomaly (GISTEMP) within the continental United States for (A) 1900–2000 and (B) 1900–2019. (C) Annual mean surface air temperature anomaly in the SEUS (black rectangle) and the rest of the United States. . . . . 62
3.11 Box-and-whisker plots of monthly values of (A) aerosol dry mass, (B) aerosol water path, (C) aerosol optical depth, (D) single scattering albedo, and (E) Ångström exponent during 2000–09 (blue) and 2010–19 (red). An × symbol below the box and whiskers denotes if the averages of the two distributions are statistically different at a 95% confidence interval. . . . . 64
3.12 Mass concentrations of elemental carbon, the primary absorber of shortwave radiation, decreased in the region over the twenty-year period by approximately 50%. . . . . 65
3.13 Box-and-whisker plot of monthly values of top of the atmosphere (A) upwelling shortwave radiation during clear-sky conditions, (B) upwelling shortwave radiation during all-sky conditions, (C) upwelling longwave radiation during clear-sky conditions, and (D) upwelling longwave radiation during all-sky conditions during 2000–09 (blue) and 2010–19 (red). An × symbol below the box and whiskers denote if the averages of the two distributions are statistically different at a 95% confidence interval. . . . . 66

4.1 Sampling locations and wind patterns. Panel A indicates the Pasadena (CalNex) sampling site in red and the Irvine (UCI) site in blue. Panels B and C shows wind speed and direction measured at the surface in Pasadena and Irvine respectively. Note the scales are different for each wind rose. . . . . 75
4.2 Measured diurnal cycles of $WSOC_g$, $O_3$, and $NO_x$ and Pasadena (CalNex) and Irvine (UCI). Shaded yellow regions represent average solar radiation in each campaign. . . . . 80
4.3 Relationship of measured $O_x$, $NO_x$ and $WSOC_g$ at Pasadena (CalNex, triangles) and Irvine (UCI, circles). The bold black points represent the overall campaign average values of $O_x$ and $NO_x$ for weekdays (solid points) and weekends (open points). . . . . 83
4.4 Correlation matrix of measured $WSOC_g$ versus other chemical and meteorological variables. Pearson's correlation coefficients are displayed in each cell, and are color-coded according to that value. . . . . 85

5.1 County-level emissions of ammonia from all source sectors reported by the 2017 EPA NEI. . . . . 93
5.2 Sulfate (A) and nitrate (B) molality (mol $kg^{-1}$) trends at CONUS IMPROVE sites from 2005-2019. Trends are described as the slope of a robust linear regression divided by median concentration over the time period (% $yr^{-1}$). . 96

# LIST OF TABLES

Page

1.1 Surface-based measurement networks employed in this dissertation. Sites describes the number of active monitor locations. Variables measured focus on the variables utilized here; other aerosol properties may be measured at these and other measurement network sites. . . . . 8

# ACKNOWLEDGMENTS

The five years of my graduate experience have been crazy and challenging in so many different ways. From the extreme demands of the Covid pandemic to social and political unrest around the nation, the world, and within this institution, very little of my PhD journey has gone "according to plan". Nonetheless, I am tremendously grateful to have spent this time at UCI. It is truly a privilege to have had this opportunity to learn and grow during such a time in the world. I am especially appreciative of the time and energy devoted by all the friends and fellow scientists who have aided and supported me in this journey.

First and foremost, I must thank my extraordinary advisor and friend Dr. Ann Marie Carlton. I am so inspired by the way Ann Marie approaches science, activism, and mentorship. Throughout all the research ups, downs, and in-betweens, Ann Marie has always been my most ardent supporter. It is an amazing privilege to have an advisor who believes in me so much, even more than I believed in myself at times. I'm really going to miss our extended chats at UCI on life and science, but I look forward to staying in touch and collaborating with in the future.

The Carlton research group has helped me in many diverse ways as I marched, sometimes erratically, to completing my PhD. Thank you to Dr. Amy Christiansen for helping me get started with research—I can't believe this all started with just one of your R scripts. Thank you to my colleagues and friends Dr. Madison Flesch, Yinting Chiu, Ellie Smith and Dr. Simon Rosanka. Our windowless office can seem a bit dreary, but I'm always so excited to come in when it means seeing and working with all of you. I am so grateful that I was able to collaborate directly with each one of you. I'm really going to miss our office chats, walks around the circle, and projector watch parties. Thank you to prior group members Jonathon Babila, Jackson Ryan, and Steven Buschmann for their contributions towards the mist chamber setup. And many thanks as well to the undergraduates I worked with: Ashley Gudino, Tiffany Hu, and Seamus Frey. It was an honor to be a part of your scientific journey, and I am so excited to see what you do in your future science endeavors.

I am immensely thankful to all of the scientists who have helped me throughout my time here. Thank you to my doctoral committee members, Professor Sergey Nizkorodov and Professor Jim Smith. It was so much fun working with both of you. I am especially thankful to Jim and the rest of the Ultrafine Aerosol Lab for their sampling support and encouragement throughout my field campaign.

I was incredibly fortunate to work with many awesome collaborators both inside and outside of UCI. One of the best times I had during my PhD research was visiting and working with the Hennigan group at UMBC. I am so grateful for the mentorship of Professor Chris Hennigan. I learned so much from him and the rest of his research group, especially Dr. Vikram Pratap, Rose Taylor, and undergrads Joy Kiguru and Shawn Serafin. I truly could not have gotten the mist chambers operating properly without their help. Similarly, I must thank our glassblower, Maik Bollhorn, for his devoted efforts to building new mist chambers for us. I also want to thank Dr. Virendra Ghate for his help on multiple projects. Virendra

was the first outside collaborator I worked with, and that experience really helped me to find my footing in atmospheric research. I am also very appreciative for the help of Dr. Gabe Chandler (go Sagehens!) and Kira Dunham towards my first paper, and I would like to thank Dr. Barry Lefer, Dr. Joost De Gouw, and Dr. Rodney Weber for the use of their CalNex datasets as a part of my Chapter 4 materials.

One of the coolest things during my PhD was learning from and engaging with all of the amazing scientists within AirUCI. I would like to thank project scientists Dr. Lisa Wingen and especially Dr. Veronique Perraud for all of their assistance in lab. Thank you to my faithful lab consultant and friend, Dr. Cynthia Wong, for all her support, as well as the rest of the Nizkorodov lab for always being there for a chat or to loan a crucial piece of Swagelok.

A significant part of my time here at UCI has been devoted to teaching and pedagogical research, and I am so grateful for all of the people I was able to collaborate with through this work. Thank you so much to Professor Kimberly Edwards for giving me a chance as Head TA. I learned so much and had so much fun working with her and the rest of the Head Instructional team. Thank you to Mel Nguyen – the general chemistry labs truly could not run without you. It is such an honor to have made such great friends throughout this endeavor – thank you so much to Yong Li, Dr. Shannon Saluga, Amanda Abiad, and Maria Flores for all of your kind help and for all of the extensive video roasting sessions. I want to also extend a huge thank you to the small army of graduate student TAs and undergraduate LAs I was privileged to work with—you guys truly make the learning happen. And for one final time, thank you all for (mostly) getting your grading done on time!

I am so fortunate to have such a mighty support system outside of the UCI bubble. My friends have truly gotten me through when everything seemed insurmountable. Thank you so much to my best friend here at UCI, Jennifer Jaimes, for all the fried chicken, questionable music choices, and late-night work/movie sessions. I am looking forward to the 10AM Sunday Yard House trips this fall. Thank you to Joanne Johnson and "the boys"— I am so glad that we somehow ended up co-located for the duration of my PhD. Thank you to Clare Hamlin, Blake Benson, and my honorary niece Adeena—our video chats and visits have brought so much joy into my life. And especially to Joanne and Clare, I cannot express how grateful I am to have had your lifelong support. Thank you to my "bf" Hope Jewell and my concert-buddy Hannah Gaines for all the talks and trips along the way. Thank you to my favorite teammate and spin-buddy Larissa Reynoso, as well as the rest of the Reynoso family. I am so thankful to have had a home-away-from-home during my PhD.

I want to give the biggest thank you to my parents, who have supported me so much throughout my life. From softball to science and so much more, they have always had my back and helped me achieve my dreams.

The text of Chapter 2 is a reprint of material as it appears in "Data Gap: Air Quality Networks Miss Air Pollution from Concentrated Animal Feeding Operations" in *Environmental Science and Technology*, used with permission from the American Chemical Society (CC BY 4.0). The coauthors listed in this publication are Gabriel Chandler, Kira J. Dunham, and

Ann Marie G. Carlton. A.G. Carlton directed and supervised research which forms the basis for this chapter.

Portions of Chapter 3 are adapted from material as it appears in "Ambient Aerosol Is Physically Larger on Cloudy Days in Bondville, IL" in *ACS Earth and Space Chemistry*, used with permission from the American Chemical Society (CC BY 4.0). The coauthors listed in this publication are Madison M. Flesch, Amy E. Christiansen, Virendra P. Ghate, and Ann Marie G. Carlton. M.M. Flesch is the primary author of this work, and A.G. Carlton directed and supervised this research project.

Portions of Chapter 3 are also adapted from material as it appears in "Changes in Aerosols, Meteorology, and Radiation in the Southeastern U.S. Warming Hole Region during 2000 to 2019" in *Journal of Climate*, used with permission from the American Meteorological Society (CC BY 4.0). The coauthors listed in this publication are Virendra P. Ghate, Thomas Surletta, and Ann Marie G. Carlton. V.P. Ghate is the primary author of this work and, with A.G. Carlton, directed and supervised this research project.

Appendix D is a reprint of material as it appears in "A Specifications-Graded, Spice-Themed, General Chemistry Laboratory Course Using an Argument-Driven Inquiry Approach" in *Journal of Chemical Education*, used with permission from the American Chemical Society (CC BY 4.0). The coauthors listed in this publication are Shannon Saluga, Yong Li, Melanie Nguyen, and Kimberly D. Edwards. K.D. Edwards directed and supervised the research which forms the basis for this appendix.

I also must acknowledge my funding sources: Chapter 2 was supported by NASA grant no. 80NSSC19K0987 and NSF-AGS grant no. 1719245. Chapter 3 was supported by NASA grant no. 80NSSC19K0987 and NSF-AGS grant no. 2024170.

# VITA

## Alyssa Marie Burns

### EDUCATION

**Doctor of Philosophy in Chemistry** **2024**
University of California, Irvine *Irvine, California*
Research Advisor: Professor Annmarie Carlton
Overall GPA: 3.963

**Masters of Science in Chemistry** **2021**
University of California, Irvine *Irvine, California*
Overall GPA: 3.941

**Bachelor of Science in Chemistry** **2018**
*Biology Minor* *Forest Grove, Oregon*
Pacific University
Overall GPA: 3.621, *cum laude*

### RESEARCH AND PROFESSIONAL EXPERIENCE

**Graduate Research Assistant** **2020-2024**
University of California, Irvine *Irvine, California*
Advisor: Professor Annmarie Carlton

**Laboratory Manager** **2018-2019**
Apical Crop Science LLC *Canby, Oregon*
Supervisor: David Knaus

**Undergraduate Research Assistant** **2017-2018**
Pacific University *Forest Grove, Oregon*
Advisor: Professor Julie Layshock

### PUBLICATIONS

*Submitted to ACS ES&T Water **2024***: Y. T. Chiu, **A. M. Burns**, S. Rosanka, T. Hu, C. Hennigan, A. G. Carlton. "Chloride Interferences in Wet Chemical Oxidation Measurements: Plausible Mechanisms and Implications."

**A. M. Burns**, G. Chandler, K. Burkhart, A. G. Carlton. "The Data Gap: Air Quality Networks Miss Air Pollution from Concentrated Animal Feeding Operations", *Environmental Science and Technology*, **2023**. 57 (49), 20718-20725. DOI: 10.1021/acs.est.3c06947
*Selected as an ACS Editor's Choice article*

S. J. Saluga*, **A. M. Burns***, Y. Li*, M. Nguyen, and K. D. Edwards. "A Specifications-Graded, Spice-Themed, General Chemistry Laboratory Course Using an Argument-Driven Inquiry Approach", *Journal of Chemical Education*, **2023**. 100 (10), 3903-3915. DOI: 10.1021/acs.jchemed.3c00433.
** denotes equal contribution*

M. M. Flesch, A. E. Christiansen, **A. M. Burns**, V. P. Ghate, and A. G. Carlton. "Ambient Aerosol Is Physically Larger on Cloudy Days in Bondville, Illinois", *ACS Earth and Space Chemistry*, **2022**. 6 (12), 2910-2918. DOI: 10.1021/acsearthspacechem.2c00207

V. P. Ghate, A. G. Carlton, T. Surletta, **A. M. Burns**, "Changes in Aerosols, Meteorology, and Radiation in the Southeastern U.S. Warming Hole Region during 2000 to 2019." *Journal of Climate*, **2022**. 35, 7725–7737. DOI: 10.1175/jcli-d-22-0073.1.

## PRESENTATIONS

***(P)–Poster, (T)–Talk, (*)–Undergraduate Mentee, Presenter(s)***

A. Gharehbagh, R. Taylor, J. Kiguru, **A. M. Burns**, A. G. Carlton, C. Hennigan. "The Influence of Inorganic Salts on the Gas-Aqueous Partitioning of Formic and Acetic Acid" at the 41st Annual American Association for Aerosol Research Conference, October 2023 **(P)**

A. Gudino*, **A. M. Burns**, A. G. Carlton. "Overcoming Chloride Salt Interferences in Water-Soluble Carbon Measurements" at the 30th Annual UCI Undergraduate Research Symposium, May 2023 **(P)**

**A. M. Burns**, A. G. Carlton. "The Data Gap: Air Quality Networks Miss Air Pollution from Concentrated Animal Feeding Operations" at the AirUCI Internal Seminar Series, Irvine, CA, March 2023 **(T)**

S. Frey*, A. Klodt, **A. M. Burns**, A. G. Carlton, S. Nizkorodov. "Uptake of Trace Gases Produced by Photooxidation of Isoprene into Atmospheric Aqueous Droplets" at the American Chemical Society National Spring Meeting, New Orleans, LA, March 2023 **(P)**

A. G. Carlton, **A. M. Burns**. *Plenary:* "Agricultural Air Pollution Policy and Impacts: an Almanac" at UNC, Institute for the Environment. September 2022 **(T)**

A. G. Carlton, **A. M. Burns**."Agricultural Emissions: Air Quality, Climate & Environmental Justice" at NASA, Student Airborne Research Program, Palmdale, CA June 2022 **(T)**

V. P. Ghate, A. G. Carlton, T. Surletta, **A. M. Burns**. "Long-Term Trends of Aerosols, Meteorology, and Radiation in the Southeastern US Warming Hole Region" at the 102nd American Meteorological Society Annual Meeting, January 2022 **(T)**

**A. M. Burns**, A. G. Carlton, V. P. Ghate, G. Chandler. "Air Pollution from Concentrated Animal Feeding Operations in the USA: A Case for Regulation" at the American Geophysical Union Fall Meeting, Virtual, December 2021 **(P)**

**A. M. Burns**, A.E. Christiansen, V.P. Ghate, A.G. Carlton. "Meteorology and Dust: Uncertainty in Ambient Aerosol Liquid Water Predictions" at the 38th Annual American Association for Aerosol Research Conference, Virtual, October 2020 **(P)**

**A. M. Burns**, J. Layshock. "Refining Extraction methods for GC/MS Detection of Phthalate Additives" at the Pacific University Senior Projects Day and the Pacific University Department of Chemistry Internal Seminar, Forest Grove, OR, April 2018 **(T)**

S. Virgen, **A. M. Burns**, L. Smith, J. Layshock. "Investigating the green claims of bio-based plastics by measuring chemical migration during simulated food contact" at the American Chemical Society National Spring Meeting, New Orleans, LA, March 2018 **(P)**

**A. M. Burns**, S. Virgen, L. Smith, J. Layshock. "Refining Migration Tests for Phthalate Additives in Bio-Plastics" at the 26th Annual Murdock College Science Research Conference, Spokane, WA, November 2017 **(P)**

## TEACHING AND MENTORING EXPERIENCE

**Instructor on Record, General Chemistry Lab I** **Fall 2023**
University of California, Irvine *Irvine, California*

**Head Teaching Assistant, General Chemistry Labs** **2022-2023**
University of California, Irvine *Irvine, California*
Supervisor: Professor Kimberly Edwards

**Chemistry Teaching Assistant Mentor** **2022-2023**
University of California, Irvine *Irvine, California*
Supervisor: Professor Renée Link

**Teaching Assistant** **6 Quarters, 2019-2022**
University of California, Irvine *Irvine, California*
Supervisors: Prof. Kimberly Edwards and Prof. Stephen Mang

**Undergraduate Mentor** **2016**
Pacific University *Forest Grove, Oregon*
Supervisors: Prof. D. W. Walls and Prof. Brent Johnson

## HONORS AND AWARDS

**Award for Contributions to the Chemistry Department Teaching Program by a TA - Continuing** **2023**
University of California, Irvine

**Minority Serving Institution Enhancement (MSIE) Award** **2019**
University of California, Irvine

**Recipient of the Dr. Harold Schimke Endowed Scholarship** **2017-2018**
Pacific University, School of Natural Sciences

**All-America Scholar Athlete** **2015-2018**
National Fastpitch Coaching Association
*Awarded four times*

**Eva C. Krebs Boxer Spirit Award** **2015-2017**
Pacific University
*Awarded three times*

**Pacesetters Scholarship** **2014-2018**
Pacific University

**California Student Achievement Scholarship** **2014-2018**
Pacific University

**Honors Scholarship** **2014-2018**
Pacific University

# ABSTRACT OF THE DISSERTATION

Aerosol Liquid Water: Sources and Partitioning

By

Alyssa Marie Burns

Doctor of Philosophy in Chemistry

University of California, Irvine, 2024

Professor Ann Marie Carlton, Chair

Despite a wealth of available techniques and preexisting data to measure and estimate atmospheric aerosol abundance, sources, and formation, many uncertainties persist. These uncertainties, in particular for aqueous aerosol and polar water-soluble organic gases ($WSOC_g$), hinder accurate prediction of atmospheric fine particulate matter ($PM_{2.5}$) and its subsequent health and radiative impacts. Emissions of ammonia ($NH_3$), a key precursor to the formation of hygroscopic aerosol mass, are poorly constrained relative to other controllable sources of aerosol precursors such as sulfur dioxide ($SO_2$) and nitrous oxides ($NO_x$). Aerosol liquid water (ALW) is a ubiquitous component of aerosol mass that directly impacts light extinction and radiative forcing, and facilitates the formation of aqueous secondary organic aerosol (aqSOA). ALW is difficult to directly measure at ambient conditions, and observational estimates are subject to errors and biases in measurements of speciated aerosol mass and meteorological variables. Partitioning of $WSOC_g$ to the aqueous phase and aqSOA formation are modulated by ALW content. Ambient $WSOC_g$ is rarely measured, and changes in the solubility of gas-phase inventories as a function of changing chemical climatology has not been systematically evaluated. My dissertation aims to utilize holistic approaches, incorporating publicly accessible datasets, remote sensing, field measurements, and modeling to understand sources and spatiotemporal trends in aqueous aerosol and its physicochemical properties. Specifically, I (1) relate surface-level particulate air quality and animal inventories with satellite retrievals

of $NH_3$ to examine air pollution from concentrated animal feeding operations (CAFOs) in the contiguous U.S.; (2) evaluate the sensitivity of thermodynamically-derived ALW observational estimates to meteorological and chemical variables; and (3) investigate $WSOC_g$ ambient concentrations in $NO_x$-limited and $NO_x$-saturated chemical regimes. Remotely sensed ammonia is spatially and temporally linked to animal unit density at medium-to-large sized CAFOs, with co-located increasing trends noted from 2002 to 2017. It is difficult to quantify the impacts on $PM_{2.5}$ mass in locations where animal density and ambient $NH_3$ is highest due to a dearth of regulatory monitors. Yet, results suggest air quality improvements lag behind the national average in rural agricultural regions. ALW predictions are more sensitive to ammonium and dust ions than to tested meteorological variables (temperature, relative humidity). Despite uncertainties, long-term trends of ALW mass consistently exhibit decreasing trends across the contiguous U.S. due to decreasing mass concentrations of hygroscopic aerosol species. Application of ALW observational estimates helps explain: (1) aerosol optical depth and Ångström exponent-derived size during cloudy and clear sky conditions in Bondville, IL; and (2) changes in surface temperature modulation related to shortwave radiation in the Southeast U.S. warming hole region over two decades. $WSOC_g$ mass concentrations in Irvine 2024 ($NO_x$-limited), are significantly less than those in Pasadena 2010 ($NO_x$-saturated). Differences in VOC emissions and actinic flux contribute to differences in $WSOC_g$ abundance between locations. $WSOC_g$ concentrations are positively correlated with $NO_x$ and $O_3$ in Pasadena. In sharp contrast, Irvine $WSOC_g$ is not correlated with $NO_x$, and is negatively correlated to $O_3$. EPA's Community Multiscale Air Quality model (CMAQ) simulations of $WSOC_g$, $NO_x$, and $O_3$ fail to accurately reproduce observed associations in both Pasadena and Irvine. These findings suggest $WSOC_g$ abundance is related to $O_3$ production chemical regimes, and that the solubility of VOC oxidation products may change with reduced anthropogenic emissions. The results of this dissertation demonstrate the ability of multidisciplinary approaches to understand ambient aerosol water, and highlights the need to chemically characterize gas- and aerosol-phase atmospheric trace species.

# Chapter 1

# Introduction

## 1.1 Background

Despite the wide array of instruments and techniques available to study aerosol formation and fate, many knowledge gaps persist and accurate quantitative assessment of subsequent health and climate impacts is difficult. Understanding the ambient burden of aerosol requires a holistic approach to elucidate under-appreciated sources of pollutants and less-understood formation pathways, such as the partitioning of water-soluble gases and aqueous condensed phase chemistry.

### 1.1.1 Atmospheric Aerosol

Atmospheric aerosols are solid or liquid particles suspended in air. Aerosols may be directly emitted or formed through secondary processes.[1] In the atmosphere, aerosol mass is ubiquitous and abundant, driving many regional and global processes relevant to public health and climate.[1,2] The exact impact of aerosols towards health and climate vary as a function

of particle physicochemical properties and location in the atmosphere. Atmospheric aerosols are physically and chemically diverse, existing in a wide variety of sizes, phase states, particle morphologies, and chemical compositions.[2–4] The most common and general way to classify particles is based on size; regulatory agencies use terms such as $PM_{2.5}$ and $PM_{10}$ to describe fine (aerodynamic diameter $\leq 2.5$ $\mu$m), and coarse particulate matter (aerodynamic diameter $\leq 10$ $\mu$m) respectively.[5] These terms are most important for health determination, as particle size controls deposition within the body.[6] Particle size and other physical properties important for health and climate effects are largely controlled by formation pathways and the chemical composition of ambient aerosol mass.

### 1.1.2 Aerosol Composition and Sources

The chemical composition of both directly emitted and secondary aerosols is complex. Primary aerosols include natural sources such as mineral dust or sea spray, in addition to anthropogenic sources such as soot from combustion and road dust.[1,7] Directly emitted aerosols are generally mechanically generated and coarse ($PM_{10}$). Most aerosol fine mass ($PM_{2.5}$) is secondary in nature, forming via complex multiphase chemical reactions.[1] Primary gaseous emissions from anthropogenic and biogenic sources undergo oxidation reactions, leading to the formation of semi-volatile to low-volatility chemical species that may condense directly or partition to pre-existing mass to produce particulate mass.[8,9] Secondary chemical reactions in the condensed phase also contribute. The resulting aerosol consists of a highly complex mixture of inorganic and organic compounds, as well as associated aerosol liquid water (ALW).

#### 1.1.2.1 Inorganic Aerosol

The primary gas-phase pollutants most important for formation of secondary inorganic aerosols are ammonia ($NH_3$), sulfur dioxide ($SO_2$), and nitrous oxides ($NO_x$; $NO_x$=NO+$NO_2$). All three species are primarily anthropogenic emissions and in the U.S. are subject to a variety of Federal, State and local regulations. Anthropogenic ammonia emissions are dominated by agriculture, and land sector emissions are substantially more uncertain relative to point sources.[10] Emissions of $SO_2$ and $NO_x$ are primarily a consequence of fossil fuel combustion.[3] Natural sources of all three species also exist such as biomass burning ($NH_3$), volcanic activity ($SO_2$), and lightning strike ($NO_x$) that can contribute to the atmospheric burden substantially in episodic events.[11–13] Gas-phase $SO_2$ and $NO_x$ react rapidly after emission with the hydroxyl radical ($^{\cdot}OH$), forming sulfuric and nitric acid respectively. These acidic species are titrated by $NH_3$, a uniquely basic and abundant gas, to form ammonium sulfate and ammonium nitrate salts. These inorganic salts make up a significant portion of aerosol mass, especially in polluted or urban regions.[14,15] Due to their contribution to acid rain, particle formation, and other pollution concerns, $SO_2$ and $NO_x$ emissions are tightly regulated, and emissions demonstrate substantial decreases since the implementation of the 1990 Clean Air Act Amendments.[16]

Primary inorganic particle mass (e.g. $Na^+$, $Cl^-$,$Ca^{2+}$, $Mg^{2+}$, $K^+$, metals, etc.) from sea spray, dust, and other sources[17,18] can also facilitate phase transfer through the formation of salts. Differences in cation valence shells may affect aerosol phase state, morphology, and pockets of density within suspended particles.[19–21] Metallic species such as iron and its oxidation state can impact condensed-phase oxidation processes and modulate brown carbon formation.[22,23] Feedbacks between inorganic aerosol constituents and the formation of aqueous secondary organic aerosol (aqSOA) are a key uncertainty.

#### 1.1.2.2 Organic Aerosol

As anthropogenic emissions of inorganic precursor species decreased in the U.S. over recent decades, organic aerosol (OA) has become a more substantial fraction of aerosol mass.[24–26] Some OA is directly emitted during combustion, and most OA mass is predominantly secondary, forming from the oxidation of volatile organic compounds (VOCs) that form semi-volatile and water-soluble species that can partition to the condensed phase and add to aerosol mass or form new particles.[27,28] VOC emissions are dominated by hydrocarbon species from the biosphere with contributions from anthropogenic sources as well. Biogenic VOCs that affect secondary organic aersol (SOA) formation are generally reactive hydrocarbon compounds, often alkenes.[29] In urban settings, anthropogenic emissions of compounds such as BTEX (benzene, toluene, ethylbenzene, and xylenes) from sectors such as mobile vehicles and solvent use can be substantial.[30,31]

Photochemical processing of VOCs entails reactions with oxidants such as OH, ozone ($O_3$), and the nitrate radical. These oxidation processes either fragment VOCs, ultimately producing $CO_2$, or add functional groups to VOCs, generally decreasing compound volatility and increasing water-solubility.[32] Following the formation of more complex, semi-volatile compounds, there are two predominant pathways for SOA formation. Historically, many studies focus on the dry condensation of semi- and low-volatility compounds to form particles.[33,34] SOA may also form through the partitioning of water soluble organic compounds (WSOC) into liquid water and subsequent reactions in the condensed phase.[9]

Despite its increasing fractional contribution to aerosol mass, OA is not well-characterized relative to the inorganic fraction of aerosol. The vast diversity of VOC emissions[32] and subsequent oxidation products[35] makes precise chemical characterization and mass closures of organic mass difficult.[36] Even in controlled laboratory experiments with a wide variety of available instrumentation, it is difficult to completely characterize the gas and particle

phase inventories.[37] Particulate organic carbon (OC) mass is routinely measured at surface networks across the U.S. in urban locations and in national parks, but provides limited information regarding the volatility of compounds present through laboratory analysis of filter samples.[38] Chemical characterization of individual organic constituents and emissions, necessary to fully elucidate formation pathways, remains difficult and uncertain.

#### 1.1.2.3 Aerosol Liquid Water

Many of the inorganic and organic components of aerosol are hygroscopic, causing liquid water uptake. Aerosol liquid water (ALW) is a ubiquitous component of aerosol mass, even in remote and in some arid locations.[39] Mass concentrations of ALW are primarily driven by hygroscopic inorganic salts, such as ammonium sulfate, ammonium nitrate, and sodium chloride, as mass concentrations of hygroscopic particle-phase species are often more limiting than water vapor mixing ratios.[40,41] While nitrate is more hygroscopic, sulfate hygroscopicity is thought to be the controlling constituent in most locations due to higher mass concentrations.[42,43] Organic compounds may also contribute substantially to ALW mass, and cloud-condensation nuclei (CCN) formation;[39,44,45] however, the lack of detailed chemical information pertaining to OA and associated uncertainties in organic hygroscopicity make assessment difficult.[46,47]

ALW is important for many physical and chemical aerosol properties. Hygroscopic uptake of water increases particle physical size, impacting the light extinction properties and by extension the radiative forcing of aerosol.[48–50] The ALW content of aerosol also largely controls the chemical potential of aqSOA formation. ALW acts as a media both for the partitioning of gaseous WSOC ($WSOC_g$) and for subsequent oxidation, functionalization and oligomerization reactions to produce SOA.[9,51] ALW similarly acts as a plasticizer in aerosol mass, reducing viscosity and allowing faster diffusivity and/or evaporation of compounds to the condensed phase.[52,53] Aerosol phase state is influenced by ALW content, with more liquid

aerosols predicted in the Eastern U.S. and more semi-solid to solid particles predicted in the West.[54] ALW and aqueous SOA formation are thought to be more important in humid and sulfate-dominated environments like the Eastern U.S. where ALW is readily abundant; however, studies suggest $WSOC_g$ concentrations and subsequent aqueous pathways may be important in arid regions as well.[55–59] Quantitative understanding of ALW at ambient conditions is limited by the difficulty and paucity of ambient measurements. ALW is lost during most measurement techniques of other nonvolatile aerosol components.[60] Optical techniques such as nephelometers and humidified differential tandem mobility analyzers (HDTMAs) can estimate ALW as a function of hygroscopic growth.[61–63] However, the drying and humidification techniques employed disturb aerosol from its ambient state. For example, drying processes may cause volatilization of other aerosol components besides ALW.[61,64] ALW can be estimated through modeling approaches when suitable co-located measurements are available. This rarely occurs outside intensive observation periods (IOPs), further complicating assessments of prediction accuracy. A limited number of studies show good agreement between measured and modeled liquid water.[44,65] Due to these limitations, ALW and aqueous processing of $WSOC_g$ remain a poorly understood property relative to pathways of SOA formation via semi-volatile condensation.

### 1.1.3 Measurements and Estimates of Ambient Aerosol

Our understanding of atmospheric aerosol burden relies upon accurate measurements and estimates regarding their formation and fate. A multitude of approaches and platforms have been developed, and can be divided into broad categories of ambient or field measurements, laboratory experiments, remote sensing via satellites and suborbital campaigns, and model studies. Each avenue offers some benefits and is also limited in various capacities.

#### 1.1.3.1 Field Measurements

The instrumental measurements techniques employed are diverse and operationally defined, and each approach senses different aerosol properties. Techniques may capture aerosol chemical and/or optical properties *in situ* or may be destructive.[66] Time resolution varies, from near real-time, or offline analysis with whole-air or filter-based particular mass samples.[66] Broadly, field measurements are divided between long-term routine and regulatory monitoring sites and IOPs.

Several different surface measurement networks exist within the U.S. to characterize precursor emissions as well as concentrations of gas and particle phase pollutants. Surface networks utilized in this dissertation are listed in Table 1.1. The target pollutants of each network vary, as well as the time and spatial resolution available. EPA supports the Interagency Monitoring of Protected Visual Environments (IMPROVE) network to enforce the Haze Rule in national parks and provides filter-based measurements of inorganic and organic particle mass from 1988 through present day.[67] EPA's Air Quality System (AQS) records measurements of species such $SO_2$, $NO_2$, $O_3$, and $PM_{2.5}$, primarily in urban and non-attainment areas.[68,69] Not all sites measure all variables, and few network sites are co-located with one another, confounding inter-network comparison.[70,71] Time-resolved meteorological measurements are often not present at long-term air quality measurement sites. Estimates of particle properties such as hygroscopic growth and light extinction that require information of meteorological variables are reliant on reanalysis products due to this limitation.[72] IMPROVE sites, for example, rarely include relative humidity (RH) measurements, despite a network mission to evaluate visibility concerns and an extinction estimate formula that relies on RH.[49]

IOPs bring together a wide array of different instrumentation techniques to specific locations and offer a wealth of data to understand complex processes. Due to the complexity of such organizational efforts, field campaign spatial and temporal coverage is episodic and are

| Network | Agency | Years Active | Sites | Variables Measured | Time Resolution |
|---|---|---|---|---|---|
| IMPROVE | NPS/EPA | 1988-present | approx. 160 | Filter-based measurements of $PM_{2.5}$ and speciated mass ($SO_4$, $NO_3$, OC, etc.) | 1-in-3-days (24-hr integrated sampling) |
| AQS/CSN | EPA | 1957-present | approx. 145 (CSN) to 500+ (PM, O3) | Gas-phase species such as $SO_2$, $NO_2$, and $O_3$. Filter-based measurements of $PM_{2.5}$ and speciated mass ($SO_4$, $NO_3$, $NH_4$, OC, etc.) | Varies for different species; hourly or sub-hourly for species such as O3 or $PM_{2.5}$ mass, 1-in-3 or 1-in-6 days for speciated mass (24-hr integrated sampling) |
| AERONET | NASA | 1993-present | 600+ (global) | Optical properties such as AOD and AE | 15 minutes |

Table 1.1: Surface-based measurement networks employed in this dissertation. Sites describes the number of active monitor locations. Variables measured focus on the variables utilized here; other aerosol properties may be measured at these and other measurement network sites.

historically biased to occur in summer, though many unique and diverse environments have been examined.[73–76] Measurement techniques vary widely and are often performed through a variety of platforms, such as surface, tower, and aircraft measurements. Quality-assured data from such campaigns are typically publicly available (e.g., CalNex 2010),[77] and re-interpretation of these measurements with more recent data and other campaigns is valuable (e.g. Nguyen et al., 2016, Chen et al., 2019).[39,78]

#### 1.1.3.2 Laboratory Experiments

Controlled laboratory experiments are valuable to elucidate the impact of specific conditions and species towards aerosol formation and other properties.[79] A variety of laboratory experiment configurations exist, from single-particle levitation techniques to atmosphere-simulating smog chambers, with correspondingly diverse characterization techniques.[80,81] Most approaches to study SOA formation involve the generation of aerosol from primary VOC and oxidant mixtures with chambers or flow tubes.[82] Conditions such as initial VOC and oxidant identities and concentrations are manipulated to represent different chemical environments.[82] For example, many studies employ $^{\cdot}OH$ or $O_3$ induced oxidation to represent daytime conditions and the nitrate radical to replicate nighttime chemistry.[83–85] Precursors such as alpha-pinene, isoprene, toluene, etc. are commonly used in binary or multicomponent systems.[86–91] Aging, browning, and other chemical processes can be simulated with produced mass.[92–94]

While these experiments provide valuable insights, they often deviate from ambient conditions. For example, the atmosphere is composed of complex mixtures, while laboratory experiments often involve single component systems.[82] Precursor concentrations and subsequent SOA yields in chamber and flow tube experiments are often much greater than ambient conditions.[95] On the other hand, wall losses of gas and particle species are ubiquitous in these types of experiments and can be difficult to quantify.[96] "High-$NO_x$" and "low-$NO_x$" conditions are often employed to understand oxidation pathways in different chemical regimes; however, definitions of these conditions vary and this confounds comparison among laboratory studies.[97] Within "low-$NO_x$" conditions alone, subtle variations in environmental and system conditions can force unrealistic product formation through different peroxy radical ($RO_2^{\cdot}$) reaction pathways.[98] These terms fail to describe the apportionment of NO and $NO_2$ within $NO_x$, and the ratio of NO to $NO_2$ also perturbs laboratory studies from ambient conditions.[99] Further, many of experiments are performed under laboratory temperature and

RH conditions, which are not representative of most atmospheric conditions.[95,100]

#### 1.1.3.3 Space-Based Remote Sensing

Remote sensing observes atmospheric trace species in situ, and unperturbed from ambient conditions. Data from instrumentation onboard satellites, such as NASA's Moderate Resolution Imaging Spectroradiometer (MODIS) aboard Aqua and Terra, is translated to surface and column concentrations of various pollutants including aerosol.[101–103] Satellite products record aerosol optical depth (AOD), single-scattering albedo (SSA), and Ångström exponent (AE), a measure of particle size, as well as other variables derived from optical properties to describe column concentrations of compounds with specific refractive properties.[101,102] Satellite retrievals are validated against surface-based column measurements and suborbital IOPs during clear sky conditions. NASA, for example, utilizes the Aerosol Robotic Network (AERONET), a surface-based optical measurement network, and field campaigns such as DISCOVER-AQ to validate their satellite retrievals.[104,105]

Retrieval algorithms and technologies continue to improve. New state-of-the-art products such as NASA's Tropospheric Emissions: Monitoring of POllution (TEMPO), for example, launched in 2023 and recently releasing initial data, is the first space-based platform to provide hourly daytime measurements of pollutants such as $NO_2$ and $O_3$ in across North America at sub-urban resolution.[106,107] Spatial, vertical, and temporal resolution of other data products varies. Some products can resolve individual plumes and point sources can be identified, though most provide coarser resolution.[108,109] Satellite retrievals have the most uncertainty during cloudy periods and in areas where background refractive properties are complex.[110–112] Clouds cover a significant portion of the Earth's surface at any given time,[113] and hygroscopic aerosol properties are different on cloudy versus clear sky days hindering understanding of aqueous aerosol processing and cloud formation.[72,114]

#### 1.1.3.4 Modeling

Modeling methods offer the unique ability to estimate conditions and chemical processes where measurements may be scarce or difficult to acquire. Ambient measurements of atmospheric pollutants demonstrate clear declines across the U.S.; models help explain these observations by filling gaps in measurement networks and and elucidating chemical sensitivities.[115,116] Modeling approaches provide insights ranging from molecular scale reactions to the prediction of future scenarios under different emission control and climate conditions.[117,118]

Accordingly, these approaches can vary in scope, ranging from kinetic 1-D box models that may simulate a select set of chemical reactions to complex Eurlerian and Lagrangian photochemical transport models that predict concentrations of pollutants during transport.[119,120] Relatively simple models are available as online platforms, including NOAA's Hybrid Single-Particle Lagrangian Integrated Trajectory model (HYSPLIT) for air parcel trajectory and dispersion[121], NCAR's Tropospheric Ultraviolet (TUV) model to predict solar radiation and photolysis rates, and the Extended Aerosol Inorganics Model (E-AIM) for thermodynamic equilibrium predictions.[122–124] Increasing complexity of specific processes in larger scale atmospheric models increases computational cost. Implementation of parameterizations to simplify and speed calculations can bias predictions of atmospheric chemical and physical processes, particularly for clouds that are often poorly resolved.[125] Models used for regulatory purposes, like EPA's Community Multiscale Air Quality (CMAQ) model, are optimized for pollutants for which they can be evaluated. For example, $O_3$ is measured at over 500 surface sites within the US with sub-hourly time resolution and is generally predicted well.[115,126] There is no routine network that measures SOA mass, and when evaluated during IOPs, predictive skill for OA is usually biased.[127–129] Model evaluation with ambient and laboratory data is vital to ensure accurate simulation of pollutants and processes to ensure sound predictions of the ambient environment under future regulatory and climate scenarios.[126]

## 1.2 Motivation

### 1.2.1 Public Health and Environmental Justice

Air pollution is a leading contributor to the global burden of disease, causing nearly 7 million excess deaths per year.[130] $PM_{2.5}$ is the most common tracer of particulate pollution. Fine particles deposit deep within the lungs, with some constituents able to diffuse into the bloodstream and affect multiple organ systems.[6,131] Short- and long-term exposures are associated with a myriad of adverse health effects, such as cardiovascular, respiratory, and neurodegenerative disease.[131–133] Regulatory definitions of safe $PM_{2.5}$ exposure differ; the US EPA recently reduced the annual standard to 9 $\mu$g $m^{-3}$, while the World Health Organization (WHO) recommends 5 $\mu$g $m^{-3}$ annual average.[134,135] Many regions of the U.S. exceed both standards.[136] The chemical composition of $PM_{2.5}$ plays a role in ultimate health outcomes. Some constituents of PM mass and precursor gaseous emissions can be directly toxic.[137] Other components, including metals and organic compounds, promote the generation of reactive oxygen species (ROS) upon deposition in the lungs, triggering oxidative stress and ultimately cell death.[138,139]

Tropospheric ozone is also an important pollutant with deleterious health and welfare effects. $O_3$ is a component of urban smog, and its formation is tightly coupled to VOC oxidation and $NO_x$ cycling.[3] Many regions of the US exceed national standards for $O_3$ pollution (70 ppb 8-hr max); more than 100 million people live in non-attainment areas.[140] Health effects for $O_3$ are typically linked to short-term exposures. $O_3$ is directly irritating and causes cardiovascular distress, and is linked to 370,000 excess deaths per year.[130] $O_3$ also damages plants and reduces crop productivity.[141]

Exposures to these pollutants are unequal. Regions with higher non-white populations and lower socioeconomic status face greater amounts of air pollutants such as $O_3$ and $PM_{2.5}$.[142]

Reductions in emissions have improved national averages of air quality, but these emission reductions and benefits are not equal.[143] In California, the combination of environmental and socioeconomic indicators highlight undue pollution burden in the Central Valley.[144] The Central Valley often exceeds $PM_{2.5}$ federal standards, and is unlikely to reach standards without considerable mitigation.[145] Uncertain budgets of primary pollutants makes assessment of such mitigation strategies difficult. The inequal pollution burden faced by frontline communities in this region, especially agricultural workers who spend much of their time outdoors,[146,147] presents a key environmental justice issue.

### 1.2.2 Radiative Forcing

The role of aerosols towards the radiative budget of the earth is a key uncertainty in climate projections.[148] Increasing average global temperature is primarily due to absorption of long wave radiation by $CO_2$ in the 'atmospheric window,' and greenhouse gas (GHG) emissions are the predominant focus of climate mitigation strategies.[149] Aerosols are short lived climate forcers (SLCF), and also exert local and regional direct and indirect effects on the Earth's radiative budget.[1,148] Direct effects pertain to the light extinction properties of aerosol. Some aerosol constituents, such as brown and black carbon (BrC and BC respectively), absorb visible and near-IR radiation and promote a warming effect both at the surface and in the upper troposphere.[150,151] Other species are more reflective and increase the amount of incoming shortwave radiation scattered by aerosol, offsetting the warming effect of GHGs and resulting in a net cooling effect.[152]

Aerosols also indirectly change radiative properties through cloud formation. Aerosol particles are the seeds for cloud and ice cloud nucleation, which efficiently scatter incoming radiation and increase Earth's albedo to promote a cooling effect in daylight hours,[152] in addition to altering local hydrological cycling.[153] The chemical composition and number-

size distribution of aerosols plays a determining role in CCN activation and ultimate cloud albedo.[41,45,154] CCN activation relies on the hygroscopic growth of aerosol under supersaturated conditions, largely controlled by aerosol composition and size distribution.[154] Under constant liquid water conditions, increasing concentrations of aerosol will produce more cloud droplets with lower water content and smaller physical size, which in turn increases the amount of light scattered, precipitation rates, and cloud lifetimes.[153,155]

Assessments of overall aerosol radiative impacts are heterogeneous and difficult to explicitly quantify. Generally, aerosol and clouds are treated as scattering species, though effects differ regionally and during events, such as biomass burning episodes.[152] While the effects of greenhouse gases are a greater overall forcing, aerosols are suggested to play a role in surface temperature modulation in regions such as the Southeast US.[156–158] Overall aerosol forcing is predicted to be slightly negative (i.e., cooling), though uncertainties in aerosol feedbacks are large relative to other climate forcers.[148,152]

### 1.2.3 Informed and Effective Action

Rapid mitigation and adaptation is required to ameliorate the most deleterious climate change impacts and to reduce the disproportionate health effects of air pollution. The power of effective and scientifically informed regulations is exemplified through the recovery of the ozone hole in the antarctic region through intergovernmental regulations of chlorofluorocarbon compounds (CFCs) and other ozone depleting substances.[159] As a part of the Clean Air Act and subsequent amendments, $SO_2$ and $NO_2$ are classified as criteria air pollutants (CAPs) due to their contributions to acid rain, particle mass, and ozone ($NO_2$) formation, and thus are measured regularly at surface sites throughout the U.S.[160,161] Reductions in these and other primary anthropogenic pollutants have dramatically improved air quality and visibility.[162] Changes in aerosol source apportionment and subsequent shifts in aerosol

burden, composition, and radiative properties may induce other unintended consequences.

For example, in 2020 international shipping fuel standards required reductions of sulfur content from 3.5% to 0.5%, with the motivation to safeguard human health and prevent ecosystem collapse in terrestrial and oceanic environments.[163] While this change is advantageous from a welfare perspective, the climate perspective is less clear. $SO_2$ shipping emissions produce reflective, cooling clouds over the ocean which help mask global warming trends. The rapid dimming of oceanic clouds as a product of these regulations is consistent with sharp recent warming trends in surface sea temperature.[164,165] While there are still many uncertainties within this problem alone, sulfur shipping regulations serve as a case study of inter-related atmospheric processes that operate synergistically and not in isolation. Unintended byproducts of mitigation strategies are widespread.[166–168] These changes are essential for human health and welfare, but complicate strategies for climate stability. Similarly, the electrification of passenger and heavy-duty vehicles is a predominant strategy to reduce both $CO_2$ and other harmful emissions like $NO_x$ and gasoline VOCs. New research indicates particle formation from brake and tire wear is substantial, enhanced due to the weight of electric vehicles, and imposes new challenges in the characterization of ambient aerosol.[169,170]

As we continue into an uncertain future, proposals for global warming mitigation strategies have become more extreme, such as "sun shades" in space and stratospheric aerosol injection.[171] The impact of fuel use and energy production changes necessary for climate stability towards atmospheric composition and emissions are unclear. Popular mitigation strategies such as carbon credits are understudied and suffer in scientific and regulatory transparency.[172] Scientific research must address the potential nature, magnitude, and distribution of both intended and unintended outcomes toward human and ecosystem health, as well as social, political and economic concerns in order to support the informed development of policy and mitigation strategies.[171]

## 1.3 Key Knowledge Gaps

Determination of effective strategies to mitigate adverse health and climate effects now and in the future requires sound scientific understanding. Despite the wide array of tools available, the ability to accurately characterize the ambient pollution burden is limited and uncertain. For example, surface $PM_{2.5}$ monitors exhibit negative mass artifacts for nitrate, ALW, and organic constituents.[100,173] Ammonia, and its particle phase counterpart, ammonium, are not measured with the spatial or temporal resolution common for other major $PM_{2.5}$ contributing species at air quality monitoring locations. The National Atmospheric Deposition Program's (NADP) Ammonia Monitoring Network (AMoN)[174] is sparse and collects biweekly passive samples that are insufficient to describe the ambient burden, which hinders appropriate assessment of particulate matter mitigation strategies.[175] The fractional contribution of the land sector to total U.S. emissions continues to grow as U.S. agriculture increasingly becomes industrialized,[176] and other controllable sectors are regulated. Ambient air pollution in rural areas is poorly characterized relative to cities, and agricultural air pollution sources lack quantitative measurements compared to other controllable sources of air pollution.

Similarly, the organic gas inventory, particularly for highly functionalized oxygenated and polar species, is highly uncertain, despite controlling effects on $O_3$ and PM production, deposition and reactive carbon budgets. The vast majority of oxygenated VOCs remain unidentified and unquantified, partly due to the vast chemical diversity of these compounds. In untargeted analysis of ambient and laboratory samples, hundreds to thousands of peaks may exist in relatively routine mass spectra.[35,177–179] While this lack of specific chemical and mechanistic information may hinder accurate prediction of SOA, some of this deficit may be overcome by measuring and modeling the chemical properties of bulk VOCs. Studies focused on gas-to-particle conversion of organic compounds typically focus on volatility. For example, particulate OC recorded in surface air quality networks is measured as a function of volatility according to specific temperature ramps. Yet, WSOC in the particulate phase

is considered as a tracer for SOA mass.[180–183] Measurements and characterization of water-soluble gases and factors that influence solubility and uptake of polar organic species to ALW remain key knowledge gaps.

## 1.4 Research Questions and Specific Aims

The studies presented in this dissertation are guided by the following research questions and specific aims:

**Question 1:** How can we reconcile measurements that sense different aerosol properties across platforms to improve holistic understanding of atmospheric trace species and their impacts?

*Specific Aims:* In the projects presented within this dissertation, I employ measurement and modeling approaches with diverse air quality and meteorology data sources to reach elusive conclusions that are not achieved in isolated approaches.

**Question 2:** How do concentrated animal feeding operations affect regional air quality in rural areas of the U.S.?

*Specific Aims:* I use the best available resources to investigate spatiotemporal changes in animal unit density, ambient ammonia concentrations, and surface air quality in the contiguous US (CONUS).

**Question 3:** To what extent can observational estimates of ALW contribute to plausible explanations to atmospheric phenomena?

*Specific Aims:* I investigate the sensitivity of thermodynamic ALW predictions to meteorology and chemical variables. Observational estimates are applied to help explain observed trends in aerosol physicochemical properties and surface temperature modulation in different

U.S. locations in the context of differing physical and chemical climatology.

**Question 4:** What is the abundance of functionalized volatile organic compounds in relation to other indicators of photochemical activity?
*Specific Aims:* I measure $WSOC_g$ in near real-time for 6 weeks in Irvine, CA in 2024 and compare values and associations with other variables to analogous measurements taken in Pasadena, CA during the 2010 CalNex campaign. CMAQ simulations are qualitatively compared to both data sets.

## 1.5 Structure of Dissertation

Chapter 2 focuses on the impact of industrial agriculture on regional air quality in the United States. While concentrated animal feeding operations (CAFOs) are established as major sources of water pollution, their air emissions remain unregulated and understudied in comparison to other controllable sources. The effects of increasingly industrialized animal husbandry towards air pollution burden in agricultural and other regions has not been established, in part due to limitations in the availability and completeness of animal and air pollution data. A variety of different data sources are used to overcome this deficit, including animal unit density derived from the USDA agricultural census, speciated $PM_{2.5}$ measurements from the EPA's Chemical Speciation Network (CSN), and remote observations of ambient ammonia mixing ratios from both NASA and ESA. The comparison of these data sources is used to highlight changes in industrial animal practices and associated effects in ammonia and particulate matter concentrations from 2002-2017.

Chapter 3 investigates sensitivities in and applications for observational estimates of particle-bound liquid water. Since ALW is difficult to measure directly, studies often rely on thermodynamic simulations of ALW content, which are affected by the meteorological and chemical

values employed. Two common meteorological reanalysis datasets, NCEP's North American Regional Reanalysis (NARR) and ECMWF's ERA5, are investigated here, as well as the effect of dust and ammonium ion inclusion. Trends in ALW across CONUS with different data inputs are also evaluated. Informed ALW estimates are then used in two different applications towards understanding aerosol optical and radiative forcing: (1) quantifying aerosol size and optical depth on clear and cloudy sky days in Bondville, IL; and (2) understanding the modulation of short wave radiation and surface air temperature in the Southeast US warming hole region.

Chapter 4 seeks to improve understanding of $WSOC_g$ abundance across different atmospheric chemical environments. Primary emissions of $NO_x$ and VOCs have dramatically reduced in the LA basin over the past 15 years; however, the impact of changing emission profiles towards the solubility of VOC oxidation products has not been investigated. Measurements of $WSOC_g$, $NO_x$, and $O_3$ in Irvine in 2024 are compared to measurements of the same variables from Pasadena in 2010. Diurnal profiles and statistical associations are compared to CMAQ simulations for the same locations in 2017. The correlations of different variables suggest differences in the formation and/or loss pathways of $WSOC_g$ in $NO_x$-saturated and $NO_x$-limited regimes, potentially with broader implications for aqSOA formation and VOC reactivity as emission controls continue to shift the proportion of VOCs to $NO_x$.

Chapter 5 focuses on future research directions. This includes (1) further use of satellite products and surface-based data to improve emissions estimates and identify "hotspots" of emissions related to animals; (2) pairing of mist chamber measurements with other on and offline measurement techniques to better characterize the soluble VOC inventory and potential salting effects on organic partitioning; and (3) development of upper-division chemistry coursework using argument-driven inquiry (ADI) and specifications grading principles.

# Chapter 2

# Data Gap: Surface Air Quality Networks Miss Air Pollution from Concentrated Animal Feeding Operations

The contents of this chapter are reproduced with permission from the following publication: Alyssa M. Burns, Gabriel Chandler, Kira J. Dunham, and Annmarie G. Carlton. Environmental Science & Technology, **2023**. 57 (49), 20718-20725. DOI: 10.1021/acs.est.3c06947.
Copyright © 2023 The Authors. Published by American Chemical Society. This publication is licensed under CC-BY 4.0.

## 2.1 Abstract

In the U.S., the agricultural sector is the largest controllable source of several air pollutants, including ammonia ($NH_3$), which is a key precursor to $PM_{2.5}$ formation. Livestock waste is the dominant contributor to ammonia emissions. In contrast to most controllable air pollutants, satellite records show ammonia mixing ratios are rising. The number of confined animal feeding operations (CAFOs) that generate considerable livestock waste is also increasing. Spatial and temporal trends in USDA-reported animal numbers normalized by county area at medium and large CAFOs provide plausible explanations for patterns in satellite-derived $NH_3$ over the contiguous U.S. (CONUS). The correlation between summertime ammonia derived from the European Space Agency's (ESA) Infrared Atmospheric Sounding Interferometer (IASI) and CAFO animal unit density in 2017 is positive and significant ($r = 0.642$; $p \approx 0$). The temporal changes from 2002 to 2017 in animal unit density and $NH_3$ derived from NASA's Atmospheric Infrared Sounder (AIRS) are spatially similar. Trends and ambient concentrations of $PM_{2.5}$ mass in agricultural regions are difficult to assess relative to those of urban population centers given the sparseness of rural monitors in regulatory surface networks. Results suggest that in agricultural areas where ammonia concentrations and animal density are highest, air quality improvement lags behind the national average.

## 2.2 Introduction

The U.S. Environmental Protection Agency (EPA) reports that agriculture is the largest source of anthropogenic emissions of ammonia ($NH_3$), nitrous oxide ($N_2O$), and methane ($CH_4$).[184,185] Emissions of nitric oxides ($NO_x$; $NO_x = NO + NO_2$), a variety of organic

species and reduced sulfur compounds, and primary $PM_{2.5}$ from agriculture are also documented.[145,186–188] These emissions adversely affect air quality and ecological welfare, destroy stratospheric ozone, and add to the global burden of greenhouse gases.[175,185,189–198]

Domestically, U.S. agricultural ammonia emissions are estimated to cause over 12,000 premature deaths and incur societal costs of roughly $160 billion each year, primarily through the formation of fine particulate matter ($PM_{2.5}$).[199,200] As the most abundant basic gas in the atmosphere, ammonia readily reacts with oxidation products of sulfur dioxide ($SO_2$) and $NO_x$ to form ammonium sulfate and ammonium nitrate, which contribute substantially to ambient $PM_{2.5}$, a criteria air pollutant (CAP). A 42% reduction in $PM_{2.5}$ mass concentrations is observed over the contiguous U.S. (CONUS) from 2000 to 2022.[201] The national average is weighted by monitoring site locations and driven largely by trends in the Northeast (73 sites, -48%), Ohio Valley (59 sites, -51%), and Southeast (63 sites, -48%). Decreased $PM_{2.5}$ mass concentrations can be attributed to environmental policies, such as acid rain and ozone mitigation. For example, $SO_2$ and $NO_2$ are CAPs regulated through the National Ambient Air Quality Standards (NAAQS) framework and performance standards at controlled sources. Measurements at approximately 500 air quality monitoring locations[160,161] document sharp reductions in ambient mixing ratios of $SO_2$ and $NO_2$ that contribute to declines in $PM_{2.5}$ mass concentrations due to reduced formation of ammonium sulfate and ammonium nitrate, respectively.[26,202,203] In sharp contrast and despite its similar contribution to $PM_{2.5}$, there is no NAAQS for ammonia, and ambient concentrations are not as routinely monitored in regulatory networks. Multiple satellite products indicate that the atmospheric burden of $NH_3$ is increasing over the U.S., most notably in agricultural regions.[204,205]

Atmospheric mixing ratios of ammonia are spatially heterogeneous and generally spike downwind in close proximity of sources due to the relatively short atmospheric lifetime (<1 day).[206–209] Physical loss mechanisms such as wet and dry deposition dominate over chemical loss.[210] Nitrogen deposition is increasing at National Atmospheric Deposition Pro-

gram (NADP) monitoring locations influenced by agriculture.[196,206,207] Similarly, since 2007, biweekly passive surface measurements from the Ammonia Monitoring Network (AMoN) document the highest ammonia concentrations are generally associated with agricultural locations.[174] The number of agricultural operations with large numbers of feedlot-confined animals, commonly called concentrated animal feeding operations (CAFOs), is increasing. The Government Accountability Office (GAO) estimates that the number of CAFOs increased 230% from 1982 to 2002,[176] in part due to economic factors that encourage increased agricultural intensity and higher animal density with the shift in market focus to exports.[211] More recently, EPA data shows the number of CAFOs increased 16% from 2011 to 2022.[212]

Despite the growing number of CAFOs and their contribution to environmental pollution, accurate understanding of the number, size, and exact location of animals housed in CAFOs is difficult to acquire[176] because consistent, public CAFO data is sparse. For example, some agricultural enterprises, including large-scale CAFOs, are not included in the USDA's Census of Agriculture (hereafter, "AgCensus") and other public data sets, due to USDA's programmatic privacy concerns.[213] CAFOs that meet certain definitions in the Clean Water Act are subject to the National Pollution Discharge Elimination System (NPDES) program, which regulates the discharge of pollutants from point sources to navigable waters of the U.S.[212] EPA records NPDES permit data, but not all CAFOs discharge to navigable waters. The precise locations and animal populations of all CAFOs are not fully disclosed in any public inventory. Both the USDA and EPA data sets represent lower bounds for the actual number of CAFO-associated animals. CAFOs are more common in high-poverty and majority-non-White communities,[214,215] and their pollution may represent an environmental justice issue.

In this work, we investigate animal density at CAFOs in the CONUS over a 15-year period (2002–2017) in relation to satellite-detected ammonia and surface level $PM_{2.5}$ mass. We examine animal density at CAFOs to the extent possible with public data sets through

analyses of the USDA Agricultural Census and EPA NPDES permit filings. We assess remotely detected ammonia and the evolving chemical climatology of rural areas in the context of surface measurements of $PM_{2.5}$ mass and its chemical constituents. We apply analyses according to the EPA and USDA's regional categories of the CONUS to explore the ability of current governmental accounting systems to accurately describe ambient air quality where ammonia pollution is greatest.

## 2.3 Materials and Methods

For all analyses, we investigate trends in the U.S. using various public, government-hosted data sets, as identified below. R statistical software is used for all data processing.[216]

### 2.3.1 County-Level Animal Unit Density Maps and CAFO Trends

Under the Clean Water Act (CWA), one animal unit (AU) is equivalent to 1000 lb of live weight, which is roughly equivalent to 1 individual cow or cattle, 2.5 swine, and/or 30-125 egg-laying or broiler chickens depending on the manure management system.[217] We employ the USDA Census of Agriculture reports, available at the county level every five years from 2002 to 2017.[213] We focus on medium- and large-scale operations that meet the following descriptions: 500+ cattle/cows, 1000+ hogs, 500,000+ broilers sold annually, or 100,000+ egg layers. To normalize emissions among species, AUs are used instead of individual head counts. In this work, we define AUs more consistent with the USDA's Economic Research Service (ERS) definitions, which account for animal lifetimes by employing "animal unit months". One AU is approximately equivalent to 1.14 beef cattle, 0.74 dairy cows, 9.09 hogs, 250 laying hens, or 455 broilers.[218] Other animal species are also industrially farmed,[10] but are not assessed here. USDA may not fully disclose animal counts at the county level

due to facility privacy concerns. We use state-level animal totals to estimate the number of undisclosed CAFO animal units in the AgCensus and assign those animals to CAFO facilities located in omitted counties. Animal data from the AgCensus are linked to county-specific land areas from USDA's ERS using the Census Service's unique Geographic Identifier (GeoID) for each county. AU density is calculated as the number of animals in each category normalized to AU definitions and divided by the county land area. Ordinary least-squares linear regression is used to examine trends in individual counties over time. Trends are defined as the slope of the regression lines (AU $km^{-2}$ $year^{-1}$).

### 2.3.2 Satellite Retrievals

Two satellite products are used to examine the spatial distributions and trends in ambient $NH_3$. We focus on summertime values (meteorological summer defined as June, July, and August), as higher temperatures favor gas-phase $NH_3$. The European Space Agency's (ESA) Infrared Atmospheric Sounding Interferometer (IASI) provides $NH_3$ observations with pixel size of 12 km in diameter at nadir and was recently evaluated with aircraft measurements over the U.S.[219] $NH_3$ values are averages over the vertical extent. The National Aeronautics and Space Administration (NASA) Atmospheric Infrared Sounder (AIRS) provides observations with a spatial resolution of 13.5 km at nadir,[220] and $NH_3$ values are taken at 918 hPa.[221] We employ version 3.1.0 of the level 2 IASI files to examine the spatial extent of $NH_3$ in 2017, the latest Census of Agriculture. AIRS data are available earlier in the record for the AgCensus and we employ this product to examine the annual trends from 2002 to 2017. To evaluate trends, we examine every grid point in the AIRS data set for which data existed for a minimum of five years in the available time window of the USDA censuses. We employ Pearson correlation to link variability between AUs and remotely sensed $NH_3$ in 2017. We use ordinary least-squares to calculate linear fits to temporal trends and report trends as the slope of the regression line (ppb $year^{-1}$).

### 2.3.3 Surface Air Quality Data and Data Set Synthesis

We employ air quality concentration and emission data from EPA public repositories. Ammonia emissions estimates are derived from the National Emissions Inventory (NEI), available every 3 years.[185] We focus on 2017 emissions estimates, as the methodology for $NH_3$ emissions from livestock waste changed substantially between the 2014 and 2017 inventories.[222] The NEI identifies more than 50 sectors that contribute to $NH_3$ emissions. We consolidate these sectors into 7 categories and keep the agricultural subsectors of fertilizer application and livestock waste separate. Ambient concentrations of $PM_{2.5}$ mass, chemical constituents ($NH_4$, $NO_3$, $SO_4$, and OC), and precursor gases ($SO_2$ and $NO_2$) are retrieved from EPA's Air Quality System (AQS) pregenerated data files for all site and monitor locations that operated continuously from 2002 to 2017.[223] We use all reported values, including Federal Reference Methods (FRM) and Federal Equivalency Methods (FEM). Measurements flagged in the AQS as exceptional events are removed. Total organic carbon values are converted to organic matter (OM) using the standard multiplier of 1.8 to better compare to other species in terms of mass concentrations.[224] Similar to trends in animal density and satellite $NH_3$, a linear regression is used to examine trends at individual monitor locations. Trends are defined as the slope of the regression line divided by the median concentration of the study time period (2002-2017), multiplied by 100% (% $year^{-1}$).

Air quality trends are examined for both individual monitor locations and, more broadly, in regional analyses. Regions are informed by the EPA and USDA definitions. EPA commonly uses 9 U.S. Climate regions to describe $PM_{2.5}$ trends.[225] USDA uses Farm Production Expenditure Regions to examine the costs incurred running a farm, and groups states with consideration of farm output and size.[226,227] Any state listed as an "estimate" for the USDA regions was included in the respective region. Employing either the EPA or USDA definitions, each region has a minimum of 10 $PM_{2.5}$ continuous sites reporting over the study period (2002-2017) and a minimum of three speciation sites. Monitor coverage is the most

sparse for ammonium ion measurements. We have more confidence in trends of $PM_{2.5}$ mass and chemical constituents for regions where monitor density is highest (Tables A1–A4).

To more closely assess trends where both AU density and ammonia mixing ratios are relatively high and rising in the Midwest, we created a "hotspot" region for the year 2017. CAFO information from AgCensus is only available for unevenly spaced county-level designations. Consequently, we associate each AU value with the corresponding county centroid. A kernel smoother is applied to this data to obtain animal density estimates over the entire CONUS. We perform an identical smoothing technique to the IASI $NH_3$ measurements. Though higher resolutions are possible with the IASI data,[228] we apply this estimate for a consistent comparison with the spatially limited animal data. A region of high AU density is identified via a regression level set estimate (i.e., the coordinates where the estimated AU density exceeds a given value). We represent this hotspot as the boundary of the level set corresponding to the $91^{st}$ percentile of the AU density across the CONUS.

## 2.4 Results and Discussion

Spatial patterns in animal unit density at medium and large CAFOs are consistent with satellite-detected $NH_3$ concentrations over the CONUS (Figure 2.1). Ammonia emission rates from livestock vary with the animal type, population size, and farm management. Practices that mitigate air pollution emissions at farms with lower animal densities, such as sustainable application of livestock waste to fields, are less feasible at the industrial scale. For example, feedlot ammonia emissions are much higher than those for pasture-raised animals due, in part, to greater reliance on manure storage and silage.[229] Livestock waste is the predominant source of controllable ammonia in the U.S., a factor of 3 higher than all other sources combined, including fertilizer use (Figure A.1), and some fraction of fertilizer is animal manure. Summertime ammonia from IASI for 2017 indicates the highest values are

over the Midwest, Central Valley of California, Arizona, and locations in the Northwest, where 2017 county-level animal unit density derived from the AgCensus is also high (Figure 2.1A,B and Movie A1. A link to all movies is provided in Appendix A.). The ammonia spatial pattern is consistent with the animal unit density of feedlot cattle and hogs in the Midwest, dairy cows in the CA Central Valley, and cattle and dairy cows in Arizona and the Northwest (Movies A2–A4). The spatial patterns for the AU density level set derived from USDA's 2017 AgCensus and IASI-detected ammonia data for 2017 are remarkably similar (Figure 2.2). Across the CONUS for 2017, there is a significant positive correlation between remotely detected $NH_3$ and area-normalized AU density (r = 0.642). Ammonia to the east of the level set for animal unit density is consistent with prevailing easterly winds over the Midwest Plains, and suggests application of wind adjustments[228] at the surface and aloft could improve correlation.

Rising emissions as a consequence of increasing animal consolidation are a plausible explanation for the temporal trends in rising ammonia mixing ratios. Over the past two decades, raw animal numbers rose approximately 6%, while the number of CAFOs rose more quickly, approximately 16% over the last 10 years (Figure A2). Farm consolidation and greater county-level animal density are found for all analyzed animal categories, including cattle, dairy cows, hogs, broiler chickens, and egg-laying hens from 2002 to 2017 (Movies A1–A6). AIRS ammonia data from 2002 to 2017 indicates an increasing atmospheric $NH_3$ burden across the CONUS, with higher rates of increase in the Midwest and CA Central Valley (Figure 2.1D). This pattern is similar to the growth in the number of CAFOs and increasing deposition of reduced nitrogen in agricultural areas.[196,198,230] Evaluation of EPA emission estimates during intensive observation periods (IOPs) and with IASI data generally find a low bias for ambient ammonia in rural Midwest regions.[231–233] This is consistent with the low bias in estimates of CAFO-associated animals in publicly available Federal archives. Recent efforts by environmental interest groups (EIGs) and some States have improved CAFO accounting. However, recent application of a deep-learning algorithm to satellite data detects

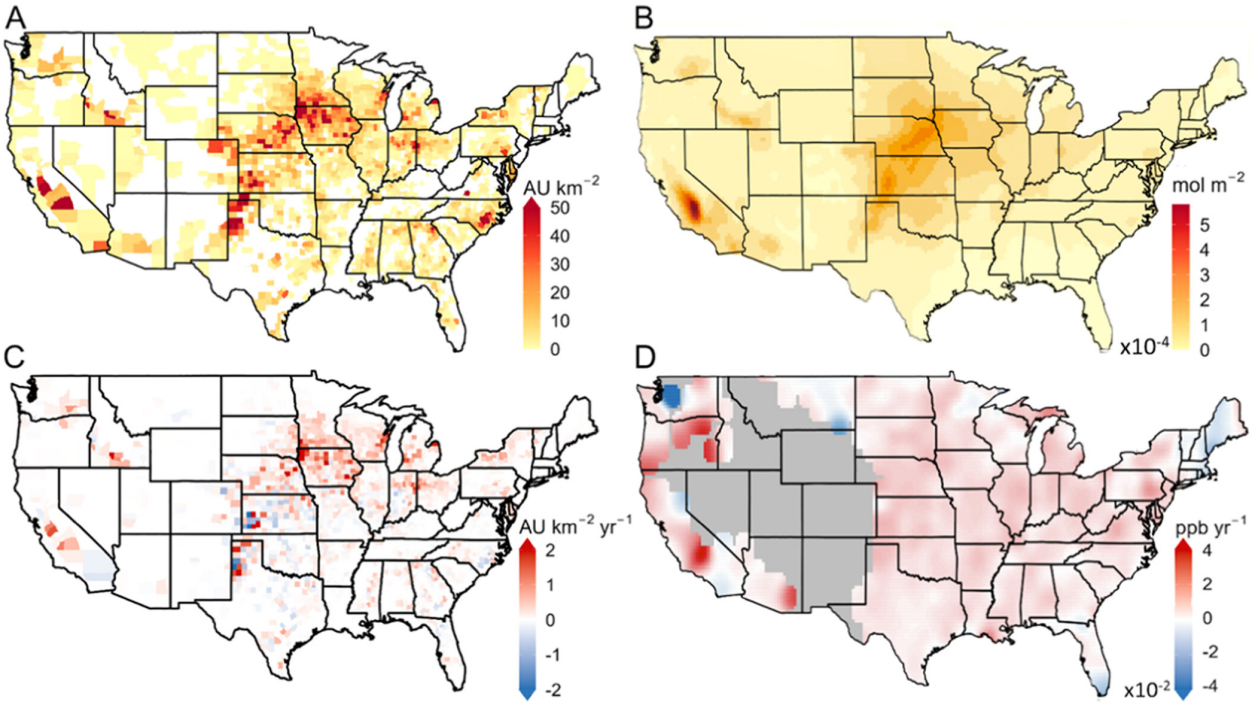


Figure 2.1: Spatial distributions and trends of animal unit density and ammonia over the CONUS. (A) Animal units (1000 lb. of live weight) at medium- and large-sized CAFOs normalized by county area for the year 2017. (B) Average summertime 2017 $NH_3$ mixing ratios from the ESA IASI product. (C) Change in county-level AU density at medium- and large-sized CAFOs from 2002 to 2017. (D) Change in summertime $NH_3$ mixing ratio from NASA AIRS product from 2002 to 2017.

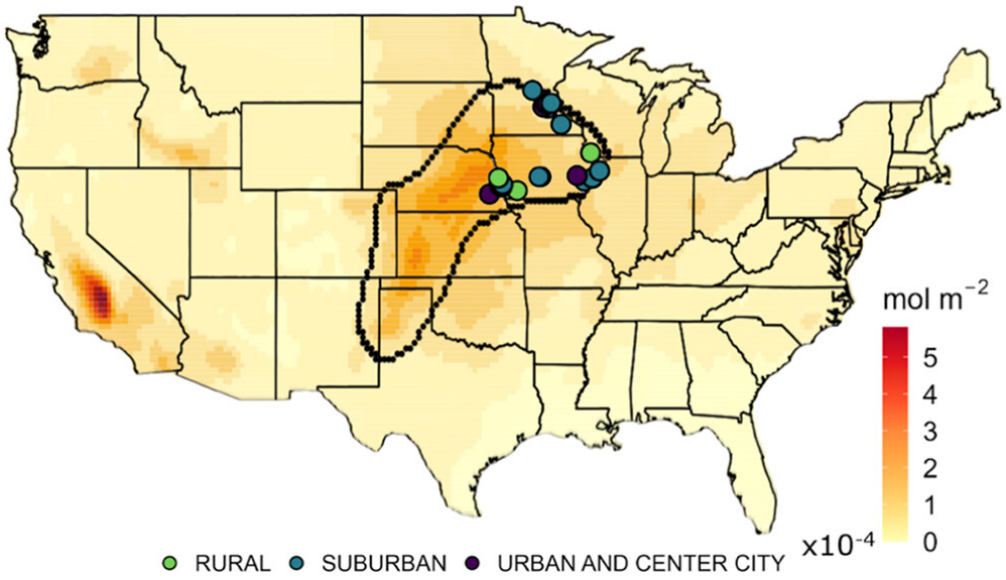


Figure 2.2: Relationship between remotely detected $NH_3$ and EPA surface $PM_{2.5}$ monitor coverage within the "hotspot" region of highest animal unit density.

15% more poultry CAFOs in North Carolina than recorded by EIGs.[234]

Accounting for animal numbers normalized by county area implicitly accounts for some degree of industrial-scale management practices that affect ammonia emissions. For example, CAFO management relies on increased use of silage and storage that results in higher emissions of air pollutants.[235,236] Measured ammonia emission rates from anaerobic lagoons are substantial,[236,237] and large dairy and swine CAFOs preferentially employ anaerobic lagoons for sanitary waste management, particularly in the Midwest Plains[236] where satellites detect ammonia hotspots. In air quality simulations, Hu et al. find that summertime ammonia observations over the Midwest Plains region are up to a factor of 4 higher than model predictions.[231] The livestock ammonia emissions employed in those air quality simulations are developed from EPA's NEI.[222] Evaluation of NEI agricultural emissions finds the highest predictive error for ammonia (90%) is for anaerobic waste lagoons.[237] In general, ambient $NH_3$ is most abundant over rural agricultural land that includes both cropland and CAFOs (Figure A3), and where surface air quality monitoring locations are thinly distributed (Figure 2.2).

Surface monitoring sites are sparsely located in rural agricultural regions, and air quality is more difficult to quantitatively assess. In and near the geographic areas with the largest increases in $NH_3$ and highest animal unit density as identified above, trends in $PM_{2.5}$ mass appear to lag behind the national average (Figure 2.3). Approximately one-third of all EPA air quality sites are located in rural settings, and approximately 10% are in agricultural locations (Figure A4). The strongest declines in $PM_{2.5}$ mass are generally observed east of the Mississippi River, particularly in urban areas and downwind of large industrial sources of the Southeast and Ohio Valley, in addition to localized monitoring sites in California (Figure 2.3). In areas where ammonia mixing ratios are rising and animal unit density is high, other air quality metrics are stagnant or also getting worse. Some specific Midwest surface sites document rising mixing ratios of $SO_2$ and $NO_2$ (Figures A5 and A6). Nonlinearities in the gas-phase oxidation of $SO_2$ and $NO_2$, the subsequent gas-to-particle partitioning, aerosol pH, and aerosol liquid water content complicate relationships between $PM_{2.5}$ and precursor emissions.[238] Within the boundaries of the animal unit level set (Figure 2.2), there are 23 surface sites active during the study period. Only three sites are classified as rural location settings. The available monitors are primarily located in the northeast corner of the geographic area, far away from satellite-detected ammonia hotspots, and are insufficient to properly assess air quality trends fully representative of the entire region.

Conventional federal-level frameworks and modeling tools, such as air quality network sites, their regional definitions, and emission estimates used in assessments, are not ideal to quantify air pollution amount or chemical composition in areas where CAFO emissions are abundant and the air pollution burden is rising. For example, in national and regional assessments, the EPA documents improving surface air quality. However, those assessments have an implicit bias that largely excludes agricultural locations, even for predominantly rural areas. For example, using EPA-defined climate regions, the largest decreases in $PM_{2.5}$ mass from 2002 to 2017 are due to sulfate and occur in the Ohio Valley (66 sites, -44%), Upper Midwest (48 sites, -39%), Southeast (60 sites, -39%), and Northeast (83 sites, -35%) (Figure 2.4A,

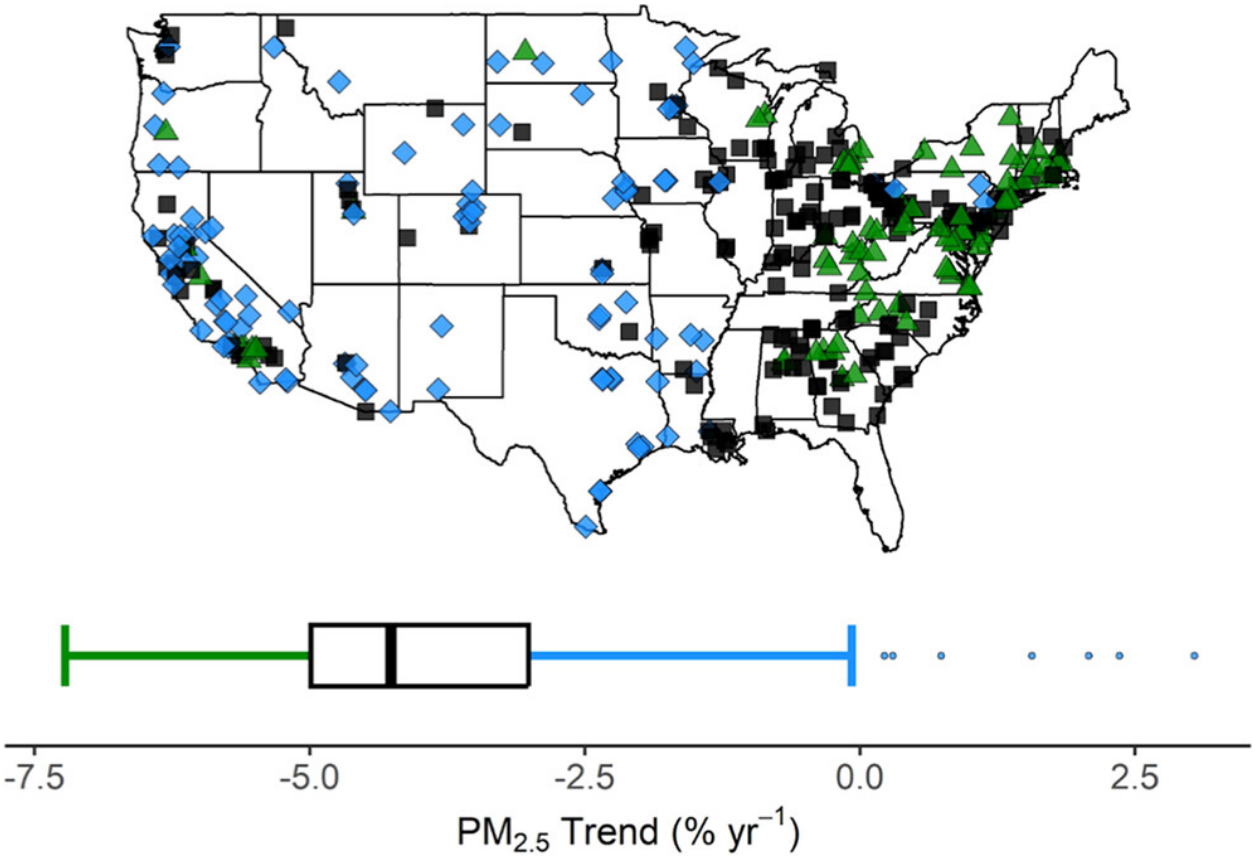


Figure 2.3: Trends in EPA measured $PM_{2.5}$. Each point represents an EPA $PM_{2.5}$ monitor active over the study period (2002–2017), and is color-coded according to the quartiles of the overall trend distribution, where black points represent trends within the interquartile range, blue points represent trends above the third quartile (less decrease than average), and green points represent trends below the first quartile (greater decrease than average).

Tables A1 and A3). Employing USDA Farm Production Expenditure regions, the largest $PM_{2.5}$ mass concentration decreases (94 sites, -43%) occur in the Midwest region (Figure 2.4B, Tables A2 and A4) and are due to sulfate. This finding reflects many earlier findings that note the success of acid rain rules that reduce $SO_2$ emissions and sulfate formation and is consistent with a primarily urban distribution of Eastern and Midwest monitoring sites (e.g., Detroit, Minneapolis). Such distribution hinders accurate assessment of air quality for the Midwest and other regions that are largely rural and agricultural.

Air pollution policy in the U.S. is primarily focused on large point sources, mobile emissions, and sources of toxic pollutants in highly populated areas. Declines in anthropogenic emissions and improved urban air quality demonstrate the successful implementation of this policy. Yet, most of the U.S. land area is not urban and approximately half is agricultural.[239] Air quality studies related to health and environmental justice typically focus on urban and suburban areas.[240–242] Rural $PM_{2.5}$ is toxic[243] and impacts human and livestock health.[244] Neglect of agricultural regions in air quality analyses may be inconsistent with national goals for environmental equity.[245] The agricultural sector relies heavily on a vulnerable immigrant workforce.[246] In one study, dairy workers in California's Central Valley, who identify primarily as Hispanic/Latino, experience decreased lung function due to particulate matter exposure in relation to work shift.[147] As air quality generally improves across the U.S., frontline communities in agricultural areas may be left behind, and a relative dearth of data prevents accurate assessment.

Strategies to reduce agricultural air pollution and its impacts are widely discussed and debated. Because a significant proportion of U.S. meat production is for export, mitigation through changes in trade strategies and production-based abatement (e.g., more efficient manure management and fertilizer use, increasing free-range farming practices) are proposed.[188,194,247] Consumer-side actions are also predicted to have a substantial influence over agricultural ammonia. Reduction of animal product consumption, red meat especially, and

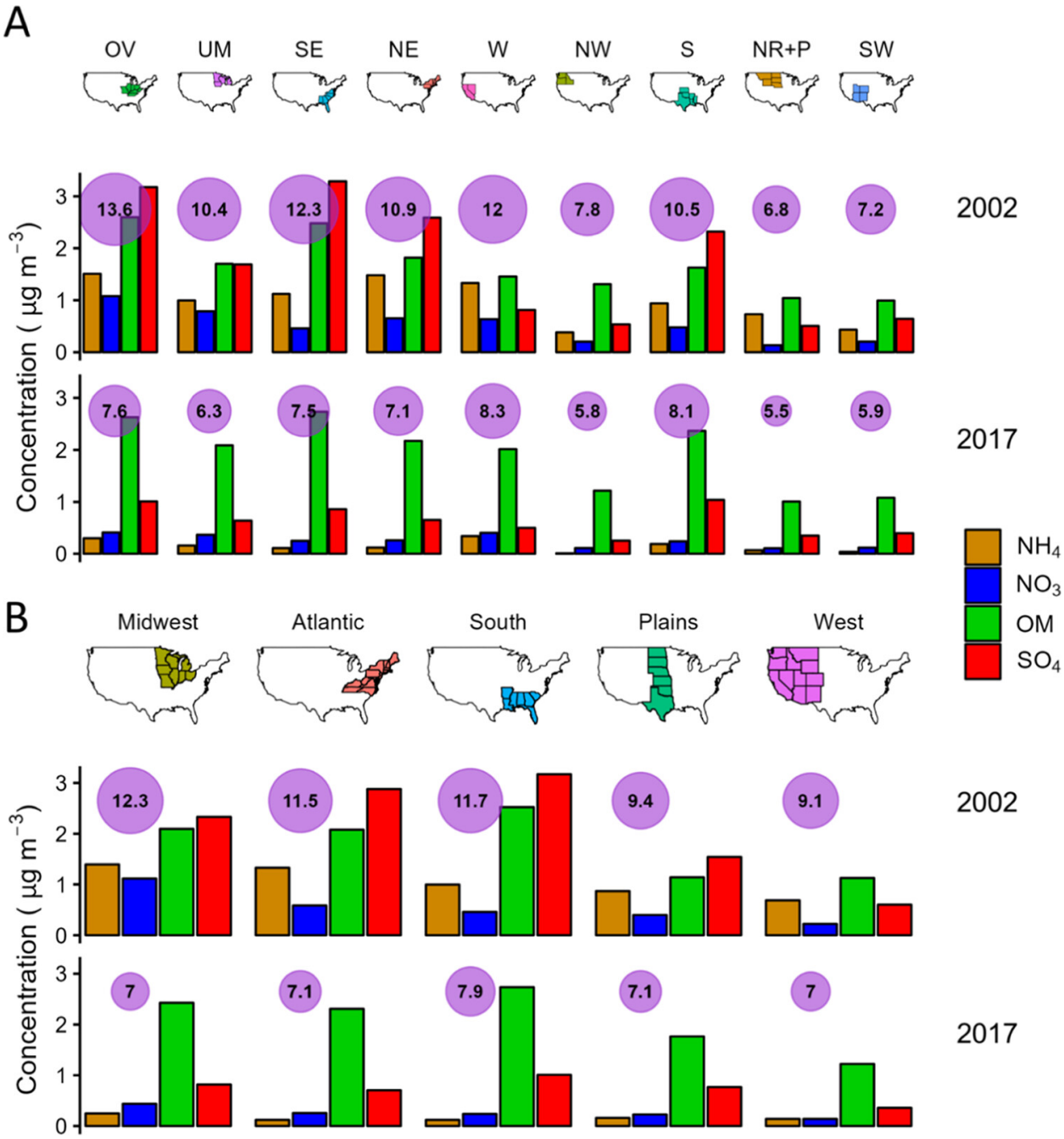


Figure 2.4: Trends in $PM_{2.5}$ mass and speciation across U.S. EPA climate regions (A) and USDA Farm production regions (B). OV refers to the Ohio Valley, UM refers to the Upper Midwest, SE refers to the Southeast, NE refers to the Northeast, W refers to the West, NW refers to the Northwest, S refers to the South, NR+P refers to the Northern Rockies and Plains, and SW refers to the Southwest. Each column represents a different EPA- or USDA-defined region, mapped in row 1. Row 2 represents average concentrations for each region in 2002, and row 3 shows the same for 2017. Purple circles display the average $PM_{2.5}$ mass for each year and are sized accordingly. Bar charts show annual average concentrations of ammonium (orange), nitrate (blue), organic matter (green), and sulfate (red), measured through EPA CSN.

utilization of more nitrogen-efficient protein sources reduce predictions of food-production-related $PM_{2.5}$ and subsequent associated mortality and societal costs.[194,199,247] Research suggests controls on agricultural ammonia emissions could be a cost-effective strategy to improve air quality and safeguard human health.[175,194,248] For example, wintertime $NH_3$ control strategies that focus on improved farm animal housing and manure management are predicted to be more cost-effective for reducing $PM_{2.5}$ mass than existing control strategies for $SO_2$ or $NO_x$.[175] However, quantitative assessment of the impacts of such strategies would be difficult given the poor spatiotemporal coverage in air quality networks at rural locations in addition to the lack of full transparency in animal data. There is precedent for satellite tools to correct ammonia seasonality in inventory estimates from the land sector within EPA.[249] Air quality policies reliant on regulation-defined surface measurements may need to evolve to incorporate advanced tools.

# Chapter 3

# Aerosol Liquid Water Predictions: Sensitivities and Application towards Aerosol Optical Properties, Radiative Forcing, and Ambient Chemistry

This chapter contains unpublished research by the author, and includes contents within Application 1, Application 2, and relevant Methods that are reproduced or adapted with permission from the publications listed below. In both publications, the author provided aerosol liquid water estimates and contributed to analyses pertaining to aerosol chemical composition and liquid water content.

1. Madison M. Flesch, Amy E. Christiansen, Alyssa M. Burns, Virendra P. Ghate, and Annmarie G. Carlton. ACS Earth and Space Chemistry, **2022**. 6 (12), 2910-2918. DOI: 10.1021/acsearthspacechem.2c00207. Copyright © The Authors. Published by American Chemical Society. This publication is licensed under CC-BY 4.0.

2. Virendra P. Ghate, Annmarie G. Carlton, Thomas Surleta, and Alyssa M. Burns. Journal of Climate, **2022**. 35, 7725–7737. DOI: 10.1175/jcli-d-22-0073.1. Copyright © The Authors. Published by the American Meteorological Society. This publication is licensed under CC-BY 4.0.

## 3.1 Abstract

Aerosol liquid water (ALW) is an important and ubiquitous component of ambient aerosol mass. Despite the well-established effects of ALW towards aerosol optical properties, radiative forcing, and secondary chemistry, ALW is difficult to measure directly and is rarely captured in field or laboratory studies. Instead, ALW can be estimated with thermodynamic modeling, using surface measurements of aerosol chemical composition paired with meteorological variables such as relative humidity and temperature. While such ALW estimates are essential towards understanding the air quality- and climate-relevant properties of ambient aerosol, uncertainties in predictions are difficult to evaluate. Not all chemical constituents that affect particle hygroscopicity such as dust ions and ammonium are routinely measured. Despite frequent observations, measurements of particle chemical composition and meteorological variables are often not co-located. This study systematically investigates meteorological and chemical uncertainties in ALW predictions. First, the differences in ALW estimates made with two meteorological reanalysis datasets, the North American Regional Reanalysis (NARR), and the European Centre for Medium-range Weather Forecasts (ECMWF) ERA5 are evaluated, in addition to the impacts of dust species and ammonium. Significant differences in ALW mass concentrations are observed, and the magnitude of these differences varies across humid and dry regions. Trends in ALW across CONUS with different data prod-

ucts are also discussed. Lastly, the impact of ALW towards different atmospheric chemistry applications is assessed. ALW offers a plausible explanation towards differences in aerosol optical depth and size distributions on clear and cloudy sky days at an agricultural location in Illinois. Similarly, wet aerosol mass helps explain surface temperature modulation in the Southeast US "warming hole" region.

## 3.2 Introduction

Ambient aerosols are well established as health-relevant pollutants and climate forcers. Despite its importance, aerosols contribute to the largest uncertainties in climate projections.[148,152] These uncertainties are due, in part, to the complex feedbacks between aerosols, clouds, and other meteorological variables. Uncertainties also stem from measurement limitations towards the ambient state of aerosol. Aerosol particles exist with a wide variety of chemical compositions, phase states, and other properties which, across variable chemical and climatological environments, may exhibit very different trends and biases. For example, particle density is highly variable under different meteorological conditions and chemical compositions,[250] which in turn affects other aerosol properties such as aerodynamic diameter.

Liquid water is a ubiquitous component of ambient aerosol. Even aerosols in some arid locations are expected to have considerable aerosol liquid water (ALW) mass concentrations due to particle chemical composition.[39] ALW is a function of aerosol size-number distributions, chemical composition and meteorological variables of temperature and relative humidity (RH). The majority of ALW is associated with hygroscopic inorganic mass, which changes in space and time.[56,251,252] Contribution to ALW from organic compounds is poorly constrained[47,253,254] and this is increasingly problematic as organic mass becomes a more dominant contributor to aerosol loading across the contiguous US (CONUS).[24,25] Mass concentrations of ALW are predicted to be highest in humid locations like the Eastern US,

and lowest in hot and dry regions such as the Southwest.[56]

ALW affects both the physical and chemical properties of aerosol. Impaired visibility on polluted, high relative humidity (RH) days is primarily driven by the hygroscopic growth of aerosols.[49,50] Changes in particulate water content will change the light scattering behavior of aerosol, which affects both visibility and the climate-relevant properties of aerosol. For example, increases in ALW can alter the amount of light an aerosol scatters, which will affect both radiative forcing and other properties like aerosol optical depth (AOD).[46,255] Similarly, ALW content will change various interrelated chemical properties of aerosol. ALW serves as a polar medium for which water-soluble gases can partition into, as well as a medium for further condensed-phase reactions that can form secondary organic aerosol (SOA). Increased ALW content may also change aerosol viscosity and phase state, promoting more liquid particles that may undergo secondary chemical reactions more quickly than semi-solid or solid aerosol mass.[52,54,118]

Despite its importance, ambient ALW mass is poorly understood relative to other aerosol components. For example, particle concentrations of non-volatile species such as sulfate are well captured in regulatory filter-based measurements. These measurements neglect ambient ALW, as filters are left to equilibriate under laboratory relative humidity conditions.[256,257] Some measurement techniques exist to estimate ALW, such as humidified tandem differential mobility analyzers (HTDMAs).[63,258,259] These techniques generally rely on optical or physical size measurements under differing RH levels, by which hygroscopic growth factors can be developed and ALW mass concentrations can be calculated. While these techniques provide some information towards ambient ALW content, the drying required to determine growth factors perturbs the ambient state of aerosol. Semi-volatile aerosol components that affect ALW mass, such as surfactants and/or hygroscopic chemical species, may be lost during such sampling procedures[61,64,260,261]. Direct and facile measurements of ALW remain elusive.

Various different models are employed to calculate ALW from available surface measure-

ments, such as ISORROPIA-II and e-AIM.[124,262] These models operate by determining thermodynamic equilibrium conditions, which can then be used to understand different aerosol properties that are difficult to measure in situ, such as ALW content or aerosol pH.[65,263,264] To determine equilibrium conditions, these methods rely upon pairing relevant meteorological information with measurements or predictions of key pollutants. Here, focus is on ISORROPIA, as it is computationally efficient and is commonly utilized in previous studies and air quality models.[114,262,265] The chemical variables employed may be from the gas-phase or the aerosol phase, such as from routine fine particle ($PM_{2.5}$) measurements. A combination of gaseous and aerosol inputs may also be employed; however, it is rare that these measurements are co-located in space and time outside of episodic field campaigns.[263]

Similarly, measurements of aerosol chemical composition are not often co-located in space and time with measurements of meteorological conditions. For example, neither the EPA's chemical speciation network (CSN) nor the interagency monitoring of protected visual environments (IMPROVE) network measure temperature and relative humidity regularly, despite their being a primary data source for long-term investigations of particle composition across the contiguous US (CONUS). Reanalysis datasets such as the North American Regional Reanalysis (NARR) and the European Centre for Medium-range Weather Forecast's (ECMWF) ERA5 are commonly used to fill gaps within observational datasets of meteorological variables.[266–268] These models utilize prognostic met predictions in retrospective simulations that employ various data assimilation techniques to nudge predictions towards observed state variables (e.g., temperature, winds, etc.). While skill for numerical weather prediction continues to improve, even reanalysis datasets exhibit biases.[269,270] The meteorological variables important for ALW mass calculations vary among reanalysis products, such as temperature, relative humidity, and broader synoptic and global scale patterns such as ENSO-forced weather variations.[269,271,272] The exact biases between models in the context of ALW predictions have not been evaluated.

The chemical composition and hygroscopicity of condensed-phase species will determine ALW content. In air quality model applications, where gas and aqueous phase concentrations can be simulated simultaneously, thermodynamic models are generally run in the forward or "closed" mode, as the total (particle + gas) concentrations are assumed to be known.[273] Because these time-resolved measurements of both phases is rarely available in the field, most ambient estimates of ALW employ the reverse or "open" problem, where only the precursor concentrations of aerosol-phase species are required to solve.[114,263,274] Sulfate ($SO_4^{2-}$) and nitrate ($NO_3^-$) are the primary hygroscopic species present in ambient aerosol and are nearly always included in these calculations.[42,275] Other common aerosol components, like sodium ($Na^+$), chloride ($Cl^-$), and other crustal species such as potassium ($K^+$), magnesium ($Mg^{2+}$), and calcium ($Ca^{2+}$) are rarely included in these predictions despite computational capabilities. These species are often left out because they are considered a minor fraction of fine aerosol in most CONUS regions;[65,276] however, fine dust concentrations can be substantial in arid regions like the Southwest U.S.,[277] and the exact impact of these ions towards ALW predictions is unclear.[46] Similarly, gaseous ammonia and ammonium ion measurements are scarce in routine regulatory networks that are often employed for determining ambient ALW across the CONUS.

Despite the importance of ALW towards ambient aerosol mass and physicochemical properties, it is often understudied in comparison to other properties toward aerosol radiative impacts and secondary aerosol formation. For example, aerosol constituents such as brown and black carbon are heavily investigated for their absorptive properties.[278] Semi-volatile condensation is the most commonly investigated pathway of SOA formation, yet aqueous processing is thought to be a dominant SOA formation pathway in humid regions.[9,56,59] Improving understanding of ALW and aerosol physicochemical state in the ambient atmosphere should help resolve aerosol uncertainties in climate projections. In this work, key uncertainties in ISORROPIA-derived ALW predictions are explored through systematic investigation of the meteorological and chemical inputs employed. The impact of these sensitivities towards

long-term trends in ALW mass is also evaluated. Predictions of ALW both at the surface and aloft are then applied to two case studies regarding aerosol optical depth, Ångström exponent-derived size, and radiative forcing. The results of this study inform appropriate calculations of ALW from surface regulatory networks, and demonstrate the importance of ALW consideration when examining the health and climatic impacts of ambient aerosol burden.

## 3.3 Methods

The methodology described here will focus on the methods used to make predictions of aerosol liquid water and understand associated uncertainties. More in-depth information pertaining to the methods used for related application analyses described in the Results and Discussion section can be found in their respective publications.[72,279] All data sources and software utilized for ALW predictions and sensitivities are publicly accessible.[262,267,268,280,281] For seasonal analyses, winter is defined as December-February, spring as March-May, summer as June-August, and fall as September-November. Various different regions and site locations in the CONUS were examined for this work to assess sensitivities and results across different chemical climatologies (Figure 3.1).

### 3.3.1 Data Sources

A summary of the data sources utilized for this analysis is displayed in Table B.1. Meteorological data necessary for ALW predictions are sourced from reanalysis databases. Here, two commonly used reanalyses are employed: the North American Regional Reanalysis (NARR) product provided by National Centers for Environmental Prediction (NCEP)[268] and the ERA5 product provided by the European Centre for Medium-range Weather Fore-

Figure 3.1: Regions and sites used for ALW sensitivity analysis and applications. The four IMPROVE/CSN colocated sites (square markers) are used for ammonium sensitivities. The Bondville location (green marker) is used for Application 1. The four SEUS sites (light and dark blue markers) are used for meteorology and dust sensitivities, as well as Application 2. Due to data limitations with urban sites in this region, just the rural SEUS sites (light blue markers) are considered for some analyses, including Application 2. The GB region (pink markers) is used for meteorology and dust sensitivities.

casts (ECMWF).[267] NARR has been employed for observational estimates of ALW in prior studies.[114,265] The NARR and ERA5 products have similar spatial resolution (32 vs 31 km resolution respectively); however, ERA5 has greater vertical resolution (137 pressure levels) versus NARR (29 levels). Temporal resolution is also finer for ERA5 (hourly) versus NARR (every 3 hours). Both products have been thoroughly evaluated and compared against other reanalysis datasets as well as surface meteorological observations, with the ERA5 generally outperforming NARR when predicting variables at the surface and aloft.[271,282,283] The NARR and ERA5 data used here is at a 0.3° and 0.2° spatial resolution respectively, paired in space and time with all IMPROVE sites active from 1988-2014 (NARR) and 1988-2019 (ERA5). Daily retrievals are available for NARR, and hourly values are available for ERA5. Temperature is available directly. Relative humidity is calculated via inputs of specific humidity (NARR) or dewpoint temperature (ERA5) paired with temperature.[284] ERA5 RH when calculated with specific humidity is nearly identical to RH calculated from dewpoint in the Southeast US (SEUS, Figure B.1).

Particle mass and speciation is primarily sourced from IMPROVE network surface sites, which provides long-term (1988-present) measurements primarily at rural national parks locations. Here, we utilize IMPROVE measurements from network origin through 2019. IMPROVE surface $PM_{2.5}$ mass concentrations of sulfate, nitrate, organic carbon (OC), sea salt, and crustal species are available as 24-hour integrated samples every 3 days. Sulfate and nitrate concentrations are determined using ion chromatography, OC fractions via thermal/optical reflectance, and crustal and sea salt species are determined by X-ray fluorescence (XRF). Measurements of sulfate and nitrate are more robust compared to other inorganic species; many days do not have quality-assured (i.e., above the detection limit and instrumental uncertainty) measurements of other ionic species. While sea salt species (sodium and chloride) are generally classified separately from other elemental ionic species (ex: calcium, potassium, and magnesium), for the purposes of sensitivity analysis, we consider both sodium and chloride to be "dust ions" with other crustal species. We make this characterization be-

cause sodium and chloride are experimentally determined via the same methods as other crustal species, and therefore suffer from the same limitations in measurement availability. Similarly, chloride has often been neglected in prior estimates of ALW using regulatory surface networks, and thus represents a similar uncertainty in overall calculations as other ionic species.[114,265] We assume all XRF species are present as fully water-soluble concentrations in our particle water estimates, as described below, although these species may be part of non-water-soluble matrices such as silicates and aggregate dust particles.

Chloride measurements from IMPROVE face additional uncertainties throughout mid-2007 to early 2011 due to high background concentrations within the filter used.[285] We suspect a negative bias on chloride concentrations reported during this time period. Similarly, methodology limitations produced substantial uncertainties for sodium concentrations in sea-salt dominant aerosol samples prior to 2011.[286] We note that further uncertainties may exist in IMPROVE gravimetric $PM_{2.5}$ prior to 2011 due to unregulated humidity conditions in the laboratory.[287] Additional biases may exist in gravimetric measurements due to the volatilization of components like ammonium nitrate from teflon filters.[173] Despite these limitations, we use the IMPROVE-reported values for these variables where available. All available valid values are used. Reported values below the method detection limit (MDL) are retained in the analysis if the value plus uncertainty is above the MDL.[58]

While the IMPROVE network provides robust measurements of species such as sulfate, nitrate, and dust ions, ammonium is not regularly measured. Ammonium is, however, regularly measured at EPA's Chemical Speciation Network (CSN). Where the IMPROVE network focuses on rural locations, CSN primarily focuses on urban and/or highly populated regions. Despite this mismatch in network objectives, a select number of locations have both IMPROVE and CSN particle speciation measurements on-site, primarily for the purpose of quality assurance between networks.[70,71] Both networks lack sufficient monitor coverage in key agricultural and rural regions with expected high ammonia and ammonium pollution.[288]

We utilize CSN $PM_{2.5}$ speciation, including $NH_4$, with the methods described above at 4 co-located CSN/IMPROVE sites to assess ammonium impacts towards ALW predictions. Only the years 2016-2019 were used to due monitor location changes.[71]

In Application 1, NASA AERONET data is used to evaluate the impact of ALW on aerosol optical depth (AOD) and Ångström exponent-derived aerosol size on clear and cloudy sky days. All surface measurements here are retrieved from a rural IMPROVE/AERONET co-located site in Bondville, Illinois (40° 05' 20" N, 88° 37' 33" W). All available surface measurements between January 2010 and December 2019 are utilized. AERONET public archives provide surface-based estimates of columnar AOD at 440, 500, 675, and 870 nm and Ångström exponents estimated for the 440–870 nm spectral range at Level 1.0 and Level 2.0 quality levels.[289] A novel cloud determination method based on the AERONET QA cloud screening algorithm assigns surface measurements into two bins, "predominantly cloudy day" or "predominantly clear sky day".[72] Hereafter, these bins will just be referred to as "cloudy sky" or "clear sky" for brevity. The Mann-Whitney U test, a nonparametric statistical test is used to determine significance of results ($p < 0.05$).

Application 2 utilizes a variety of observations to resolve the impact of aerosols and meteorology towards surface temperature modulation in the SEUS from January 2000 to December 2019. The SEUS study area is bounded by the northwest corner at 36°N, 90°W and the southeast corner at 32°N, 84°W (Figure 3.10). We focus on the rural SEUS sites shown in Figure 3.1 because the urban sites (BIRM and ATLA) were not operational over the entire two decades. As most of the meteorological, cloud, aerosol, and land surface properties in the region exhibit a distinct annual cycle, changes within different seasons are explored. In addition, the differences in all the monthly data within the two decades ("All") are also examined to understand the seasons most impacting the annual means that are usually used in studies focused on long-term statistics. Statistical significance is determined at the 95% confidence level assuming a two-tailed Gaussian distribution.

The Goddard Institute of Space Studies surface temperature analysis version 4 (GISTEMP) data are used to examine monthly surface air temperature anomalies from the climatological mean.[290] Monthly averaged cloud and aerosol properties as observed by the Moderate Resolution Imaging Spectroradiometer (MODIS) onboard the Terra satellite are used in this work.[113,291] We utilize the aerosol properties as derived from the Deep Blue algorithm[292] as we mainly focus on aerosols that influence the visible spectral region, rather than other aerosols that influence the near-infrared or infrared region (e.g., dust). Hence, the MODIS-derived AOD and the single scattering albedo (SSA) at 470 nm along with the calculated Ångström exponent (412–470 nm) are analyzed in this work. The integrated water vapor (IWV) values are used as derived from the near-infrared algorithm, and thus correspond to the daytime values during cloud-free periods.[293] The cloud liquid water path (LWP) as derived by the visible/near-infrared algorithm, as derived through its relationship with cloud optical thickness and drop effective radius are used.[294] The MODIS Terra data are available at a uniform 1° spatial resolution on monthly time scales beginning from February 2000 and are averaged within the study area.

The top of the atmosphere (TOA) shortwave and longwave fluxes during cloudy and clear-sky (cloud-free) periods as reported by the Clouds and the Earth's Radiant Energy System (CERES) project are utilized. The CERES Energy Balanced and Filled fluxes utilize the MODIS observed cloud properties and other variables as reported by Loeb et al. (2018)[295] and Kato et al. (2018)[296] and are available at 1° spatial and monthly temporal resolution.

### 3.3.2 ALW Observational Estimates

All ALW predictions are made using ISORROPIAv2.1, a computationally efficient thermodynamic model commonly employed in air quality models.[262] Comparison of ISORROPIA with more explicit models such as E-AIM for aerosol pH predictions shows similar results.[263,264] In

ISORROPIA, inputs of chemical species are used to determine the ratios of sulfate, sodium, and other crustal species for each observation. These ratios are used to determine the major species present within the system. This determination, with temperature and RH, is used to determine the appropriate set of equilibrium equations to solve. After mass conservation, electroneutrality, water activity equations and activity coefficients are calculated, the thermodynamic equilibrium concentrations are attained as an output, including mass concentrations of liquid water.[262]

We assume a well mixed boundary layer and metastable particles (i.e, particles are always assumed to be liquid, with no solid precipitation), and run in the reverse, open-system direction because only particulate chemical inputs are available. The approach introduces uncertainties; for example, forward-mode predictions are recommended over reverse mode for aerosol pH predictions but are insensitive to different phase-state assumptions (i.e., stable vs metastable).[263,297] To investigate uncertainties in the meteorological reanalysis datasets, a "base case" simulation is run for all IMPROVE sites with both meteorological models (NARR: 1988-2014, ERA5: 1988-2019) using just sulfate and nitrate inputs. Prior studies employ these or similar conditions because these are the most hygroscopic inorganic constituents of aerosol mass and are often the most abundant.[42,275,298] Only the ERA5 dataset is used to examine dust ion and ammonium sensitivities in order to isolate chemical uncertainties from those due to meteorology. To examine the effects of both meteorology and dust ions, two different regions are examined: the great basin (GB), an arid region and the total/rural SEUS, a humid region (Figure 3.1).

Integrated ALW predictions are often employed to more robustly compare surface-based measurements to column-based retrievals such as AOD.[265,276] Integrated ALW is often referred to as the Aerosol Water Path (AWP). Prior work has shown that the boundary layer is well-mixed in regions like the SEUS.[299] Likewise, CALIPSO results indicate that most aerosol scattering occurs within the planetary boundary layer (PBL), which adds validity to

this approach for AOD comparisons.[265] In this work, AWP is only investigated for the rural SEUS warming hole region (Figure 3.1). Surface chemical measurements are extrapolated through the boundary layer with vertically resolved meteorological inputs of temperature and relative humidity to determine ALW mass concentrations at all pressure levels below the PBL. Similarly, these columnar ALW mass concentrations can be utilized to understand properties such as aloft extinction.[276]

Trends in ALW are investigated using daily averages, matching IMPROVE network sampling frequency, of ALW and other chemical components are used at all continuous sites from 2005-2019. This time period was selected as spatial coverage of the IMPROVE network greatly improved between 2000-2005. Only ERA5 meteorology is used for this analysis. An iterated reweighted least squares (IWLS) regression is used to determine trends. Unlike traditional ordinary least squares (OLS) regression, IWLS is robust to outlier influences and is more suitable for variable environmental data.[300] Outliers in chemical data are relatively scarce here; however, extreme values in ALW observational estimates confound OLS regression methods. Trends are defined as the slope of the regression line divided by the median concentration of the study time period, multiplied by 100% (% year$^{-1}$).

For Application 1, organic ALW predictions are also considered following the methodology described in Christiansen et al 2019.[276] Organic carbon (OC) fractions, available from IMPROVE, are converted to organic mass (OM) using seasonal and site-specific calculated OM/OC ratios.[58,301] Key uncertainties in organic hygroscopicity affect these predictions, and the inclusion of organic ALW does not change the overall trends or conclusions determined here.[72] Due to this, and because organic ALW is most often a minor contributor to aerosol mass compared to inorganic-associated ALW,[275,276,302] organic ALW is not considered in other analyses.

## 3.4 Results and Discussion

### 3.4.1 ALW Sensitivities

ALW predicted with different reanalysis datasets exhibit statistically significant differences. ISORROPIA simulations generally predict larger mass concentrations of surface-level ALW in the rural SEUS using NARR than when using ERA5 (Figure 3.2). This discrepancy becomes more apparent when examining AWP through the vertical column, where the median AWP predicted by NARR is nearly 50% higher than ERA5. Surface temperature predicted by NARR in this region is slightly elevated compared to ERA5 (approximately 0.6% higher on average), though the variables are well correlated with an $R^2 = 0.98$ (Figure B.2). Comparison of RH shows poor correlation between NARR and ERA5 in this region ($R^2$=0.42). Similar to temperature, NARR routinely predicts a higher PBL than ERA5 (Figure B.3). All together, these differences produce a positive bias in NARR predicted water relative to ERA5 in the SEUS.

Biases in renalysis meteorology may cause different effects in different regions of the CONUS. Figure 3.3 shows the difference between NARR and ERA5 predicted surface-level ALW in 2014. Positive biases are noted in eastern and northern regions, where NARR predicts a higher yearly-average ALW compared to ERA5. In contrast, NARR appears to underpredict surface-level ALW across the southwest. Comparison of NARR and ERA5 outputs for a more arid region, GB, helps explain this trend (Figure B.2). Similar to the SEUS, NARR overpredicts temperature, though the magnitude of this difference is much larger for GB (approx. 5%). Calculated RH, on the other hand, is generally lower for NARR relative to ERA5, in part due to the routine overprediction of air temperature. As a result, predicted ALW is generally lower for NARR than ERA5 in more arid regions. We note that the metastable assumption is used for all ALW calculations provided here, which may be less valid in locations where RH is routinely below the deliquescence RH.[262] The deliquescence

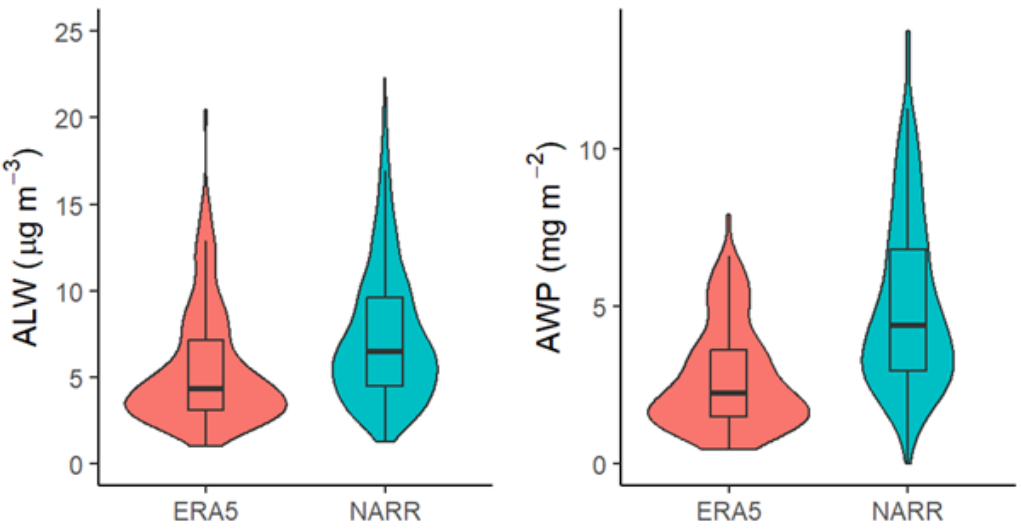


Figure 3.2: Comparison between reanalysis datasets for surface-level monthly average ALW and AWP for the rural SEUS region (2000-2014). NARR significantly overestimates both ALW and AWP in comparison to ERA5 (p-values $< 0.05$ via Mann-Whitney U test). Only sulfate and nitrate were used as chemical inputs for water calculations.

relative humidity for aerosol of mixed composition is often in the range of 20-70%; however the hysteresis of efflorescence makes it difficult to determine if aerosol exists in a mixed phase state or supersaturated state.[303,304] In the GB arid region, monthly average RH profiles are all above 20%. While dry particles are likely to occur under low RH conditions, it is difficult to assess these effects on longer time resolutions, such as the one-in-three day resolution of IMPROVE chemical data.

Together, these differences show that meteorological inputs have a substantial effect towards the prediction of ambient ALW. The NARR data assimilation protocol is less advanced than ERA5 and other more contemporary data sources, in addition to having lower resolution in time, pressure levels, and space. NARR has been shown to underperform compared to other reanalysis datasets for predictions of precipitation and other hydrological variables.[305,306] ERA-5, in contrast, has been shown to outperform NARR and other models for the prediction of surface temperatures.[271,282] Following these findings, ERA5-predicted ALW is likely more representative of ambient mass concentrations, and so all subsequent sensitivities and

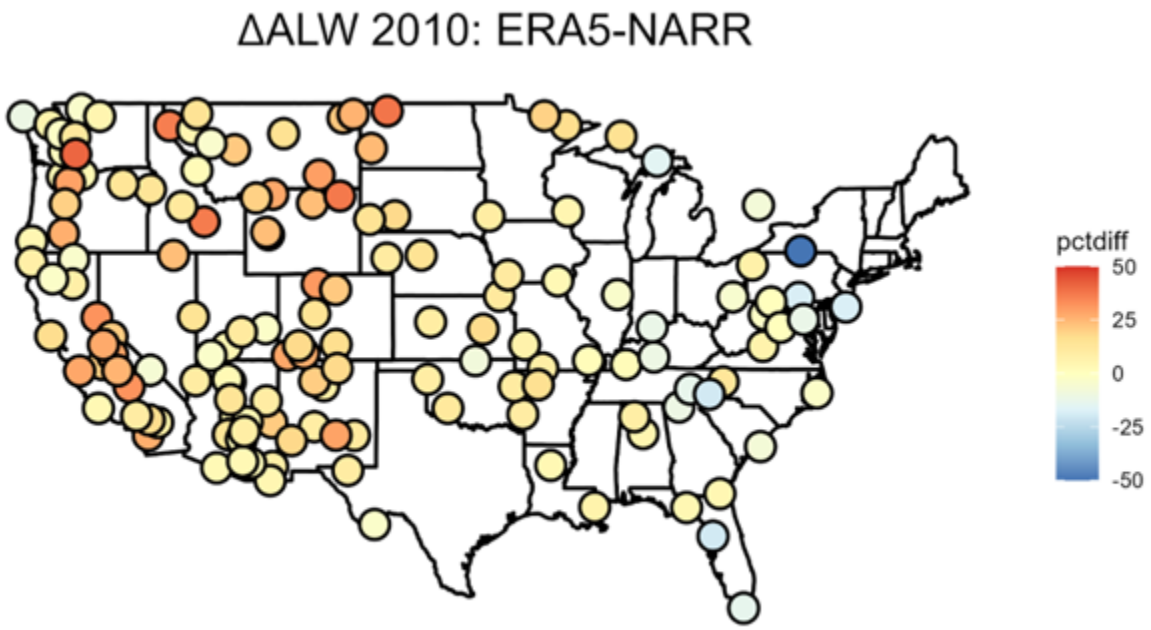


Figure 3.3: Comparison (percent difference) between ERA5 and NARR derived average surface-level ALW for the year 2010. Only sulfate and nitrate were used as chemical inputs for water calculations.

applications employ ERA5 meteorology.

The inclusion of ammonium reduces predicted ALW at all 4 available CSN locations (Figure 3.4). This decrease is most apparent at Birmingham, AL, which is a more suburban site than the others investigated. These decreases are primarily due to shifts in the sulfate ratio and chemical regimes determined by ISORROPIA. In the absence of ammonium and dust ions, all equilibrium conditions are determined for a sulfate-rich regime. Under these conditions, sulfate is a major aqueous species and increases water activity substantially. When ammonium is included, many observations shift to a sulfate-poor regime, where aqueous $HSO_4^-$ is considered a minor species and other, less hygroscopic components are the major species. This shift in equilibrium conditions generally results in reduced ALW mass. While these uncertainties due to ammonium are significant, it is difficult to examine the impact this may have across the CONUS due to a paucity of surface measurements, particularly in key regions like the Midwest/Plains.

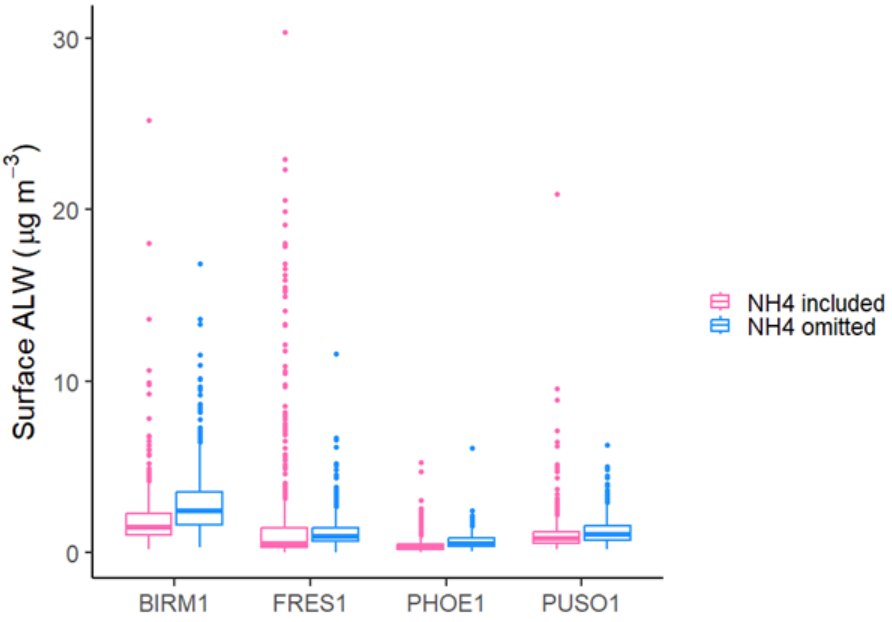


Figure 3.4: Comparison between daily surface-level ALW calculated with and without ammonium ion ($NH_4$) at EPA CSN sites. ERA5 meteorology is used for both calculations. Temporal resolution is limited to just 2016-19 due to analytical lab uncertainties.

In both humid and dry regions, the inclusion of dust ions reduces the ALW mass concentrations predicted by ISORROPIA-II (Figure 3.5). While the differences are significant in both regions, the magnitude of dust impacts are much more substantial in the arid GB region compared to the humid SEUS. This is primarily due to the abundance of dust ions between the two locations. Dust is often a minor constituent in aerosol mass in the SEUS, whereas fine dust mass concentrations and dust events are both more prevalent in the arid regions like GB.[277] Across the CONUS, inclusion of dust ions in yearly average surface ALW predictions generally reduce predicted mass concentrations (Figure 3.6). A few coastal sites show increased ALW when dust is included; however, this effect is driven by high chloride concentrations from sea spray aerosol at those locations.

Similar to ammonium, chemical regime shifts can explain some of the decreases observed when dust is included. At sites where fine dust is a significant contributor to aerosol mass, regimes can shift out of the sulfate-rich regime and into a sulfate-poor domain. Most sites;

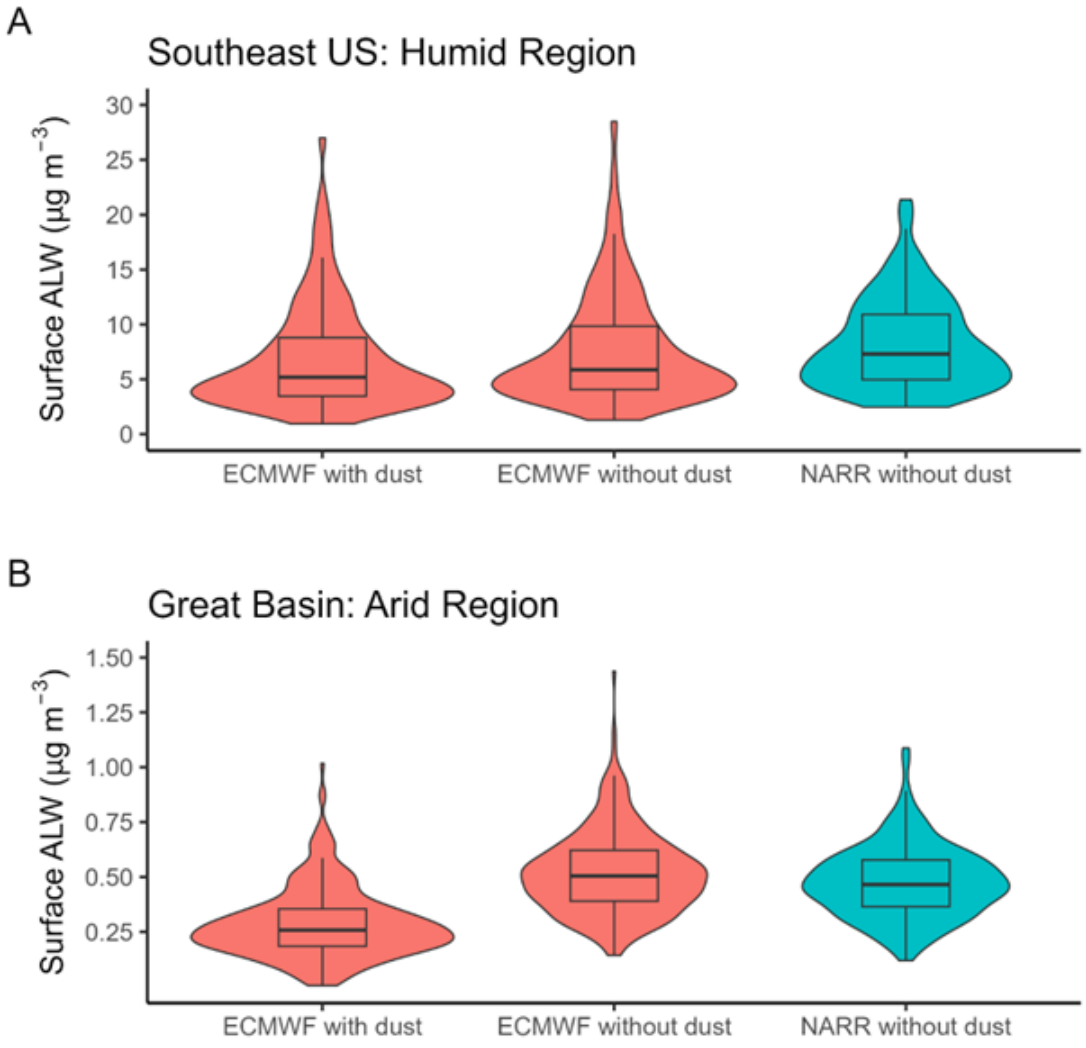


Figure 3.5: Comparison of meteorological and dust sensitivities in monthly average surface-level ALW predictions for a humid region (total SEUS, left) and an arid region (Great Basin, right). All available measurement days are used (1988-2014).

however, still remain in the sulfate-rich regime when dust ions are included. The absence of ammonium in these calculations makes it difficult to shift the value of R1, the "total sulfate ratio" greater than 2, which signifies a sulfate-poor regime. Even without a change in overall regime, the inclusion of less-hygroscopic species such as $Ca^{2+}$, $K^{+}$, and $Mg^{2+}$ as major aqueous-phase species still perturbs equilibrium calculations to significantly reduce overall estimates of ALW mass. Should ammonium and dust both be considered, ALW concentrations would be expected to decrease further at most locations.

It is difficult to assess the uncertainty of ammonium relative to meteorology and dust ions due to measurement limitations. For the SEUS, the relative uncertainty between meteorology and dust ion inclusion is similar, with ERA5 predicting a 20% reduction in ALW relative to NARR and dust ion inclusion showing a 12% reduction relative to just a sulfate/nitrate system (Figure 3.5). In contrast, dust ion inclusion in the arid GB region clearly changes ALW observational estimates more than meteorology, even though the meteorological variables show greater deviation between datasets in the arid region (Figure B.2). As shown in Figure 3.6, the impact of dust ion inclusion seems to be more prevalent with time, where there is little change induced by dust over the eastern U.S. in 2005, but by 2019 decreased ALW is apparent at all non-coastal locations. As controllable aerosol components like sulfate and nitrate continue to decrease, dust ions will make greater contributions to fine aerosol mass[277,307,308] and therefore be more important to consider in ALW estimates. Similarly, with increasing surface temperatures and increasing propensity for drought conditions, fine dust abundance and dust storms and are likely to become even more important in the southwest U.S. and other arid regions.[307,309]

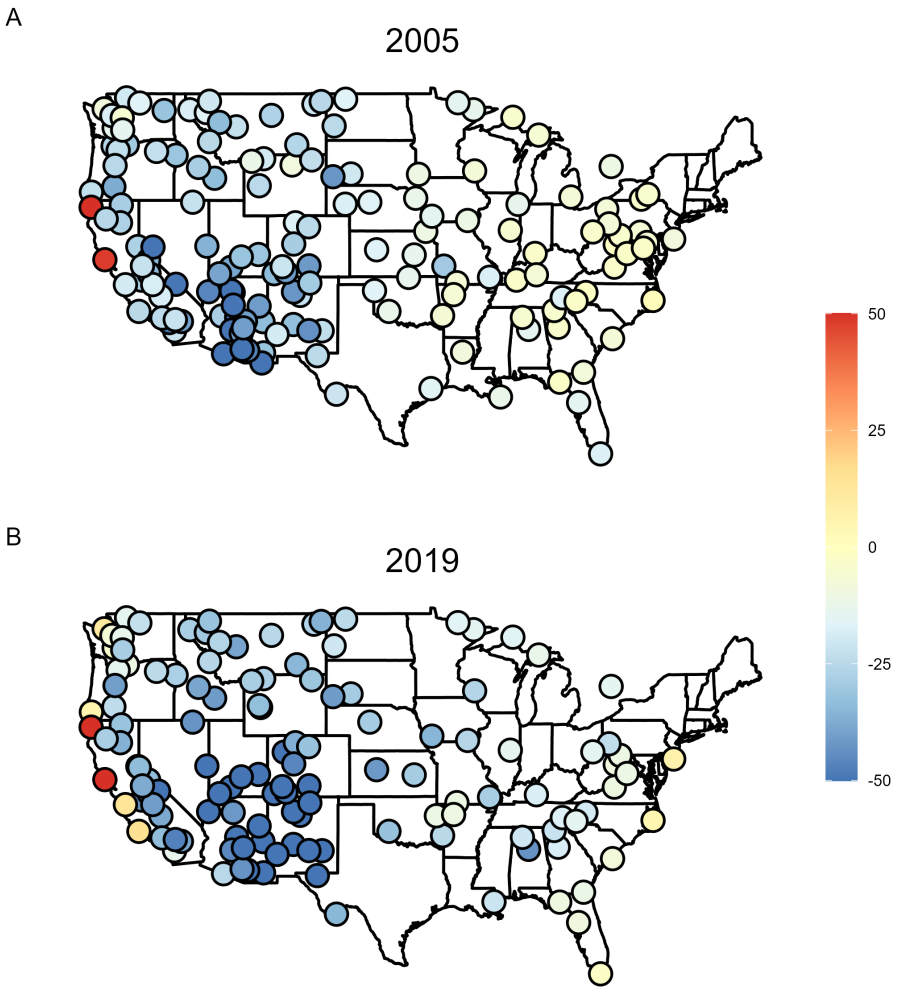


Figure 3.6: Comparison (percent difference) of dust sensitivities (Dust - No Dust) in yearly average surface-level ALW predictions across CONUS IMPROVE sites for 2005 (A) and 2019 (B). ERA5 meteorology is used for both calculations.

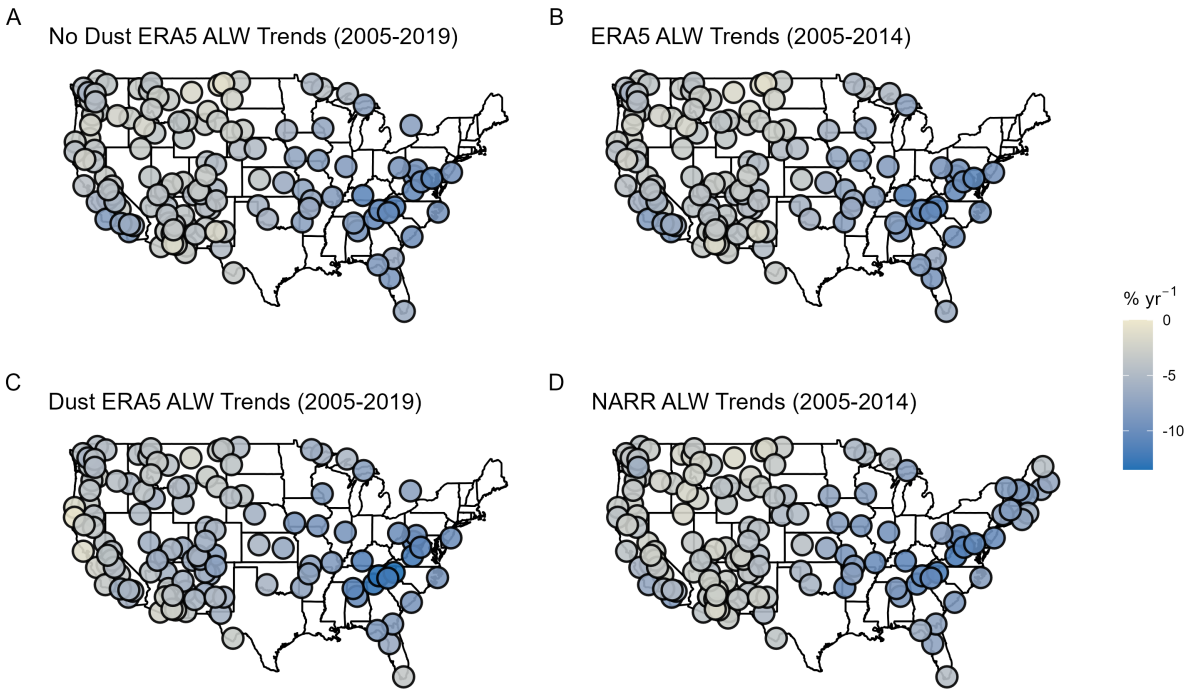


Figure 3.7: Trends (percent yr$^{-1}$) in predicted ALW mass concentrations at CONUS IMPROVE sites with different data products. Panels A and C show trends from 2005 with and without dust ions respectively, both using ERA5 meteorology. Panels B and D show trends from 2005-2014 with ERA5 and NARR meteorology respectively.

### 3.4.2 Trends in ALW Mass Concentrations

Across all CONUS IMPROVE sites active from 2005-2019, surface level ALW mass concentrations are decreasing (Figure 3.7). These trends persist in similar magnitude and spatial distribution regardless of the meteorological and chemical inputs employed. Trends are more sensitive to dust than meteorological inputs. Prior studies have acknowledged uncertainties in the influence of the meteorological and chemical inputs employed from ALW observational estimates, and note higher confidence in the trends observed rather than absolute mass concentrations.[58,114,274] The trends reported here confirm those findings; on broader timescales, ALW observational estimates show a clear spatiotemporal trend despite input uncertainties. On shorter timescales, when concentrations of ammonium and/or dust are high, or when absolute concentrations of ALW are required, these sensitivities may be more important.

Decreases in ALW mass are most notable over the eastern U.S., with more stagnant trends observed in the west. These trends are primarily driven by changes in particle chemical composition over time rather than meteorological forcing. RH controls the amount of water available for particles to uptake. Both NARR and ERA5 meteorology lack clear trends in RH, with nearly all sites reporting a trend $< \pm 0.5$ % yr$^{-1}$ (Figure B.4). Successful emission regulations have decreased mass concentrations of primary hygroscopic species such sulfate, which results in the decreasing trend in surface level ALW mass. Sulfate decreases are most notable in the coal-influenced eastern U.S., which is also reflected in the spatial pattern of ALW surface trends.[26,203,310]

Broadly, these results suggest significant changes in aerosol media since 2005, with a median 5.2% yr$^{-1}$ reduction in ALW mass observed across the CONUS (dust included, ERA5 meteorology). These changes are likely to affect both chemical and physical aerosol properties. For example, decreasing ALW may impact the available media for partitioning of water-soluble organic gases, limiting aqueous SOA formation.[180] Reduced ALW may also impact aerosol ionic strength and pH, with broader implications towards phase state and secondary chemical processes.[19,311,312] The physical size and light extinction properties of particles are likely to change as well. The following applications investigate the effects of declining ALW towards physical aerosol properties in two unique chemical environments.

### 3.4.3 Application 1: Explaining Clear and Cloudy Sky Differences in Aerosol Optical Depth and Size in Bondville, IL

Atmospheric chemistry field measurements are often prone to a "clear sky bias". Satellite retrievals and surface optical measurements often strategically avoid cloudy conditions as a part of quality assurance protocols. Prior work has shown that chemical composition is different between clear and cloudy sky conditions across the CONUS, with higher mass

concentrations of ALW generally observed during cloudy sky conditions.[114] This suggests aerosol optical properties such as aerosol optical depth and size should also be different between clear and cloudy sky conditions. Here, we use an IMPROVE/AERONET co-located site in Bondville, Illinois to examine clear/cloudy sky differences in aerosol physicochemical properties.

During the study period in Bondville, population distributions for values of AOD at all measured wavelengths, demonstrated by the 440 nm channel, are significantly different on clear sky days than on cloudy days in every season (Figure 3.8). On clear days, Ångström exponents (AE) are significantly larger, indicating a smaller average physical size for the ambient aerosol distribution with the sole exception of winter. Median AOD values are greatest at all examined wavelengths and differences between cloudy and clear sky days are most pronounced in the spring and summer seasons (Table B.2). The difference in medians is small, yet more often than not, is more than the 0.02 instrumental uncertainty. Meteorological variables such as surface temperature and relative humidity are statistically similar between cloudy/clear sky days across all seasons. PBL height is significantly lower on cloudy days in the spring and summer, which could be a contributing factor to the observed differences in AOD, but does not provide sufficient explanation for the differences in AE.[72]

Chemical composition of $PM_{2.5}$ provides a plausible explanation for AOD and AE observations at the Bondville monitoring site. Particle composition affects AOD and AE via intrinsic properties such as refractive index and through influences on particle size via changes in hygroscopicity and water uptake.[313,314] Cloudy versus clear sky differences in overall $PM_{2.5}$ and ALW mass are sharpest during spring and summer, exhibiting similar patterns to AOD and AE measurements for those categories. In the summer when $PM_{2.5}$ and ALW mass are the highest, AOD is also the highest. IMPROVE-measured $PM_{2.5}$ mass concentrations that include ALW are the highest on cloudy days in every season but winter (Figure 3.9). This is similar to patterns in AOD and is physically consistent with an abundance of hygroscopic

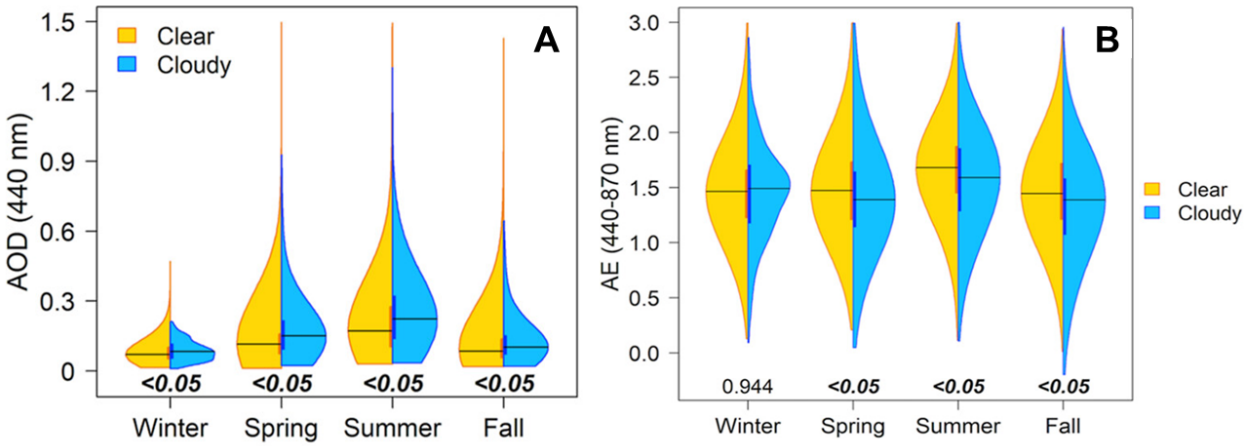


Figure 3.8: Seasonal distributions from 2010 to 2019 of AOD at 440 nm (A) and AE for the 440–870 nm (B) wavelength range on clear sky (gold) and cloudy (blue) days as binned by the AERONET quality assurance algorithm method. Vertical gold (clear sky) and blue (cloudy) bars represent the $25^{th}$ to $75^{th}$ quartile of each distribution, with the black horizontal line as the median. Black numbers are p-values from two-sided Mann-Whitney U tests, with bold italicized font indicating statistical significance between distributions where a p value $< 0.05$ indicates the two populations are not equal.

particles that take up water to grow in size on cloudy days. Aqueous-phase processing of air parcels is documented to shift accumulation mode aerosol to a larger population size.[315,316]

ALW provides a plausible explanation towards the differences observed in AOD and AE. These observations support prior work demonstrating the ability of ALW to help explain discrepancies between surface level observations of $PM_{2.5}$ and columnar observations of AOD.[265] We note that this explanation relies on the assumption that surface measurements adequately represent the boundary layer column. Consideration of vertically resolved meteorology and AWP instead of just surface-level ALW may improve this understanding even further.

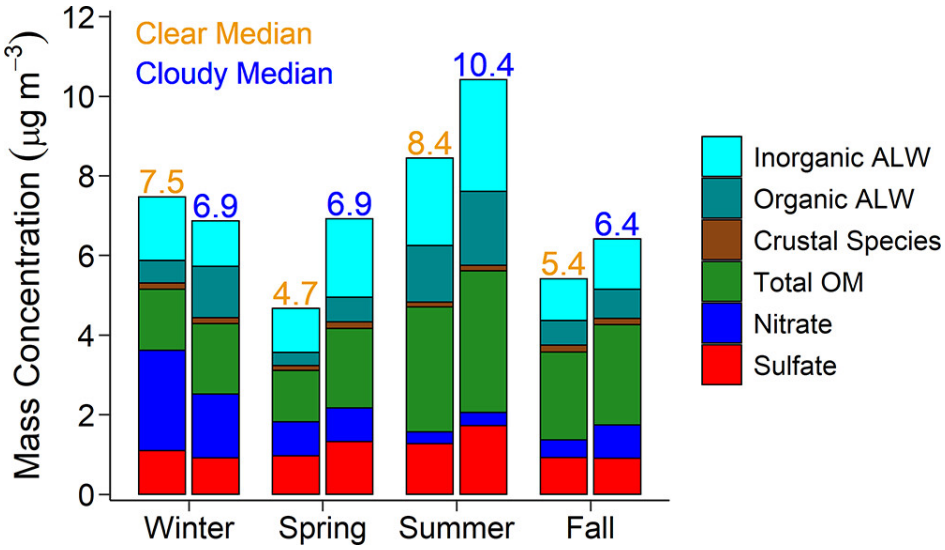


Figure 3.9: Stacked bars of median total $PM_{2.5}$ chemical composition and ALW observation-based estimates during clear sky (left bars, gold numbers) and cloudy (right bars, blue numbers) days as binned using the AERONET QA algorithm for 2010-2019. Crustal species include calcium, potassium, magnesium, and sea salt species of sodium and chloride. Table B.3 identifies statistical significance for individual chemical constituents.

### 3.4.4 Application 2: Elucidating Aerosol Radiative Impacts on Surface Air Temperature Modulation in the Southeast US

The emergence of a "warming hole" in the SEUS has not been clearly explained. In this region, and in sharp contrast to much of the world, surface temperatures did not rise over the period of 1901-2000, though some warming has been noted in recent decades (Figure 3.10). Physical meteorology provides a plausible explanation for the strength and spatial extent of the warming hole in the winter season, but cannot fully explain weakened warming trends in other seasons.[317,318] The processes responsible for the formation and modulation of the warming hole have been much studied (e.g., Carlton et al. 2018)[74] and debated with studies proposing a wide variety and/or combination of potential meteorological and aerosol effects.[129,156–158,319–329] It remains unclear to what extent the recent warming was controlled by wintertime temperature advection versus increased greenhouse gas (GHG) concentrations. It is further unclear how changes in factors (other than GHG) that govern

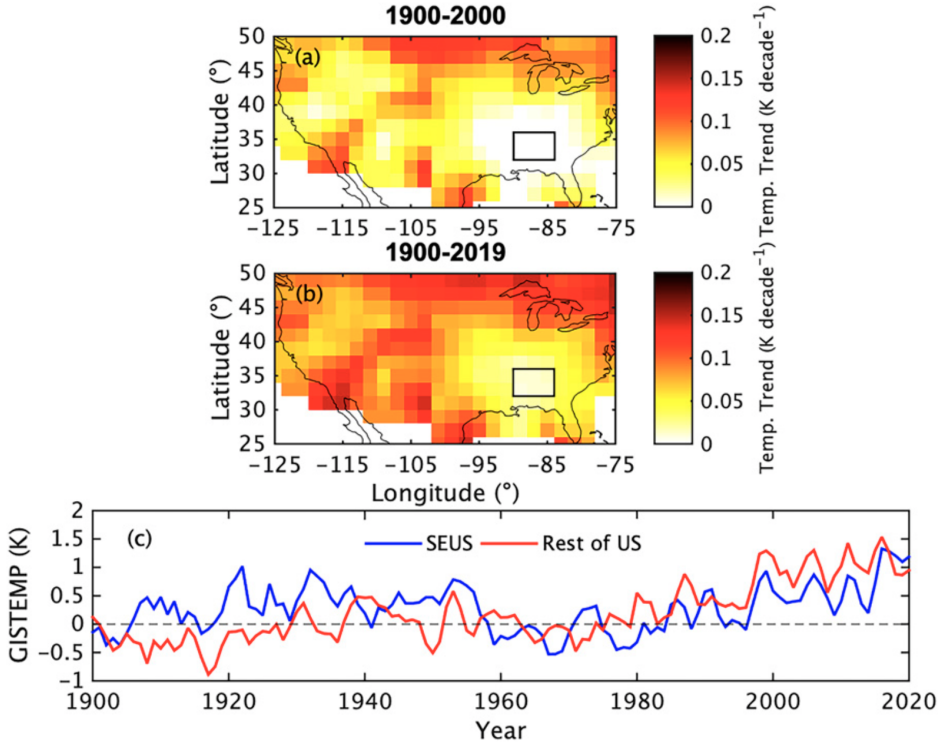


Figure 3.10: Long-term trend of annual averaged surface air temperature anomaly (GISTEMP) within the continental United States for (A) 1900–2000 and (B) 1900–2019. (C) Annual mean surface air temperature anomaly in the SEUS (black rectangle) and the rest of the United States.

regional radiation budgets (e.g., cloud, aerosol, land surface properties) and their seasonality affect the annual and seasonal temperature trends. To address these issues, we analyzed two decades (2000–09 and 2010-19) of meteorological, cloud, aerosol, chemical, and optical data collected by a variety of satellite remote sensing instruments, reanalysis models, and surface aerosol measurements. Examination of cloud fields and other meteorological variables is consistent with other studies, showing that warm air advection drives the observed trends in the winter season.[279,318] Here, we just focus on aerosol properties and their relation to the radiative budget in the region.

In contrast to most meteorological variables, aerosol fields show substantial changes between the two decades (Figure 3.11). Aerosol dry mass concentration and AWP exhibit a statistically significant decrease in all seasons during 2010–19, compared to the values during

2000–09. Both dry mass and AWP exhibit a distinct annual cycle with the highest values during the summer months and lowest values during the winter months. Absolute differences in dry mass are relatively small, with more substantial population differences observed for AWP, especially in the summer. These findings are consistent with prior work demonstrating regional and national air quality improvements. The implementation of the Clean Air Act and subsequent amendments have greatly reduced ambient concentrations of various pollutants, in particular sulfate, a chemical species that modulates water uptake.[202,265] Sulfate reductions are especially notable in the summer as a result of peak energy consumption and shifts in fuel use.[330] AOD also exhibits a statistically significant decrease in the decadal mean values; however, while dry mass and AWP decreases were significant every season, significance in AOD was observed only in the spring and summer seasons. The percent decrease in AOD was highest in the summer season, indicating the aerosol impact on radiation budget to be highest in summer months. This surface-based observation is consistent with earlier findings that demonstrate a summertime enhancement in space-based AOD over the region.[265,298] Aerosol size as determined by AE is generally similar across seasons and time, with only the fall showing significant differences.

The single scattering albedo (SSA) measures the ratio of scattering efficiency to extinction efficiency, with a value of 1 denoting a fully scattering particle and a value of zero denoting a particle completely absorbing the radiation. SSA exhibits a distinct annual cycle with the highest values during the winter months and the lowest during the summer months. Comparing decades, SSA shows a statistically significant increase in the later decade during winter, spring and summer months as compared to the earlier decade. Although small, this increase suggests that the particles became more efficient in scattering the radiation during the later decade as compared to the earlier decade. This finding is in sharp contrast to decreasing AOD trends, but may still be explained by changing aerosol composition. Mass concentrations of elemental carbon, the primary absorber of shortwave radiation, decreased in the region over the 20-yr period by approximately 50% and could induce observed changes in

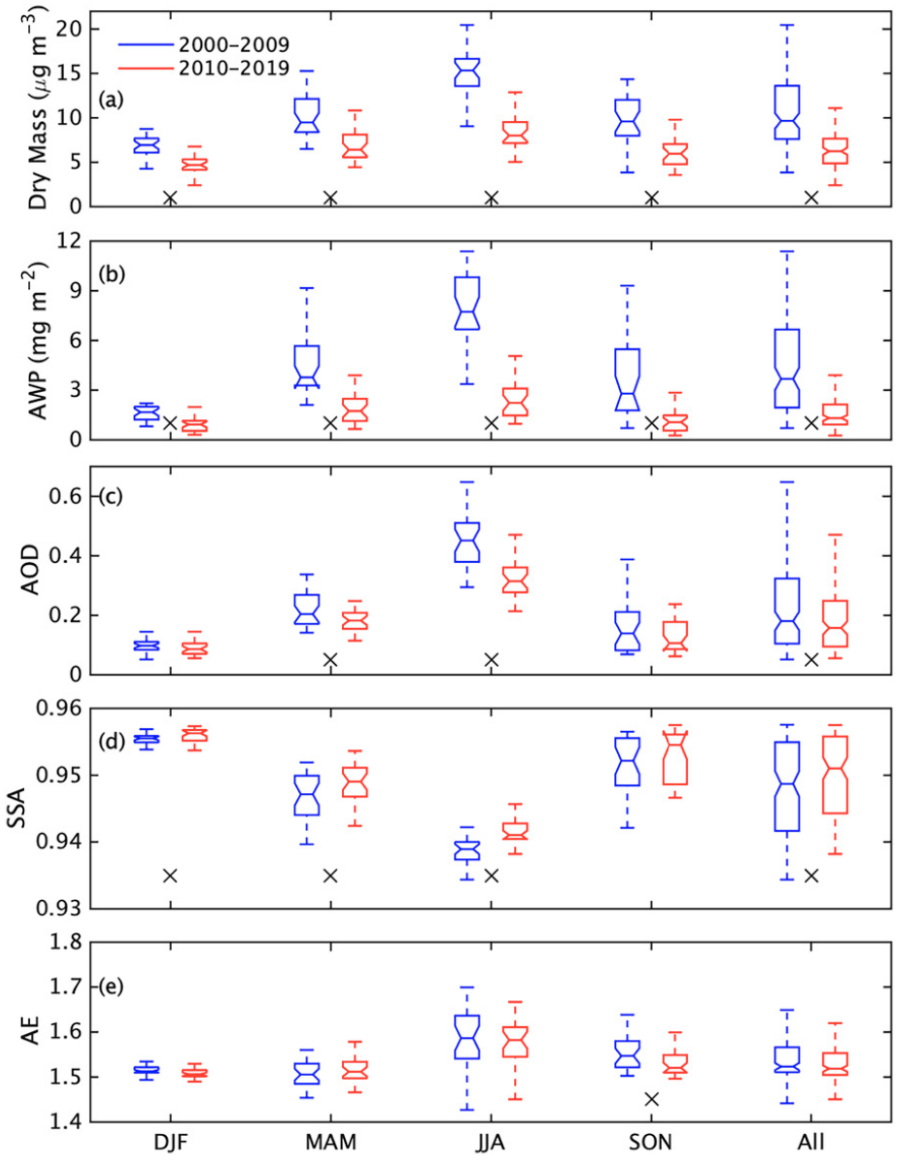


Figure 3.11: Box-and-whisker plots of monthly values of (A) aerosol dry mass, (B) aerosol water path, (C) aerosol optical depth, (D) single scattering albedo, and (E) Ångström exponent during 2000–09 (blue) and 2010–19 (red). An × symbol below the box and whiskers denotes if the averages of the two distributions are statistically different at a 95% confidence interval.

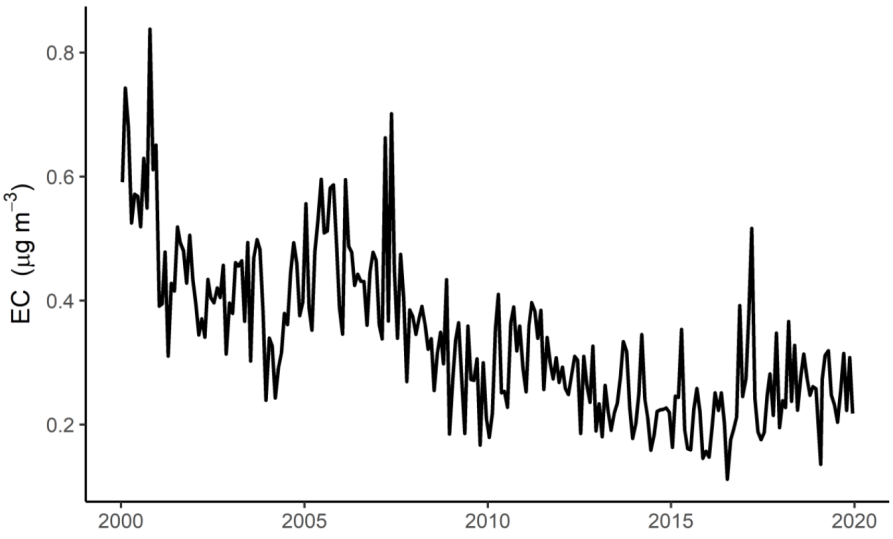


Figure 3.12: Mass concentrations of elemental carbon, the primary absorber of shortwave radiation, decreased in the region over the twenty-year period by approximately 50%.

scattering properties (Figure 3.12). The reductions noted in AWP in the latter decade could also increase scattering efficiency, as water coated aerosol particles have lower scattering as compared to dry aerosols.

In a one-dimensional radiation budget framework, radiative fluxes at the top of the atmosphere (TOA) and at the surface will determine surface air temperature. We focus on TOA parameters, as surface radiative fluxes did not exhibit any significant changes between the two decades.[279] Both the all-sky and clear-sky TOA upwelling shortwave and longwave radiative fluxes exhibit a distinct annual cycle with higher values in the summer months and lower values in the winter months (Figure 3.13). The TOA clear-sky upwelling shortwave radiation during the summer months was lower during 2010–19 as compared to that during 2000–09. All other TOA radiation parameters, including TOA all-sky upwelling shortwave radiation, are similar between decades, which points towards AOD as a determining factor. The lack of changes in the TOA all-sky longwave and shortwave fluxes suggest the influence of clouds on the radiation budget to be unchanged during the 20-yr period.

Collectively, these results suggest that aerosols are primary modulators to surface air tem-

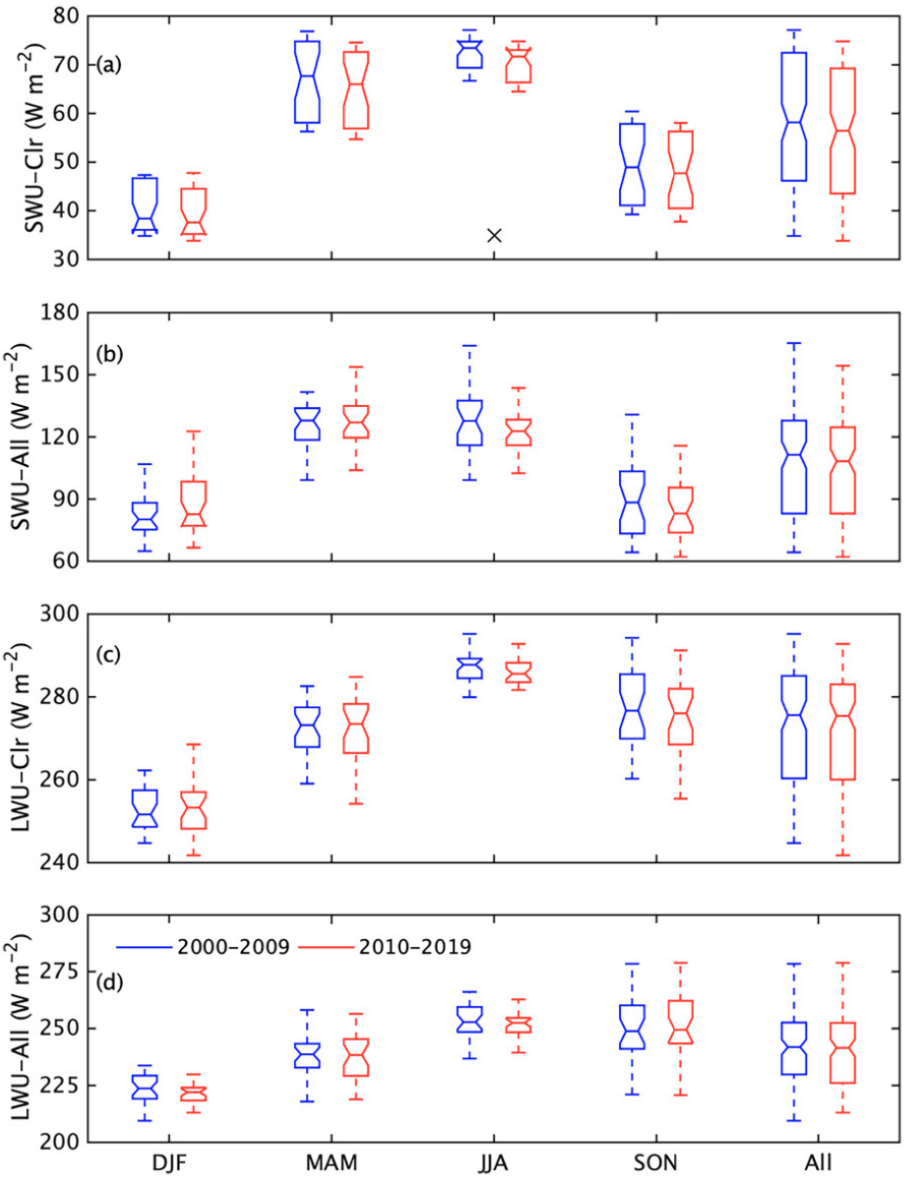


Figure 3.13: Box-and-whisker plot of monthly values of top of the atmosphere (A) upwelling shortwave radiation during clear-sky conditions, (B) upwelling shortwave radiation during all-sky conditions, (C) upwelling longwave radiation during clear-sky conditions, and (D) upwelling longwave radiation during all-sky conditions during 2000–09 (blue) and 2010–19 (red). An × symbol below the box and whiskers denote if the averages of the two distributions are statistically different at a 95% confidence interval.

peratures in the region, at least during the summer months. The coincident decrease in summertime AOD and TOA outgoing shortwave radiation during cloud-free conditions, paired with an increase in surface temperatures highlights the ability of aerosol to modulate surface air temperatures. Changes observed in AOD are consistent with the decreases observed in dry mass and AWP. These findings are broadly consistent with Application 1, as the change in summertime AOD seems to be the result of changes in columnar aerosol composition and associated ALW. Ambient aerosol composition and ALW content may also help explain the anomalous increase in SSA observed in this study, and warrants further examination.

## 3.5 Conclusions

The meteorological models and chemical inputs employed induce substantial uncertainties in ALW predictions. Differences in meteorological reanalysis datasets will significantly change predicted ALW and AWP. It is difficult to predict an overall bias, as the datasets may be better or worse at predicting different variables in different locations and times. It is thus highly important to evaluate the quality of reanalysis data towards the variables necessary for ALW calculations. Between the two reanalysis datasets examined here, ERA5 generally produces higher ALW estimates than NARR, though the magnitude of these differences is variable in space and time. ERA5 is established to have more reliable surface temperature observations and therefore likely produces more accurate ALW estimates than NARR.[271,282] Ammonium inclusion generally decreases predicted ALW from the $SO_4$-$NO_3$ base case conditions. Dust ion inclusion, on the other hand, significantly decreases ALW predictions in nearly all locations.

While many studies may neglect dust ions and/or ammonium for various reasons, namely measurement limitations, these results suggest that sensitivities should be performed for each case to justify these omissions. Ammonium, as a primary species within the ISORROPIA

solution framework, may be the most important uncertainty investigated here; however, the lack of reliable measurements in ammonia-influenced regions makes quantitative assessment difficult. Dust ion inclusion will likely become more important to consider as drought conditions and dust event frequency becomes more common.[307–309] While ISORROPIA does include some parameterization for differing chemical climatologies, the impacts of different ion inclusions may still have a substantial effect even within the same regime, as shown in Chapter 3. Future work should include discrete parameterization of acceptable dust prevalence, ammonium concentration, etc. at which these species can be neglected or at which point they must be considered in order to attain realistic predictions. Similarly, the influence of sea salt is clear at sites with coastal influence (Figure 3.6). Because chloride is a chemical constituent that faces a great amount of measurement uncertainty and data availability limitations,[285] it may be difficult to attain an accurate understanding of ALW mass concentrations at sites with coastal influence.

Though the analysis here seeks to resolve some key uncertainties in ALW predictions, it is difficult at this time to quantitatively assess the accuracy of these predictions due to the dearth of ambient measurements. Prior works have compared ISORROPIA outputs with growth-factor derived measurements of ambient ALW, with good agreement noted, especially for high RH ($> 60\%$) conditions.[65,331] Predictions may improve when organic-associated ALW is considered, though uncertainties in organic composition and hygroscopicity across different environments complicate comparisons.[44,47,302] Since most ambient measurement techniques rely on drying ambient aerosol and risk losing volatile and potentially hygroscopic aerosol mass, it is even more difficult to assess how well the observational estimates provided here reflect the ALW content of ambient aerosol. Emergent technologies like lidar show promise in making ALW measurements more feasible on a greater scale and without changing the ambient state of aerosol mass.[332,333] Despite the sensitivity of ALW observational estimates to meteorology and chemical constituents, trends in surface ALW mass are consistent and decreasing across the CONUS (Figure 3.7).

ALW and AWP predictions are vital towards understanding ambient aerosol state in relation to optical, radiative, and chemical properties. Applications 1 and 2 both highlight the significance of ALW towards understanding optical and radiative properties of aerosols, a key uncertainty within climate models.[148,152] ALW provides a plausible explanation for elevated AOD and larger particle size on cloudy days in Bondville, Illinois. Similarly, consideration of dry and wet aerosol concentrations helps explain decadal trends in summertime AOD and related aerosol-driven surface temperature modulation in the SEUS warming hole region. Future work towards either of these projects would benefit greatly from a greater suite of colocated and high time-resolution measurements of aerosol composition, radiative forcing, and meteorological factors to help better elucidate the driving factors behind observed trends. Collectively, the applications presented here demonstrate the importance of ALW towards understanding ambient aerosol chemistry, and emphasize the need for robust and accurate observational estimates across different chemical regimes.

# Chapter 4

# Gas-Phase Water Soluble Organic Carbon in the South Coast Air Basin: $NO_x$ and VOC solubility

This chapter contains unpublished research carried out in collaboration with the Carlton Research Group, UCI Ultrafine Aerosol Lab, and CalNex 2010 PIs Dr. Barry Lefer, Dr. Joost De Gouw, and Dr. Rodney Weber. All Irvine mist chamber measurements, dataset synthesis, and data analysis were completed by the author. $NO_x$ and $O_3$ measurements in Irvine were taken by the Ultrafine Aerosol Lab. Carlton group members Dr. Simon Rosanka and Ellie Smith contributed to air quality simulations. All Pasadena measurements were taken by the CalNex PIs listed above.

## 4.1 Abstract

Gas-phase water-soluble organic carbon ($WSOC_g$) is an important yet understudied portion of the volatile organic carbon (VOC) inventory. The chemical coupling of hydroxyl radical ($^{\cdot}OH$) induced photooxidation of VOCs and $NO_x$ controls tropospheric ozone ($O_3$) production. These chemical cycles also lead to the formation of functionalized VOCs such as $WSOC_g$, which can form secondary organic aerosol (SOA) through condensational and aqueous processes. Changes in primary $NO_x$ and VOC emissions are well studied in the context of $O_3$ chemistry, such as weekend effects; however, the effects of these chemical regimes towards the products of VOC oxidation, such as $WSOC_g$, are not as extensively studied. Here, near real-time measurements of $WSOC_g$, $NO_x$, and $O_3$ are compared between two locations within the California South Coast Air Basin (SoCAB): Irvine from 12 Feb to 31 Mar 2024 and Pasadena during the CalNex field campaign (15 May to 15 June 2010). $WSOC_g$ mass concentrations are approximately 50% lower in Irvine compared to Pasadena, while $O_3$ mixing ratios are similar. $WSOC_g$ is positively correlated with NO at both locations. In Pasadena, $WSOC_g$ is also positively correlated with $NO_2$ and $O_3$. In contrast, Irvine data lacks correlation with $NO_2$ and is negatively correlated with $O_3$. Spatiotemporal variation in primary emissions, as well as lower actinic flux during Irvine sampling, contribute to some of these differences but cannot fully explain observed correlations. Results are consistent with a $NO_x$-saturated chemical regime for $O_3$ production in Pasadena, whereas Irvine appears to be a more $NO_x$-limited or transitional regime, suggesting that $O_3$ production regimes affect $WSOC_g$ abundance. EPA's Community Multiscale Air Quality model (CMAQ) cannot fully reproduce the observed diurnal profiles nor associations with $WSOC_g$ in either location. Results suggest that lower $NO_x$ conditions in Irvine may inhibit the formation of $WSOC_g$ and/or increase depositional losses via pathways that are not well-described in current gas-phase chemical mechanisms. This implies VOC product distributions, relevant for both semi-volatile and aqueous SOA formation, may vary in locations as a function of

$NO_x$-influenced $O_3$ production.

## 4.2 Introduction

The effects of $NO_x$ ($NO_x = NO + NO_2$) and volatile organic compounds (VOCs) towards tropospheric ozone ($O_3$) production, a key health concern, are heavily investigated.[115,130,334,335] $O_3$ production relies on complex chemistry between $NO_x$ and VOCs. Regions are generally described as $NO_x$-limited or $NO_x$-saturated depending on $NO_x$ and VOC emissions as well as the response of $O_3$ to changes in these emissions.[3,336,337] The South Coast Air Basin (SoCAB) is a historic case study of $NO_x$-saturated conditions.[336,338–345] Under these conditions, $O_3$ production responds non-linearly to $NO_x$ reductions. For example, a "weekend effect" is noted, where reductions in $NO_x$ emissions on weekends promotes an increase in $O_3$ relative to weekday values. This effect is well-documented in SoCAB over time[338,342], though more recent studies point towards a weakening of this effect and a shift towards more $NO_x$-limited conditions.[340,341]

Perturbations in $NO_x$ that change the production efficiency of $O_3$ will also change the oxidation pathways and efficiency of VOCs through changes in the reactions of the hydroxyl radical ($^{\cdot}OH$), nitric oxide (NO), and organic peroxy radicals ($RO_2^{\cdot}$).[346–348] For example, the formation of highly oxygenated molecules (HOMs) is suppressed under higher $NO_x$ conditions due to the dominant termination reaction of NO with $RO_2^{\cdot}$.[98,347,349] A prior study during the 2010 CalNex field campaign found evidence for faster photochemical processing and increased OH concentrations on weekends relative to weekdays in SoCAB.[346] The effect of short- and long-term $NO_x$ emission changes; however, have not been evaluated towards the properties of the ambient gas-phase VOC inventory, such as volatility and solubility.

As primary VOCs undergo oxidation reactions, they generally become more oxygenated,

less volatile, and more water-soluble.[32] As such, water-soluble organic carbon (WSOC) is often used as a tracer for secondary organic aerosols.[180–183] WSOC may exist in either the gas ($WSOC_g$) or condensed ($WSOC_p$) phase, of which the latter is often a large portion of secondary organic aerosol (SOA) mass.[350] $WSOC_g$ may partition reversibly or irreversibly to aerosol liquid water, promoting secondary condensed phase chemistry and the formation of aqueous SOA.[351,352] Aqueous SOA (aqSOA) formation is predicted to be important in the eastern United States, where liquid water is more available; however, studies suggest it may be an important pathway in more arid regions as well.[56–59]

Relative to $WSOC_p$, measurements of $WSOC_g$ are sparse across space and time. Surface measurements of bulk WSOCg in the U.S. are limited to seven distinct sampling locations, with most measurements occurring prior to 2010 (Figure C.1). Prior works generally collect $WSOC_g$ in tandem with $WSOC_p$ to examine partitioning behavior, and do not thoroughly investigate the ambient abundance or diurnal profile of $WSOC_g$. As anthropogenic VOC and $NO_x$ emissions are reduced in recent decades, changes to the solubility of the gas-phase VOC inventory remain a critical knowledge gap. Here, recent measurements of $WSOC_g$, $NO_x$, and $O_3$ taken in Irvine, CA, a site expected to be $NO_x$-limited, are compared with measurements taken during CalNex 2010 in Pasadena, CA, an established $NO_x$-saturated location.[338] Measurements are paired in space and time at both locations with EPA's Community Multiscale Air Quality (CMAQ) model predictions and qualitatively compared to diurnal patterns and statistical associations among species. Techniques established for $O_3$ studies are utilized to infer broad changes in VOC oxidation product solubility.

## 4.3 Methods

### 4.3.1 Sampling Locations

Ambient measurements were taken in Pasadena and Irvine, distinct locations within the SoCAB region (Figure 4.1). Ambient measurements in Pasadena, CA were taken as a part of the CalNex-LA 2010 field campaign.[73] All Pasadena data is sourced from the publicly-available online CalNex data repository, and all datasets are used with the permission of their respective authors.[77] Data was collected at the LA ground site located on the California Institute of Technology campus (34.140582, -118.122455). Prevailing winds are from the southwest, which transports urban air plumes from downtown LA to Pasadena (Figure 4.1B).[353] All measurements were taken during the late spring/early summer season, from 15 May to 16 June 2010. This sampling location has been described in more detail by prior publications.[354,355] All data evaluated here, including meteorological variables, were collected at the LA ground site from either a trailer ($WSOC_g$, meteorology) or top of tower (10m, $NO_x$ and $O_3$). Temperature was noted to be significantly higher than the campaign average during Memorial Day weekend (29 to 31 May 2010), and these dates are removed from analysis.[356]

In this study, measurements were taken on the University of California, Irvine campus (33.644708, -117.844277) from late winter through early spring (12 February to 31 March 2024). Measurements of $WSOC_g$, $NO_x$, and $O_3$ were taken from a loading dock on campus, with sporadic traffic from cars and trucks during weekdays and minimal activity on weekends. Measurements of meteorological variables were retrieved from nearby weather stations. Temperature, relative humidity, solar radiation, and precipitation were measured close to the sampling site ($\sim$ 0.5 mi away).[357] Wind speed and direction were measured at a separate site (SNA, $\sim$ 2 mi inland).[358] Wind direction is predominantly from the south and southwest (Figure 4.1C). Urban plume influence is minimal relative to Pasadena. Rainy (hourly

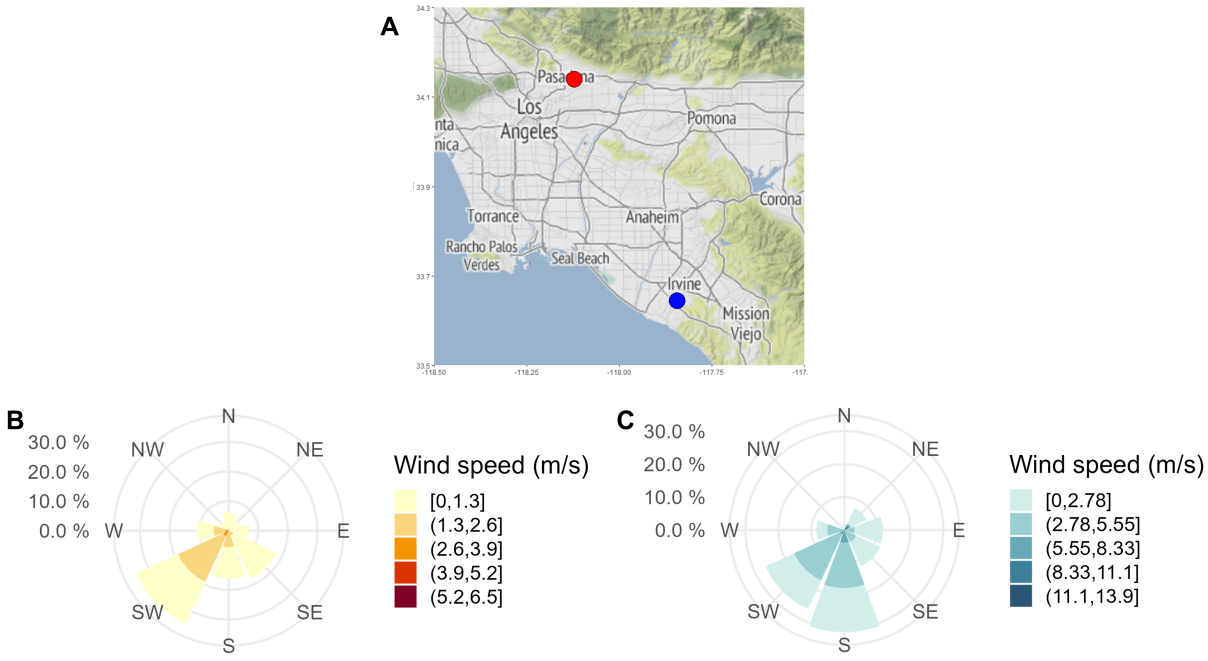


Figure 4.1: Sampling locations and wind patterns. Panel A indicates the Pasadena (CalNex) sampling site in red and the Irvine (UCI) site in blue. Panels B and C shows wind speed and direction measured at the surface in Pasadena and Irvine respectively. Note the scales are different for each wind rose.

average rain rate > 0 in) and rain-influenced periods (hourly average rain accumulation > 0 in) were removed from this analysis, as wet depositional losses may confound comparison to Pasadena where conditions were dry (Figure C.2). Data collected on the evening of March 2, 2024 are also removed from analysis due to the influence of fresh firework emissions during a campus event (Figure C.3).

### 4.3.2 Ambient Measurements and Chemical Analysis

Mass concentrations of $WSOC_g$ were determined using a mist chamber (MC) paired with a total organic carbon (TOC) analyzer (Sievers M9 Portable TOC Analyzer, Veolia Water Technologies). MCs are wet scrubbers that operate by concentrating water soluble gases from a large volume of air into a small volume of water through turbulent mixing of air with water as a mist.[359] MCs are an efficient collection system for water soluble gases ($K_H \geq 10^2$ M $atm^{-1}$).[360,361] The collection efficiency of the MC used in this study was verified using serial measurements[360] with formic acid and was determined to be 97.1% ± 0.9% (mean ± 1$\sigma$).The general sampling procedure has been employed in a number of ambient studies, including CalNex.[180,362–364] A schematic of the sampling apparatus is shown in Figure C.4. The sampling inlet was ∼ 3 m above ground level, with the MC-TOC system kept inside a laboratory room. Particles were scrubbed from the sampling stream using a PTFE membrane filter (1.0 $\mu$m pore size, 47 mm diameter). 10 mL of nanopure (18.2 MΩ cm) was sampled in the MCs for 5 min. The chamber was rinsed in between samples; total sample cycle time was approximately 14 min. A programmable syringe pump was used to automatically route water through the system. A vacuum pump and automated value were used to control air flow. Flow rates were measured throughout the campaign and were consistent at 29.15 ± 0.07 L air $min^{-1}$. Mass concentrations of $WSOC_g$ ($\mu$g C $m^{-3}$) were determined using the flow rate and final sample volume. Evaporative loss in MC sampling is expected, and final sample volume for these sampling conditions is determined to be 9.22 ± 0.18 mL.

After collection, an aliquot of the sample is routed to the TOC analyzer through an automated port (VICI). The TOC analyzer is operated in Turbo mode, taking one measurement every 4 s, and samples each aliquot for approximately 2 min. An average value ($n \geq 10$) is presented for each sample. Factory calibration of the analyzer is verified periodically throughout the campaign using sucrose ($\geq 99.5\%$ purity, Sigma Aldrich BioXtra) standards in the range of 25-1000 ppbC. All measured ambient concentrations in Irvine are within the range of the verification standards. Nanopure water was used for all samples and was replaced once a day. A dynamic blank was taken each time the water was replaced, where the vacuum pump was turned off and the rest of the sampling procedure was performed as usual. Dynamic blank values were generally $< 10$ ppbC throughout the campaign. The limit of detection was determined as 3 times the standard deviation ($\sigma$) of the dynamic blanks, 0.40 $\mu$g C m$^{-3}$ after unit conversion.[364] All WSOC$_g$ mass concentrations presented here are blank subtracted to account for background TOC. The overall uncertainty in this method, based on the propagation of the uncertainties described above, is estimated to be 10%, similar to the reported uncertainty of the Pasadena WSOC$_g$ measurements (8%).[362]

NO, $NO_2$, $O_3$ were measured in both campaigns. In Pasadena, $NO_x$ species were measured using chemiluminescence (model 42i-TL, Thermo Electron Instruments), and $O_3$ was measured using UV differential absorption (model 49c, Thermo Environmental Instruments).[338] Mixing ratios are available as one-minute averages for each species. Similar measurement techniques were employed in Irvine. $NO_x$ was measured using a commercial instrument that measures $NO_2$ by direct absorption and NO by reaction with ozone to produce $NO_2$ (model 405 nm, 2B Tech). This instrument was calibrated using a commercially prepared gas cylinder (Linde Plc.). Ozone was measured using a commercial instrument that measures absorption at 254 nm (model 106-L, 2B Tech). Measurements of both $NO_x$ and ozone were performed every 10 s. Odd oxygen ($O_x$) is defined as the sum of $O_3$ and $NO_2$, a quantity that is preserved on longer timescales due to the rapid interconversion of these species during the day.[336,365]

To account for differences in time resolution between measurement techniques, hourly averages are used with both Pasadena and Irvine datasets. Apart from campaign data, the 2011 and 2020 National Emissions Inventory (NEI) reports are used to determine changes in VOC and $NO_x$ emissions by sector with time and location.[366,367] The NEI provides emissions estimates for more than 50 granular source sectors, which are consolidated into 11 broad categories (e.g., all solvent-related sectors are aggregated into one Solvent category). Methodologies change between different NEI versions, and inter-annual comparability is limited.[366,367] The 2011 NEI is noted for underestimating VOC emissions from volatile chemical products (VCPs).[368] All emissions attributed to fires are removed. All data analysis was performed using R.[216] Statistical significance is determined using the Mann-Whitney U test, a nonparametric approach appropriate for the comparison of non-normal population distributions, or through Pearson's correlation coefficients.

### 4.3.3 Modeling

Location-specific CMAQ (version 5.4) model simulations of $WSOC_g$, $NO_x$, and $O_3$ are compared to ambient data collected at both sampling locations. We perform a simulation at a 12 km x 12 km horizontal grid resolution over the contiguous United States (CONUS) and employ the Weather Research and Forecasting model (WRFv4.1.1). Gas-phase chemistry and particle microphysics are represented by the Carbon Bond (version 6.3) mechanism and the aero7 submodel, respectively.[369] Anthropogenic and biogenic emissions are from the EPA's Air Quality Time Series (EQUATES).[370] We perform one simulation for July and August in 2017, where July is regarded as spin up period and is not included in the analysis. To determine CMAQ $WSOC_g$, mass concentrations of each species were calculated from model-predicted mixing ratios with the ideal gas law and WRF-predicted meteorology. Mist chamber collection efficiency is simulated for each individual organic gas predicted by CMAQ using Henry's Law coefficients as established by Hennigan et al., 2018.[360]

## 4.4 Results

### 4.4.1 $WSOC_g$ Mass Concentrations in Irvine and Pasadena

The ambient abundance of $WSOC_g$ and $NO_x$ is significantly higher in 2010 in Pasadena relative to Irvine in 2024 (Figure C.5). The median mass concentration of $WSOC_g$ is over 50% higher for Pasadena. Differences are more modest for $NO_x$, with Pasadena mixing ratios ∼30% higher than Irvine. $O_3$ in Irvine is insignificantly higher. Diurnal profiles of each campaign show clear differences in $WSOC_g$ production (Figure 4.2). At Pasadena, $WSOC_g$ concentrations increase rapidly in daylight hours, nearly mirroring the profile of $O_3$. This is indicative of photochemical production of both species, as identified by prior studies.[338,362] $NO_x$ concentrations are lowest in daylight hours and are relatively elevated at night. Strong peaks corresponding to rush hour traffic are absent. In Irvine, $O_3$ follows the expected cycle of photochemical production, with peak values at 15:00. In contrast, $WSOC_g$ and $NO_x$ show little diurnal variation. $WSOC_g$ reaches a maximum value of ∼3 $\mu$g C $m^{-3}$ at 10:00.

Differences observed between the two sampling locations, time periods, and seasons can be attributed to differences in meteorology, emissions, and chemical regimes. Temperature was significantly lower in Irvine and relative humidity was significantly higher, corresponding to the early-spring sampling season and closer proximity to the Pacific Ocean relative to sampling at Pasadena (Figure C.5). County-level emission estimates from the 2011 and 2020 EPA National Emission Inventories (NEI) demonstrate significant VOC reductions in both counties over time, particularly from the Mobile source sector (Figure C.6). Contributions from other sectors are do not change dramatically in terms of fractional contribution, and sector contribution to total emissions is similar between both counties. Regional biogenic emissions are likely less during the Irvine campaign relative to Pasadena. Temperature-dependent VOC emissions are likely to be higher on average in Pasadena, which experiences

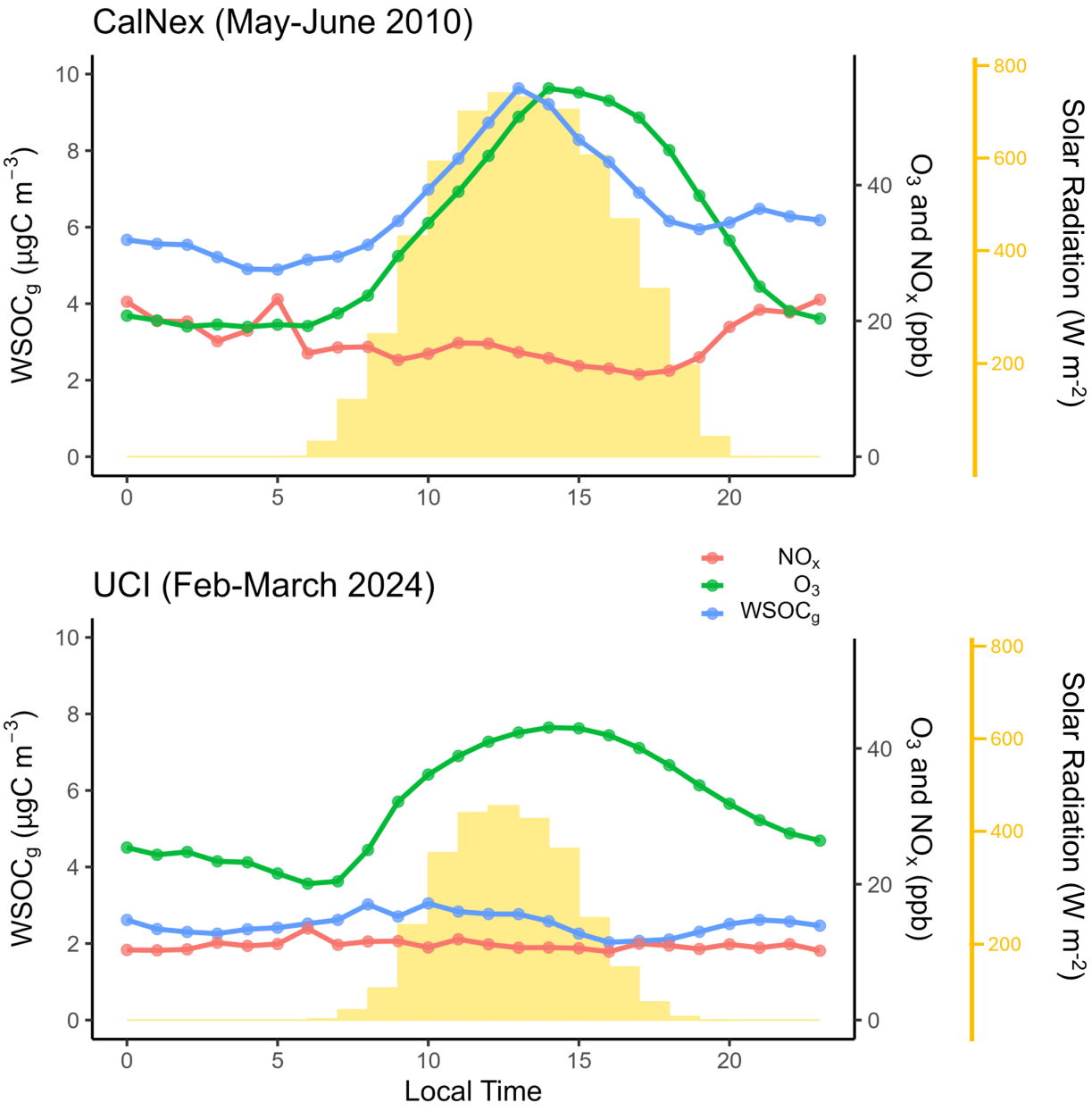


Figure 4.2: Measured diurnal cycles of $WSOC_g$, $O_3$, and $NO_x$ and Pasadena (CalNex) and Irvine (UCI). Shaded yellow regions represent average solar radiation in each campaign.

higher temperatures at its inland location relative to the more coastal Irvine. Emissions of isoprene, a highly reactive dialkene with the greatest mass flux to the atmosphere, exhibit positive associations with temperature and solar flux.[371] Studies suggest that temperature-dependent biogenic VOCs, despite making up a minor fraction of total VOC mixing ratios, contribute significantly to $^{\cdot}$OH reactivity and subsequent $O_3$ and SOA production in SoCAB.[372,373] The greater mass abundance observed and the afternoon peaks in $WSOC_g$ observed in summertime Pasadena relative to spring in Irvine are consistent with these prior findings.

CMAQ predictions are consistent with the spatial differences in abundance (Figure C.7). $WSOC_g$ concentrations are simulated to be over 2x greater in Pasadena than Irvine. The CMAQ simulation is for August of 2017, and differences in actinic flux do not exist within the model and cannot explain the spatial differences in predictions. In both locations, CMAQ appears to overpredict mass concentrations of $WSOC_g$. Mean $WSOC_g$ measured in Pasadena were 5.86 $\mu$g C $m^{-3}$ and simulated mean $WSOC_g$ is 7.62 $\mu$g C $m^{-3}$. In Irvine, measured $WSOC_g$ (mean 2.31 $\mu$g C $m^{-3}$) is more comparable to simulated values (mean 2.61 $\mu$g C $m^{-3}$). CMAQ reproduces the measured diurnal profiles of $O_3$, but fails to describe the diurnal variations in $NO_x$ and $WSOC_g$ (Figure C.8). Simulated $NO_x$ exhibits pronounced peaks in the late morning and evening in both locations, corresponding to rush-hour traffic times, that are not observed in measured values. $WSOC_g$ is simulated to be high throughout the day in Pasadena, with a notable drop in concentrations in the afternoon when $O_3$ is at its maximum, similar to $NO_x$. In Irvine, simulated $WSOC_g$ mass concentrations peak in the morning and evening, also similar to $NO_x$.

### 4.4.2 Associations among $WSOC_g$, $O_x$, and $NO_x$

The relationship between $O_x$ ($O_x = O_3 + NO_2$), $NO_x$, and VOCs helps to elucidate changes in $O_3$ production as a function of emission changes. For example, under $NO_x$-saturated conditions, a decrease in $NO_x$ will increase $O_x$ production.[336] This effect has often been observed in real measurements as a weekend enhancement of $O_3$, i.e., the "weekend effect".[338,342] Increasing concentrations of VOCs are associated with higher maxima of $O_x$ in this regime. In the $NO_x$-limited regime, reductions in $NO_x$ are associated with decreases in $O_x$ production. This regime is much less sensitive to VOC emissions, though increasing VOC is still associated with higher peak $O_x$. Using this method, we can identify the $NO_x$ regimes of each sample location by comparing $O_x$:$NO_x$ on weekdays and weekends (Figure 4.3).

Despite similar $O_3$ concentrations in each study (Figure C.5), $O_x$:$NO_x$ curves indicate different production regimes at each location. $NO_x$ concentrations were significantly lower on weekends in both locations (Figure C.9). In Pasadena, reductions in ambient $NO_x$ concentrations on weekends results in higher weekend $O_x$ concentrations, indicating a $NO_x$-saturated regime. This is consistent with prior studies establishing the weekend ozone effect in LA, including studies from the CalNex data set.[338,342] In Irvine, a slight reduction in $NO_x$ concentrations is observed on the weekends and, in response, a small reduction in $O_x$ occurs. This indicates that Irvine is $NO_x$-limited or transitional regime during the campaign period. The overall downward-left shift in peak $O_x$ and overall data distributions from Calnex 2010 to UCI 2024 suggest reductions in VOC emissions contributed to the long-term reductions observed in $O_3$ across the region.[340,365]

The relationships between $NO_x$ and $O_x$ in both Irvine and Pasadena are consistent with other studies of $O_3$ production in the SoCAB. The relationship of these variables with VOCs and $WSOC_g$ is less clear. $WSOC_g$ is an index of the sum of the polar products of VOC oxidation. This suggests $WSOC_g$ should have discernible statistical associations to VOCs

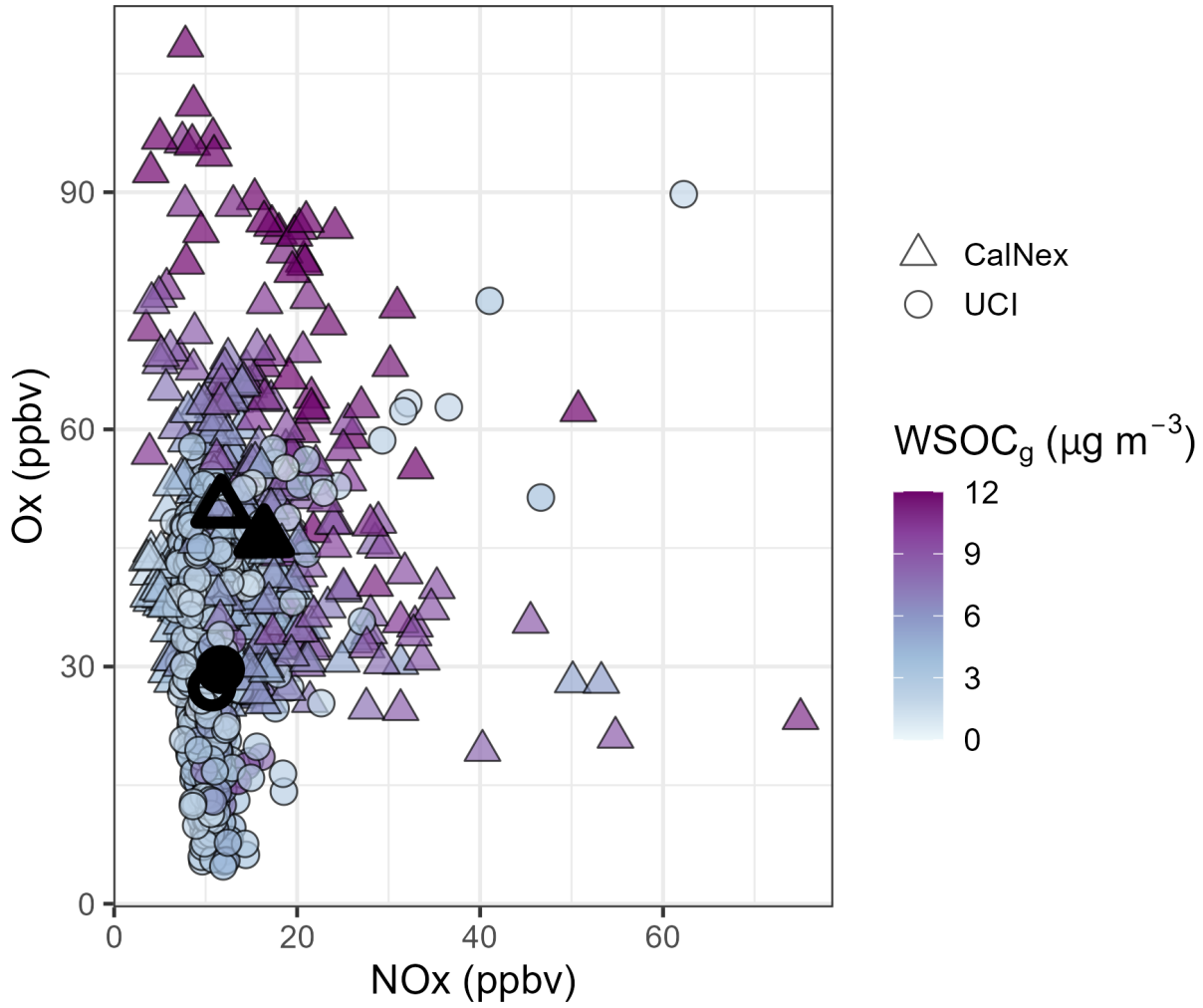


Figure 4.3: Relationship of measured $O_x$, $NO_x$ and $WSOC_g$ at Pasadena (CalNex, triangles) and Irvine (UCI, circles). The bold black points represent the overall campaign average values of $O_x$ and $NO_x$ for weekdays (solid points) and weekends (open points).

in the context of the $O_x$:$NO_x$ curve, with the high $WSOC_g$ concentrations associated with high $O_x$ production. This relationship is clear in Pasadena, where $WSOC_g$ concentrations are greatest when $O_x$ is at its maximum (Figure 4.3). In sharp contrast, the highest $WSOC_g$ mass concentrations observed in Irvine are associated with low $O_x$ concentrations. This suggests $WSOC_g$ production or loss follows different pathways in Pasadena and Irvine. These relationships persist on both weekends and weekdays in both locations (Figure C.10). Weekends show the most similarities between campaigns, though $O_x$ influence on $WSOC_g$ is still clear in Pasadena and absent in Irvine.

$WSOC_g$ in Pasadena is strongly correlated with $O_x$ ($r = 0.62$) across the full campaign dataset (Figure 4.4). More modest correlations are observed with $NO_x$. Irvine, on the other hand, exhibits a negative correlation with $O_x$ ($r = -0.38$). $WSOC_g$ in Irvine is not correlated with $NO_x$. Differences in $NO_x$ associations between locations appear to be driven by $NO_2$. Both Pasadena and Irvine $WSOC_g$ are correlated to NO, but only Pasadena shows correlations between $WSOC_g$ and $NO_2$. These relationships may be influenced by the sampling location on each campus; Irvine measurements were taken adjacent to a loading dock with intermittent fresh $NO_x$ emissions, whereas Pasadena generally receives more aged urban emissions from downtown LA (Figure 4.1).[353] The ratio of NO:$NO_2$ is higher near roadways than in aged plumes.[374] These associations generally remain consistent on weekdays and weekends, though on weekends, the correlation between $WSOC_g$ and $NO_x/NO_2$ in Pasadena is absent, as also observed in $O_x$:$NO_x$ curves (Figure C.10). The persistence of positive $O_x$:$WSOC_g$ correlations in Pasadena and negative $O_x$:$WSOC_g$ in Irvine indicate $NO_x$-regime influence on $WSOC_g$ abundance.

These results suggest that the gas-phase inventory at Irvine in 2024 is less soluble than observed at Pasadena in 2010 as a product of changing $NO_x$ regimes. This chemical shift, however, is not represented by CMAQ outputs (Figure C.11, Figure C.12). In both locations, $WSOC_g$ and $NO_x$ are strongly correlated ($r = 0$ .77 and 0.76 in Irvine and Pasadena respec-

| $WSOC_g$ vs... | NO | $NO_2$ | $NO_x$ | $O_3$ | $O_x$ | Temperature | RH |
|---|---|---|---|---|---|---|---|
| Overall CN | 0.32 | 0.38 | 0.42 | 0.29 | 0.61 | 0.69 | -0.38 |
| Overall UCI | 0.46 | -0.12 | 0.004 | -0.31 | -0.32 | 0.06 | 0.005 |
| Weekday CN | 0.36 | 0.52 | 0.54 | 0.25 | 0.60 | 0.69 | -0.45 |
| Weekday UCI | 0.45 | -0.12 | -0.004 | -0.25 | -0.26 | 0.12 | -0.01 |
| Weekend CN | 0.28 | 0.03 | 0.03 | 0.42 | 0.64 | 0.69 | -0.20 |
| Weekend UCI | 0.51 | -0.17 | 0.09 | -0.44 | -0.46 | -0.09 | 0.03 |

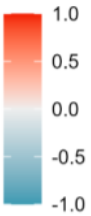


Figure 4.4: Correlation matrix of measured $WSOC_g$ versus other chemical and meteorological variables. Pearson's correlation coefficients are displayed in each cell, and are color-coded according to that value.

tively). $WSOC_g$ and $O_3$, on the other hand, have no strong correlation in either sampling location (r = -0.11 and 0.08 in Irvine and Pasadena respectively). $O_x$:$NO_x$ relationships simulated by CMAQ are also different, with no significant change in $O_x$ concentrations on weekends in either location despite significant decreases in $NO_x$ concentrations (Figure C.11). This indicates that the chemistry governing $WSOC_g$ formation and/or loss is not well represented within the model.

### 4.4.3 Discussion

The exact mechanisms driving differences between $WSOC_g$ abundance and $NO_x$ dependence in Pasadena and Irvine are not fully elucidated. $WSOC_g$ production does not appear to be well-represented in air quality models such as CMAQ. Mass concentrations are overpredicted, and associations among simulated $WSOC_g$, $NO_x$, and $O_3$ species are different from ambient

data at both locations. In contrast, the $O_3$ concentrations and diurnal profiles simulated are similar to ambient measurements. CMAQ is thoroughly evaluated for the prediction of $O_3$ and $PM_{2.5}$, but is not often evaluated for simulating the VOC inventory.[115,375–378] CMAQ's lack of predictive skill towards $WSOC_g$:$O_3$ correlations in both locations reflects poor understanding and/or missing chemical pathways in air quality modeling frameworks. Improved understanding of $WSOC_g$ abundance is important to improve simulations of aqSOA formation and ambient pollution burden.

Much of the focus in ambient and chamber studies is towards semi-volatile partitioning and associated SOA formation. However, the oxidation processes that lead to the formation of semi-volatile or low-volatility products also lead to the formation of more soluble products. While volatility and solubility are highly correlated, they are still distinct variables from one another. Prior works examining volatility and solubility for model applications suggest many functionalized products of anthropogenic and biogenic VOCs are both highly soluble and volatile, especially under high-$NO_x$ conditions.[379] Other modeling studies suggest enhanced aqSOA formation under high $NO_x$ concentrations due to increased availability of $WSOC_g$ in the aqueous phase. In high-$NO_x$ conditions, more low-volatility products form with greater potential to condense onto particles.[380]

These prior findings may help explain the observed trends in $WSOC_g$. In a more $NO_x$-limited environment such as Irvine in 2024, the products of VOC oxidation may be more highly functionalized than those in a $NO_x$-saturated environment such as Pasadena in 2010. These highly functionalized, low-volatility products then may be more prone to depositional loss and dry condensation, resulting in low gas-phase concentrations of WSOC. In Pasadena, the fragmentation and higher volatility of products may enhance gas-phase concentrations and subsequent partitioning to form aq.SOA. Praske et al. 2018[381] suggest autooxidation processes that form highly oxygenated compounds are becoming more important in urban areas as $NO_x$ emissions are reduced, which could be reflected in our findings. More research

is needed to resolve $WSOC_g$ formation and loss pathways in differing chemical regimes.

## 4.5 Conclusions and Future Directions

These results suggest that the ambient VOC inventory is less soluble under low-$NO_x$ and/or $NO_x$-limited conditions. Mass concentrations of $WSOC_g$ are over 50% lower in Irvine in 2024, a $NO_x$-limited or transitional region, relative to Pasadena in 2010, a $NO_x$-saturated regime. Differences in primary VOC emissions, wind patterns, and actinic flux explain some of this decrease; however, differences in the correlation of $WSOC_g$, $NO_x$, and $O_3$ between locations suggest perturbations in VOC oxidation chemistry that either (1) reduce the amount of $WSOC_g$ formed, or (2) increase the amount of $WSOC_g$ lost through partitioning to the condensed phase or deposition.

The differences noted in sampling locations and seasons makes quantitative assessment difficult, and more measurements are warranted. Here, we cannot conclusively determine if changes in $WSOC_g$ relationships are due to emission changes, urban transport, changes in oxidation pathways, or the difference in actinic flux between seasons. Several studies have pointed towards a weakening of the weekend effect in SoCAB,[340,341] and suggests that the region is moving towards more $NO_x$-limited conditions overall. $WSOC_g$ measurements in general are quite sparse across the globe, and measurements across a greater variety of chemical environments could better elucidate production mechanisms and the impact towards SOA.

Speciated organic compound information would be valuable to help confirm the findings presented here, available via modeling or measurement approaches. The chemical speciation of $WSOC_g$ has not been widely investigated and remains unclear. CMAQ simulations can provide information on specific compounds and compound classes, which could help reveal which species drive the differences in mass abundances observed here. A more resolved un-

derstanding of the volatility and functionalization of $WSOC_g$ at each site will help inform the mechanisms controlling ambient abundance. A wide variety of chemical information is available from the CalNex Pasadena ground site, which could similarly help confirm shifts in $WSOC_g$ abundance or production pathways. PTR-MS measurements of VOCs are also available at both locations, and the direct comparison of gas-phase species could be elucidating. Immediate next steps on this project include analysis of PTR-MS detected VOCs and further analysis of CMAQ simulations with better time-matching to each campaign to help better resolve the findings presented here.

# Chapter 5

# Summary and Future Directions

## 5.1 Summary

Collectively, the results presented in this dissertation demonstrate the effectiveness of multi-disciplinary approaches to understand the amount and properties of ambient aerosols. The combination of different data sources and products allows for the development of a holistic scientific understanding that represents ambient conditions and pollution burden more robustly than laboratory, remote, or model studies alone. These results also highlight several areas for further research.

### 5.1.1 Data Gap: Air Quality Networks Miss Air Pollution from Concentrated Animal Feeding Operations

Despite the importance of livestock waste for ambient air emissions of ammonia, the effects of animal husbandry practices towards regional particulate air pollution in the CONUS remains unclear. Part of this uncertainty stems from the dearth of surface chemical measure-

ments in agricultural regions and the lack of complete and accessible information pertaining to the locations and sizes of industrial animal operations. Using county-level information from the USDA Census of Agriculture (2002-2017), I find animal unit density at CAFOs is increasing, most notably in the Midwest. I observe concurrent and spatially-similar increases in remotely-detected mixing ratios of ambient ammonia. The correlation between 2017 summertime ammonia derived from ESA's IASI product and 2017 animal unit density at medium-to-large CAFOs is positive and significant ($r = 0.642$; $p \approx 0$). Both AU density and NASA AIRS ammonia show increasing trends over the analyzed time period. Quantitative assessment of air quality impacts remains difficult due to the urban bias of regulatory air quality monitoring sites. Results suggest that air quality improvements in rural and agricultural regions lag behind the national average, presenting an environmental justice issue. These findings also highlight the ability of remote sensing to fill gaps within surface measurements.

### 5.1.2 Aerosol Liquid Water Predictions: Sensitivities and Application towards Aerosol Optical Properties, Radiative Forcing, and Ambient Chemistry

Liquid water is a ubiquitous and important component of ambient aerosol that is challenging to analytically characterize. Due to these measurement limitations, many atmospheric studies rely on thermodynamic models paired with observations of hygroscopic aerosol components to determine ambient mass concentrations and trends. Several uncertainties exist in both the chemical and meteorological inputs used. ALW determined by reverse-mode ISORROPIA-II simulations is significantly different when two common meteorological reanalysis datasets (NARR and ERA5) are employed for observations of temperature and relative humidity. ALW is also sensitive to the chemical composition data used. Inclusion of

both dust ions and ammonium appears to reduce predicted ALW mass relative to calculations employing just sulfate and nitrate mass concentrations. Despite these sensitivities, all data combinations produce a similar, universally decreasing trend at IMPROVE sites across the CONUS. Decreases in ALW mass have important implications for aerosol chemical and physical properties. The role of ALW in aerosol optical and radiative properties is further explored in Applications 1 and 2. In Application 1, wet PM mass provides a plausible explanation for increased AOD and larger particle sizes on cloudy days relative to clear sky conditions in Bondville, IL. Application 2 demonstrates the importance of ALW and other aerosol chemical properties towards surface temperature modulation in the Southeast US warming hole region.

### 5.1.3 Gas-Phase Water Soluble Organic Carbon in the South Coast Air Basin: $NO_x$ Influence on VOC Solubility

The solubility of gas-phase VOCs is an important yet understudied property. Measurements of $WSOC_g$ are sparse in space and time. As such, the chemical composition, formation pathways, and partitioning behavior are uncertain, especially in the context of changing chemical regimes. Mass concentrations of $WSOC_g$ are much lower in Irvine 2024 than Pasadena 2010, likely due to reduced primary emissions of anthropogenic $NO_x$ and VOCs between sampling periods and locations, as well as lower seasonal actinic flux during spring in Irvine that reduces biogenic VOC emission as well as photochemical activity. The correlation between $WSOC_g$, $NO_x$, and $O_x$ is different between the two locations, and points towards $NO_x$ influence on $WSOC_g$ abundance. CMAQ simulations, which are highly tuned to $NO_x$-saturated conditions, fail to reproduce these observed correlations. These results suggest that VOC product distributions are different in $NO_x$ limited and saturated conditions such as Irvine and Pasadena respectively. Correlations in both datasets with NO suggests branching $RO_2$ chemistry in different $NO_x$ regimes plays a role. This may have implications towards the

formation and fate of aqueous SOA as more regions shift towards $NO_x$ limited conditions.

## 5.2 Future Directions

### 5.2.1 Bridging Data Sources and Emission Discrepancies

All three projects investigated here highlight the use of freely available and public data sources, such as long-term weather data and surface air quality measurements, in combination with modeling tools to better quantify ambient conditions. Despite this holistic approach, uncertainties persist. As demonstrated in Chapter 2, regional air quality remains difficult to quantify in key regions. The spatial representativeness of regulatory air quality monitoring sites is generally improving with time across CONUS, but significant gaps in surface measurements still remain. Remote sensing techniques such as the ESA IASI and NASA AIRS satellite products employed here make it harder for pollution to "hide" in such regions, but often lack sufficient spatiotemporal resolution to robustly identify hot spots and hot moments. Likewise, regulatory agencies such as EPA must employ techniques that will withstand court scrutiny and rarely use the latest state-of-the art technologies to record or predict pollutant concentrations. Because the atmospheric lifetime of ammonia is short, ambient concentrations should be spatially reflective of consistent emission sources. EPA's NEI currently employs USDA-reported animal head counts and lookup tables for animal activity and waste treatment to approximate ammonia emissions from livestock. As shown in Chapter 2, animal density may be a more important factor to consider as EPA's current estimates of $NH_3$ emissions do not reflect remotely-detected burden (Figure 5.1, Figure 2.1B).

Beyond ammonia emissions and associated particle pollution, animal husbandry also co-emits species such as methane ($CH_4$) and nitrous oxide ($N_2O$), potent greenhouse gases.[382] $N_2O$ is also an ozone-destructive species, and contributes to $O_3$ depletion in polar regions.[383] The

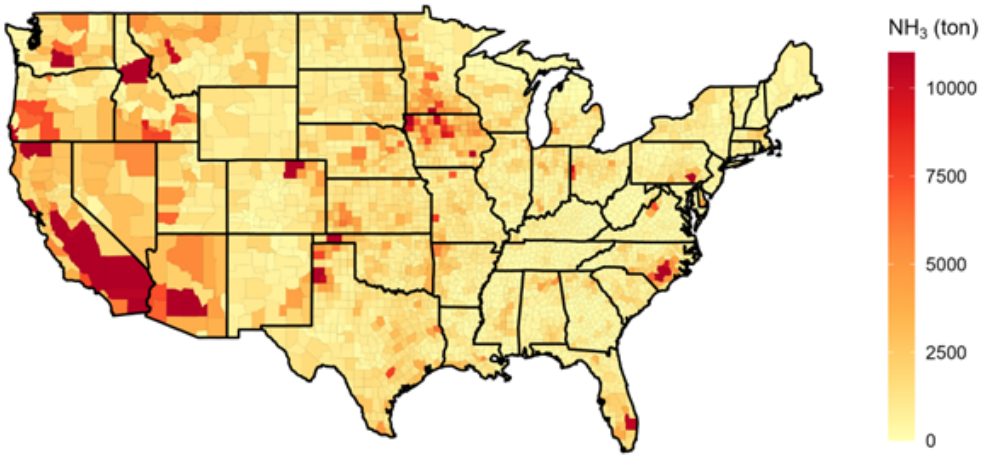


Figure 5.1: County-level emissions of ammonia from all source sectors reported by the 2017 EPA NEI.

budgets of these species remain unclear, and will become increasingly important as we shift towards renewable fuels and reduce $CO_2$ emissions.[384–386] The majority of animal husbandry occurs in the Northern hemisphere, thus presenting a global environmental justice issue as isolated emissions cause warming and destruction of stratospheric ozone elsewhere.

The combination of satellite records and surface datasets may offer the opportunity to better elucidate the budgets and emissions of these species. Some tools already exist to pinpoint sources of $NH_3$, $CH_4$, and $N_2O$ from satellite and aircraft observations; however, these tools suffer for determination of agricultural emissions and temporal resolution. For example, the IASI product has been used to identify ammonia point sources, but identifies much fewer hotspots of agricultural sources than industrial or natural sources, despite the dominance of livestock waste towards overall emissions.[109] Agricultural emissions are highly dependent upon ephemeral soil conditions and microbial activity,[387,388] which may not be well-captured with satellite passover times.

A combination of ground observations of animal unit density with satellite data of emissions and landsat imagery could be employed to positively identify CAFOs and emission plumes for key agricultural pollutants ($CH_4$, $NH_3$, $N_2O$). Landsat data have been used previously for

CAFO identification,[234] and could be used to better elucidate exact farming practices such as silage methods that favor higher gaseous emissions in different regions. This data could be used to inform county-level emissions estimates to better represent ambient pollution burden from agriculture in national inventories.[101] The incorporation of other remote and/or surface measurements such as AOD, $NO_2$, etc. could also help resolve unresolved findings from Chapter 2 regarding the regional air quality impacts and exposures for agricultural workers and rural populations.

### 5.2.2 Aerosol Molality: Effects towards Partitioning and other Physicochemical Properties

The decreasing trends observed in ALW and $WSOC_g$ highlight unquantified changes in aerosol physical and chemical properties. Our understanding of $WSOC_g$ burden and chemical identity is highly uncertain. Surface measurements of $WSOC_g$ are scarce, especially outside the East Coast.[180,363,364] Chapter 4 demonstrates differences in $WSOC_g$ mass concentrations that seem to be driven by differences in $NO_x$ regimes. Model simulations of $WSOC_g$ suggest ambient concentrations are greatest in arid regions, where $WSOC_g$ measurements are especially sparse.[56] A greater amount of $WSOC_g$ measurements in a greater number of chemically diverse locations and seasons will help resolve an uncertain budget. Likewise, chemical characterization of $WSOC_g$ could help confirm the pathways proposed in Chapter 4. Other factors, such as ALW mass and aerosol ionic strength, not well-understood or well-captured in the ambient environment, could have influence over gas- and particle-phase WSOC concentrations as well.

In chapter 3, reductions in ALW mass concentrations appear to be largely driven by reductions in hygroscopic nitrate and sulfate mass. Despite large decreases in the mass concentrations of both salts and ALW, sulfate and nitrate molality in ambient aerosols are increasing

across much of the US (Figure 5.2), suggesting that these components may still influence atmospheric chemistry significantly. As inorganic aerosol components are more easily mitigated, organic aerosol is becoming a more dominant fraction of total mass.[24,25] The feedback between inorganic, organic, and liquid water mass presents a key uncertainty in secondary organic aerosol formation through aqueous pathways.

Salts are well-established to have an effect over gas partitioning. The Hofmeister series, first noted in the 19th century, describes the effect of salts on the stability and solubility of proteins (organic compounds) in biological systems.[389] This series shows a reproducible trend, with varying effects depending on the identity and concentration of the salt.[389] These effects are generally described as "salting in", where salts promote gas partitioning to the condensed phase, and "salting out" where the prescence of salts inhibits partitioning. In ambient aerosol in Baltimore, a "salting out" effect has generally been observed with chloride and sulfate salts, even at low aerosol molalities (<2 mol kg).[311] Aerosol media is expected to surpass 12 mol $kg^{-1}$ in many locations, especially where ALW mass is more limited such as the Southwest.[390] Salting effects are often parameterized through Setschenow coefficients[391], determined through modeling or experimental data. Several studies have developed Setschenow coefficients for a select number of atmospherically-relevant compounds[392–396], but a full understanding of salting effects on ambient aerosol formation remains elusive, especially as aerosol media becomes more concentrated (Figure 5.2). A better understanding of aerosol molality and salting effects may help explain some of the differences observed in $WSOC_g$ concentrations in Chapter 4.

Part of these uncertainties stem from larger uncertainties in the chemical identity of the $WSOC_g$ inventory. While direct measurements of bulk $WSOC_g$ in units of carbon mass are relatively straightforward and easy to automate for field measurements, it is more difficult to chemically identify $WSOC_g$ in mist chamber samples. Mist chamber sample volume is high (10 mL) and organic concentrations are generally low ($\leq$2000 ppbC). Methods to

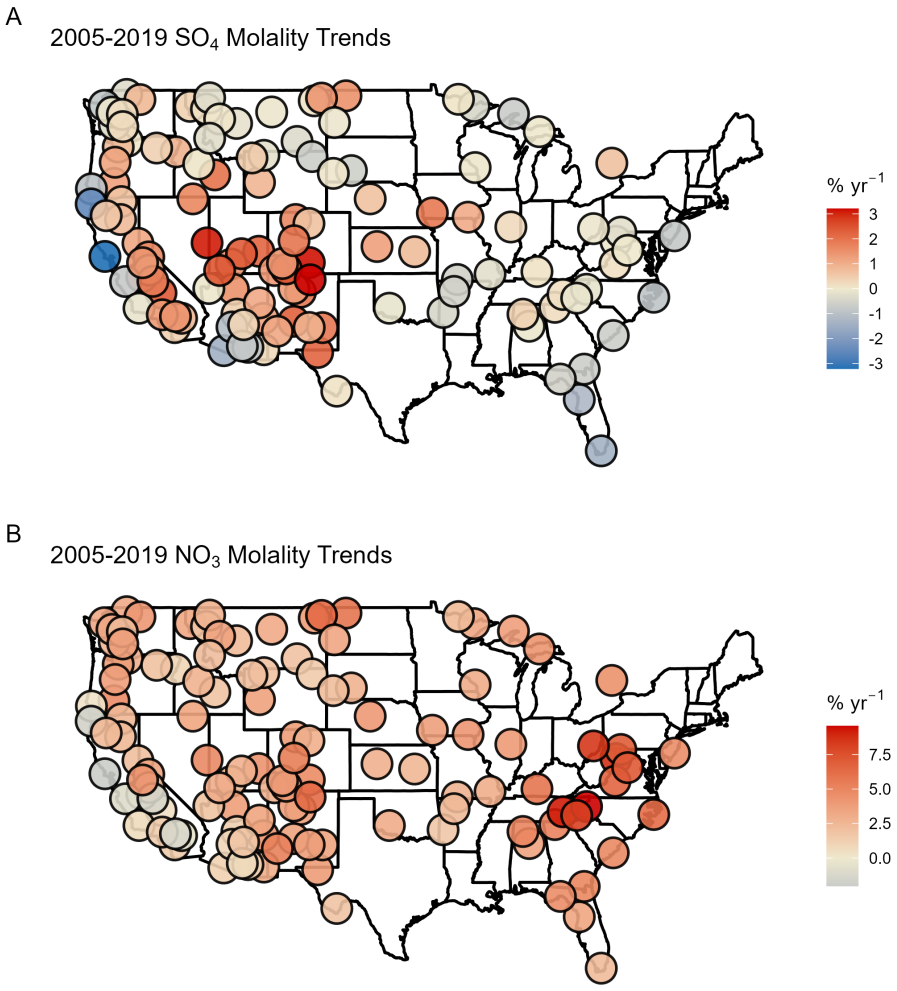


Figure 5.2: Sulfate (A) and nitrate (B) molality (mol $kg^{-1}$) trends at CONUS IMPROVE sites from 2005-2019. Trends are described as the slope of a robust linear regression divided by median concentration over the time period (% $yr^{-1}$).

concentrate and/or remove salts from aqueous samples such as these often involve drying or solvent transfer steps that will drive away volatile species. It is likely that the bulk of ambient $WSOC_g$ largely consists of small (<200 amu) and volatile compounds containing some degree of functionalization, such as acetic or formic acids.[397–399] Salts may also interfere directly with many characterization techniques; even relatively simple approaches such as total organic carbon (TOC) analyzers face interferences in the presence of halogens.[400]

Pairing mist chambers with other online gas-phase measurements may help identify the compounds that primarily contribute to $WSOC_g$ mass, and may also elucidate which compounds drive salting effects observed in prior work.[311] PTR-MS techniques, for example, can detect a wide array of hydrocarbon and oxygenated volatile gas-phase compounds.[401] Mist chamber collection of $WSOC_g$ can be paired with collocated PTR-MS measurements to quantify $WSOC_g$ present in the ambient air, and identify which species were scrubbed efficiently from the mist chamber outflow. Ambient air PTR-MS data is available for both CalNex and Irvine $WSOC_g$ sampling campaigns and may help confirm findings in Chapter 4. Where Setschenow coefficients are available, salt-impacted concentrations could also be estimated to help better resolve online TOC measurements. Other techniques should also be explored to investigate MC samples after collection. Raman spectroscopy, for example, is relatively insensitive to water and can provide information about functional groups, sources, and/or specific chemical constituents.[402,403]

Ambient evidence for salting effects could be found through further examination of environmental databases and prior field campaigns. While $WSOC_g$ measurements are fairly sparse, VOC measurements and particle phase measurements of organic aerosol are more abundant. OC fractions, for example, from regulatory networks could provide information on salting effects towards semivolatile compound and SOA formation. New ASCENT network sites include high time resolution measurements of non-refractory mass[404], which could be used to help further resolve the response of OA to salt molality. The effects of ionic strength

on aerosol properties such as phase state[19] (which will also affect partitioning and diffusion) could also be better elucidated with higher time resolution measurements of chemical constituents paired with AERONET or other optical measurements.

### 5.2.3 Chemical Education: Active and Inclusive Practices in Upper-Division Chemistry Courses

Apart from my atmospheric chemistry research, I also helped develop and implement a themed, argument-driven inquiry, and specifications-grading based curriculum for the second quarter of general chemistry lab (Chem 1LD) at UCI under the guidance of Professor Kimberly Edwards. These efforts resulted in one publication, for which I share first-authorship with Dr. Shannon Saluga and Yong Li.[405] The scope of that work is beyond this dissertation, but the main text of this publication is included here as Appendix D for reference.

In a post-pandemic classroom, garnering student engagement and excitement is especially challenging. Attention spans are generally low,[406]and this problem can become exacerbated for courses like general chemistry lecture and lab, which are commonly a part of "general education" requirements for non-chemistry-major students. Even in majors-series coursework, information retention and the building of cross-course connections between techniques and scientific principles can be a challenge. Some of these issues stem from traditional grading metrics and course schema. For example, typical points-based coursework often promotes competition between students and puts the emphasis on earning points versus mastering course material.[407] Traditional lectures and confirmation-based lab assignments require students to just follow along, without much emphasis on essential scientific skills like collaboration and inquiry.[408,409] Engagement in upper-division coursework especially can be challenging as problems and principles tend to be less tangible and more theoretical.[410]

My publication, "A Specifications-Graded Spice-themed, General Chemistry Laboratory

Course Using an Argument-Driven Inquiry Approach" demonstrates that some of these issues can be overcome through the implementation of active learning and grading practices. Specifications grading practices are becoming more and more common; for example, nearly all undergraduate chemistry lab courses at UCI now employ specifications grading in some capacity. This style of grading is advantageous as it promotes greater mastery of subject matter for students, while still allowing flexibility and cooperation by incorporating peer-review and revisions into assignments and exams.[407] Argument-driven inquiry (ADI) helps build student engagement and scientific thinking skills by allowing students to develop their own procedures and arguments for guiding questions instead of traditional confirmation-based, more "cookbook" style of experiments.[411] The theme employed here serves to keep subject matter relatable for students and to also keep all experiments green and scalable for large-scale courses.[412,413] Surveys of student attitudes for this new course show positive shifts for nearly all parameters, notably with students finding this course to be more relaxed, more organized, and more exciting than the first quarter of general chemistry lab (Figure D7).

While the success of alternative approaches such as these has promoted greater development and implementation for lower-division and non-majors coursework, these practices, especially ADI, are more rarely applied to more advanced chemistry courses. I aim to continue developing these approaches for advanced chemistry courses such as physical and analytical chemistry lecture and lab. Both of these subdisciplines are often barriers for students and traditionally focus heavily towards confirmation-based experiments and problem sets. Greater emphasis on inquiry could improve student engagement and connection-making between topics when tackling upper-division coursework.[414] Similarly, use of specifications and other mastery-based grading schemes can help prevent students from becoming discouraged in these often more-challenging disciplines. The aim of any courses developed would be to focus on environmental applications, easy for students to relate to and with real-world applicability.

# References


[1] McNeill, V. F. Atmospheric Aerosols: Clouds, Chemistry, and Climate. *Annual Review of Chemical and Biomolecular Engineering* **2017**, *8*, 427–444.

[2] Pöschl, U. Atmospheric Aerosols: Composition, Transformation, Climate and Health Effects. *Angewandte Chemie International Edition* **2005**, *44*, 7520–7540, _eprint: https://onlinelibrary.wiley.com/doi/pdf/10.1002/anie.200501122.

[3] Finlayson-Pitts, B. J.; Pitts, J. N. Chemistry of the Upper and Lower Atmosphere. 2000.

[4] Shiraiwa, M.; Li, Y.; Tsimpidi, A. P.; Karydis, V. A.; Berkemeier, T.; Pandis, S. N.; Lelieveld, J.; Koop, T.; Pöschl, U. Global distribution of particle phase state in atmospheric secondary organic aerosols. *Nature Communications* **2017**, *8*, 15002, Publisher: Nature Publishing Group.

[5] EPA, U. Particulate Matter (PM) Basics. 2024; `https://www.epa.gov/pm-pollution/particulate-matter-pm-basics`.

[6] Morawska, L.; Buonanno, G. The physics of particle formation and deposition during breathing. *Nature Reviews Physics* **2021**, *3*, 300–301, Publisher: Nature Publishing Group.

[7] Calvo, A. I.; Alves, C.; Castro, A.; Pont, V.; Vicente, A. M.; Fraile, R. Research on aerosol sources and chemical composition: Past, current and emerging issues. *Atmospheric Research* **2013**, *120-121*, 1–28.

[8] Hallquist, M. et al. The formation, properties and impact of secondary organic aerosol: current and emerging issues. *Atmos. Chem. Phys.* **2009**, *9*, 5155–5236, Number: 14.

[9] Ervens, B.; Turpin, B. J.; Weber, R. J. Secondary organic aerosol formation in cloud droplets and aqueous particles (aqSOA): a review of laboratory, field and model studies. *Atmospheric Chemistry and Physics* **2011**, *11*, 11069–11102, Number: 21 WOS:000296967900020.

[10] Liu, L.; Xu, W.; Lu, X.; Zhong, B.; Guo, Y.; Lu, X.; Zhao, Y.; He, W.; Wang, S.; Zhang, X.; Liu, X.; Vitousek, P. Exploring global changes in agricultural ammonia emissions and their contribution to nitrogen deposition since 1980. *Proceedings of the National Academy of Sciences* **2022**, *119*, e2121998119, Publisher: Proceedings of the National Academy of Sciences.

[11] Bray, C. D.; Battye, W.; Aneja, V. P.; Tong, D. Q.; Lee, P.; Tang, Y. Ammonia emissions from biomass burning in the continental United States. *Atmospheric Environment* **2018**, *187*, 50–61.

[12] Ge, C.; Wang, J.; Carn, S.; Yang, K.; Ginoux, P.; Krotkov, N. Satellite-based global volcanic SO2 emissions and sulfate direct radiative forcing during 2005–2012.

*Journal of Geophysical Research: Atmospheres* **2016**, *121*, 3446–3464, _eprint: https://onlinelibrary.wiley.com/doi/pdf/10.1002/2015JD023134.

[13] Nault, B. A.; Laughner, J. L.; Wooldridge, P. J.; Crounse, J. D.; Dibb, J.; Diskin, G.; Peischl, J.; Podolske, J. R.; Pollack, I. B.; Ryerson, T. B.; Scheuer, E.; Wennberg, P. O.; Cohen, R. C. Lightning NOx Emissions: Reconciling Measured and Modeled Estimates With Updated NOx Chemistry. *Geophysical Research Letters* **2017**, *44*, 9479–9488, _eprint: https://onlinelibrary.wiley.com/doi/pdf/10.1002/2017GL074436.

[14] Sun, Y.-L.; Zhang, Q.; Schwab, J. J.; Demerjian, K. L.; Chen, W.-N.; Bae, M.-S.; Hung, H.-M.; Hogrefe, O.; Frank, B.; Rattigan, O. V.; Lin, Y.-C. Characterization of the sources and processes of organic and inorganic aerosols in New York city with a high-resolution time-of-flight aerosol mass apectrometer. *Atmospheric Chemistry and Physics* **2011**, *11*, 1581–1602, Publisher: Copernicus GmbH.

[15] Wexler, A. S.; Seinfeld, J. H. Second-generation inorganic aerosol model. *Atmospheric Environment. Part A. General Topics* **1991**, *25*, 2731–2748.

[16] LaCount, M. D.; Haeuber, R. A.; Macy, T. R.; Murray, B. A. Reducing power sector emissions under the 1990 Clean Air Act Amendments: A retrospective on 30 years of program development and implementation. *Atmospheric Environment* **2021**, *245*, 118012.

[17] Silva, P. J.; Carlin, R. A.; Prather, K. A. Single particle analysis of suspended soil dust from Southern California. *Atmospheric Environment* **2000**, *34*, 1811–1820.

[18] Cochran, R. E.; Ryder, O. S.; Grassian, V. H.; Prather, K. A. Sea Spray Aerosol: The Chemical Link between the Oceans, Atmosphere, and Climate. *Accounts of Chemical Research* **2017**, *50*, 599–604, Publisher: American Chemical Society.

[19] Richards, D. S.; Trobaugh, K. L.; Hajek-Herrera, J.; Price, C. L.; Sheldon, C. S.; Davies, J. F.; Davis, R. D. Ion-molecule interactions enable unexpected phase transitions in organic-inorganic aerosol. *Science Advances* **2020**, *6*, eabb5643, Publisher: American Association for the Advancement of Science.

[20] Ott, E.-J. E.; Freedman, M. A. Influence of Ions on the Size Dependent Morphology of Aerosol Particles. *ACS Earth and Space Chemistry* **2021**, *5*, 2320–2328, Publisher: American Chemical Society.

[21] Mikhailov, E.; Vlasenko, S.; Martin, S. T.; Koop, T.; Pöschl, U. Amorphous and crystalline aerosol particles interacting with water vapor: conceptual framework and experimental evidence for restructuring, phase transitions and kinetic limitations. *Atmospheric Chemistry and Physics* **2009**, *9*, 9491–9522, Number: 24.

[22] Hopstock, K.; Carpenter, B.; Patterson, J.; Al-Abadleh, H.; Nizkorodov, S. A. Formation of insoluble brown carbon through iron-catalyzed reaction of biomass burning organics. *Environmental Science: Atmospheres* **2023**, *3*, 207–220, Publisher: Royal Society of Chemistry.

[23] Al-Abadleh, H. Aging of atmospheric aerosols and the role of iron in catalyzing brown carbon formation. *Environmental Science: Atmospheres* **2021**, *1*, 297–345, Publisher: Royal Society of Chemistry.

[24] Hass-Mitchell, T. et al. Increasing Contributions of Temperature-Dependent Oxygenated Organic Aerosol to Summertime Particulate Matter in New York City. *ACS ES&T Air* **2024**, *1*, 113–128, Publisher: American Chemical Society.

[25] Milando, C.; Huang, L.; Batterman, S. Trends in PM2.5 emissions, concentrations and apportionments in Detroit and Chicago. *Atmospheric Environment* **2016**, *129*, 197–209.

[26] Blanchard, C. L.; Hidy, G. M.; Tanenbaum, S.; Edgerton, E. S.; Hartsell, B. E. The Southeastern Aerosol Research and Characterization (SEARCH) study: Temporal trends in gas and PM concentrations and composition, 1999-2010. *Journal of the Air & Waste Management Association* **2013**, *63*, 247–259, Number: 3 WOS:000322633600001.

[27] Shrivastava, M. et al. Recent advances in understanding secondary organic aerosol: Implications for global climate forcing. *Reviews of Geophysics* **2017**, *55*, 509–559, Number: 2 WOS:000405304200008.

[28] Smith, J. N.; Barsanti, K. C.; Friedli, H. R.; Ehn, M.; Kulmala, M.; Collins, D. R.; Scheckman, J. H.; Williams, B. J.; McMurry, P. H. Observations of aminium salts in atmospheric nanoparticles and possible climatic implications. *Proceedings of the National Academy of Sciences* **2010**, *107*, 6634–6639, Publisher: Proceedings of the National Academy of Sciences.

[29] Guenther, A. B.; Jiang, X.; Heald, C. L.; Sakulyanontvittaya, T.; Duhl, T.; Emmons, L. K.; Wang, X. The Model of Emissions of Gases and Aerosols from Nature version 2.1 (MEGAN2.1): an extended and updated framework for modeling biogenic emissions. *Geoscientific Model Development* **2012**, *5*, 1471–1492, Number: 6.

[30] Gu, P.; Dallmann, T. R.; Li, H. Z.; Tan, Y.; Presto, A. A. Quantifying Urban Spatial Variations of Anthropogenic VOC Concentrations and Source Contributions with a Mobile Sampling Platform. *International Journal of Environmental Research and Public Health* **2019**, *16*, 1632, Number: 9 Publisher: Multidisciplinary Digital Publishing Institute.

[31] Lee, S. C.; Chiu, M. Y.; Ho, K. F.; Zou, S. C.; Wang, X. Volatile organic compounds (VOCs) in urban atmosphere of Hong Kong. *Chemosphere* **2002**, *48*, 375–382.

[32] Goldstein, A. H.; Galbally, I. E. Known and unknown organic constituents in the Earth' s atmosphere. *Environmental Science & Technology* **2007**, *41*, 1514–1521.

[33] Donahue, N. M.; Robinson, A. L.; Stanier, C. O.; Pandis, S. N. Coupled partitioning, dilution, and chemical aging of semivolatile organics. *Environmental Science & Technology* **2006**, *40*, 2635–2643, Number: 8 WOS:000236992700026.

[34] Pankow, J. F. An absorption model of the gas/aerosol partitioning involved in the formation of secondary organic aerosol. *Atmospheric Environment* **1994**, *28*, 189–193.

[35] Ditto, J. C.; Barnes, E. B.; Khare, P.; Takeuchi, M.; Joo, T.; Bui, A. A. T.; Lee-Taylor, J.; Eris, G.; Chen, Y.; Aumont, B.; Jimenez, J. L.; Ng, N. L.; Griffin, R. J.; Gentner, D. R. An omnipresent diversity and variability in the chemical composition of atmospheric functionalized organic aerosol. *Communications Chemistry* **2018**, *1*, 1–13, Publisher: Nature Publishing Group.

[36] Zhang, H. et al. Monoterpenes are the largest source of summertime organic aerosol in the southeastern United States. *Proceedings of the National Academy of Sciences* **2018**, *115*, 2038–2043, Publisher: Proceedings of the National Academy of Sciences.

[37] Isaacman-VanWertz, G. et al. Chemical evolution of atmospheric organic carbon over multiple generations of oxidation. *Nature Chemistry* **2018**, *10*, 462–468, Number: 4 Publisher: Nature Publishing Group.

[38] Chow, J. C.; Watson, J. G.; Chen, L.-W. A.; Chang, M. O.; Robinson, N. F.; Trimble, D.; Kohl, S. The IMPROVE_A Temperature Protocol for Thermal/Optical Carbon Analysis: Maintaining Consistency with a Long-Term Database. *Journal of the Air & Waste Management Association* **2007**, *57*, 1014–1023.

[39] Nguyen, T. K. V.; Zhang, Q.; Jimenez, J. L.; Pike, M.; Carlton, A. G. Liquid Water: Ubiquitous Contributor to Aerosol Mass. *Environmental Science & Technology Letters* **2016**, *3*, 257–263, Number: 7.

[40] Allan, R. P.; Willett, K. M.; John, V. O.; Trent, T. Global Changes in Water Vapor 1979–2020. *Journal of Geophysical Research: Atmospheres* **2022**, *127*, e2022JD036728, _eprint: https://onlinelibrary.wiley.com/doi/pdf/10.1029/2022JD036728.

[41] Pöhlker, M. L. et al. Global organic and inorganic aerosol hygroscopicity and its effect on radiative forcing. *Nature Communications* **2023**, *14*, 6139, Publisher: Nature Publishing Group.

[42] Ford, B.; Heald, C. L. Aerosol loading in the Southeastern United States: reconciling surface and satellite observations. *Atmospheric Chemistry and Physics* **2013**, *13*, 9269–9283.

[43] Attwood, A. R. et al. Trends in sulfate and organic aerosol mass in the Southeast U.S.: Impact on aerosol optical depth and radiative forcing. *Geophysical Research Letters* **2014**, *41*, 7701–7709, Number: 21 WOS:000345518300038.

[44] Jin, X.; Wang, Y.; Li, Z.; Zhang, F.; Xu, W.; Sun, Y.; Fan, X.; Chen, G.; Wu, H.; Ren, J.; Wang, Q.; Cribb, M. Significant contribution of organics to aerosol liquid water content in winter in Beijing, China. *Atmospheric Chemistry and Physics* **2020**, *20*, 901–914, Publisher: Copernicus GmbH.

[45] Novakov, T.; Penner, J. E. Large contribution of organic aerosols to cloud-condensation-nuclei concentrations. *Nature* **1993**, *365*, 823–826, Number: 6449 Publisher: Nature Publishing Group.

[46] Metzger, S.; Abdelkader, M.; Steil, B.; Klingmüller, K. Aerosol water parameterization: long-term evaluation and importance for climate studies. *Atmospheric Chemistry and Physics* **2018**, *18*, 16747–16774, Publisher: Copernicus GmbH.

[47] Jathar, S. H.; Mahmud, A.; Barsanti, K. C.; Asher, W. E.; Pankow, J. F.; Kleeman, M. J. Water uptake by organic aerosol and its influence on gas/particle partitioning of secondary organic aerosol in the United States. *Atmospheric Environment* **2016**, *129*, 142–154.

[48] Bian, H.; Chin, M.; Rodriguez, J. M.; Yu, H.; Penner, J. E.; Strahan, S. Sensitivity of aerosol optical thickness and aerosol direct radiative effect to relative humidity. *Atmospheric Chemistry and Physics* **2009**, *9*, 2375–2386, Publisher: Copernicus GmbH.

[49] Pitchford, M.; Malm, W.; Schichtel, B.; Kumar, N.; Lowenthal, D.; Hand, J. Revised Algorithm for Estimating Light Extinction from IMPROVE Particle Speciation Data. *Journal of the Air & Waste Management Association* **2007**, *57*, 1326–1336, Number: 11.

[50] Malm, W. C.; Sisler, J. F.; Huffman, D.; Eldred, R. A.; Cahill, T. A. Spatial and seasonal trends in particle concentration and optical extinction in the United States. *Journal of Geophysical Research: Atmospheres* **1994**, *99*, 1347–1370, _eprint: https://onlinelibrary.wiley.com/doi/pdf/10.1029/93JD02916.

[51] Tan, Y.; Lim, Y. B.; Altieri, K. E.; Seitzinger, S. P.; Turpin, B. J. Mechanisms leading to oligomers and SOA through aqueous photooxidation: insights from OH radical oxidation of acetic acid and methylglyoxal. *Atmospheric Chemistry and Physics* **2012**, *12*, 801–813, Publisher: Copernicus GmbH.

[52] Reid, J. P.; Bertram, A. K.; Topping, D. O.; Laskin, A.; Martin, S. T.; Petters, M. D.; Pope, F. D.; Rovelli, G. The viscosity of atmospherically relevant organic particles. *Nature Communications* **2018**, *9*, 956, Publisher: Nature Publishing Group.

[53] Tong, H.-J.; Reid, J. P.; Bones, D. L.; Luo, B. P.; Krieger, U. K. Measurements of the timescales for the mass transfer of water in glassy aerosol at low relative humidity and ambient temperature. *Atmospheric Chemistry and Physics* **2011**, *11*, 4739–4754, Publisher: Copernicus GmbH.

[54] Li, Y.; Carlton, A. G.; Shiraiwa, M. Diurnal and Seasonal Variations in the Phase State of Secondary Organic Aerosol Material over the Contiguous US Simulated in CMAQ. *ACS Earth and Space Chemistry* **2021**, *5*, 1971–1982, Publisher: American Chemical Society.

[55] Budisulistiorini, S. H.; Nenes, A.; Carlton, A. G.; Surratt, J. D.; McNeill, V. F.; Pye, H. O. T. Simulating Aqueous-Phase Isoprene-Epoxydiol (IEPOX) Secondary

Organic Aerosol Production During the 2013 Southern Oxidant and Aerosol Study (SOAS). *Environmental Science & Technology* **2017**, *51*, 5026–5034, Number: 9.

[56] Carlton, A. G.; Turpin, B. J. Particle partitioning potential of organic compounds is highest in the Eastern US and driven by anthropogenic water. *Atmospheric Chemistry and Physics* **2013**, *13*, 10203–10214, Publisher: Copernicus GmbH.

[57] Youn, J.-S.; Wang, Z.; Wonaschuetz, A.; Arellano, A.; Betterton, E. A.; Sorooshian, A. Evidence of aqueous secondary organic aerosol formation from biogenic emissions in the North American Sonoran Desert. *Geophysical Research Letters* **2013**, *40*, 3468–3472, Number: 13 WOS:000326396600046.

[58] Christiansen, A. E.; Carlton, A. G.; Porter, W. C. The changing nature of organic carbon over the United States. *Environmental Science & Technology* **2020**, 1052410532, Number: 54.

[59] Sareen, N.; Waxman, E. M.; Turpin, B. J.; Volkamer, R.; Carlton, A. G. Potential of Aerosol Liquid Water to Facilitate Organic Aerosol Formation: Assessing Knowledge Gaps about Precursors and Partitioning. *Environmental Science & Technology* **2017**, *51*, 3327–3335, Publisher: American Chemical Society.

[60] Babila, J. E.; Carlton, A. G.; Hennigan, C. J.; Ghate, V. P. On Aerosol Liquid Water and Sulfate Associations: The Potential for Fine Particulate Matter Biases. *Atmosphere* **2020**, *11*, 194, Number: 2.

[61] Nguyen, T. K. V.; Petters, M. D.; Suda, S. R.; Guo, H.; Weber, R. J.; Carlton, A. G. Trends in particle-phase liquid water during the Southern Oxidant and Aerosol Study. *Atmospheric Chemistry and Physics* **2014**, *14*, 10911–10930, Publisher: Copernicus GmbH.

[62] Titos, G.; Cazorla, A.; Zieger, P.; Andrews, E.; Lyamani, H.; Granados-Muñoz, M. J.; Olmo, F. J.; Alados-Arboledas, L. Effect of hygroscopic growth on the aerosol light-scattering coefficient: A review of measurements, techniques and error sources. *Atmospheric Environment* **2016**, *141*, 494–507.

[63] Sorooshian, A.; Hersey, S.; Brechtel, F. J.; Corless, A.; Flagan, R. C.; Seinfeld, J. H. Rapid, Size-Resolved Aerosol Hygroscopic Growth Measurements: Differential Aerosol Sizing and Hygroscopicity Spectrometer Probe (DASH-SP). *Aerosol Science and Technology* **2008**, *42*, 445–464, Publisher: Taylor & Francis _eprint: https://doi.org/10.1080/02786820802178506.

[64] Wang, Y.; Voliotis, A.; Hu, D.; Shao, Y.; Du, M.; Chen, Y.; Kleinheins, J.; Marcolli, C.; Alfarra, M. R.; McFiggans, G. On the evolution of sub- and super-saturated water uptake of secondary organic aerosol in chamber experiments from mixed precursors. *Atmospheric Chemistry and Physics* **2022**, *22*, 4149–4166, Publisher: Copernicus GmbH.

[65] Guo, H.; Xu, L.; Bougiatioti, A.; Cerully, K. M.; Capps, S. L.; Hite, J. R. J.; Carlton, A. G.; Lee, S.-H.; Bergin, M. H.; Ng, N. L.; Nenes, A.; Weber, R. J. Fine-particle water and pH in the southeastern United States. *Atmospheric Chemistry and Physics* **2015**, *15*, 5211–5228, Publisher: Copernicus GmbH.

[66] Prather, K. A.; Hatch, C. D.; Grassian, V. H. Analysis of Atmospheric Aerosols. *Annual Review of Analytical Chemistry* **2008**, *1*, 485–514, Publisher: Annual Reviews.

[67] IMPROVE Improve – Interagency Monitoring of Protected Visual Environments. 2024; `https://vista.cira.colostate.edu/Improve/`.

[68] EPA, U. Quality Assurance Guidance Document 2.12–Monitoring PM2.5 in Ambient Air Using Designated Reference or Class I Equivalent Methods. 2016; `https://www3.epa.gov/ttnamti1/files/ambient/pm25/qa/m212.pdf`.

[69] EPA, U. Quality Assurance Project Plan for the Photochemical Assessment Monitoring Stations (PAMS) Required Site Network for Speciated Volatile Organic Compounds, Carbonyls, and Meteorological Parameters Including Mixing Layer Height - Revision 1 Model QAPP. 2023; `https://www.epa.gov/system/files/documents/2024-04/pams-qapp-r1-may-2023.pdf`.

[70] Solomon, P. A.; Crumpler, D.; Flanagan, J. B.; Jayanty, R.; Rickman, E. E.; McDade, C. E. U.S. National PM2.5 Chemical Speciation Monitoring Networks—CSN and IMPROVE: Description of networks. *Journal of the Air & Waste Management Association* **2014**, *64*, 1410–1438, Publisher: Taylor & Francis _eprint: https://doi.org/10.1080/10962247.2014.956904.

[71] Gorham, K. A. Comparison of recent speciated PM2.5 data from collocated CSN and IMPROVE measurements. *Atmospheric Environment* **2021**, *244*, 117977, Publisher: Pergamon.

[72] Flesch, M. M.; Christiansen, A. E.; Burns, A. M.; Ghate, V. P.; Carlton, A. G. Ambient Aerosol Is Physically Larger on Cloudy Days in Bondville, Illinois. *ACS Earth and Space Chemistry* **2022**, *6*, 2910–2918, Publisher: American Chemical Society.

[73] Ryerson, T. B. et al. The 2010 California Research at the Nexus of Air Quality and Climate Change (CalNex) field study. *Journal of Geophysical Research: Atmospheres* **2013**, *118*, 5830–5866, _eprint: https://onlinelibrary.wiley.com/doi/pdf/10.1002/jgrd.50331.

[74] Carlton, A. G. et al. Synthesis of the Southeast Atmosphere Studies: Investigating Fundamental Atmospheric Chemistry Questions. *Bulletin of the American Meteorological Society* **2018**, *99*, 547 – 567, Place: Boston MA, USA Publisher: American Meteorological Society.

[75] Martin, S. T. et al. Introduction: Observations and Modeling of the Green Ocean Amazon (GoAmazon2014/5). *Atmospheric Chemistry and Physics* **2016**, *16*, 4785–4797, Publisher: Copernicus GmbH.

[76] Zhang, Q.; Parworth, C. L.; Lechner, M.; Jimenez, J. L. Aerosol Mass Spectrometer Global Database.

[77] NOAA CalNex 2010 LA Ground Site Data Download. `https://csl.noaa.gov/groups/csl7/measurements/2010calnex/Ground/DataDownload/`.

[78] Chen, X. et al. On the sources and sinks of atmospheric VOCs: an integrated analysis of recent aircraft campaigns over North America. *Atmospheric Chemistry and Physics* **2019**, *19*, 9097–9123, Publisher: Copernicus GmbH.

[79] Burkholder, J. B. et al. The Essential Role for Laboratory Studies in Atmospheric Chemistry. *Environmental Science & Technology* **2017**, *51*, 2519–2528.

[80] McMurry, P. H. A review of atmospheric aerosol measurements. *Atmospheric Environment* **2000**, *34*, 1959–1999.

[81] Nizkorodov, S. A.; Laskin, J.; Laskin, A. Molecular chemistry of organic aerosols through the application of high resolution mass spectrometry. *Physical Chemistry Chemical Physics* **2011**, *13*, 3612–3629, Publisher: The Royal Society of Chemistry.

[82] Srivastava, D.; Vu, T. V.; Tong, S.; Shi, Z.; Harrison, R. M. Formation of secondary organic aerosols from anthropogenic precursors in laboratory studies. *npj Climate and Atmospheric Science* **2022**, *5*, 1–30, Publisher: Nature Publishing Group.

[83] Klodt, A. L.; Aiona, P. K.; MacMillan, A. C.; Lee, H. J. J.; Zhang, X.; Helgestad, T.; Novak, G. A.; Lin, P.; Laskin, J.; Laskin, A.; Bertram, T. H.; Cappa, C. D.; Nizkorodov, S. A. Effect of relative humidity, NOx, and ammonia on the physical properties of naphthalene secondary organic aerosols. *Environmental Science: Atmospheres* **2023**, *3*, 991–1007, Publisher: RSC.

[84] Dam, M.; Thomas, A. E.; Smith, J. N. Formation of Highly Oxidized Organic Compounds and Secondary Organic Aerosol from -Thujene Ozonolysis. *The Journal of Physical Chemistry A* **2023**, *127*, 6989–6998, Publisher: American Chemical Society.

[85] Dam, M.; Draper, D. C.; Marsavin, A.; Fry, J. L.; Smith, J. N. Observations of gas-phase products from the nitrate radical-initiated oxidation of four monoterpenes. 2022; `https://acp.copernicus.org/preprints/acp-2021-1020/acp-2021-1020.pdf`.

[86] Klodt, A. L.; Adamek, M.; Dibley, M.; Nizkorodov, S. A.; O'Brien, R. E. Effects of the sample matrix on the photobleaching and photodegradation of toluene-derived secondary organic aerosol compounds. *Atmospheric Chemistry and Physics* **2022**, *22*, 10155–10171, Publisher: Copernicus GmbH.

[87] Ng, N. L.; Chhabra, P. S.; Chan, A. W. H.; Surratt, J. D.; Kroll, J. H.; Kwan, A. J.; McCabe, D. C.; Wennberg, P. O.; Sorooshian, A.; Murphy, S. M.; Dalleska, N. F.; Flagan, R. C.; Seinfeld, J. H. Effect of $NO_x$ level on secondary organic aerosol (SOA) formation from the photooxidation of terpenes. *Atmospheric Chemistry and Physics* **2007**, *7*, 5159–5174, Publisher: Copernicus GmbH.

[88] Zhang, D.; Zhang, R. Ozonolysis of -pinene and -pinene: Kinetics and mechanism. *The Journal of Chemical Physics* **2005**, *122*, 114308.

[89] McVay, R. C.; Zhang, X.; Aumont, B.; Valorso, R.; Camredon, M.; La, Y. S.; Wennberg, P. O.; Seinfeld, J. H. SOA formation from the photooxidation of -pinene: systematic exploration of the simulation of chamber data. *Atmospheric Chemistry and Physics* **2016**, *16*, 2785–2802, Publisher: Copernicus GmbH.

[90] Voliotis, A.; Du, M.; Wang, Y.; Shao, Y.; Alfarra, M. R.; Bannan, T. J.; Hu, D.; Pereira, K. L.; Hamilton, J. F.; Hallquist, M.; Mentel, T. F.; McFiggans, G. Chamber investigation of the formation and transformation of secondary organic aerosol in mixtures of biogenic and anthropogenic volatile organic compounds. *Atmospheric Chemistry and Physics* **2022**, *22*, 14147–14175, Publisher: Copernicus GmbH.

[91] Surratt, J. D.; Chan, A. W. H.; Eddingsaas, N. C.; Chan, M.; Loza, C. L.; Kwan, A. J.; Hersey, S. P.; Flagan, R. C.; Wennberg, P. O.; Seinfeld, J. H. Reactive intermediates revealed in secondary organic aerosol formation from isoprene. *Proceedings of the National Academy of Sciences* **2010**, *107*, 6640–6645, Publisher: Proceedings of the National Academy of Sciences.

[92] Wong, C.; Pazienza, J. E.; Rychnovsky, S. D.; Nizkorodov, S. A. Formation of Chromophores from cis-Pinonaldehyde Aged in Highly Acidic Conditions. *Journal of the American Chemical Society* **2024**, *146*, 11702–11710, Publisher: American Chemical Society.

[93] Hopstock, K. S.; Klodt, A. L.; Xie, Q.; Alvarado, M. A.; Laskin, A.; Nizkorodov, S. A. Photolytic aging of organic aerosol from pyrolyzed urban materials. *Environmental Science: Atmospheres* **2023**, *3*, 1272–1285.

[94] Loza, C. L.; Chhabra, P. S.; Yee, L. D.; Craven, J. S.; Flagan, R. C.; Seinfeld, J. H. Chemical aging of *m*-xylene secondary organic aerosol: laboratory chamber study. *Atmospheric Chemistry and Physics* **2012**, *12*, 151–167, Publisher: Copernicus GmbH.

[95] Porter, W. C.; Jimenez, J. L.; Barsanti, K. C. Quantifying Atmospheric Parameter Ranges for Ambient Secondary Organic Aerosol Formation. *ACS Earth and Space Chemistry* **2021**, *5*, 2380–2397, Publisher: American Chemical Society.

[96] Bilsback, K. R.; He, Y.; Cappa, C. D.; Chang, R. Y.-W.; Croft, B.; Martin, R. V.; Ng, N. L.; Seinfeld, J. H.; Pierce, J. R.; Jathar, S. H. Vapors Are Lost to Walls, Not to Particles on the Wall: Artifact-Corrected Parameters from Chamber Experiments and Implications for Global Secondary Organic Aerosol. *Environmental Science & Technology* **2023**, *57*, 53–63, Publisher: American Chemical Society.

[97] Wennberg, P. O. Let's Abandon the "High NOx" and "Low NOx" Terminology. *ACS ES&T Air* **2024**, *1*, 3–4, Publisher: American Chemical Society.

[98] Peng, Z.; Lee-Taylor, J.; Orlando, J. J.; Tyndall, G. S.; Jimenez, J. L. Organic peroxy radical chemistry in oxidation flow reactors and environmental chambers and their

atmospheric relevance. *Atmospheric Chemistry and Physics* **2019**, *19*, 813–834, Publisher: Copernicus GmbH.

[99] Nihill, K. J.; Ye, Q.; Majluf, F.; Krechmer, J. E.; Canagaratna, M. R.; Kroll, J. H. Influence of the NO/NO2 Ratio on Oxidation Product Distributions under High-NO Conditions. *Environmental Science & Technology* **2021**, *55*, 6594–6601, Publisher: American Chemical Society.

[100] Chow, J. C.; Lowenthal, D. H.; Chen, L.-W. A.; Wang, X.; Watson, J. G. Mass reconstruction methods for PM2.5: a review. *Air Quality, Atmosphere & Health* **2015**, *8*, 243–263.

[101] Streets, D. G. et al. Emissions estimation from satellite retrievals: A review of current capability. *Atmospheric Environment* **2013**, *77*, 1011–1042.

[102] Martin, R. V. Satellite remote sensing of surface air quality. *Atmospheric Environment* **2008**, *42*, 7823–7843.

[103] Coops, N. C.; Duro, D. C.; Wulder, M. A.; Han, T. Estimating afternoon MODIS land surface temperatures (LST) based on morning MODIS overpass, location and elevation information. *International Journal of Remote Sensing* **2007**, *28*, 2391–2396, Publisher: Taylor & Francis _eprint: https://doi.org/10.1080/01431160701294653.

[104] Giles, D. M.; Sinyuk, A.; Sorokin, M. G.; Schafer, J. S.; Smirnov, A.; Slutsker, I.; Eck, T. F.; Holben, B. N.; Lewis, J. R.; Campbell, J. R.; Welton, E. J.; Korkin, S. V.; Lyapustin, A. I. Advancements in the Aerosol Robotic Network (AERONET) Version 3 database – automated near-real-time quality control algorithm with improved cloud screening for Sun photometer aerosol optical depth (AOD) measurements. *Atmospheric Measurement Techniques* **2019**, *12*, 169–209, Publisher: Copernicus GmbH.

[105] Crawford, J.; Pickering, K. E., K.E. DISCOVER-AQ: Advancing strategies for air quality observations in the next decade. *EM Magazine, Air & Waste Management Association* **2014**, *9*, 4–7.

[106] Naeger, A. R.; Newchurch, M. J.; Moore, T.; Chance, K.; Liu, X.; Alexander, S.; Murphy, K.; Wang, B. Revolutionary Air-Pollution Applications from Future Tropospheric Emissions: Monitoring of Pollution (TEMPO) Observations. **2021**, Section: Bulletin of the American Meteorological Society.

[107] NASA TEMPO Mission Overview. `https://tempo.si.edu/overview.html`.

[108] Duren, R. M. et al. California's methane super-emitters. *Nature* **2019**, *575*, 180–184, Publisher: Nature Publishing Group.

[109] Van Damme, M.; Clarisse, L.; Whitburn, S.; Hadji-Lazaro, J.; Hurtmans, D.; Clerbaux, C.; Coheur, P.-F. Industrial and agricultural ammonia point sources exposed. *Nature* **2018**, *564*, 99–103, Number: 7734 Publisher: Nature Publishing Group.

[110] Bulgin, C. E.; Merchant, C. J.; Ghent, D.; Klüser, L.; Popp, T.; Poulsen, C.; Sogacheva, L. Quantifying Uncertainty in Satellite-Retrieved Land Surface Temperature from Cloud Detection Errors. *Remote Sensing* **2018**, *10*, 616, Number: 4 Publisher: Multidisciplinary Digital Publishing Institute.

[111] Liu, B.; Ma, Y.; Gong, W.; Zhang, M.; Wang, W.; Shi, Y. Comparison of AOD from CALIPSO, MODIS, and Sun Photometer under Different Conditions over Central China. *Scientific Reports* **2018**, *8*, 10066, Publisher: Nature Publishing Group.

[112] Kokhanovsky, A. A.; Breon, F. M.; Cacciari, A.; Carboni, E.; Diner, D.; Di Nicolantonio, W.; Grainger, R. G.; Grey, W. M. F.; Höller, R.; Lee, K. H.; Li, Z.; North, P. R. J.; Sayer, A. M.; Thomas, G. E.; von Hoyningen-Huene, W. Aerosol remote sensing over land: A comparison of satellite retrievals using different algorithms and instruments. *Atmospheric Research* **2007**, *85*, 372–394.

[113] King, M. D.; Platnick, S.; Menzel, W. P.; Ackerman, S. A.; Hubanks, P. A. Spatial and Temporal Distribution of Clouds Observed by MODIS Onboard the Terra and Aqua Satellites. *IEEE Transactions on Geoscience and Remote Sensing* **2013**, *51*, 3826–3852.

[114] Christiansen, A. E.; Carlton, A. G.; Henderson, B. H. Differences in fine particle chemical composition on clear and cloudy days. *Atmospheric Chemistry and Physics* **2020**, *20*, 11607–11624.

[115] He, H.; Liang, X.-Z.; Sun, C.; Tao, Z.; Tong, D. Q. The long-term trend and production sensitivity change in the US ozone pollution from observations and model simulations. *Atmospheric Chemistry and Physics* **2020**, *20*, 3191–3208, Publisher: Copernicus GmbH.

[116] Liu, J. C.; Mickley, L. J.; Sulprizio, M. P.; Dominici, F.; Yue, X.; Ebisu, K.; Anderson, G. B.; Khan, R. F. A.; Bravo, M. A.; Bell, M. L. Particulate air pollution from wildfires in the Western US under climate change. *Climatic Change* **2016**, *138*, 655–666.

[117] Elm, J. Toward a Holistic Understanding of the Formation and Growth of Atmospheric Molecular Clusters: A Quantum Machine Learning Perspective. *The Journal of Physical Chemistry A* **2021**, *125*, 895–902, Publisher: American Chemical Society.

[118] Schmedding, R.; Rasool, Q. Z.; Zhang, Y.; Pye, H. O. T.; Zhang, H.; Chen, Y.; Surratt, J. D.; Lopez-Hilfiker, F. D.; Thornton, J. A.; Goldstein, A. H.; Vizuete, W. Predicting secondary organic aerosol phase state and viscosity and its effect on multiphase chemistry in a regional-scale air quality model. *Atmospheric Chemistry and Physics* **2020**, *20*, 8201–8225, Publisher: Copernicus GmbH.

[119] Jin, S.; Demerjian, K. A photochemical box model for urban air quality study. *Atmospheric Environment. Part B. Urban Atmosphere* **1993**, *27*, 371–387.

[120] Fowler, D.; Cape, J. N.; Coyle, M.; Smith, R. I.; Hjellbrekke, A. G.; Simpson, D.; Derwent, R. G.; Johnson, C. E. Modelling photochemical oxidant formation, transport, deposition and exposure of terrestrial ecosystems. *Environmental Pollution* **1999**, *100*, 43–55.

[121] Stein, A. F.; Draxler, R. R.; Rolph, G. D.; Stunder, B. J. B.; Cohen, M. D.; Ngan, F. NOAA's HYSPLIT Atmospheric Transport and Dispersion Modeling System. **2015**, Section: Bulletin of the American Meteorological Society.

[122] Koepke, P. et al. Comparison of Models Used for UV Index Calculations. *Photochemistry and Photobiology* **1998**, *67*, 657–662, _eprint: https://onlinelibrary.wiley.com/doi/pdf/10.1111/j.1751-1097.1998.tb09109.x.

[123] NCAR ACOM: Quick TUV. `https://www.acom.ucar.edu/Models/TUV/Interactive_TUV/`.

[124] Friese, E.; Ebel, A. Temperature Dependent Thermodynamic Model of the System H+NH4+Na+SO42NO3ClH2O. *The Journal of Physical Chemistry A* **2010**, *114*, 11595–11631, Publisher: American Chemical Society.

[125] Gong, W.; Stroud, C.; Zhang, L. Cloud Processing of Gases and Aerosols in Air Quality Modeling. *Atmosphere* **2011**, *2*, 567–616, Number: 4 Publisher: Molecular Diversity Preservation International.

[126] Appel, K. W. et al. The Community Multiscale Air Quality (CMAQ) model versions 5.3 and 5.3.1: system updates and evaluation. *Geoscientific Model Development* **2021**, *14*, 2867–2897, Publisher: Copernicus GmbH.

[127] Shrivastava, M.; Fast, J.; Easter, R.; Gustafson, W. I. J.; Zaveri, R. A.; Jimenez, J. L.; Saide, P.; Hodzic, A. Modeling organic aerosols in a megacity: comparison of simple and complex representations of the volatility basis set approach. *Atmospheric Chemistry and Physics* **2011**, *11*, 6639–6662, Publisher: Copernicus GmbH.

[128] Kanakidou, M. et al. Organic aerosol and global climate modelling: a review. *Atmospheric Chemistry and Physics* **2005**, *5*, 1053–1123, Publisher: Copernicus GmbH.

[129] Zheng, Y.; Thornton, J. A.; Ng, N. L.; Cao, H.; Henze, D. K.; McDuffie, E. E.; Hu, W.; Jimenez, J. L.; Marais, E. A.; Edgerton, E.; Mao, J. Long-term observational constraints of organic aerosol dependence on inorganic species in the southeast US. *Atmospheric Chemistry and Physics* **2020**, *20*, 13091–13107, Publisher: Copernicus GmbH.

[130] Fuller, R. et al. Pollution and health: a progress update. *The Lancet Planetary Health* **2022**, *6*, e535–e547, Publisher: Elsevier.

[131] Calderón-Garcidueñas, L.; Ayala, A. Air Pollution, Ultrafine Particles, and Your Brain: Are Combustion Nanoparticle Emissions and Engineered Nanoparticles Causing Preventable Fatal Neurodegenerative Diseases and Common Neuropsychiatric Outcomes?

*Environmental Science & Technology* **2022**, *56*, 6847–6856, Publisher: American Chemical Society.

[132] Pope III, C. A. Review: Epidemiological Basis for Particulate Air Pollution Health Standards. *Aerosol Science and Technology* **2000**, *32*, 4–14, Publisher: Taylor & Francis _eprint: https://doi.org/10.1080/027868200303885.

[133] Pope, C. A.; Coleman, N.; Pond, Z. A.; Burnett, R. T. Fine particulate air pollution and human mortality: 25+ years of cohort studies. *Environmental Research* **2020**, *183*, 108924.

[134] Organization, W. H. WHO Global Air Quality Guidelines. 2021; `https://iris.who.int/bitstream/handle/10665/345334/9789240034433-eng.pdf`.

[135] EPA, U. Final Rule to Strengthen the National Air Quality Health Standard for Particulate Matter. 2024; `https://www.epa.gov/system/files/documents/2024-02/pm-naaqs-overview.pdf`.

[136] Pai, S. J.; Carter, T. S.; Heald, C. L.; Kroll, J. H. Updated World Health Organization Air Quality Guidelines Highlight the Importance of Non-anthropogenic PM2.5. *Environmental Science & Technology Letters* **2022**, *9*, 501–506, Publisher: American Chemical Society.

[137] Kampa, M.; Castanas, E. Human health effects of air pollution. *Environmental Pollution* **2008**, *151*, 362–367.

[138] Fang, T.; Lakey, P. S. J.; Weber, R. J.; Shiraiwa, M. Oxidative Potential of Particulate Matter and Generation of Reactive Oxygen Species in Epithelial Lining Fluid. *Environmental Science & Technology* **2019**, *53*, 12784–12792, Publisher: American Chemical Society.

[139] Verma, V.; Fang, T.; Xu, L.; Peltier, R. E.; Russell, A. G.; Ng, N. L.; Weber, R. J. Organic Aerosols Associated with the Generation of Reactive Oxygen Species (ROS) by Water-Soluble PM2.5. *Environmental Science & Technology* **2015**, *49*, 4646–4656, Number: 7 WOS:000352659000077.

[140] Jaffe, D. A.; Ninneman, M.; Chan, H. C. NOx and O3 Trends at U.S. Non-Attainment Areas for 1995–2020: Influence of COVID-19 Reductions and Wildland Fires on Policy-Relevant Concentrations. *Journal of Geophysical Research: Atmospheres* **2022**, *127*, e2021JD036385, _eprint: https://onlinelibrary.wiley.com/doi/pdf/10.1029/2021JD036385.

[141] Ainsworth, E. A.; Yendrek, C. R.; Sitch, S.; Collins, W. J.; Emberson, L. D. The Effects of Tropospheric Ozone on Net Primary Productivity and Implications for Climate Change*. *Annual Review of Plant Biology* **2012**, *63*, 637–661, Publisher: Annual Reviews.

[142] Jbaily, A.; Zhou, X.; Liu, J.; Lee, T.-H.; Kamareddine, L.; Verguet, S.; Dominici, F. Air pollution exposure disparities across US population and income groups. *Nature* **2022**, *601*, 228–233, Publisher: Nature Publishing Group.

[143] Colmer, J.; Hardman, I.; Shimshack, J.; Voorheis, J. Disparities in PM2.5 air pollution in the United States. *Science* **2020**, *369*, 575–578, Publisher: American Association for the Advancement of Science.

[144] Zeise, L.; Blumenfeld, J.; August, L.; Bangia, K.; Plummer, L.; Prasad, S.; Ranjbar, K.; Slocombe, A.; Wieland, W. CalEnviroScreen 4.0. **2021**,

[145] Almaraz, M.; Bai, E.; Wang, C.; Trousdell, J.; Conley, S.; Faloona, I.; Houlton, B. Z. Agriculture is a major source of NOx pollution in California. *Science Advances* **2018**, *4*, eaao3477, Number: 1 Publisher: American Association for the Advancement of Science Section: Research Article.

[146] Burnett, R. et al. Global estimates of mortality associated with long-term exposure to outdoor fine particulate matter. *Proceedings of the National Academy of Sciences* **2018**, *115*, 9592–9597, Publisher: Proceedings of the National Academy of Sciences.

[147] Mitchell, D. C.; Armitage, T. L.; Schenker, M. B.; Bennett, D. H.; Tancredi, D. J.; Langer, C. E.; Reynolds, S. J.; Dooley, G.; Mehaffy, J.; Mitloehner, F. M. Particulate Matter, Endotoxin, and Worker Respiratory Health on Large Californian Dairies. *Journal of Occupational and Environmental Medicine* **2015**, *57*, 79–87, Number: 1 Publisher: Lippincott Williams & Wilkins.

[148] on Climate Change (IPCC)ange (IPCC), I. P. *Climate Change 2021 – The Physical Science Basis: Working Group I Contribution to the Sixth Assessment Report of the Intergovernmental Panel on Climate Change*; Cambridge University Press, 2023; pp 817–922.

[149] Shukla, P. R.; Skea, J.; Slade, R. Working Group III Contribution to the Sixth Assessment Report of the Intergovernmental Panel on Climate Change. **2021**,

[150] Zhang, Y.; Forrister, H.; Liu, J.; Dibb, J.; Anderson, B.; Schwarz, J. P.; Perring, A. E.; Jimenez, J. L.; Campuzano-Jost, P.; Wang, Y.; Nenes, A.; Weber, R. J. Top-of-atmosphere radiative forcing affected by brown carbon in the upper troposphere. *Nature Geoscience* **2017**, *10*, 486–489, Publisher: Nature Publishing Group.

[151] Ban-Weiss, G. A.; Cao, L.; Bala, G.; Caldeira, K. Dependence of climate forcing and response on the altitude of black carbon aerosols. *Climate Dynamics* **2012**, *38*, 897–911.

[152] Li, J.; Carlson, B. E.; Yung, Y. L.; Lv, D.; Hansen, J.; Penner, J. E.; Liao, H.; Ramaswamy, V.; Kahn, R. A.; Zhang, P.; Dubovik, O.; Ding, A.; Lacis, A. A.; Zhang, L.; Dong, Y. Scattering and absorbing aerosols in the climate system. *Nature Reviews Earth & Environment* **2022**, *3*, 363–379, Publisher: Nature Publishing Group.

[153] Christensen, M. W.; Jones, W. K.; Stier, P. Aerosols enhance cloud lifetime and brightness along the stratus-to-cumulus transition. *Proceedings of the National Academy of Sciences* **2020**, *117*, 17591–17598, Publisher: Proceedings of the National Academy of Sciences.

[154] McFiggans, G. et al. The effect of physical and chemical aerosol properties on warm cloud droplet activation. *Atmos. Chem. Phys.* **2006**,

[155] Twomey, S. The Influence of Pollution on the Shortwave Albedo of Clouds. **1977**, Section: Journal of the Atmospheric Sciences.

[156] Leibensperger, E. M.; Mickley, L. J.; Jacob, D. J.; Chen, W.-T.; Seinfeld, J. H.; Nenes, A.; Adams, P. J.; Streets, D. G.; Kumar, N.; Rind, D. Climatic effects of 1950–2050 changes in US anthropogenic aerosols – Part 2: Climate response. *Atmospheric Chemistry and Physics* **2012**, *12*, 3349–3362, Publisher: Copernicus GmbH.

[157] Mickley, L. J.; Leibensperger, E. M.; Jacob, D. J.; Rind, D. Regional warming from aerosol removal over the United States: Results from a transient 2010–2050 climate simulation. *Atmospheric Environment* **2012**, *46*, 545–553.

[158] Silvern, R. F.; Jacob, D. J.; Kim, P. S.; Marais, E. A.; Turner, J. R.; Campuzano-Jost, P.; Jimenez, J. L. Inconsistency of ammonium–sulfate aerosol ratios with thermodynamic models in the eastern US: a possible role of organic aerosol. *Atmospheric Chemistry and Physics* **2017**, *17*, 5107–5118, Publisher: Copernicus GmbH.

[159] DeSombre, E. R. The Experience of the Montreal Protocol: Particularly Remarkable, and Remarkably Particular. *UCLA Journal of Environmental Law and Policy* **2000**, *19*, 49–82.

[160] Overview of Sulfur Dioxide (SO2) Air Quality in the United States.

[161] Overview of Nitrogen Dioxide (NO2) Air Quality in the United States.

[162] Hand, J. L.; Prenni, A. J.; Copeland, S.; Schichtel, B. A.; Malm, W. C. Thirty years of the Clean Air Act Amendments: Impacts on haze in remote regions of the United States (1990–2018). *Atmospheric Environment* **2020**, *243*, 117865.

[163] Organization, I. M. RESOLUTION MEPC.320(74) 2019 GUIDELINES FOR CONSISTENT IMPLEMENTATION OF THE 0.50% SULPHUR LIMIT UNDER MARPOL ANNEX VI. 2019; `https://wwwcdn.imo.org/localresources/en/OurWork/Environment/Documents/Resolution%20MEPC.320(74).pdf`.

[164] Diamond, M. S. Detection of large-scale cloud microphysical changes within a major shipping corridor after implementation of the International Maritime Organization 2020 fuel sulfur regulations. *Atmospheric Chemistry and Physics* **2023**, *23*, 8259–8269, Publisher: Copernicus GmbH.

[165] Yuan, T.; Song, H.; Oreopoulos, L.; Wood, R.; Bian, H.; Breen, K.; Chin, M.; Yu, H.; Barahona, D.; Meyer, K.; Platnick, S. Abrupt reduction in shipping emission as an inadvertent geoengineering termination shock produces substantial radiative warming. *Communications Earth & Environment* **2024**, *5*, 1–8, Publisher: Nature Publishing Group.

[166] Collins, D. B.; Farmer, D. K. Unintended Consequences of Air Cleaning Chemistry. *Environmental Science & Technology* **2021**, *55*, 12172–12179, Publisher: American Chemical Society.

[167] Roy, J. California's plastic bag ban is failing. Here's why. 2023; `https://www.latimes.com/environment/story/2023-08-24/whats-the-deal-with-single-use-plastic-bag-bans`, Section: Climate & Environment.

[168] Jones, B. Climate change: How to plant trillions of trees without hurting people and the planet - Vox. *Vox* **2021**,

[169] Thomas, A. E.; Bauer, P. S.; Dam, M.; Perraud, V.; Wingen, L. M.; Smith, J. N. Automotive braking is a source of highly charged aerosol particles. *Proceedings of the National Academy of Sciences* **2024**, *121*, e2313897121, Publisher: Proceedings of the National Academy of Sciences.

[170] Timmers, V. R. J. H.; Achten, P. A. J. Non-exhaust PM emissions from electric vehicles. *Atmospheric Environment* **2016**, *134*, 10–17.

[171] Committee on Developing a Research Agenda and Research Governance Approaches for Climate Intervention Strategies that Reflect Sunlight to Cool Earth; Board on Atmospheric Sciences and Climate; Committee on Science, Technology, and Law; Division on Earth and Life Studies; Policy and Global Affairs; National Academies of Sciences, Engineering, and Medicine *Reflecting Sunlight: Recommendations for Solar Geoengineering Research and Research Governance*; National Academies Press: Washington, D.C., 2021; Pages: 25762.

[172] Delacote, P.; L'Horty, T.; Kontoleon, A.; West, T. A. P.; Creti, A.; Filewod, B.; LeVelly, G.; Guizar-Coutiño, A.; Groom, B.; Elias, M. Strong transparency required for carbon credit mechanisms. *Nature Sustainability* **2024**, *7*, 706–713, Publisher: Nature Publishing Group.

[173] Chiu, Y. T. T.; Carlton, A. G. Aerosol Thermodynamics: Nitrate Loss from Regulatory PM2.5 Filters in California. *ACS ES&T Air* **2024**, *1*, 25–32, Publisher: American Chemical Society.

[174] (NRSP-3), N. A. D. P. Ammonia Monitoring Network (AMoN). 2022.

[175] Pinder, R. W.; Adams, P. J.; Pandis, S. N. Ammonia Emission Controls as a Cost-Effective Strategy for Reducing Atmospheric Particulate Matter in the Eastern United States. *Environmental Science & Technology* **2007**, *41*, 380–386, Number: 2.

[176] Office, U. S. G. A. Concentrated Animal Feeding Operations: EPA Needs More Information and a Clearly Defined Strategy to Protect Air and Water Quality from Pollutants of Concern. 2023; https://www.gao.gov/products/gao-08-944.

[177] Nozière, B. et al. The Molecular Identification of Organic Compounds in the Atmosphere: State of the Art and Challenges. *Chemical Reviews* **2015**, *115*, 3919–3983, Publisher: American Chemical Society.

[178] Worton, D. R.; Decker, M.; Isaacman-VanWertz, G.; Chan, A. W. H.; Wilson, K. R.; Goldstein, A. H. Improved molecular level identification of organic compounds using comprehensive two-dimensional chromatography, dual ionization energies and high resolution mass spectrometry. *Analyst* **2017**, *142*, 2395–2403, Publisher: The Royal Society of Chemistry.

[179] Hamilton, J. F.; Webb, P. J.; Lewis, A. C.; Hopkins, J. R.; Smith, S.; Davy, P. Partially oxidised organic components in urban aerosol using GCXGC-TOF/MS. *Atmospheric Chemistry and Physics* **2004**, *4*, 1279–1290, Publisher: Copernicus GmbH.

[180] Hennigan, C. J.; Bergin, M. H.; Russell, A. G.; Nenes, A.; Weber, R. J. Gas/particle partitioning of water-soluble organic aerosol in Atlanta. *Atmospheric Chemistry and Physics* **2009**, *9*, 3613–3628, Publisher: Copernicus GmbH.

[181] Weber, R. J.; Sullivan, A. P.; Peltier, R. E.; Russell, A.; Yan, B.; Zheng, M.; de Gouw, J.; Warneke, C.; Brock, C.; Holloway, J. S.; Atlas, E. L.; Edgerton, E. A study of secondary organic aerosol formation in the anthropogenic-influenced southeastern United States. *Journal of Geophysical Research: Atmospheres* **2007**, *112*, _eprint: https://onlinelibrary.wiley.com/doi/pdf/10.1029/2007JD008408.

[182] Miyazaki, Y.; Kondo, Y.; Takegawa, N.; Komazaki, Y.; Fukuda, M.; Kawamura, K.; Mochida, M.; Okuzawa, K.; Weber, R. J. Time-resolved measurements of water-soluble organic carbon in Tokyo. *Journal of Geophysical Research: Atmospheres* **2006**, *111*, _eprint: https://onlinelibrary.wiley.com/doi/pdf/10.1029/2006JD007125.

[183] Zhang, X.; Liu, Z.; Hecobian, A.; Zheng, M.; Frank, N. H.; Edgerton, E. S.; Weber, R. J. Spatial and seasonal variations of fine particle water-soluble organic carbon (WSOC) over the southeastern United States: implications for secondary organic aerosol formation. *Atmospheric Chemistry and Physics* **2012**, *12*, 6593–6607, Publisher: Copernicus GmbH.

[184] US EPA, O. Overview of Greenhouse Gases. 2015; https://www.epa.gov/ghgemissions/overview-greenhouse-gases.

[185] US EPA, O. 2017 National Emissions Inventory (NEI) Data. 2017; https://www.epa.gov/air-emissions-inventories/2017-national-emissions-inventory-nei-data.

[186] Aneja, V. P.; Schlesinger, W. H.; Erisman, J. W. Effects of Agriculture upon the Air Quality and Climate: Research, Policy, and Regulations. *Environmental Science & Technology* **2009**, *43*, 4234–4240, Number: 12 Publisher: American Chemical Society.

[187] Hafner, S. D.; Howard, C.; Muck, R. E.; Franco, R. B.; Montes, F.; Green, P. G.; Mitloehner, F.; Trabue, S. L.; Rotz, C. A. Emission of volatile organic compounds from silage: Compounds, sources, and implications. *Atmospheric Environment* **2013**, *77*, 827–839.

[188] Chamanara, S.; Goldstein, B.; Newell, J. P. Where's the beef? Costco's meat supply chain and environmental justice in California. *Journal of Cleaner Production* **2021**, *278*, 123744.

[189] EIA - Greenhouse Gas Emissions - Nitrous Oxide Emissions. 2021; `https://www.eia.gov/environment/emissions/ghg_report/ghg_nitrous.php`.

[190] Portmann, R. W.; Daniel, J. S.; Ravishankara, A. R. Stratospheric ozone depletion due to nitrous oxide: influences of other gases. *Philosophical Transactions of the Royal Society B: Biological Sciences* **2012**, *367*, 1256–1264, Number: 1593.

[191] Bouwman, A. F.; Lee, D. S.; Asman, W. a. H.; Dentener, F. J.; Hoek, K. W. V. D.; Olivier, J. G. J. A global high-resolution emission inventory for ammonia. *Global Biogeochemical Cycles* **1997**, *11*, 561–587, Number: 4 _eprint: https://agupubs.onlinelibrary.wiley.com/doi/pdf/10.1029/97GB02266.

[192] Meng, W.; Zhong, Q.; Yun, X.; Zhu, X.; Huang, T.; Shen, H.; Chen, Y.; Chen, H.; Zhou, F.; Liu, J.; Wang, X.; Zeng, E. Y.; Tao, S. Improvement of a Global High-Resolution Ammonia Emission Inventory for Combustion and Industrial Sources with New Data from the Residential and Transportation Sectors. *Environmental Science & Technology* **2017**, *51*, 2821–2829, Number: 5 Publisher: American Chemical Society.

[193] Pozzer, A.; Tsimpidi, A. P.; Karydis, V. A.; de Meij, A.; Lelieveld, J. Impact of agricultural emission reductions on fine-particulate matter and public health. *Atmospheric Chemistry and Physics* **2017**, *17*, 12813–12826, Publisher: Copernicus GmbH.

[194] Paulot, F.; Jacob, D. J. Hidden Cost of U.S. Agricultural Exports: Particulate Matter from Ammonia Emissions. *Environmental Science & Technology* **2014**, *48*, 903–908, Number: 2 Publisher: American Chemical Society.

[195] Bauer, S. E.; Tsigaridis, K.; Miller, R. Significant atmospheric aerosol pollution caused by world food cultivation. *Geophysical Research Letters* **2016**, *43*, 5394–5400, Number: 10 _eprint: https://agupubs.onlinelibrary.wiley.com/doi/pdf/10.1002/2016GL068354.

[196] Beachley, G.; Rogers, C.; Lavery, T.; Walker, J.; Puchalski, M. Long-Term Trends in Reactive Nitrogen Deposition in the United States. *EM (Pittsburgh, Pa.)* **2019**, *1*, http://nadp.slh.wisc.edu/committees/tdep/reports/EMissue2019/Long–term%20Trends%20in%20N%20Dep.pdf.

[197] Behera, S. N.; Sharma, M.; Aneja, V. P.; Balasubramanian, R. Ammonia in the atmosphere: a review on emission sources, atmospheric chemistry and deposition on terrestrial bodies. *Environmental Science and Pollution Research* **2013**, *20*, 8092–8131.

[198] Li, Y.; Schichtel, B. A.; Walker, J. T.; Schwede, D. B.; Chen, X.; Lehmann, C. M. B.; Puchalski, M. A.; Gay, D. A.; Collett, J. L. Increasing importance of deposition of reduced nitrogen in the United States. *Proceedings of the National Academy of Sciences* **2016**, *113*, 5874–5879, Publisher: Proceedings of the National Academy of Sciences.

[199] Domingo, N. G. G.; Balasubramanian, S.; Thakrar, S. K.; Clark, M. A.; Adams, P. J.; Marshall, J. D.; Muller, N. Z.; Pandis, S. N.; Polasky, S.; Robinson, A. L.; Tessum, C. W.; Tilman, D.; Tschofen, P.; Hill, J. D. Air quality–related health damages of food. *Proceedings of the National Academy of Sciences* **2021**, *118*, Number: 20 Publisher: National Academy of Sciences Section: Physical Sciences.

[200] Heo, J.; Adams, P. J.; Gao, H. O. Public Health Costs of Primary PM2.5 and Inorganic PM2.5 Precursor Emissions in the United States. *Environmental Science & Technology* **2016**, *50*, 6061–6070, Publisher: American Chemical Society.

[201] US EPA, O. Particulate Matter (PM2.5) Trends. 2016; `https://www.epa.gov/air-trends/particulate-matter-pm25-trends`.

[202] Hand, J. L.; Schichtel, B. A.; Malm, W. C.; Pitchford, M. L. Particulate sulfate ion concentration and SO2 emission trends in the United States from the early 1990s through 2010. *Atmospheric Chemistry and Physics* **2012**, *12*, 10353–10365, Number: 21 WOS:000310954400022.

[203] Butler, T. J.; Vermeylen, F. M.; Rury, M.; Likens, G. E.; Lee, B.; Bowker, G. E.; McCluney, L. Response of ozone and nitrate to stationary source NOx emission reductions in the eastern USA. *Atmospheric Environment* **2011**, *45*, 1084–1094.

[204] Warner, J. X.; Dickerson, R. R.; Wei, Z.; Strow, L. L.; Wang, Y.; Liang, Q. Increased atmospheric ammonia over the world's major agricultural areas detected from space. *Geophysical Research Letters* **2017**, *44*, 2875–2884, Number: 6 _eprint: https://agupubs.onlinelibrary.wiley.com/doi/pdf/10.1002/2016GL072305.

[205] Damme, M. V.; Clarisse, L.; Franco, B.; Sutton, M. A.; Erisman, J. W.; Kruit, R. W.; Zanten, M. v.; Whitburn, S.; Hadji-Lazaro, J.; Hurtmans, D.; Clerbaux, C.; Coheur, P.-F. Global, regional and national trends of atmospheric ammonia derived from a decadal (2008–2018) satellite record. *Environmental Research Letters* **2021**, *16*, 055017, Number: 5 Publisher: IOP Publishing.

[206] Hiranuma, N.; Brooks, S. D.; Thornton, D. C. O.; Auvermann, B. W. Atmospheric ammonia mixing ratios at an open-air cattle feeding facility. *Journal of the Air & Waste Management Association (1995)* **2010**, *60*, 210–218, Number: 2.

[207] Miller, D. J.; Sun, K.; Tao, L.; Pan, D.; Zondlo, M. A.; Nowak, J. B.; Liu, Z.; Diskin, G.; Sachse, G.; Beyersdorf, A.; Ferrare, R.; Scarino, A. J. Ammonia and methane dairy emission plumes in the San Joaquin Valley of California from individual feedlot to regional scales. *Journal of Geophysical Research: Atmospheres* **2015**, *120*, 9718–9738, _eprint: https://onlinelibrary.wiley.com/doi/pdf/10.1002/2015JD023241.

[208] Xu, L.; Penner, J. E. Global simulations of nitrate and ammonium aerosols and their radiative effects. *Atmospheric Chemistry and Physics* **2012**, *12*, 9479–9504, Publisher: Copernicus GmbH.

[209] Dennis, R. L.; Mathur, R.; Pleim, J. E.; Walker, J. T. Fate of ammonia emissions at the local to regional scale as simulated by the Community Multiscale Air Quality model. *Atmospheric Pollution Research* **2010**, *1*, 207–214.

[210] Dentener, F. J.; Crutzen, P. J. A three-dimensional model of the global ammonia cycle. *Journal of atmospheric chemistry* **1994**, *19*, 331–369, Publisher: Springer Verlag.

[211] Lencucha, R.; Pal, N. E.; Appau, A.; Thow, A.-M.; Drope, J. Government policy and agricultural production: a scoping review to inform research and policy on healthy agricultural commodities. *Globalization and Health* **2020**, *16*, 11, Number: 1.

[212] US EPA, O. National Pollutant Discharge Elimination System (NPDES). 2014; `https://www.epa.gov/npdes`.

[213] USDA - National Agricultural Statistics Service - Census of Agriculture. 2021; `https://www.nass.usda.gov/AgCensus/`.

[214] Son, J.-Y.; Muenich, R. L.; Schaffer-Smith, D.; Miranda, M. L.; Bell, M. L. Distribution of environmental justice metrics for exposure to CAFOs in North Carolina, USA. *Environmental Research* **2021**, *195*, 110862.

[215] Casey, J. A.; Cushing, L.; Depsky, N.; Morello-Frosch, R. Climate Justice and California's Methane Superemitters: Environmental Equity Assessment of Community Proximity and Exposure Intensity. *Environmental Science & Technology* **2021**, *55*, 14746–14757, Publisher: American Chemical Society.

[216] Team, R. C. R: A language and Environment for Statistical Computing. 2020.

[217] 40 CFR 122.23 – Concentrated animal feeding operations (applicable to State NPDES programs, see § 123.25). 2021; `https://www.ecfr.gov/current/title-40/chapter-I/subchapter-D/part-122/subpart-B/section-122.23`.

[218] Gollehon, N.; Caswell, M.; Ribaudo, M.; Kellogg, R.; Lander, C.; Letson, D. Confined Animal Production and Manure Nutrients.

[219] Guo, X. et al. Validation of IASI Satellite Ammonia Observations at the Pixel Scale Using In Situ Vertical Profiles. *Journal of Geophysical Research: Atmospheres* **2021**, *126*, e2020JD033475, Number: 9 _eprint: https://onlinelibrary.wiley.com/doi/pdf/10.1029/2020JD033475.

[220] Bowman, K. W. TROPESS AIRS-Aqua L2 Ammonia for Forward Stream, Standard Product V1. `https://disc.gsfc.nasa.gov/datasets/TRPSDL2NH3AIRSFS_1/summary`.

[221] Warner, J. X.; Wei, Z.; Strow, L. L.; Dickerson, R. R.; Nowak, J. B. The global tropospheric ammonia distribution as seen in the 13-year AIRS measurement record. *Atmospheric Chemistry and Physics* **2016**, *16*, 5467–5479, Number: 8 Place: Gottingen Publisher: Copernicus Gesellschaft Mbh WOS:000376937000042.

[222] US EPA, O. 2017 National Emissions Inventory (NEI) Technical Support Document (TSD). 2019; https://www.epa.gov/air-emissions-inventories/2017-national-emissions-inventory-nei-technical-support-document-tsd.

[223] AirData website File Download page. 2021; https://aqs.epa.gov/aqsweb/airdata/download_files.html.

[224] Hand, J. L.; Copeland, S. A.; Day, D. E.; Dilner, A. M.; Indresand, H.; Malm, W. C.; McDade, C. E.; Moore, C. T.; Pitchford, M. L.; Schichtel, B. A.; Watson, J. G. Spatial and Seasonal Patterns and Temporal Variability of Haze and its Constituents in the United States: Report V. 2011; https://tinyurl.com/4e4f5xc4.

[225] Karl, T.; Koss, W. J., 1931 Regional and national monthly, seasonal, and annual temperature weighted by area, 1895-1983. **1984**,

[226] ARMS III Farm Production Regions Map. 2022; https://www.nass.usda.gov/Charts_and_Maps/Farm_Production_Expenditures/reg_map_c.php.

[227] USDA ERS - Land and Natural Resources. https://www.ers.usda.gov/data-products/ag-and-food-statistics-charting-the-essentials/land-and-natural-resources/?topicId=a7a658d4-f209-4641-9172-066ca0896abe.

[228] Clarisse, L.; Van Damme, M.; Clerbaux, C.; Coheur, P.-F. Tracking down global $NH_3$ point sources with wind-adjusted superresolution. *Atmospheric Measurement Techniques* **2019**, *12*, 5457–5473, Publisher: Copernicus GmbH.

[229] McQuilling, A. M.; Adams, P. J. Semi-empirical process-based models for ammonia emissions from beef, swine, and poultry operations in the United States. *Atmospheric Environment* **2015**, *120*, 127–136.

[230] Schwede, D. B.; Lear, G. G. A novel hybrid approach for estimating total deposition in the United States. *Atmospheric Environment* **2014**, *92*, 207–220.

[231] Hu, C.; Griffis, T. J.; Frie, A.; Baker, J. M.; Wood, J. D.; Millet, D. B.; Yu, Z.; Yu, X.; Czarnetzki, A. C. A Multiyear Constraint on Ammonia Emissions and Deposition Within the US Corn Belt. *Geophysical Research Letters* **2021**, *48*, e2020GL090865, Number: 6 _eprint: https://agupubs.onlinelibrary.wiley.com/doi/pdf/10.1029/2020GL090865.

[232] Chen, Y. et al. High-resolution hybrid inversion of IASI ammonia columns to constrain US ammonia emissions using the CMAQ adjoint model. *Atmospheric Chemistry and Physics* **2021**, *21*, 2067–2082, Publisher: Copernicus GmbH.

[233] Wang, R.; Guo, X.; Pan, D.; Kelly, J. T.; Bash, J. O.; Sun, K.; Paulot, F.; Clarisse, L.; Van Damme, M.; Whitburn, S.; Coheur, P.-F.; Clerbaux, C.; Zondlo, M. A. Monthly Patterns of Ammonia Over the Contiguous United States at 2-km Resolution. *Geophysical Research Letters* **2021**, *48*, e2020GL090579, _eprint: https://onlinelibrary.wiley.com/doi/pdf/10.1029/2020GL090579.

[234] Handan-Nader, C.; Ho, D. E. Deep learning to map concentrated animal feeding operations. *Nature Sustainability* **2019**, *2*, 298–306, Number: 4 Publisher: Nature Publishing Group.

[235] Kupper, T.; Häni, C.; Neftel, A.; Kincaid, C.; Bühler, M.; Amon, B.; VanderZaag, A. Ammonia and greenhouse gas emissions from slurry storage - A review. *Agriculture, Ecosystems & Environment* **2020**, *300*, 106963.

[236] ICF International Managing Agricultural Land for Greenhouse Gas Mitigation within the United States. 2016; `https://www.usda.gov/sites/default/files/documents/White_Paper_WEB71816.pdf`.

[237] McQuiling, A. Ammonia Emissions from Livestock in the United States: From Farm-Level Models to a New National Inventory. Dissertation, Carneige Mellon University, Pittsburgh, PA, 2016.

[238] Nenes, A.; Pandis, S. N.; Kanakidou, M.; Russell, A. G.; Song, S.; Vasilakos, P.; Weber, R. J. Aerosol acidity and liquid water content regulate the dry deposition of inorganic reactive nitrogen. *Atmospheric Chemistry and Physics* **2021**, *21*, 6023–6033, Publisher: Copernicus GmbH.

[239] USDA ERS - Land and Natural Resources. 2022; `https://www.ers.usda.gov/data-products/ag-and-food-statistics-charting-the-essentials/land-and-natural-resources/?topicId=a7a658d4-f209-4641-9172-066ca0896abe`.

[240] Sicard, P.; Agathokleous, E.; Anenberg, S. C.; De Marco, A.; Paoletti, E.; Calatayud, V. Trends in urban air pollution over the last two decades: A global perspective. *Science of The Total Environment* **2023**, *858*, 160064.

[241] Farkas, C. M.; Moeller, M. D.; Felder, F. A.; Henderson, B. H.; Carlton, A. G. High Electricity Demand in the Northeast U.S.: PJM Reliability Network and Peaking Unit Impacts on Air Quality. *Environmental Science & Technology* **2016**, *50*, 8375–8384, Number: 15 Publisher: American Chemical Society.

[242] Southerland, V. A.; Brauer, M.; Mohegh, A.; Hammer, M. S.; Donkelaar, A. v.; Martin, R. V.; Apte, J. S.; Anenberg, S. C. Global urban temporal trends in fine particulate matter (PM2·5) and attributable health burdens: estimates from global datasets. *The Lancet Planetary Health* **2022**, *6*, e139–e146, Publisher: Elsevier.

[243] Wang, Y.; Puthussery, J. V.; Yu, H.; Liu, Y.; Salana, S.; Verma, V. Sources of cellular oxidative potential of water-soluble fine ambient particulate matter in the Midwestern United States. *Journal of Hazardous Materials* **2022**, *425*, 127777.

[244] Beaupied, B. L.; Martinez, H.; Martenies, S.; McConnel, C. S.; Pollack, I. B.; Giardina, D.; Fischer, E. V.; Jathar, S.; Duncan, C. G.; Magzamen, S. Cows as canaries: The effects of ambient air pollution exposure on milk production and somatic cell count in dairy cows. *Environmental Research* **2022**, *207*, 112197.

[245] Rural Playbook | Build.gov. `https://www.whitehouse.gov/build/resources/rural/`.

[246] USDA ERS - Farm Labor. `https://www.ers.usda.gov/topics/farm-economy/farm-labor/`.

[247] Ma, R.; Li, K.; Guo, Y.; Zhang, B.; Zhao, X.; Linder, S.; Guan, C.; Chen, G.; Gan, Y.; Meng, J. Mitigation potential of global ammonia emissions and related health impacts in the trade network. *Nature Communications* **2021**, *12*, 6308, Number: 1 Publisher: Nature Publishing Group.

[248] Gu, B. et al. Abating ammonia is more cost-effective than nitrogen oxides for mitigating PM2.5 air pollution. *Science* **2021**, *374*, 758–762, Publisher: American Association for the Advancement of Science.

[249] Gilliland, A. B.; Dennis, R. L.; Roselle, S. J.; Pierce, T. E. Seasonal NH3 emission estimates for the eastern United States based on ammonium wet concentrations and an inverse modeling method. *Journal of Geophysical Research: Atmospheres* **2003**, *108*, _eprint: https://onlinelibrary.wiley.com/doi/pdf/10.1029/2002JD003063.

[250] Spencer, M. T.; Shields, L. G.; Prather, K. A. Simultaneous Measurement of the Effective Density and Chemical Composition of Ambient Aerosol Particles. *Environmental Science & Technology* **2007**, *41*, 1303–1309, Publisher: American Chemical Society.

[251] Hodas, N.; Sullivan, A. P.; Skog, K.; Keutsch, F. N.; Collett, J. L. J.; Decesari, S.; Facchini, M. C.; Carlton, A. G.; Laaksonen, A.; Turpin, B. J. Aerosol Liquid Water Driven by Anthropogenic Nitrate: Implications for Lifetimes of Water-Soluble Organic Gases and Potential for Secondary Organic Aerosol Formation. *Environmental Science & Technology* **2014**, *48*, 11127–11136, Publisher: American Chemical Society.

[252] Wu, Z.; Wang, Y.; Tan, T.; Zhu, Y.; Li, M.; Shang, D.; Wang, H.; Lu, K.; Guo, S.; Zeng, L.; Zhang, Y. Aerosol Liquid Water Driven by Anthropogenic Inorganic Salts: Implying Its Key Role in Haze Formation over the North China Plain. *Environmental Science & Technology Letters* **2018**, *5*, 160–166, Number: 3 Publisher: American Chemical Society.

[253] Petters, M. D.; Kreidenweis, S. M. A single parameter representation of hygroscopic growth and cloud condensation nucleus activity. *Atmospheric Chemistry and Physics* **2007**, *7*, 1961–1971, Number: 8.

[254] Engelhart, G. J.; Hildebrandt, L.; Kostenidou, E.; Mihalopoulos, N.; Donahue, N. M.; Pandis, S. N. Water content of aged aerosol. *Atmospheric Chemistry and Physics* **2011**, *11*, 911–920, Publisher: Copernicus GmbH.

[255] Pilinis, C.; Pandis, S. N.; Seinfield, J. H. Sensitivity of direct climate forcing by atmospheric aerosols to aerosol size and composition. *Journal of Geophysical Research: Atmospheres* **1995**, *100*, 18739–18754, _eprint: https://onlinelibrary.wiley.com/doi/pdf/10.1029/95JD02119.

[256] Agency, U. E. P. *Quality Assurance Handbook for Air Pollution Measurement Systems*; Office of Air Quality Planning and Standards Air Quality Assessment Division, 2017; Vol. II.

[257] Noble, C. A.; Vanderpool, R. W.; Peters, T. M.; McElroy, F. F.; Gemmill, D. B.; Wiener, R. W. Federal Reference and Equivalent Methods for Measuring Fine Particulate Matter. *Aerosol Science and Technology* **2001**, *34*, 457–464.

[258] Liu, B. Y. H.; Pui, D. Y. H.; Whitby, K. T.; Kittelson, D. B.; Kousaka, Y.; Mckenzie, R. L. In *Sulfur in the Atmosphere*; Husar, R. B., Lodge, J. P., Moore, D. J., Eds.; Pergamon, 1978; pp 99–104.

[259] Swietlicki, E. et al. Hygroscopic properties of submicrometer atmospheric aerosol particles measured with H-TDMA instruments in various environments—a review. *Tellus B* **2008**, *60*, 432–469, _eprint: https://onlinelibrary.wiley.com/doi/pdf/10.1111/j.1600-0889.2008.00350.x.

[260] Gysel, M.; Crosier, J.; Topping, D. O.; Whitehead, J. D.; Bower, K. N.; Cubison, M. J.; Williams, P. I.; Flynn, M. J.; McFiggans, G. B.; Coe, H. Closure study between chemical composition and hygroscopic growth of aerosol particles during TORCH2. *Atmospheric Chemistry and Physics* **2007**, *7*, 6131–6144, Publisher: Copernicus GmbH.

[261] Andrews, E.; Larson, S. M. Effect of surfactant layers on the size changes of aerosol particles as a function of relative humidity. *Environmental Science & Technology* **1993**, *27*, 857–865.

[262] Fountoukis, C.; Nenes, A. ISORROPIA II: a computationally efficient thermodynamic equilibrium model for K+–Ca2+–Mg2+–NH4+–Na+–SO42–NO3–Cl–H2O aerosols. *Atmos. Chem. Phys.* **2007**, *7*, 4639–4659, Number: 17.

[263] Hennigan, C. J.; Izumi, J.; Sullivan, A. P.; Weber, R. J.; Nenes, A. A critical evaluation of proxy methods used to estimate the acidity of atmospheric particles. *Atmospheric Chemistry and Physics* **2015**, *15*, 2775–2790, Publisher: Copernicus GmbH.

[264] Pye, H. O. T. et al. The Acidity of Atmospheric Particles and Clouds. *Atmospheric Chemistry and Physics Discussions* **2019**, 1–143.

[265] Nguyen, T. K. V.; Ghate, V. P.; Carlton, A. G. Reconciling satellite aerosol optical thickness and surface fine particle mass through aerosol liquid water. *Geophysical Research Letters* **2016**, *43*, 11903–11912, Number: 22 WOS:000393208100049.

[266] Schneider, D. P.; Deser, C.; Fasullo, J.; Trenberth, K. E. Climate Data Guide Spurs Discovery and Understanding. *Eos, Transactions American Geophysical Union* **2013**, *94*, 121–122, _eprint: https://onlinelibrary.wiley.com/doi/pdf/10.1002/2013EO130001.

[267] Hersbach, H. et al. The ERA5 global reanalysis. *Quarterly Journal of the Royal Meteorological Society* **2020**, *146*, 1999–2049, _eprint: https://onlinelibrary.wiley.com/doi/pdf/10.1002/qj.3803.

[268] Mesinger, F. et al. North American Regional Reanalysis. *Bulletin of the American Meteorological Society* **2006**, *87*, 343–360, Publisher: American Meteorological Society Section: Bulletin of the American Meteorological Society.

[269] Keller, J. D.; Wahl, S. Representation of Climate in Reanalyses: An Intercomparison for Europe and North America. **2021**, Section: Journal of Climate.

[270] Fujiwara, M. et al. Introduction to the SPARC Reanalysis Intercomparison Project (S-RIP) and overview of the reanalysis systems. *Atmospheric Chemistry and Physics* **2017**, *17*, 1417–1452, Publisher: Copernicus GmbH.

[271] Sheridan, S. C.; Lee, C. C.; Smith, E. T. A Comparison Between Station Observations and Reanalysis Data in the Identification of Extreme Temperature Events. *Geophysical Research Letters* **2020**, *47*, e2020GL088120, _eprint: https://onlinelibrary.wiley.com/doi/pdf/10.1029/2020GL088120.

[272] Liu, Y.-C.; Di, P.; Chen, S.-H.; Chen, X.; Fan, J.; DaMassa, J.; Avise, J. Climatology of diablo winds in Northern California and their relationships with large-scale climate variabilities. *Climate Dynamics* **2021**, *56*, 1335–1356.

[273] Liu, J.; Chen, E.; Capps, S. L. The first application of a numerically exact, higher-order sensitivity analysis approach for atmospheric modelling: implementation of the hyperdual-step method in the Community Multiscale Air Quality Model (CMAQ) version 5.3.2. *Geoscientific Model Development* **2024**, *17*, 567–585, Publisher: Copernicus GmbH.

[274] Nguyen, T. K. V.; Capps, S. L.; Carlton, A. G. Decreasing Aerosol Water Is Consistent with OC Trends in the Southeast U.S. *Environmental Science & Technology* **2015**, *49*, 7843–7850, Number: 13.

[275] Speer, R. E.; Edney, E. O.; Kleindienst, T. E. Impact of organic compounds on the concentrations of liquid water in ambient PM2.5. *Journal of Aerosol Science* **2003**, *34*, 63–77.

[276] Christiansen, A. E.; Ghate, V. P.; Carlton, A. G. Aerosol Optical Thickness: Organic Composition, Associated Particle Water, and Aloft Extinction. *ACS Earth and Space Chemistry* **2019**, *3*, 403–412, Publisher: American Chemical Society.

[277] Hand, J. L.; Gill, T. E.; Schichtel, B. A. Spatial and seasonal variability in fine mineral dust and coarse aerosol mass at remote sites across the United States. *Journal of Geophysical Research: Atmospheres* **2017**, *122*, 3080–3097, _eprint: https://onlinelibrary.wiley.com/doi/pdf/10.1002/2016JD026290.

[278] Laskin, A.; Laskin, J.; Nizkorodov, S. A. Chemistry of Atmospheric Brown Carbon. *Chemical Reviews* **2015**, *115*, 4335–4382, Publisher: American Chemical Society.

[279] Ghate, V. P.; Carlton, A. G.; Surleta, T.; Burns, A. M. Changes in Aerosols, Meteorology, and Radiation in the Southeastern U.S. Warming Hole Region during 2000 to 2019. **2022**, Section: Journal of Climate.

[280] Improve – Interagency Monitoring of Protected Visual Environments. 2021; `http://vista.cira.colostate.edu/Improve/`.

[281] Agency, U. S. E. P. AirData Pre-Generated Data Files. `https://aqs.epa.gov/aqsweb/airdata/download_files.html`.

[282] Ibebuchi, C. C.; Lee, C. C.; Silva, A.; Sheridan, S. C. Evaluating Apparent Temperature in the Contiguous United States From Four Reanalysis Products Using Artificial Neural Networks. *Journal of Geophysical Research: Machine Learning and Computation* **2024**, *1*, e2023JH000102, _eprint: https://onlinelibrary.wiley.com/doi/pdf/10.1029/2023JH000102.

[283] Gualtieri, G. Analysing the uncertainties of reanalysis data used for wind resource assessment: A critical review. *Renewable and Sustainable Energy Reviews* **2022**, *167*, 112741.

[284] Huang, J. A Simple Accurate Formula for Calculating Saturation Vapor Pressure of Water and Ice. **2018**, Section: Journal of Applied Meteorology and Climatology.

[285] Zhang, X. Data Advisory: Correction of chloride concentrations for filter blank levels. 2019; `https://vista.cira.colostate.edu/improve/Data/QA_QC/Advisory/da0039/da0039_ChlorideOverCorrection.pdf`.

[286] White, W. H. Data Advisory: Over-reporting of sodium in salt-rich samples. 2017; `https://vista.cira.colostate.edu/improve/Data/QA_QC/Advisory/da0037/da0037_Na_matrix.pdf`.

[287] White, W. H. Data Advisory: Increased variation of humidity in the weighing laboratory. 2016; `https://vista.cira.colostate.edu/improve/Data/QA_QC/Advisory/da0035/da0035_IncreasedRH.pdf`.

[288] Burns, A. M.; Chandler, G.; Dunham, K. J.; Carlton, A. G. Data Gap: Air Quality Networks Miss Air Pollution from Concentrated Animal Feeding Operations. *Environmental Science & Technology* **2023**, *57*, 20718–20725, Publisher: American Chemical Society.

[289] AERONET Data Download Tool. `https://aeronet.gsfc.nasa.gov/cgi-bin/webtool_aod_v3`.

[290] Lenssen, N. J. L.; Schmidt, G. A.; Hansen, J. E.; Menne, M. J.; Persin, A.; Ruedy, R.; Zyss, D. Improvements in the GISTEMP Uncertainty Model. *Journal of Geophysical Research: Atmospheres* **2019**, *124*, 6307–6326, _eprint: https://onlinelibrary.wiley.com/doi/pdf/10.1029/2018JD029522.

[291] Platnick, S.; King, M.; Hubanks, P. MODIS Atmosphere L3 Monthly Product. 2017.

[292] Sayer, A. M.; Hsu, N. C.; Bettenhausen, C.; Jeong, M.-J. Validation and uncertainty estimates for MODIS Collection 6 "Deep Blue" aerosol data. *Journal of Geophysical Research: Atmospheres* **2013**, *118*, 7864–7872, _eprint: https://onlinelibrary.wiley.com/doi/pdf/10.1002/jgrd.50600.

[293] Gao, B; Coauthors MOD05_L2 MODIS/Terra Total Precipitable Water Vapor 5-Min L2 Swath 1km and 5km. 2015; `http://modaps.modaps.eosdis.nasa.gov/services/about/products/c6/MOD05_L2.html`.

[294] Zhou, L.; Liu, Q.; Liu, D.; Xie, L.; Qi, L.; Liu, X. Validation of MODIS liquid water path for oceanic nonraining warm clouds: Implications on the vertical profile of cloud water content. *Journal of Geophysical Research: Atmospheres* **2016**, *121*, 4855–4876, _eprint: https://onlinelibrary.wiley.com/doi/pdf/10.1002/2015JD024499.

[295] Loeb, N. G.; Doelling, D. R.; Wang, H.; Su, W.; Nguyen, C.; Corbett, J. G.; Liang, L.; Mitrescu, C.; Rose, F. G.; Kato, S. Clouds and the Earth's Radiant Energy System (CERES) Energy Balanced and Filled (EBAF) Top-of-Atmosphere (TOA) Edition-4.0 Data Product. *Journal of Climate* **2018**, *31*, 895 – 918, Place: Boston MA, USA Publisher: American Meteorological Society.

[296] Kato, S.; Rose, F. G.; Rutan, D. A.; Thorsen, T. J.; Loeb, N. G.; Doelling, D. R.; Huang, X.; Smith, W. L.; Su, W.; Ham, S.-H. Surface Irradiances of Edition 4.0 Clouds and the Earth's Radiant Energy System (CERES) Energy Balanced and Filled (EBAF) Data Product. *Journal of Climate* **2018**, *31*, 4501 – 4527, Place: Boston MA, USA Publisher: American Meteorological Society.

[297] Song, S.; Gao, M.; Xu, W.; Shao, J.; Shi, G.; Wang, S.; Wang, Y.; Sun, Y.; McElroy, M. B. Fine-particle pH for Beijing winter haze as inferred from different thermodynamic equilibrium models. *Atmospheric Chemistry and Physics* **2018**, *18*, 7423–7438, Publisher: Copernicus GmbH.

[298] Goldstein, A. H.; Koven, C. D.; Heald, C. L.; Fung, I. Y. Biogenic carbon and anthropogenic pollutants combine to form a cooling haze over the southeastern United States. *Proceedings of the National Academy of Sciences* **2009**, *106*, 8835–8840, Publisher: Proceedings of the National Academy of Sciences.

[299] Wagner, N. L. et al. In situ vertical profiles of aerosol extinction, mass, and composition over the southeast United States during SENEX and SEAC(4)RS: observations of a modest aerosol enhancement aloft. *Atmospheric Chemistry and Physics* **2015**, *15*, 7085–7102, Number: 12 WOS:000357117500036.

[300] Taskinen, S.; Nordhausen, K. In *Encyclopedia of Mathematical Geosciences*; Daya Sagar, B., Cheng, Q., McKinley, J., Agterberg, F., Eds.; Springer International Publishing: Cham, 2020; pp 1–4.

[301] Malm, W. C.; Schichtel, B. A.; Hand, J. L.; Prenni, A. J. Implications of Organic Mass to Carbon Ratios Increasing Over Time in the Rural United States. *Journal of Geophysical Research: Atmospheres* **2020**, *n/a*, e2019JD031480, Number: n/a.

[302] Khlystov, A.; Stanier, C. O.; Takahama, S.; Pandis, S. N. Water content of ambient aerosol during the Pittsburgh Air Quality Study. *Journal of Geophysical Research: Atmospheres* **2005**, *110*, _eprint: https://onlinelibrary.wiley.com/doi/pdf/10.1029/2004JD004651.

[303] Santarpia, J. L.; Li, R.; Collins, D. R. Direct measurement of the hydration state of ambient aerosol populations. *Journal of Geophysical Research: Atmospheres* **2004**, *109*, _eprint: https://onlinelibrary.wiley.com/doi/pdf/10.1029/2004JD004653.

[304] Rood, M. J.; Shaw, M. A.; Larson, T. V.; Covert, D. S. Ubiquitous nature of ambient metastable aerosol. *Nature* **1989**, *337*, 537–539, Number: 6207.

[305] Yang, Z.; Qian, Y.; Xue, P.; Wang, J.; Chakraborty, T. C.; Pringle, W. J.; Li, J.; Chen, X. Moisture Sources of Precipitation in the Great Lakes Region: Climatology and Recent Changes. *Geophysical Research Letters* **2023**, *50*, e2022GL100682, _eprint: https://onlinelibrary.wiley.com/doi/pdf/10.1029/2022GL100682.

[306] Srivastava, A. K.; Grotjahn, R.; Ullrich, P. A.; Zarzycki, C. Evaluation of precipitation indices in suites of dynamically and statistically downscaled regional climate models over Florida. *Climate Dynamics* **2022**, *58*, 1587–1611.

[307] Achakulwisut, P.; Mickley, L. J.; Anenberg, S. C. Drought-sensitivity of fine dust in the US Southwest: Implications for air quality and public health under future climate change. *Environmental Research Letters* **2018**, *13*, 054025, Publisher: IOP Publishing.

[308] Achakulwisut, P.; Shen, L.; Mickley, L. J. What Controls Springtime Fine Dust Variability in the Western United States? Investigating the 2002–2015 Increase in Fine Dust in the U.S. Southwest. *Journal of Geophysical Research: Atmospheres* **2017**, *122*, 12,449–12,467, _eprint: https://onlinelibrary.wiley.com/doi/pdf/10.1002/2017JD027208.

[309] Tong, D. Q.; Wang, J. X. L.; Gill, T. E.; Lei, H.; Wang, B. Intensified dust storm activity and Valley fever infection in the southwestern United States. *Geophysical Research Letters* **2017**, *44*, 4304–4312, _eprint: https://onlinelibrary.wiley.com/doi/pdf/10.1002/2017GL073524.

[310] Hand, J. L.; Gebhart, K. A.; Schichtel, B. A.; Malm, W. C. Increasing trends in wintertime particulate sulfate and nitrate ion concentrations in the Great Plains of the United States (2000–2010). *Atmospheric Environment* **2012**, *55*, 107–110.

[311] Pratap, V.; Carlton, A. G.; Christiansen, A. E.; Hennigan, C. J. Partitioning of Ambient Organic Gases to Inorganic Salt Solutions: Influence of Salt Identity, Ionic Strength, and pH. *Geophysical Research Letters* **2021**, *48*, e2021GL095247, _eprint: https://onlinelibrary.wiley.com/doi/pdf/10.1029/2021GL095247.

[312] Song, Y.-C.; Lilek, J.; Lee, J. B.; Chan, M. N.; Wu, Z.; Zuend, A.; Song, M. Viscosity and phase state of aerosol particles consisting of sucrose mixed with inorganic salts. *Atmospheric Chemistry and Physics* **2021**, *21*, 10215–10228, Publisher: Copernicus GmbH.

[313] Bohren, C. F.; Huffman, D. R. *Absorption and Scattering of Light by Small Particles*; 1998.

[314] Kupc, A.; Williamson, C.; Wagner, N. L.; Richardson, M.; Brock, C. A. Modification, calibration, and performance of the Ultra-High Sensitivity Aerosol Spectrometer for particle size distribution and volatility measurements during the Atmospheric Tomography Mission (ATom) airborne campaign. *Atmospheric Measurement Techniques* **2018**, *11*, 369–383, Publisher: Copernicus GmbH.

[315] Hering, S.; Eldering, A.; Seinfeld, J. H. Bimodal character of accumulation mode aerosol mass distributions in Southern California. *Atmospheric Environment* **1997**, *31*, 1–11.

[316] Walter, J.; Wall, S. M.; Ondo, J. L.; Winklmayr, W. Modes in the size distributions of atmospheric inorganic aerosol. *Atmospheric Environment. Part A. General Topics* **1990**, *24*, 2349–2359.

[317] Meehl, G. A.; Washington, W. M.; Arblaster, J. M.; Hu, A.; Teng, H.; Tebaldi, C.; Sanderson, B. N.; Lamarque, J.-F.; Conley, A.; Strand, W. G.; White, J. B. Climate System Response to External Forcings and Climate Change Projections in CCSM4. *Journal of Climate* **2012**, *25*, 3661 – 3683, Place: Boston MA, USA Publisher: American Meteorological Society.

[318] Meehl, G. A.; Arblaster, J. M.; Chung, C. T. Y. Disappearance of the southeast U.S. "warming hole" with the late 1990s transition of the Interdecadal Pacific Oscillation. *Geophysical Research Letters* **2015**, *42*, 5564–5570, _eprint: https://onlinelibrary.wiley.com/doi/pdf/10.1002/2015GL064586.

[319] Saxena, V. K.; Yu, S. Searching for a regional fingerprint of aerosol radiative forcing in the southeastern US. *Geophysical Research Letters* **1998**, *25*, 2833–2836, _eprint: https://onlinelibrary.wiley.com/doi/pdf/10.1029/98GL02106.

[320] Tosca, M. G.; Campbell, J.; Garay, M.; Lolli, S.; Seidel, F. C.; Marquis, J.; Kalashnikova, O. Attributing Accelerated Summertime Warming in the Southeast United States to Recent Reductions in Aerosol Burden: Indications from Vertically-Resolved Observations. *Remote Sensing* **2017**, *9*, 674, Number: 7 Publisher: Multidisciplinary Digital Publishing Institute.

[321] Napton, D. E.; Auch, R. F.; Headley, R.; Taylor, J. L. Land changes and their driving forces in the Southeastern United States. *Regional Environmental Change* **2010**, *10*, 37–53.

[322] Liang, X.-Z.; Pan, J.; Zhu, J.; Kunkel, K. E.; Wang, J. X. L.; Dai, A. Regional climate model downscaling of the U.S. summer climate and future change. *Journal of Geophysical Research: Atmospheres* **2006**, *111*, _eprint: https://onlinelibrary.wiley.com/doi/pdf/10.1029/2005JD006685.

[323] Yu, S.; Alapaty, K.; Mathur, R.; Pleim, J.; Zhang, Y.; Nolte, C.; Eder, B.; Foley, K.; Nagashima, T. Attribution of the United States "warming hole": Aerosol indirect effect and precipitable water vapor. *Scientific Reports* **2014**, *4*, 6929, Publisher: Nature Publishing Group.

[324] Cusworth, D. H.; Mickley, L. J.; Leibensperger, E. M.; Iacono, M. J. Aerosol trends as a potential driver of regional climate in the central United States: evidence from observations. *Atmospheric Chemistry and Physics* **2017**, *17*, 13559–13572, Publisher: Copernicus GmbH.

[325] Kunkel, K. E.; Liang, X.-Z.; Zhu, J.; Lin, Y. Can CGCMs Simulate the Twentieth-Century "Warming Hole" in the Central United States? *Journal of Climate* **2006**, *19*, 4137 – 4153, Place: Boston MA, USA Publisher: American Meteorological Society.

[326] Wang, H.; Schubert, S.; Suarez, M.; Chen, J.; Hoerling, M.; Kumar, A.; Pegion, P. Attribution of the Seasonality and Regionality in Climate Trends over the United States during 1950–2000. *Journal of Climate* **2009**, *22*, 2571 – 2590, Place: Boston MA, USA Publisher: American Meteorological Society.

[327] Puma, M. J.; Cook, B. I. Effects of irrigation on global climate during the 20th century. *Journal of Geophysical Research: Atmospheres* **2010**, *115*, _eprint: https://onlinelibrary.wiley.com/doi/pdf/10.1029/2010JD014122.

[328] Misra, V.; Michael, J.-P.; Boyles, R.; Chassignet, E. P.; Griffin, M.; O'Brien, J. J. Reconciling the Spatial Distribution of the Surface Temperature Trends in the Southeastern United States. *Journal of Climate* **2012**, *25*, 3610 – 3618, Place: Boston MA, USA Publisher: American Meteorological Society.

[329] Ellenburg, W. L.; McNider, R. T.; Cruise, J. F.; Christy, J. R. Towards an Understanding of the Twentieth-Century Cooling Trend in the Southeastern United States: Biogeophysical Impacts of Land-Use Change. **2016**, Section: Earth Interactions.

[330] Chan, E. A. W.; Gantt, B.; McDow, S. The reduction of summer sulfate and switch from summertime to wintertime PM2.5 concentration maxima in the United States. *Atmospheric Environment* **2018**, *175*, 25–32.

[331] Bian, Y. X.; Zhao, C. S.; Ma, N.; Chen, J.; Xu, W. Y. A study of aerosol liquid water content based on hygroscopicity measurements at high relative humidity in the North China Plain. *Atmospheric Chemistry and Physics* **2014**, *14*, 6417–6426, Publisher: Copernicus GmbH.

[332] Tan, W.; Yu, Y.; Li, C.; Li, J.; Kang, L.; Dong, H.; Zeng, L.; Zhu, T. Profiling Aerosol Liquid Water Content Using a Polarization Lidar. *Environmental Science & Technology* **2020**, *54*, 3129–3137, Publisher: American Chemical Society.

[333] Ren, J.; Tan, W.; Tian, X.; Wu, Z.; Li, C.; Li, J.; Zhao, C.; Liu, D.; Kang, L.; Zhu, T. Retrieval of aerosol liquid water content from high spectral resolution lidar. *Science of The Total Environment* **2021**, *799*, 149423.

[334] Pusede, S. E.; Steiner, A. L.; Cohen, R. C. Temperature and Recent Trends in the Chemistry of Continental Surface Ozone. *Chemical Reviews* **2015**, *115*, 3898–3918, Publisher: American Chemical Society.

[335] Cooper, O. R. et al. Global distribution and trends of tropospheric ozone: An observation-based review. *Elementa: Science of the Anthropocene* **2014**, *2*, 000029.

[336] Nussbaumer, C. M.; Cohen, R. C. The Role of Temperature and NOx in Ozone Trends in the Los Angeles Basin. *Environmental Science & Technology* **2020**, *54*, 15652–15659, Publisher: American Chemical Society.

[337] Chameides, W.; Fehsenfeld, F.; Rodgers, M.; Cardelino, C.; Martinez, J.; Parrish, D.; Lonneman, W.; Lawson, D.; Rasmussen, R.; Zimmerman, P.; Greenberg, J.; Middleton, P.; Wang, T. Ozone Precursor Relationships in the Ambient Atmosphere. *Journal of Geophysical Research-Atmospheres* **1992**, *97*, 6037–6055, Number: D5 WOS:A1992HQ64400021.

[338] Pollack, I. B. et al. Airborne and ground-based observations of a weekend effect in ozone, precursors, and oxidation products in the California South Coast Air Basin. *Journal of Geophysical Research: Atmospheres* **2012**, *117*, _eprint: https://onlinelibrary.wiley.com/doi/pdf/10.1029/2011JD016772.

[339] Pollack, I. B.; Ryerson, T. B.; Trainer, M.; Neuman, J. A.; Roberts, J. M.; Parrish, D. D. Trends in ozone, its precursors, and related secondary oxidation products in Los Angeles, California: A synthesis of measurements from 1960 to 2010. *Journal of Geophysical Research: Atmospheres* **2013**, *118*, 5893–5911, _eprint: https://onlinelibrary.wiley.com/doi/pdf/10.1002/jgrd.50472.

[340] Simon, H.; Hogrefe, C.; Whitehill, A.; Foley, K. M.; Liljegren, J.; Possiel, N.; Wells, B.; Henderson, B. H.; Valin, L. C.; Tonnesen, G.; Appel, K. W.; Koplitz, S. Revisiting day-of-week ozone patterns in an era of evolving US air quality. *Atmospheric Chemistry and Physics* **2024**, *24*, 1855–1871, Publisher: Copernicus GmbH.

[341] Schroeder, J. R.; Cai, C.; Xu, J.; Ridley, D.; Lu, J.; Bui, N.; Yan, F.; Avise, J. Changing ozone sensitivity in the South Coast Air Basin during the COVID-19 period. *Atmospheric Chemistry and Physics* **2022**, *22*, 12985–13000, Publisher: Copernicus GmbH.

[342] Blanchard, C. L.; Tanenbaum, S. J. Differences between Weekday and Weekend Air Pollutant Levels in Southern California. *Journal of the Air & Waste Management Association* **2003**, *53*, 816–828, Publisher: Taylor & Francis _eprint: https://doi.org/10.1080/10473289.2003.10466222.

[343] Wu, S. et al. O3 Sensitivity to NOx and VOC During RECAP-CA: Implication for Emissions Control Strategies. *ACS ES&T Air* **2024**, *1*, 536–546, Publisher: American Chemical Society.

[344] Fujita, E. M.; Campbell, D. E.; Stockwell, W. R.; Saunders, E.; Fitzgerald, R.; Perea, R. Projected ozone trends and changes in the ozone-precursor relationship in the South Coast Air Basin in response to varying reductions of precursor emissions. *Journal of the Air & Waste Management Association* **2016**, *66*, 201–214, Publisher: Taylor & Francis _eprint: https://doi.org/10.1080/10962247.2015.1106991.

[345] Perdigones, B. C.; Lee, S.; Cohen, R. C.; Park, J.-H.; Min, K.-E. Two Decades of Changes in Summertime Ozone Production in California's South Coast Air Basin. *Environmental Science & Technology* **2022**, *56*, 10586–10595, Publisher: American Chemical Society.

[346] Warneke, C. et al. Photochemical aging of volatile organic compounds in the Los Angeles basin: Weekday-weekend effect. *Journal of Geophysical Research: Atmospheres* **2013**, *118*, 5018–5028, _eprint: https://onlinelibrary.wiley.com/doi/pdf/10.1002/jgrd.50423.

[347] Jenkin, M. E.; Saunders, S. M.; Wagner, V.; Pilling, M. J. Protocol for the development of the Master Chemical Mechanism, MCM v3 (Part B): tropospheric degradation of aromatic volatile organic compounds. *Atmospheric Chemistry and Physics* **2003**, *3*, 181–193, Publisher: Copernicus GmbH.

[348] Saunders, S. M.; Jenkin, M. E.; Derwent, R. G.; Pilling, M. J. Protocol for the development of the Master Chemical Mechanism, MCM v3 (Part A): tropospheric degradation of non-aromatic volatile organic compounds. *Atmospheric Chemistry and Physics* **2003**, *3*, 161–180, Publisher: Copernicus GmbH.

[349] Nie, W. et al. NO at low concentration can enhance the formation of highly oxygenated biogenic molecules in the atmosphere. *Nature Communications* **2023**, *14*, 3347, Publisher: Nature Publishing Group.

[350] Xu, L.; Guo, H.; Weber, R. J.; Ng, N. L. Chemical Characterization of Water-Soluble Organic Aerosol in Contrasting Rural and Urban Environments in the Southeastern United States. *Environmental Science & Technology* **2017**, *51*, 78–88, Publisher: American Chemical Society.

[351] McNeill, V. F. Aqueous Organic Chemistry in the Atmosphere: Sources and Chemical Processing of Organic Aerosols. *Environmental Science & Technology* **2015**, *49*, 1237–1244, Publisher: American Chemical Society.

[352] El-Sayed, M. M. H.; Ortiz-Montalvo, D. L.; Hennigan, C. J. The effects of isoprene and $NO_x$ on secondary organic aerosols formed through reversible and irreversible uptake to aerosol water. *Atmospheric Chemistry and Physics* **2018**, *18*, 1171–1184, Number: 2.

[353] Veres, P. R.; Roberts, J. M.; Cochran, A. K.; Gilman, J. B.; Kuster, W. C.; Holloway, J. S.; Graus, M.; Flynn, J.; Lefer, B.; Warneke, C.; de Gouw, J. Evidence of rapid production of organic acids in an urban air mass. *Geophysical Research Letters* **2011**, *38*, _eprint: https://onlinelibrary.wiley.com/doi/pdf/10.1029/2011GL048420.

[354] Hersey, S. P.; Craven, J. S.; Schilling, K. A.; Metcalf, A. R.; Sorooshian, A.; Chan, M. N.; Flagan, R. C.; Seinfeld, J. H. The Pasadena Aerosol Characterization Observatory (PACO): chemical and physical analysis of the Western Los Angeles basin aerosol. *Atmospheric Chemistry and Physics* **2011**, *11*, 7417–7443, Publisher: Copernicus GmbH.

[355] Washenfelder, R. A. et al. The glyoxal budget and its contribution to organic aerosol for Los Angeles, California, during CalNex 2010. *Journal of Geophysical Research: Atmospheres* **2011**, *116*, _eprint: https://onlinelibrary.wiley.com/doi/pdf/10.1029/2011JD016314.

[356] Griffith, S. M. et al. Measurements of hydroxyl and hydroperoxy radicals during CalNex-LA: Model comparisons and radical budgets. *Journal of Geophysical Research: Atmospheres* **2016**, *121*, 4211–4232, _eprint: https://onlinelibrary.wiley.com/doi/pdf/10.1002/2015JD024358.

[357] Personal Weather Station Dashboard | Weather Underground. `https://www.wunderground.com/dashboard/pws/KCAIRVIN137`.

[358] Herzmann, D. IEM :: Download ASOS/AWOS/METAR Data. `https://mesonet.agron.iastate.edu/request/download.phtml?network=CA_ASOS`.

[359] Cofer, W. R.; Collins, V. G.; Talbot, R. W. Improved aqueous scrubber for collection of soluble atmospheric trace gases. *Environmental Science & Technology* **1985**, *19*, 557–560, Publisher: American Chemical Society.

[360] Hennigan, C. J.; El-Sayed, M. M. H.; Hodzic, A. Detailed characterization of a mist chamber for the collection of water-soluble organic gases. *Atmospheric Environment* **2018**, *188*, 12–17, WOS:000440119000002.

[361] Spaulding, R. S.; Talbot, R. W.; Charles, M. J. Optimization of a Mist Chamber (Cofer Scrubber) for Sampling Water-Soluble Organics in Air. *Environmental Science & Technology* **2002**, *36*, 1798–1808, Number: 8.

[362] Zhang, X.; Liu, J.; Parker, E. T.; Hayes, P. L.; Jimenez, J. L.; de Gouw, J. A.; Flynn, J. H.; Grossberg, N.; Lefer, B. L.; Weber, R. J. On the gas-particle partitioning of soluble organic aerosol in two urban atmospheres with contrasting emissions: 1. Bulk water-soluble organic carbon. *Journal of Geophysical Research: Atmospheres* **2012**, *117*, _eprint: https://onlinelibrary.wiley.com/doi/pdf/10.1029/2012JD017908.

[363] Hennigan, C. J.; Bergin, M. H.; Dibb, J. E.; Weber, R. J. Enhanced secondary organic aerosol formation due to water uptake by fine particles. *Geophysical Research Letters* **2008**, *35*, L18801, Number: 18 WOS:000259395400003.

[364] El-Sayed, M. M. H.; Wang, Y.; Hennigan, C. J. Direct atmospheric evidence for the irreversible formation of aqueous secondary organic aerosol. *Geophysical Research Letters* **2015**, *42*, 5577–5586, Number: 13 WOS:000358691300062.

[365] Li, C.; Zhu, Q.; Jin, X.; Cohen, R. C. Elucidating Contributions of Anthropogenic Volatile Organic Compounds and Particulate Matter to Ozone Trends over China. *Environmental Science & Technology* **2022**, *56*, 12906–12916, Publisher: American Chemical Society.

[366] US EPA, O. 2020 National Emissions Inventory (NEI) Technical Support Document (TSD). 2023; https://www.epa.gov/air-emissions-inventories/2020-national-emissions-inventory-nei-technical-support-document-tsd.

[367] US EPA, O. 2011 National Emissions Inventory (NEI) Technical Support Document. 2015; https://www.epa.gov/air-emissions-inventories/2011-national-emissions-inventory-nei-technical-support-document.

[368] McDonald, B. C. et al. Volatile chemical products emerging as largest petrochemical source of urban organic emissions. *Science* **2018**, *359*, 760–764, Publisher: American Association for the Advancement of Science.

[369] Luecken, D. J.; Yarwood, G.; Hutzell, W. T. Multipollutant modeling of ozone, reactive nitrogen and HAPs across the continental US with CMAQ-CB6. *Atmospheric Environment* **2019**, *201*, 62–72.

[370] EPA, U. EQUATESv1.0: Emissions, WRF/MCIP, CMAQv5.3.2 Data – 2002-2019 US_12km and NHEMI_108km. 2024; https://dataverse.unc.edu/dataset.xhtml?persistentId=doi:10.15139/S3/F2KJSK.

[371] Sharkey, T. D.; Singsaas, E. L.; Vanderveer, P. J.; Geron, C. Field measurements of isoprene emission from trees in response to temperature and light. *Tree Physiology* **1996**, *16*, 649–654.

[372] Liu, S. et al. Composition and reactivity of volatile organic compounds in the South Coast Air Basin and San Joaquin Valley of California. *Atmospheric Chemistry and Physics* **2022**, *22*, 10937–10954, Publisher: Copernicus GmbH.

[373] Pfannerstill, E. Y.; Arata, C.; Zhu, Q.; Schulze, B. C.; Ward, R.; Woods, R.; Harkins, C.; Schwantes, R. H.; Seinfeld, J. H.; Bucholtz, A.; Cohen, R. C.; Goldstein, A. H. Temperature-dependent emissions dominate aerosol and ozone formation in Los Angeles. *Science* **2024**, *384*, 1324–1329, Publisher: American Association for the Advancement of Science.

[374] Richmond-Bryant, J.; Chris Owen, R.; Graham, S.; Snyder, M.; McDow, S.; Oakes, M.; Kimbrough, S. Estimation of on-road NO2 concentrations, NO2/NOX ratios, and related roadway gradients from near-road monitoring data. *Air Quality, Atmosphere & Health* **2017**, *10*, 611–625.

[375] Gilliland, A. B.; Hogrefe, C.; Pinder, R. W.; Godowitch, J. M.; Foley, K. L.; Rao, S. T. Dynamic evaluation of regional air quality models: Assessing changes in O3 stemming from changes in emissions and meteorology. *Atmospheric Environment* **2008**, *42*, 5110–5123.

[376] Smyth, S. C.; Jiang, W.; Roth, H.; Moran, M. D.; Makar, P. A.; Yang, F.; Bouchet, V. S.; Landry, H. A comparative performance evaluation of the AURAMS and CMAQ air-quality modelling systems. *Atmospheric Environment* **2009**, *43*, 1059–1070.

[377] Seltzer, K. M.; Nolte, C. G.; Spero, T. L.; Appel, K. W.; Xing, J. Evaluation of near surface ozone and particulate matter in air quality simulations driven by dynamically downscaled historical meteorological fields. *Atmospheric Environment* **2016**, *138*, 42–54.

[378] Zhu, S.; Kinnon, M. M.; Shaffer, B. P.; Samuelsen, G. S.; Brouwer, J.; Dabdub, D. An uncertainty for clean air: Air quality modeling implications of underestimating VOC emissions in urban inventories. *Atmospheric Environment* **2019**, *211*, 256–267.

[379] Hodzic, A.; Aumont, B.; Knote, C.; Lee-Taylor, J.; Madronich, S.; Tyndall, G. Volatility dependence of Henry's law constants of condensable organics: Application to estimate depositional loss of secondary organic aerosols. *Geophysical Research Letters* **2014**, *41*, 4795–4804, _eprint: https://onlinelibrary.wiley.com/doi/pdf/10.1002/2014GL060649.

[380] Ervens, B.; Carlton, A. G.; Turpin, B. J.; Altieri, K. E.; Kreidenweis, S. M.; Feingold, G. Secondary organic aerosol yields from cloud-processing of isoprene oxidation products. *Geophysical Research Letters* **2008**, *35*, Number: 2.

[381] Praske, E.; Otkjær, R. V.; Crounse, J. D.; Hethcox, J. C.; Stoltz, B. M.; Kjaergaard, H. G.; Wennberg, P. O. Atmospheric autoxidation is increasingly important in urban and suburban North America. *Proceedings of the National Academy of Sciences* **2018**, *115*, 64–69.

[382] Eilerman, S. J.; Peischl, J.; Neuman, J. A.; Ryerson, T. B.; Aikin, K. C.; Holloway, M. W.; Zondlo, M. A.; Golston, L. M.; Pan, D.; Floerchinger, C.; Herndon, S. Characterization of Ammonia, Methane, and Nitrous Oxide Emissions from Concentrated Animal Feeding Operations in Northeastern Colorado. *Environmental Science & Technology* **2016**, *50*, 10885–10893, Number: 20 Publisher: American Chemical Society.

[383] Ravishankara, A. R.; Daniel, J. S.; Portmann, R. W. Nitrous Oxide (N2O): The Dominant Ozone-Depleting Substance Emitted in the 21st Century. *Science* **2009**, *326*, 123–125, Publisher: American Association for the Advancement of Science.

[384] Tian, H. et al. Global nitrous oxide budget (1980–2020). *Earth System Science Data* **2024**, *16*, 2543–2604, Publisher: Copernicus GmbH.

[385] Saunois, M. et al. The Global Methane Budget 2000–2017. *Earth System Science Data* **2020**, *12*, 1561–1623, Publisher: Copernicus GmbH.

[386] Nisbet, E. G.; Dlugokencky, E. J.; Fisher, R. E.; France, J. L.; Lowry, D.; Manning, M. R.; Michel, S. E.; Warwick, N. J. Atmospheric methane and nitrous oxide:

challenges alongthe path to Net Zero. *Philosophical Transactions of the Royal Society A: Mathematical, Physical and Engineering Sciences* **2021**, *379*, 20200457, Publisher: Royal Society.

[387] Anthony, T. L.; Silver, W. L. Hot moments drive extreme nitrous oxide and methane emissions from agricultural peatlands. *Global Change Biology* **2021**, *27*, 5141–5153, Number: 20 Publisher: John Wiley & Sons, Ltd.

[388] Meinhardt, K. A.; Stopnisek, N.; Pannu, M. W.; Strand, S. E.; Fransen, S. C.; Casciotti, K. L.; Stahl, D. A. Ammonia-oxidizing bacteria are the primary N2O producers in an ammonia-oxidizing archaea dominated alkaline agricultural soil. *Environmental Microbiology* **2018**, *20*, 2195–2206, Number: 6 _eprint: https://onlinelibrary.wiley.com/doi/pdf/10.1111/1462-2920.14246.

[389] Zhang, Y.; Cremer, P. S. Interactions between macromolecules and ions: the Hofmeister series. *Current Opinion in Chemical Biology* **2006**, *10*, 658–663, Number: 6 WOS:000242919700020.

[390] Carlton, A. G.; Christiansen, A. E.; Flesch, M. M.; Hennigan, C. J.; Sareen, N. Multiphase Atmospheric Chemistry in Liquid Water: Impacts and Controllability of Organic Aerosol. *Accounts of Chemical Research* **2020**, *53*, 1715–1723, Number: 9 Publisher: American Chemical Society.

[391] Setschenow, J. Über die Konstitution der Salzlösungen auf Grund ihres Verhaltens zu Kohlensäure. *Zeitschrift für Physikalische Chemie* **1889**, *4U*, 117–125, Publisher: De Gruyter (O).

[392] Waxman, E. M.; Elm, J.; Kurtén, T.; Mikkelsen, K. V.; Ziemann, P. J.; Volkamer, R. Glyoxal and Methylglyoxal Setschenow Salting Constants in Sulfate, Nitrate, and Chloride Solutions: Measurements and Gibbs Energies. *Environmental Science & Technology* **2015**, *49*, 11500–11508, Number: 19.

[393] Wang, C.; Lei, Y. D.; Endo, S.; Wania, F. Measuring and Modeling the Salting-out Effect in Ammonium Sulfate Solutions. *Environmental Science & Technology* **2014**, *48*, 13238–13245, Number: 22.

[394] Wang, C.; Lei, Y. D.; Wania, F. Effect of Sodium Sulfate, Ammonium Chloride, Ammonium Nitrate, and Salt Mixtures on Aqueous Phase Partitioning of Organic Compounds. *Environmental Science & Technology* **2016**, *50*, 12742–12749, Number: 23 Place: Washington Publisher: Amer Chemical Soc WOS:000389557100025.

[395] Kampf, C. J.; Waxman, E. M.; Slowik, J. G.; Dommen, J.; Pfaffenberger, L.; Praplan, A. P.; Prévôt, A. S. H.; Baltensperger, U.; Hoffmann, T.; Volkamer, R. Effective Henry's Law Partitioning and the Salting Constant of Glyoxal in Aerosols Containing Sulfate. *Environmental Science & Technology* **2013**, *47*, 4236–4244, Number: 9.

[396] McFall, A. S.; Johnson, A. W.; Anastasio, C. Air–Water Partitioning of Biomass-Burning Phenols and the Effects of Temperature and Salinity. *Environmental Science & Technology* **2020**, *54*, 3823–3830, Number: 7 Publisher: American Chemical Society.

[397] Anderson, C. H.; Dibb, J. E.; Griffin, R. J.; Hagler, G. S. W.; Bergin, M. H. Atmospheric water-soluble organic carbon measurements at Summit, Greenland. *Atmospheric Environment* **2008**, *42*, 5612–5621.

[398] Yang, L.; Budisulistiorini, S. H.; Chen, G.; Wang, X.; Kuwata, M. The Relationship between Molecular Size and Polarity of Atmospheric Organic Aerosol in Singapore and Its Implications for Volatility and Light Absorption Properties. *ACS Earth and Space Chemistry* **2021**, *5*, 3182–3196, Publisher: American Chemical Society.

[399] Liu, J.; Zhang, X.; Parker, E. T.; Veres, P. R.; Roberts, J. M.; de Gouw, J. A.; Hayes, P. L.; Jimenez, J. L.; Murphy, J. G.; Ellis, R. A.; Huey, L. G.; Weber, R. J. On the gas-particle partitioning of soluble organic aerosol in two urban atmospheres with contrasting emissions: 2. Gas and particle phase formic acid. *Journal of Geophysical Research: Atmospheres* **2012**, *117*, _eprint: https://onlinelibrary.wiley.com/doi/pdf/10.1029/2012JD017912.

[400] van Zomeren, A.; Koper, R.; Dijkstra, J. J.; Comans, R. N. J. Chloride Interference during Analysis of Dissolved Organic Carbon Using Wet Chemical Oxidation Methods. *ACS ES&T Water* **2021**, *1*, 1295–1301, Publisher: American Chemical Society.

[401] Yuan, B.; Koss, A. R.; Warneke, C.; Coggon, M.; Sekimoto, K.; de Gouw, J. A. Proton-Transfer-Reaction Mass Spectrometry: Applications in Atmospheric Sciences. *Chemical Reviews* **2017**, *117*, 13187–13229, Publisher: American Chemical Society.

[402] Estefany, C.; Sun, Z.; Hong, Z.; Du, J. Raman spectroscopy for profiling physical and chemical properties of atmospheric aerosol particles: A review. *Ecotoxicology and Environmental Safety* **2023**, *249*, 114405.

[403] Huang, Q.; Vikesland, P. J. In Situ pH Measurement of Water Droplets Using Flash-Freeze Surface-Enhanced Raman Spectroscopy. *Environmental Science & Technology Letters* **2022**, *9*, 459–465, Publisher: American Chemical Society.

[404] About | ASCENT. `https://ascent.research.gatech.edu/about`.

[405] Saluga, S. J.; Burns, A. M.; Li, Y.; Nguyen, M. M.; Edwards, K. D. A Specifications-Graded, Spice-Themed, General Chemistry Laboratory Course Using an Argument-Driven Inquiry Approach. *Journal of Chemical Education* **2023**, *100*, 3903–3915, Publisher: American Chemical Society.

[406] Lorenz-Spreen, P.; Mønsted, B. M.; Hövel, P.; Lehmann, S. Accelerating dynamics of collective attention. *Nature Communications* **2019**, *10*, 1759, Publisher: Nature Publishing Group.

[407] Nilson, L. B. *Specifications Grading: Restoring Rigor, Motivating Students, and Saving Faculty Time*; Routledge: New York, 2023.

[408] Domin, D. S. A Review of Laboratory Instruction Styles. *Journal of Chemical Education* **1999**, *76*, 543, Publisher: American Chemical Society.

[409] Abraham, M. R. What Can Be Learned from Laboratory Activities? Revisiting 32 Years of Research. *Journal of Chemical Education* **2011**, *88*, 1020–1025, Publisher: American Chemical Society.

[410] Closser, K. D.; Hawker, M. J.; Muchalski, H. Quantized Grading: An ab Initio Approach to Using Specifications Grading in Physical Chemistry. *Journal of Chemical Education* **2024**, *101*, 474–482, Publisher: American Chemical Society.

[411] Walker, J. P.; Sampson, V.; Zimmerman, C. O. Argument-Driven Inquiry: An Introduction to a New Instructional Model for Use in Undergraduate Chemistry Labs. *Journal of Chemical Education* **2011**, *88*, 1048–1056, Publisher: American Chemical Society.

[412] Tessier, L.; Tessier, J. Theme-based courses foster student learning and promote comfort with learning new material. *Journal for Learning through the Arts* **2015**, *11*.

[413] Howitz, W. J.; Frey, T.; Saluga, S. J.; Nguyen, M.; Denaro, K.; Edwards, K. D. A Specifications-Graded, Sports Drink-Themed General Chemistry Laboratory Course Using an Argument-Driven Inquiry Approach. *Journal of Chemical Education* **2023**, *100*, 672–680, Publisher: American Chemical Society.

[414] Stanford, C.; Moon, A.; Towns, M.; Cole, R. Analysis of Instructor Facilitation Strategies and Their Influences on Student Argumentation: A Case Study of a Process Oriented Guided Inquiry Learning Physical Chemistry Classroom. *Journal of Chemical Education* **2016**, *93*, 1501–1513, Publisher: American Chemical Society.

# Appendix A

# Supporting Information for Chapter 2

Movies A1-A6 can be found in the online supporting information:

https://pubs.acs.org/doi/10.1021/acs.est.3c06947?goto=supporting-info

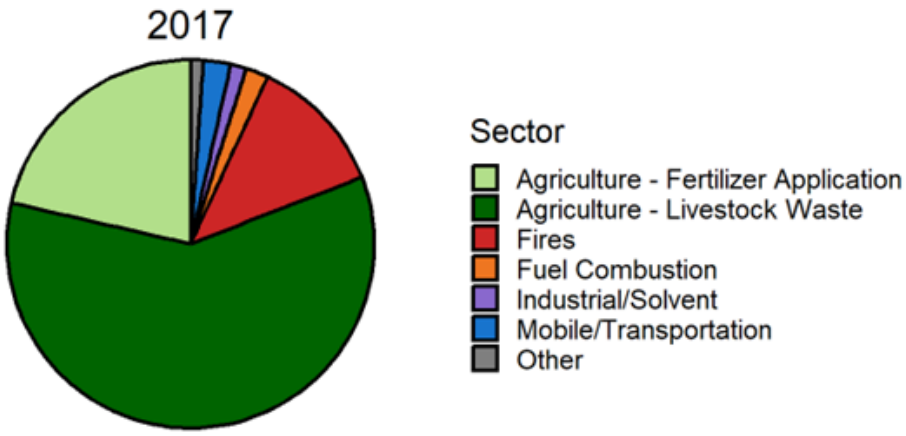


Figure A.1: Fractional contribution by source sector to total 2017 annual ammonia emission in the contiguous U.S. according EPA's National Emissions Inventory.

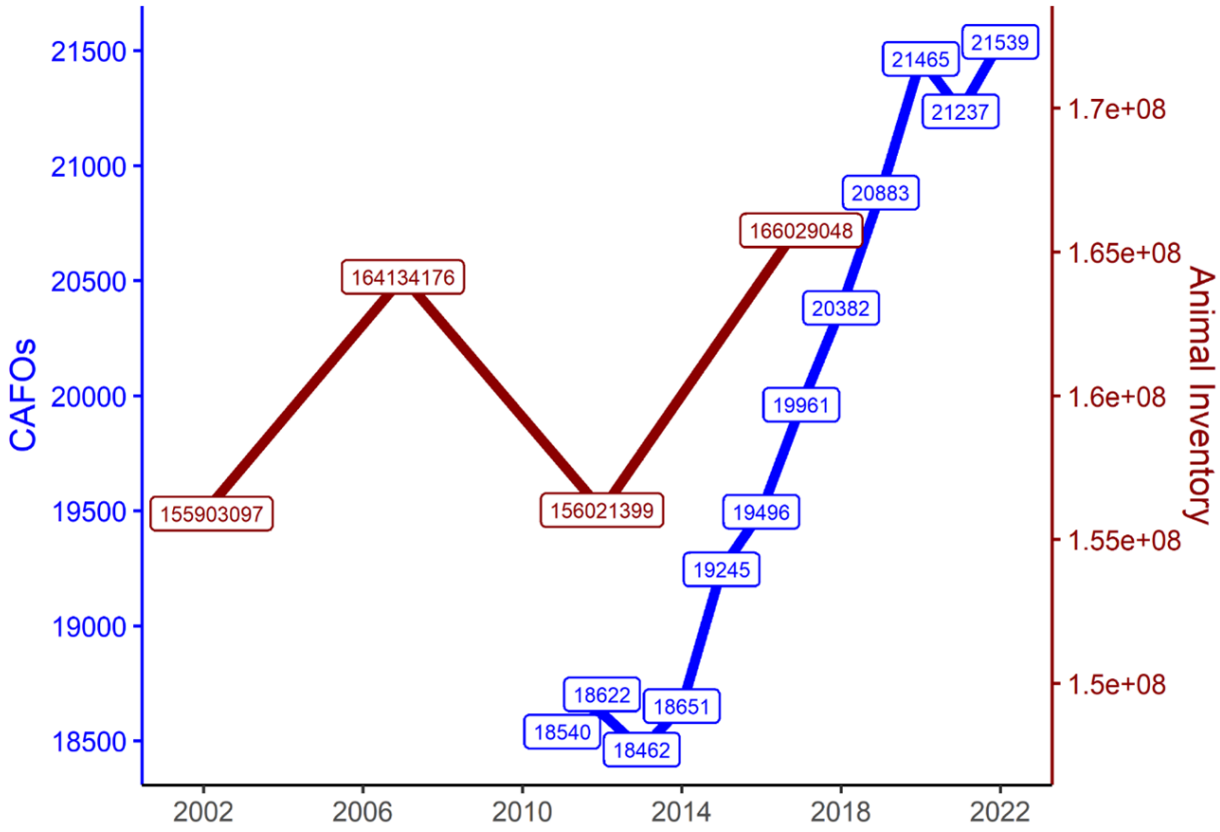


Figure A.2: Annual farm animal and CAFO numbers from National Pollution Discharge Elimination System (NPDES) reporting to the EPA. All available State-level data (2011-2022) is used and aggregated across the CONUS. Animal inventory represents USDA Ag-Census reported head counts for cows and swine, which are often in open air confinements

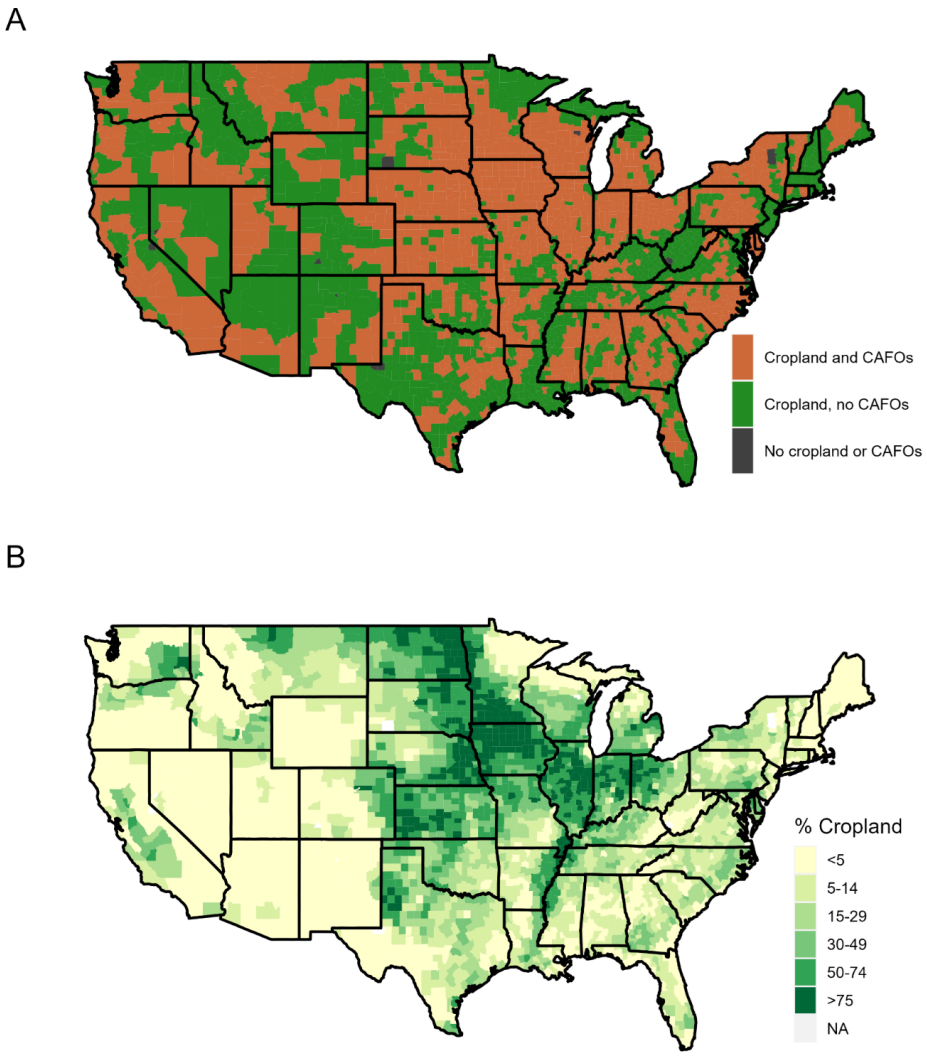


Figure A.3: USDA-reported cropland cover and industrial farming practices from the 2017 AgCensus over the CONUS (A). USDA-reported cropland at the county level (B). Satellite $NH_3$ patterns are more similar to the spatial extent of CAFOs than cropland cover.

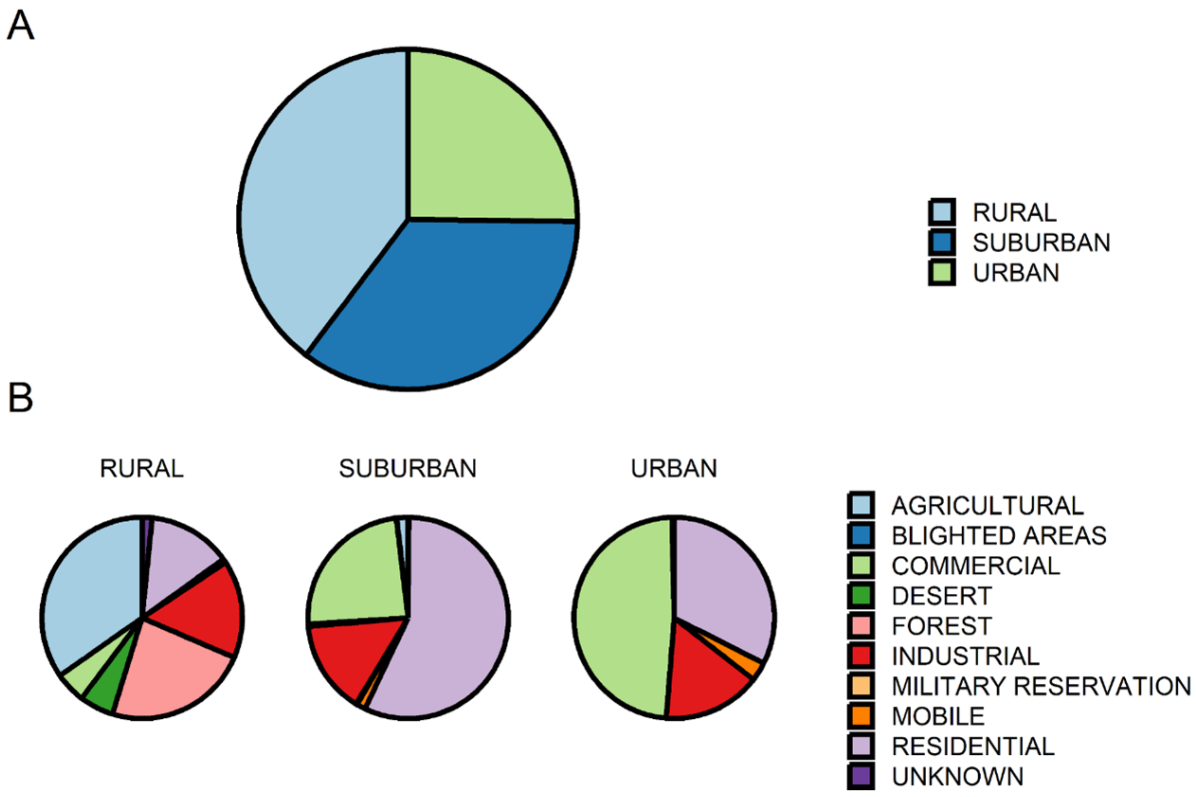


Figure A.4: EPA-reported AQS site location setting (A) and site land use (B).

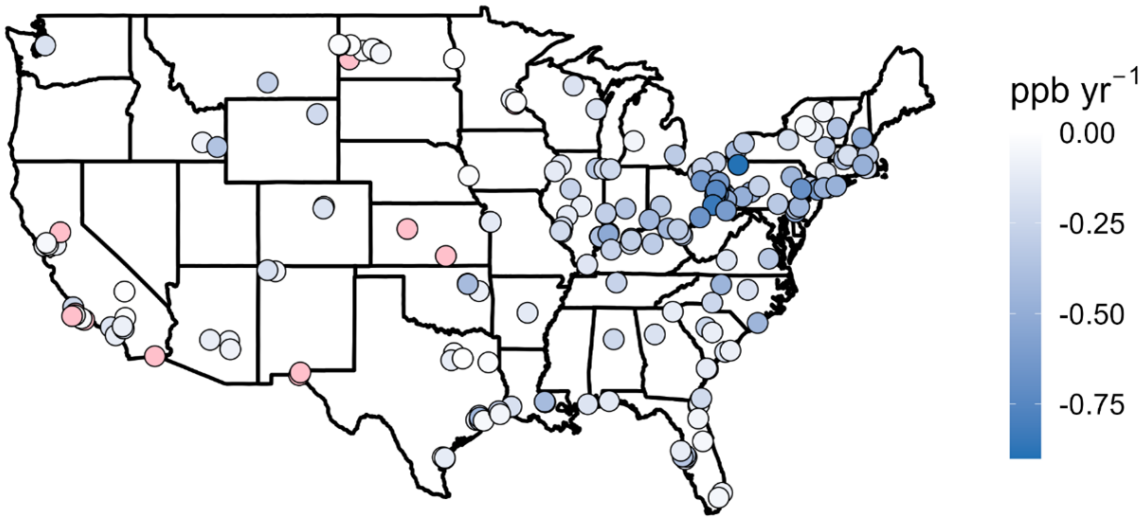


Figure A.5: Trends in ambient $SO_2$ concentrations from 2002-2017. Blue points represent a decreasing trend according to the colorbar. Pink points represent sites that experience a slightly positive trend (<0.1 ppb yr$^{-1}$).

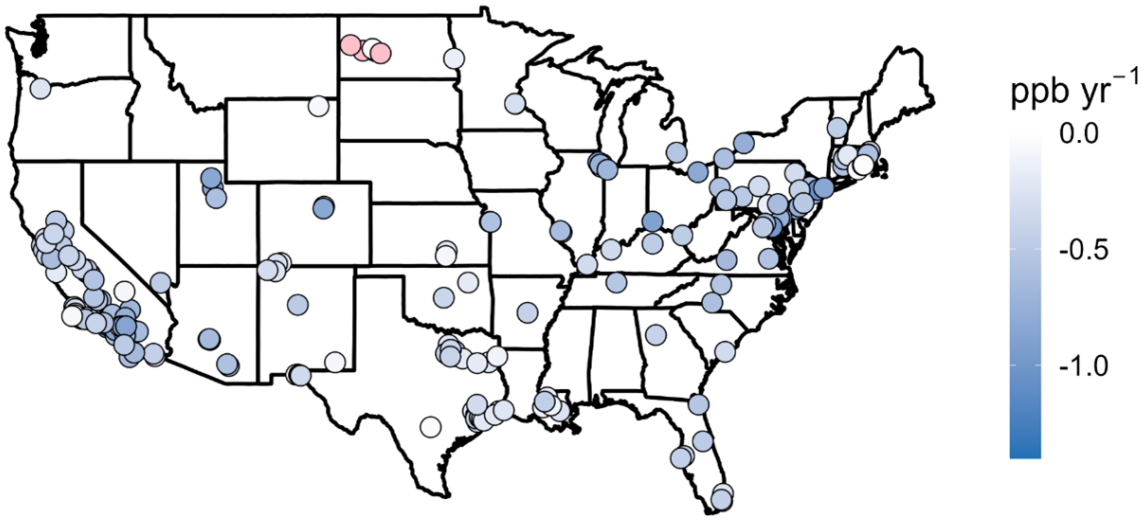


Figure A.6: Trends in ambient $NO_2$ concentrations from 2002-2017. Blue points represent a decreasing trend according to the colorbar. Pink points represent sites that experience a slightly positive trend (<0.05 ppb yr$^{-1}$).

| EPA Region (total sites) | Median 2002 conc. ($\mu$g m$^{-3}$) | 2002 SD | Median 2017 conc. ($\mu$g m$^{-3}$) | 2017 SD | Percent Change |
|---|---|---|---|---|---|
| Ohio Valley (66) | 13.6 | 8.2 | 7.6 | 4.3 | -44.1 |
| Upper Midwest (48) | 10.4 | 7.7 | 6.3 | 4.4 | -39.4 |
| Southeast (60) | 12.3 | 7.0 | 7.5 | 4.1 | -38.7 |
| Northeast (83) | 10.9 | 8.6 | 7.1 | 4.8 | -34.9 |
| West (56) | 12.0 | 13.1 | 8.3 | 8.8 | -30.9 |
| Northwest (10) | 7.8 | 9.4 | 5.8 | 10.5 | -25.6 |
| South (34) | 10.5 | 6.2 | 8.1 | 4.1 | -23.3 |
| Northern Rockies and Plains (18) | 6.8 | 6.5 | 5.5 | 6.1 | -19.4 |
| Southwest (24) | 7.2 | 7.7 | 5.9 | 6.3 | -18.0 |
| CONUS (399) | 11.0 | 8.9 | 7.1 | 5.9 | -35.2 |

Table A.1: Average $PM_{2.5}$ mass concentrations, standard deviations (SD), and regional site numbers for EPA-defined U.S. climate regions.

| USDA Region (total sites) | Median 2002 conc. ($\mu$g m$^{-3}$) | 2002 SD | Median 2017 conc. ($\mu$g m$^{-3}$) | 2017 SD | Percent Change |
|---|---|---|---|---|---|
| Midwest (94) | 12.3 | 8.1 | 7.0 | 4.5 | -43.2 |
| Atlantic (126) | 11.5 | 8.4 | 7.1 | 4.5 | -38.3 |
| South (51) | 11.7 | 6.5 | 7.9 | 4.2 | -32.4 |
| Plains (32) | 9.4 | 6.4 | 7.1 | 5.1 | -24.5 |
| West (96) | 9.1 | 11.5 | 7.0 | 8.3 | -23.1 |
| CONUS (399) | 11.0 | 8.9 | 7.1 | 5.9 | -35.2 |

Table A.2: Average $PM_{2.5}$ mass concentrations, standard deviations (SD), and regional site numbers for USDA-defined Farm Production regions.

| EPA Region (total sites) | Chemical Species (sites) | Median 2002 conc. ($\mu$g m$^{-3}$) | 2002 SD | Median 2017 conc. ($\mu$g m$^{-3}$) | 2017 SD | Percent Change |
|---|---|---|---|---|---|---|
| Ohio Valley (32) | $SO_4$ (32) | 3.2 | 3.2 | 1.0 | 0.8 | -68.2 |
| | $NO_3$ (32) | 1.1 | 1.4 | 0.4 | 1.4 | -62.0 |
| | $NH_4$ (29) | 1.5 | 1.3 | 0.3 | 0.6 | -80.1 |
| | OM (26) | 2.6 | 1.6 | 2.6 | 2.1 | 1.2 |
| Upper Midwest (18) | $SO_4$ (18) | 1.7 | 2.6 | 0.6 | 0.6 | -62.4 |
| | $NO_3$ (18) | 0.8 | 2.4 | 0.4 | 1.4 | -53.5 |
| | $NH_4$ (14) | 1.0 | 1.4 | 0.2 | 0.5 | -83.9 |
| | OM (15) | 1.7 | 3.7 | 2.1 | 1.9 | 22.8 |
| Southeast (37) | $SO_4$ (37) | 3.3 | 2.9 | 0.9 | 0.6 | -73.9 |
| | $NO_3$ (36) | 0.5 | 0.7 | 0.3 | 0.5 | -45.3 |
| | $NH_4$ (34) | 1.1 | 0.9 | 0.1 | 0.2 | -90.1 |
| | OM (27) | 2.5 | 3.8 | 2.7 | 5.4 | 10.2 |
| Northeast (31) | $SO_4$ (31) | 2.6 | 3.8 | 0.7 | 0.5 | -74.9 |
| | $NO_3$ (31) | 0.7 | 1.6 | 0.3 | 0.9 | -60.0 |
| | $NH_4$ (22) | 1.5 | 1.5 | 0.1 | 0.4 | -91.9 |
| | OM (29) | 1.8 | 4.4 | 2.2 | 1.9 | 19.5 |
| West (27) | $SO_4$ (27) | 0.8 | 1.4 | 0.5 | 0.6 | -38.8 |
| | $NO_3$ (27) | 0.6 | 6.0 | 0.4 | 2.5 | -36.3 |
| | $NH_4$ (12) | 1.3 | 3.1 | 0.3 | 1.3 | -74.4 |
| | OM (23) | 1.5 | 4.0 | 2.0 | 5.7 | 38.5 |
| Northwest (20) | $SO_4$ (20) | 0.5 | 0.8 | 0.3 | 0.3 | -52.5 |
| | $NO_3$ (20) | 0.2 | 0.8 | 0.1 | 0.6 | -45.3 |
| | $NH_4$ (5) | 0.4 | 0.4 | 0.01 | 0.1 | -97.4 |
| | OM (18) | 1.3 | 8.9 | 1.2 | 10.0 | -7.0 |
| South (23) | $SO_4$ (23) | 2.3 | 2.5 | 1.0 | 0.9 | -55.3 |
| | $NO_3$ (21) | 0.5 | 1.3 | 0.2 | 0.7 | -49.6 |
| | $NH_4$ (17) | 0.9 | 0.9 | 2.4 | 0.3 | -79.8 |
| | OM (17) | 1.6 | 1.5 | 0.2 | 2.5 | 45.5 |
| Northern Rockies and Plains (22) | $SO_4$ (22) | 0.5 | 0.9 | 0.3 | 0.4 | -30.6 |
| | $NO_3$ (22) | 0.1 | 0.7 | 0.1 | 0.5 | -19.9 |
| | $NH_4$ (3) | 0.7 | 0.9 | 0.1 | 0.3 | -90.4 |
| | OM (22) | 1.0 | 2.2 | 1.0 | 13.8 | -3.3 |
| Southwest (30) | $SO_4$ (30) | 0.6 | 0.6 | 0.4 | 0.4 | -38.3 |
| | $NO_3$ (30) | 0.2 | 1.7 | 0.1 | 1.1 | -41.6 |
| | $NH_4$ (5) | 0.4 | 1.5 | 0.04 | 1.0 | -90.7 |
| | OM (30) | 1.0 | 4.2 | 1.1 | 2.4 | 8.7 |
| CONUS (240) | $SO_4$ (240) | 1.3 | 2.7 | 0.6 | 0.7 | -56.0 |
| | $NO_3$ (237) | 0.4 | 2.6 | 0.2 | 1.3 | -45.9 |
| | $NH_4$ (141) | 1.1 | 1.6 | 0.2 | 0.7 | -85.6 |
| | OM (207) | 1.4 | 4.8 | 1.9 | 6.4 | 31.6 |

Table A.3: Average mass concentrations for major $PM_{2.5}$ constituents, standard deviations (SD), and regional site numbers for EPA-defined U.S. climate regions.

| USDA Region (total sites) | Chemical Species (sites) | Median 2002 conc. ($\mu$g m$^{-3}$) | 2002 SD | Median 2017 conc. ($\mu$g m$^{-3}$) | 2017 SD | Percent Change |
|---|---|---|---|---|---|---|
| Midwest (41) | $SO_4$ (41) | 2.3 | 3.0 | 0.8 | 0.8 | -64.9 |
| | $NO_3$ (41) | 1.1 | 2.2 | 0.4 | 1.5 | -60.5 |
| | $NH_4$ (34) | 1.4 | 1.4 | 0.3 | 0.5 | -82.1 |
| | OM (36) | 2.1 | 3.1 | 2.4 | 2.0 | 15.7 |
| Atlantic (55) | $SO_4$ (55) | 2.9 | 3.6 | 0.7 | 0.5 | -75.5 |
| | $NO_3$ (55) | 0.6 | 1.4 | 0.3 | 0.8 | -56.1 |
| | $NH_4$ (46) | 1.3 | 1.3 | 0.1 | 0.4 | -91.0 |
| | OM (44) | 2.1 | 3.7 | 2.3 | 2.0 | 11.0 |
| South (30) | $SO_4$ (30) | 3.2 | 2.7 | 1.0 | 0.7 | -68.1 |
| | $NO_3$ (29) | 0.5 | 0.7 | 0.2 | 0.4 | -47.9 |
| | $NH_4$ (25) | 1.0 | 0.9 | 0.1 | 0.3 | -88.0 |
| | OM (21) | 2.5 | 4.0 | 2.7 | 6.0 | 8.5 |
| Plains (22) | $SO_4$ (22) | 1.5 | 2.2 | 0.8 | 0.8 | -50.2 |
| | $NO_3$ (20) | 0.4 | 1.4 | 0.2 | 0.7 | -42.5 |
| | $NH_4$ (22) | 0.9 | 0.9 | 0.2 | 0.3 | -81.6 |
| | OM (20) | 1.1 | 1.4 | 1.8 | 3.0 | 55.1 |
| West (92) | $SO_4$ (92) | 0.6 | 0.9 | 0.4 | 0.5 | -40.3 |
| | $NO_3$ (92) | 0.2 | 3.5 | 0.1 | 1.6 | -36.8 |
| | $NH_4$ (23) | 0.7 | 2.7 | 0.1 | 1.2 | -79.7 |
| | OM (23) | 1.1 | 5.5 | 1.2 | 9.0 | 8.8 |
| CONUS (240) | $SO_4$ (240) | 1.3 | 2.7 | 0.6 | 0.7 | -56.0 |
| | $NO_3$ (237) | 0.4 | 2.6 | 0.2 | 1.3 | -45.9 |
| | $NH_4$ (141) | 1.1 | 1.6 | 0.2 | 0.7 | -85.6 |
| | OM (207) | 1.4 | 4.8 | 1.9 | 6.4 | 31.6 |

Table A.4: Average mass concentrations for major $PM_{2.5}$ constituents, standard deviations (SD), and regional site numbers for USDA-defined Farm Production Regions.

# Appendix B

# Supporting Information for Chapter 3

| Source Platform | Variables Used | Characteristics |
|---|---|---|
| Interagency Monitoring of Protected Visual Environments (IMPROVE) | Calicium, magnesium, nitrate, potassium, sodium, sulfate, and total fine mass concentrations | 1-in-3 day surface measurements from sites COHU1, SIPS1, BIRM1, ATLA1, JARB1, and GRBA1 . Uncertainties are reported as a measure of standard deviation and are generally low (<10%) for most species |
| EPA Chemical Speciation Network (CSN) | Ammonium, nitrate, and sulfate mass concentrations | 1-in-3 day surface measurements from sites 01-073-0023, 04-013-9997, 06-019-011, and 53-033-0080. Uncertainties are reported as a measure of standard deviation and are generally low (<10%) for all species |
| European Centre for Medium-Range Weather Forecasts (ECMWF) reanalysis model (ERA5) | Profiles of temperature, water vapor mixing ratio, and boundary layer height | – |
| National Centers for Environmental Prediction (NCEP) North American Regional Reanalysis (NARR) | Profiles of temperature, water vapor mixing ratio, and boundary layer height | – |
| NASA Aerosol Robotic Network (AERONET)[a] | Aerosol optical depth (AOD) and Ångström exponents (AE) in the 440-870 nm spectral range | Level 1.0 and Level 2.0 quality levels employed |
| Goddard Institute of Space Studies (GISS) surface temperature analysis (GISTEMP)[b] | Surface air temperature anomalies from 2000-2019 | 2° spatial and monthly temporal; uncertainty of 0.17 K |
| Moderate Resolution Imaging Spectroradiometer (MODIS)[b] | AOD, single scattering albedo (SSA), and AE | 1° spatial and monthly temporal; uncertainty in AOD of 0.03 + 20% |
| Clouds and the Earth's Radiant Energy System (CERES) Energy Blanaced and Filled (EBAF) fluxes[b] | Top-of-atmosphere (TOA) longwave (LW) and shortwave (SW) fluxes during clear sky and all-sky conditions | Monthly averages at 1° spatial resolution; uncertainty of 5 W $m^{-2}$ in both longwave and short wave fluxes |

Table B.1: Data sources utilized for ALW observational estimates, sensitivity analyses, and applications. Adapted from Ghate et al., 2022. [a]Only utilized in Application 1. [b]Only utilized in Application 2.

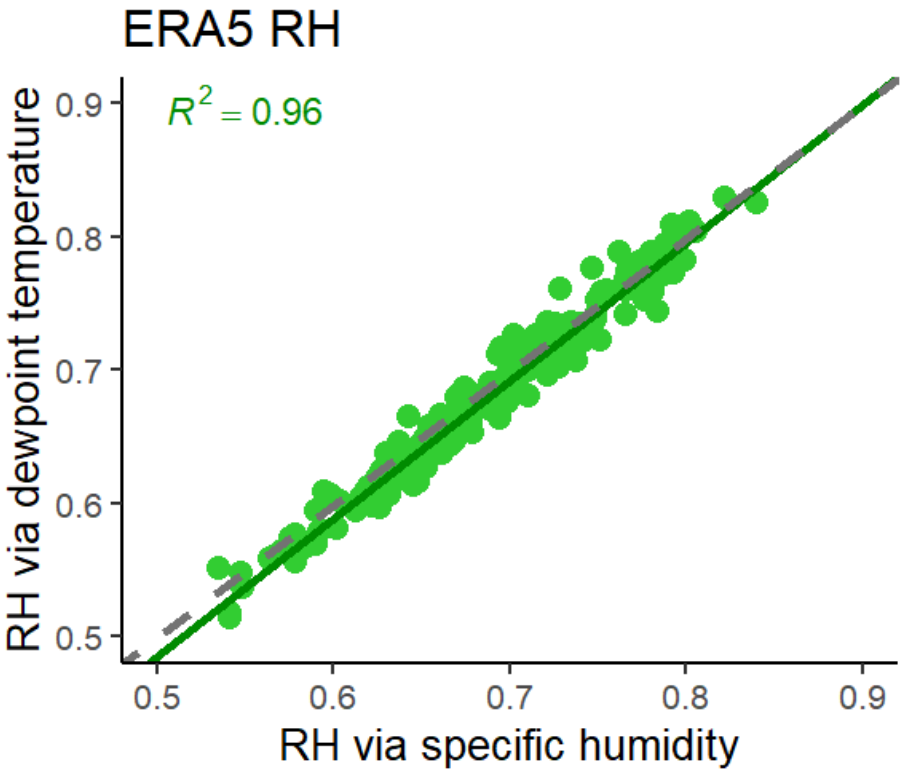


Figure B.1: Comparison between monthly average RH calculated with specific humidity and dewpoint temperature inputs with ERA5 meteorology for the total SEUS. Colored lines represent a linear fit of the data, with a 1:1 line added for visual reference (dashed line). All available measurement days are used (1988-2019).

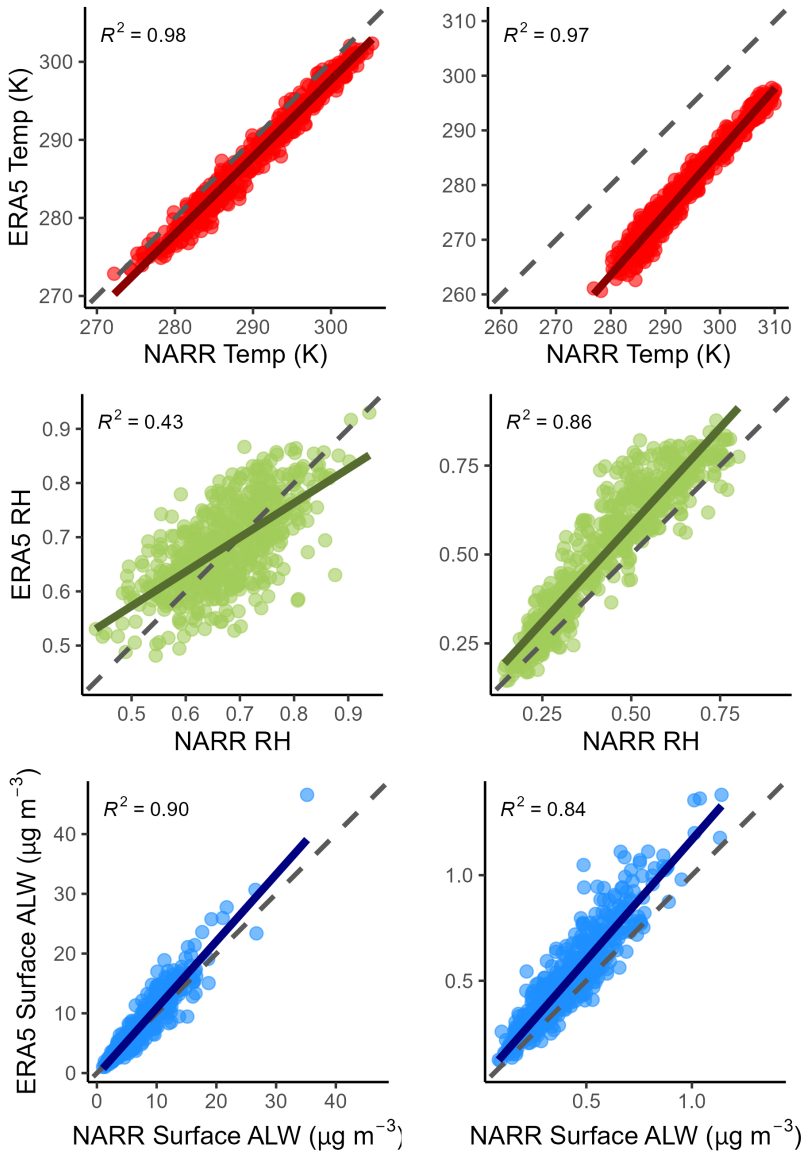


Figure B.2: Comparison between meteorological variables and predicted monthly average surface-level ALW in a humid region (total SEUS, left) and an arid region (GB, right). Colored lines represent a linear fit of the data, with a 1:1 line added for visual reference (dashed line). All available measurement days are used (1988-2014).

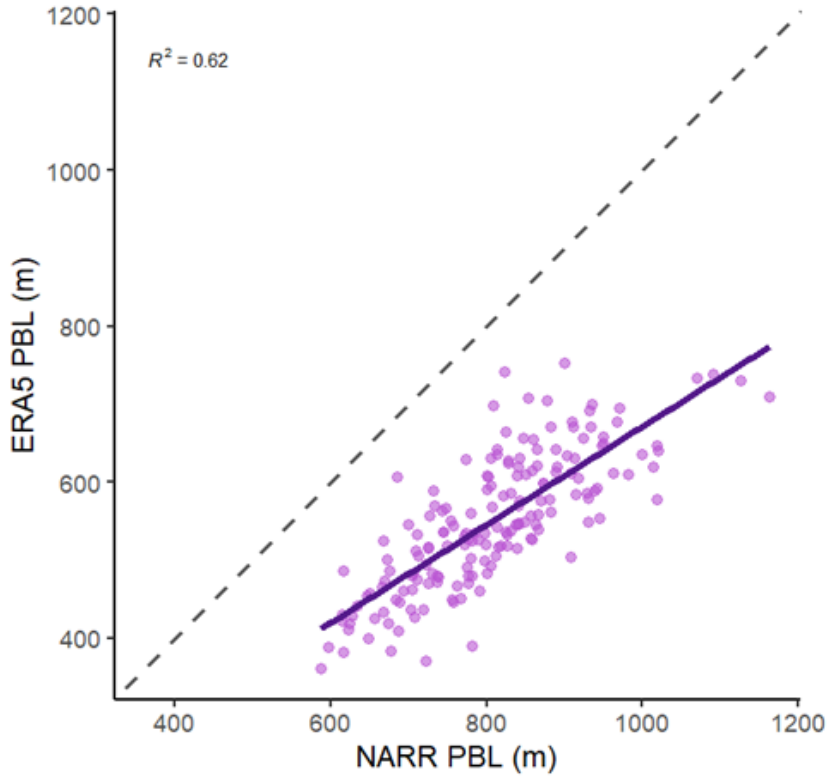


Figure B.3: Comparison between predicted monthly average PBL height in a humid region (rural SEUS). Colored lines represent a linear fit of the data, with a 1:1 line added for visual reference (dashed line). All available measurement days are used (1988-2014).

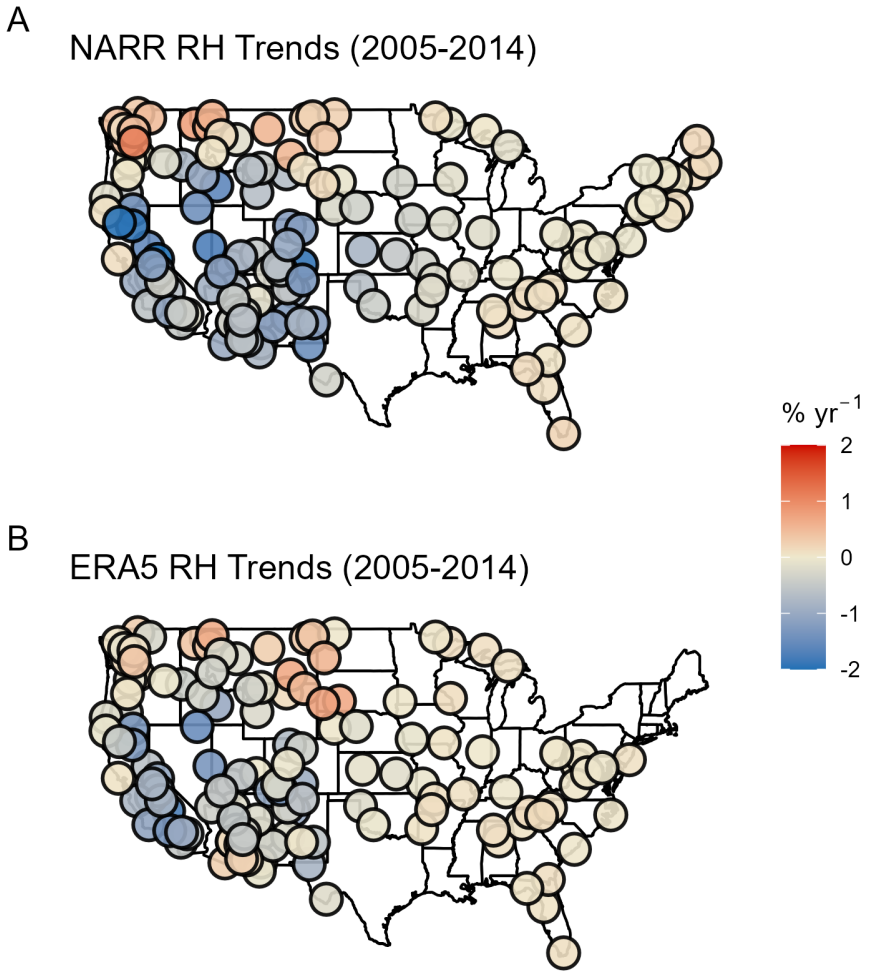


Figure B.4: Trends (% yr$^{-1}$) in RH with NARR (A) and ERA5 (B) reanalysis datasets from 2005-2014.

| Parameter | Season | Clear Median | Cloudy Median | Mann-Whitney U test p-value | Medians > 0.02 Experimental Uncertainty |
|---|---|---|---|---|---|
| Ångström exponent (440-870 nm) | Winter | 1.46 | 1.49 | 0.944 | Y |
| | **Spring** | **1.47** | **1.39** | **<0.05** | Y |
| | **Summer** | **1.68** | **1.59** | **<0.05** | Y |
| | **Fall** | **1.45** | **1.39** | **<0.05** | Y |
| Aerosol optical depth (440 nm) | **Winter** | **0.07** | **0.08** | **<0.05** | N |
| | **Spring** | **0.11** | **0.15** | **<0.05** | Y |
| | **Summer** | **0.17** | **0.22** | **<0.05** | Y |
| | Fall | **0.08** | **0.10** | **<0.05** | Y |
| Aerosol optical depth (500 nm) | **Winter** | **0.06** | **0.07** | **<0.05** | N |
| | **Spring** | **0.10** | **0.12** | **<0.05** | Y |
| | **Summer** | **0.14** | **0.18** | **<0.05** | Y |
| | **Fall** | **0.07** | **0.09** | **<0.05** | N |
| Aerosol optical depth (675 nm) | **Winter** | **0.04** | **0.05** | **<0.05** | N |
| | **Spring** | **0.06** | **0.08** | **<0.05** | Y |
| | **Summer** | **0.08** | **0.11** | **<0.05** | Y |
| | **Fall** | **0.04** | **0.06** | **<0.05** | N |
| Aerosol optical depth (870 nm) | **Winter** | **0.03** | **0.03** | **<0.05** | N |
| | **Spring** | **0.04** | **0.06** | **<0.05** | N |
| | **Summer** | **0.06** | **0.08** | **<0.05** | Y |
| | **Fall** | **0.03** | **0.04** | **<0.05** | N |

Table B.2: Predominantly clear sky and cloudy medians and two-sided Mann-Whitney U test p values of aerosol optical depth (AOD) and Ångström exponents. For clarity, p values significantly less than 0.05 are listed as "<0.05" and statistically significant seasons are bolded.

| Parameter ($\mu$g $m^{-3}$) | Season | Clear Median | Cloudy Median | Mann-Whitney U test p value |
|---|---|---|---|---|
| Inorganic Aerosol Liquid Water | Winter | 1.60 | 1.14 | 0.329 |
| | **Spring** | **1.10** | **1.97** | **<0.05** |
| | Summer | 2.19 | 2.81 | 0.093 |
| | Fall | 1.05 | 1.27 | 0.183 |
| Organic Aerosol Liquid Water | Winter | 0.58 | 1.29 | 0.898 |
| | **Spring** | **0.34** | **0.62** | **<0.05** |
| | Summer | 1.42 | 1.86 | 0.116 |
| | Fall | 0.62 | 0.73 | 0.235 |
| Nitrate | Winter | 2.52 | 1.60 | 0.650 |
| | Spring | 0.56 | 0.85 | 0.621 |
| | Summer | 0.30 | 0.33 | 0.443 |
| | Fall | 0.45 | 0.84 | 0.052 |
| Sulfate | Winter | 1.10 | 0.92 | 0.301 |
| | **Spring** | **0.97** | **1.32** | **<0.05** |
| | Summer | 1.27 | 1.72 | 0.113 |
| | Fall | 0.45 | 0.90 | 0.599 |
| Organic Mass | Winter | 1.55 | 1.77 | 0.961 |
| | **Spring** | **1.31** | **1.99** | **<0.05** |
| | Summer | 3.13 | 3.55 | 0.110 |
| | Fall | 2.20 | 2.52 | 0.536 |
| Potassium | Winter | 0.032 | 0.038 | 0.595 |

Continued on next page

**Table B.3 – continued from previous page**

| Parameter ($\mu$g $m^{-3}$) | Season | Clear Median | Cloudy Median | Mann-Whitney U test p value |
|---|---|---|---|---|
| | **Spring** | **0.032** | **0.041** | **<0.05** |
| | Summer | 0.031 | 0.031 | 0.387 |
| | Fall | 0.036 | 0.037 | 0.496 |
| Chloride | Winter | 0.058 | 0.038 | 0.258 |
| | Spring | 0.020 | 0.026 | 0.093 |
| | Summer | 0.016 | 0.016 | 0.425 |
| | Fall | 0.020 | 0.016 | 0.546 |
| Calcium | Winter | 0.024 | 0.033 | 0.602 |
| | Spring | 0.035 | 0.031 | 0.907 |
| | Summer | 0.052 | 0.041 | 0.743 |
| | Fall | 0.066 | 0.058 | 0.193 |
| Magnesium | Winter | 0.007 | 0.006 | 0.549 |
| | Spring | 0.012 | 0.017 | 0.073 |
| | Summer | 0.014 | 0.007 | 0.112 |
| | Fall | 0.013 | 0.007 | 0.256 |
| Sodium | Winter | 0.020 | 0.018 | 0.816 |
| | Spring | 0.012 | 0.014 | 0.149 |
| | Summer | 0.010 | 0.013 | 0.249 |
| | Fall | 0.010 | 0.006 | 0.300 |
| $PM_{2.5}$ + Aerosol Liquid Water | Winter | 10.20 | 10.20 | 0.746 |
| | **Spring** | **6.22** | **10.47** | **<0.05** |
| | Summer | 10.30 | 13.40 | 0.083 |

Continued on next page

**Table B.3 – continued from previous page**

| Parameter ($\mu$g $m^{-3}$) | Season | Clear Median | Cloudy Median | Mann-Whitney U test p value |
|---|---|---|---|---|
| | Fall | 7.18 | 8.81 | 0.415 |

Table B.3: Predominantly clear sky and cloudy medians and two-sided Mann-Whitney U test p values for IMPROVE-measured $PM_{2.5}$ chemical species and aerosol liquid water estimates. For clarity, p values significantly less than 0.05 are listed as "<0.05" and statistically significant seasons are bolded.

# Appendix C

# Supporting Information for Chapter 4

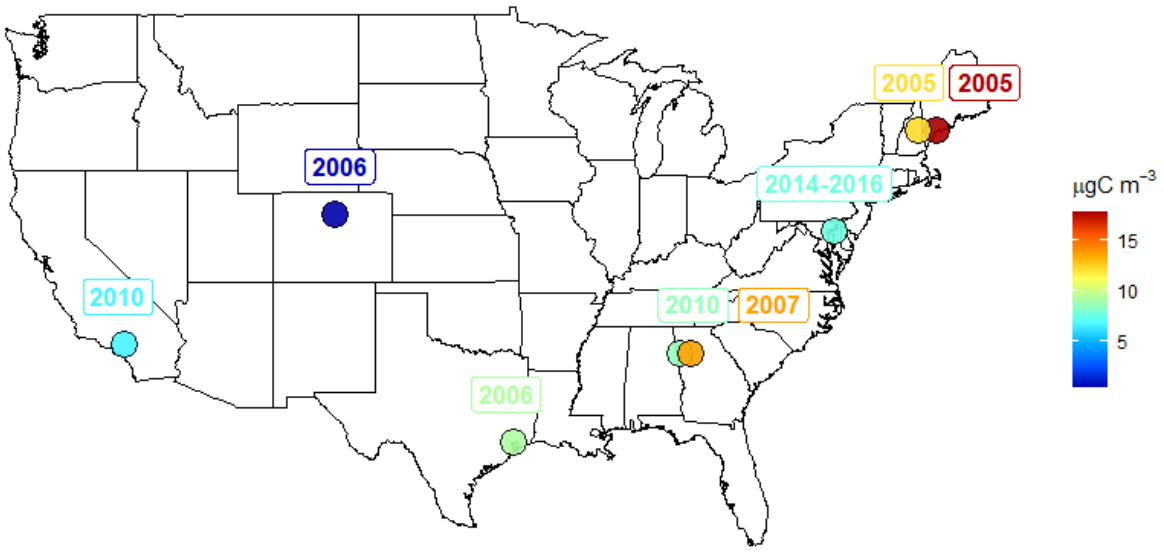


Figure C.1: Summary of prior surface mist chamber measurement campaigns of $WSOC_g$ in the CONUS. Median concentrations ($\mu$g C $m^{-3}$) observed at each site are represented by the color of site labels

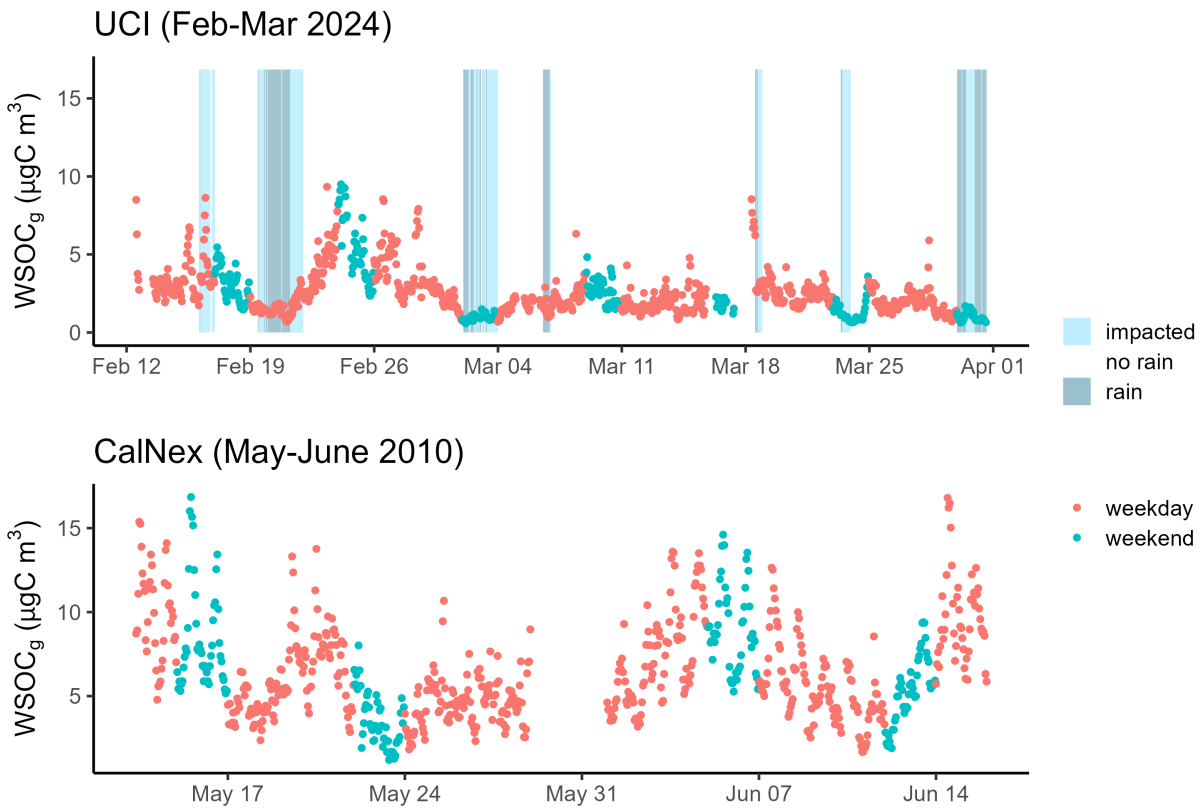


Figure C.2: Time series of hourly-averaged WSOC$_g$ measured in Irvine (UCI, top) and Pasadena (CalNex, bottom). Weekend data points are shown in blue and weekdays are shown in red. Periods with active rain ("rain", rain rate $> 0$ in) or rain influence ("impacted", rain accumulation $> 0$ in) that were removed from subsequent Irvine analysis are highlighted by the blue background. No rain was recorded during CalNex sampling. Noted events within datasets (i.e., fireworks at UCI, memorial day weekend at CalNex) are not shown.

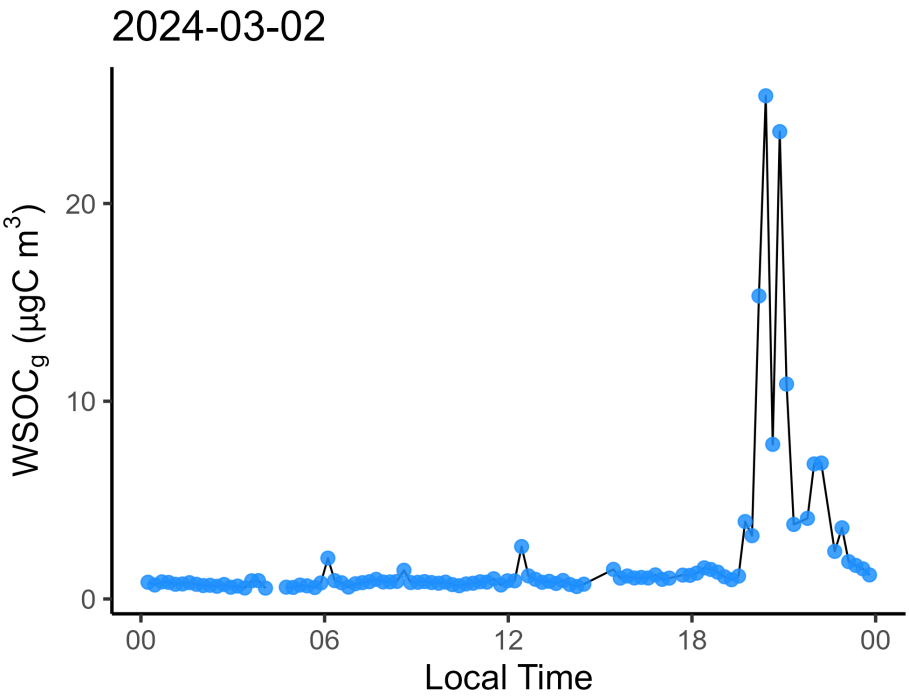


Figure C.3: Time series of all data points on March 2$^{nd}$ 2024 in Irvine. The sharp increase in the evening coincides with firework activity on UCI's campus. All data points on this day after 6PM were removed from the analysis.

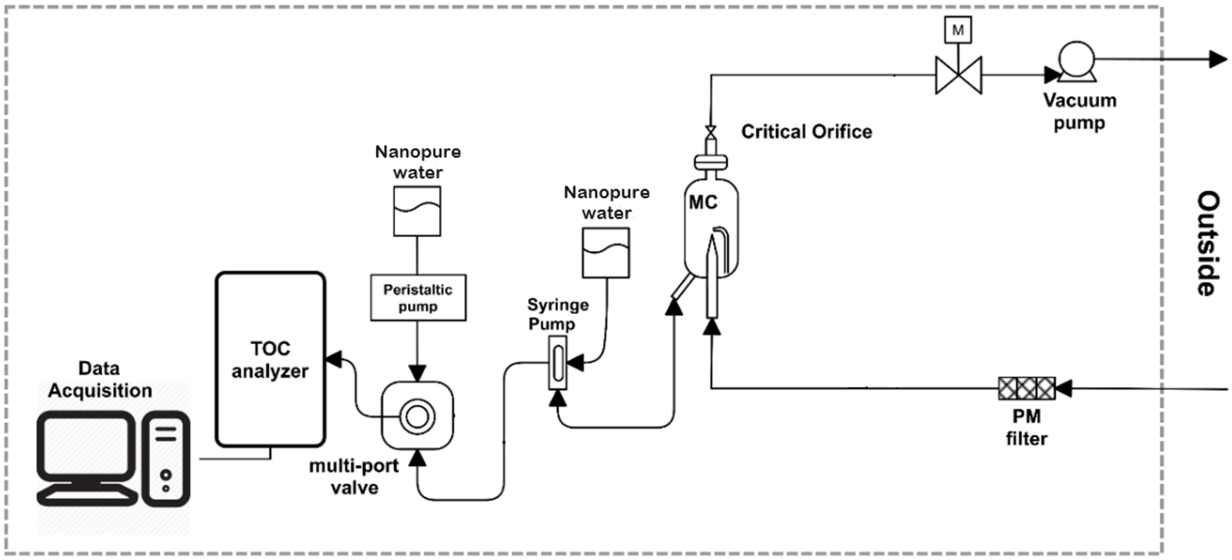


Figure C.4: Schematic of the MC experimental setup. Adapted from Pratap et al. 2021.

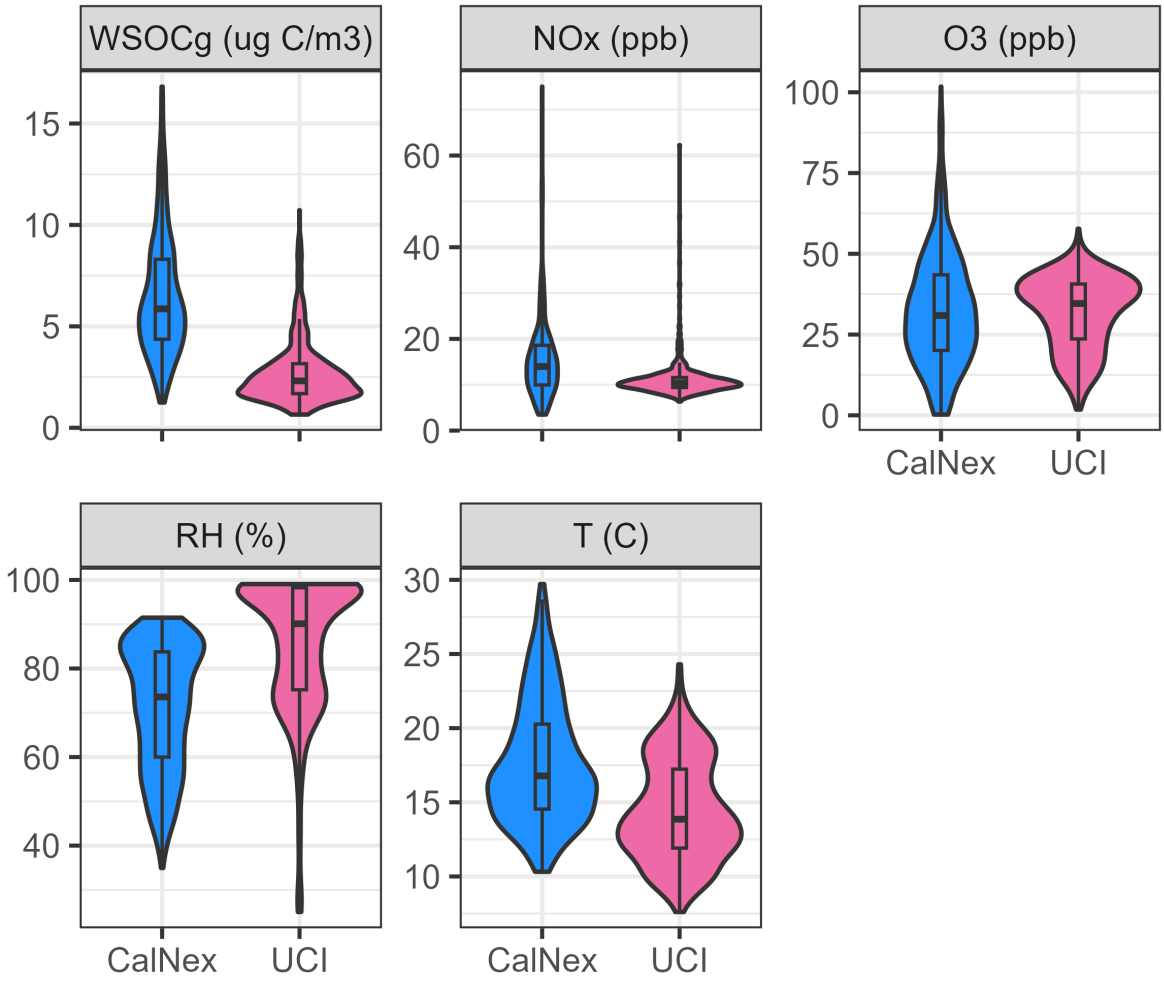


Figure C.5: Differences in measured chemical and meteorological variables at Pasadena (CalNex, Blue) and Irvine (UCI, pink). All population differences are significant at the 95% level ($p < 0.05$) aside from $O_3$ ($p = 0.22$).

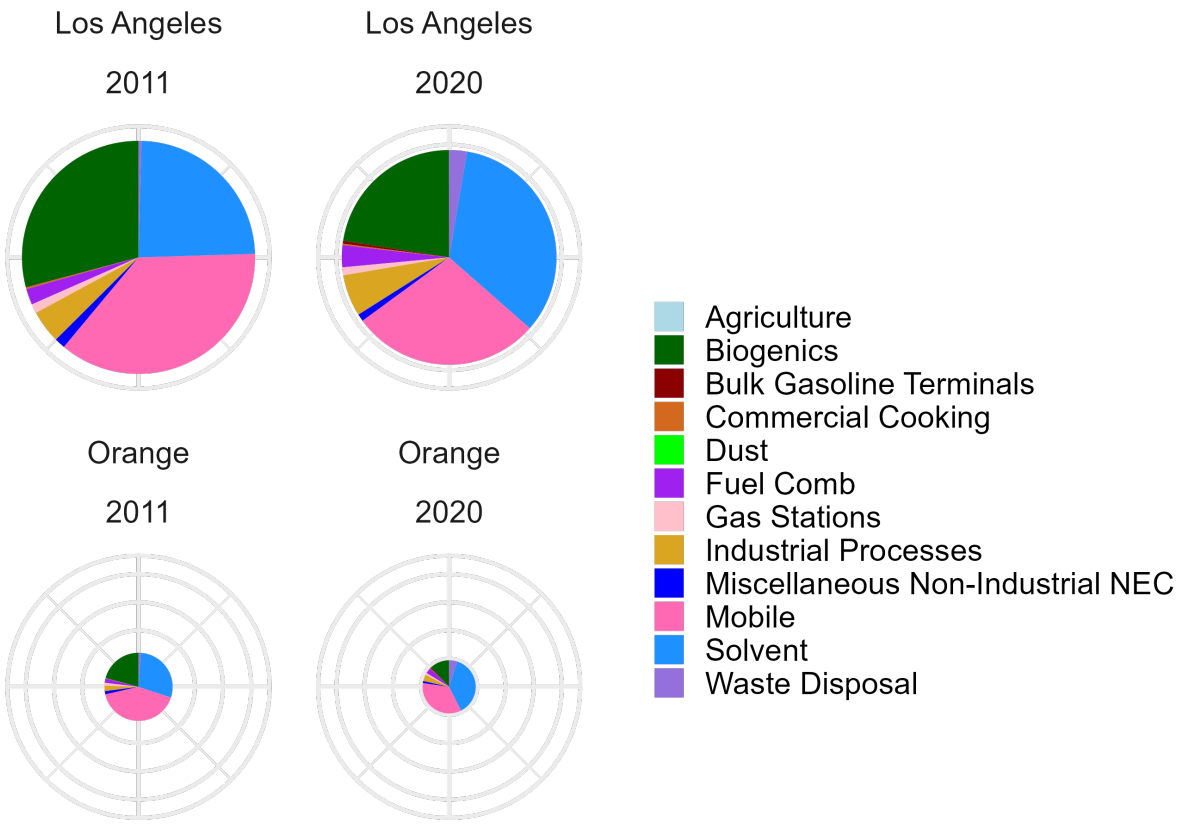


Figure C.6: NEI-reported VOC emissions (tons $yr^{-1}$) for Los Angeles county (Pasadena) and Orange county (Irvine) in 2011 and 2020, the best available matches to sampling times.

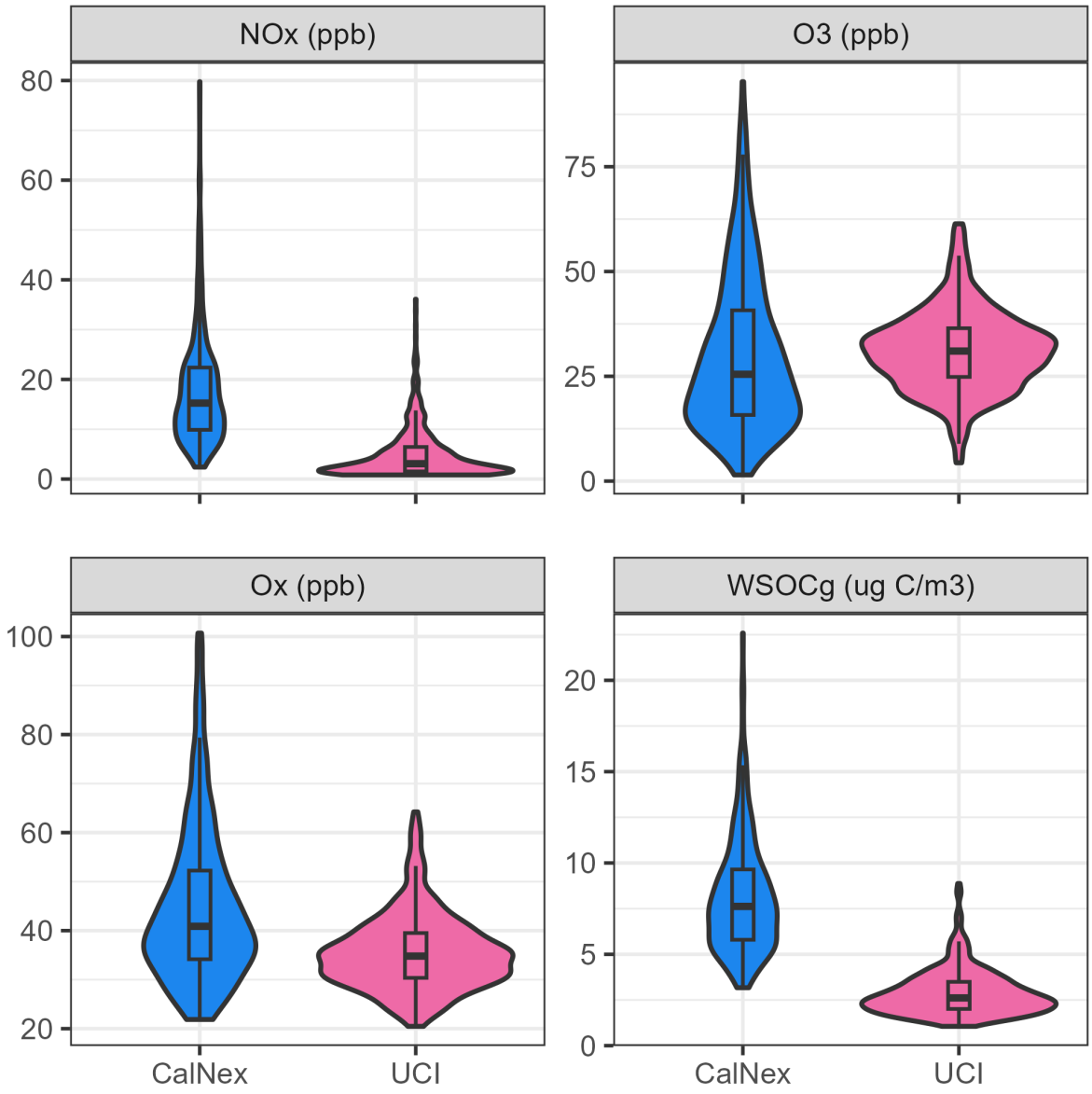


Figure C.7: Differences in CMAQ-simulated chemical variables at Pasadena (CalNex, Blue) and Irvine (UCI, pink). All population differences are significant at the 95% level ($p < 0.05$).

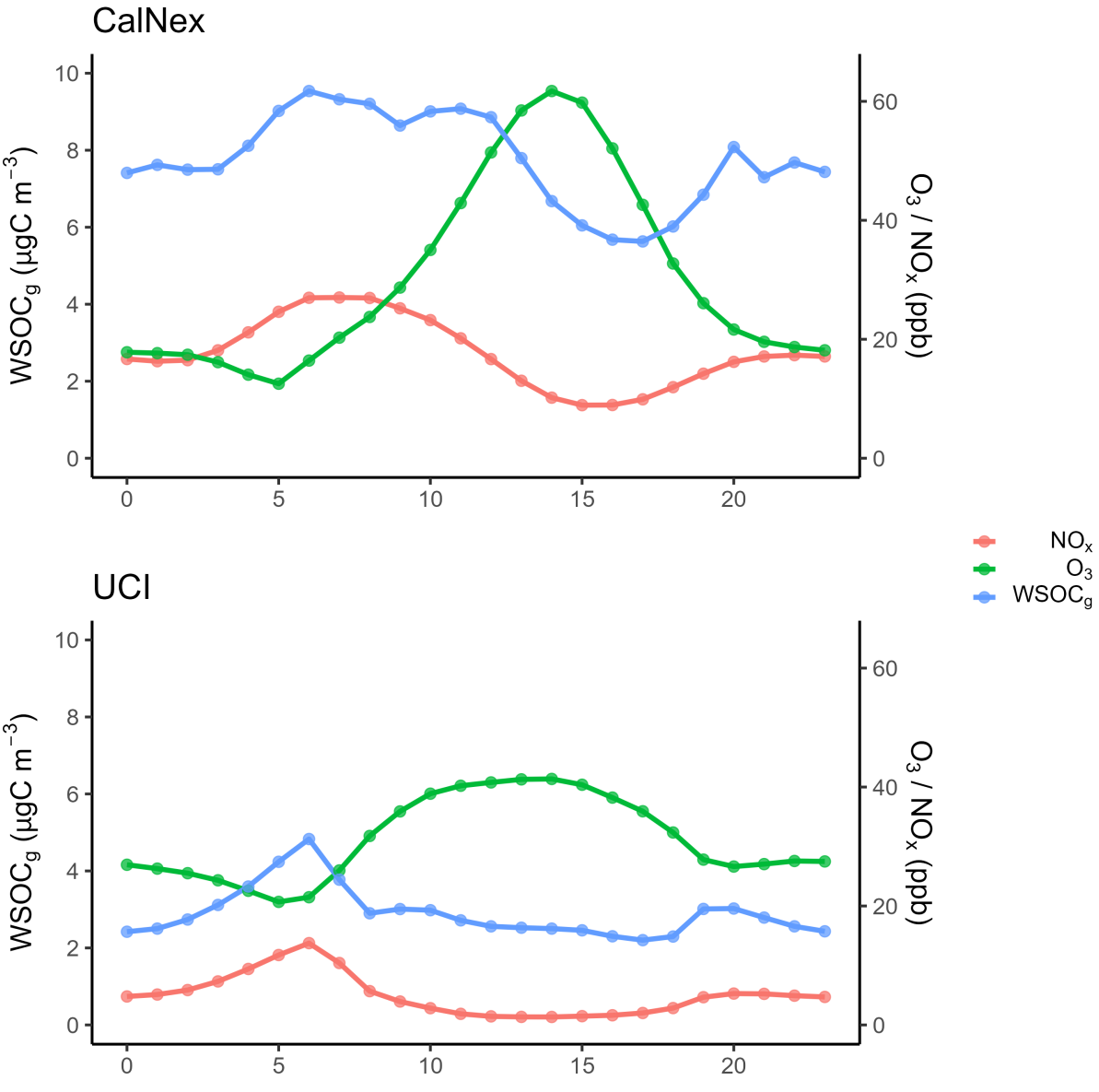


Figure C.8: CMAQ-simulated diurnal cycles of $WSOC_g$, $O_3$, and $NO_x$ and Pasadena (CalNex) and Irvine (UCI).

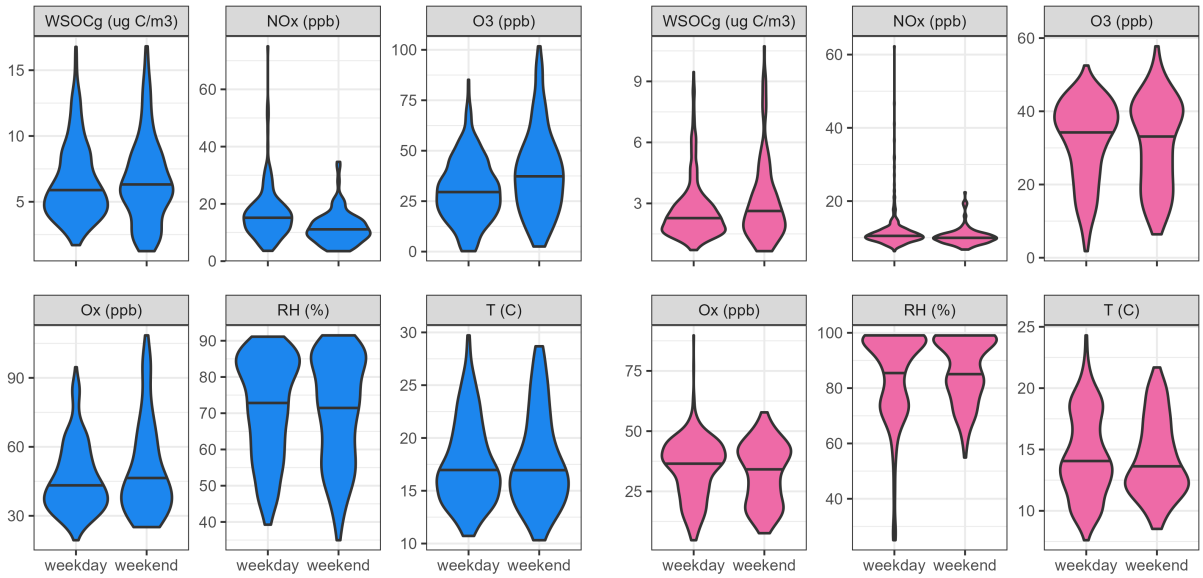


Figure C.9: Differences in measured chemical and meteorological variables on weekends and weekdays at Pasadena (CalNex, Blue) and Irvine (UCI, pink). No population differences are significant at the 95% level ($p < 0.05$) aside from $WSOC_g$ at Irvine ($p = 0.03$), $NO_x$ at both sites($p \approx 0$), and $O_3$ at Pasadena ($p \approx 0$).

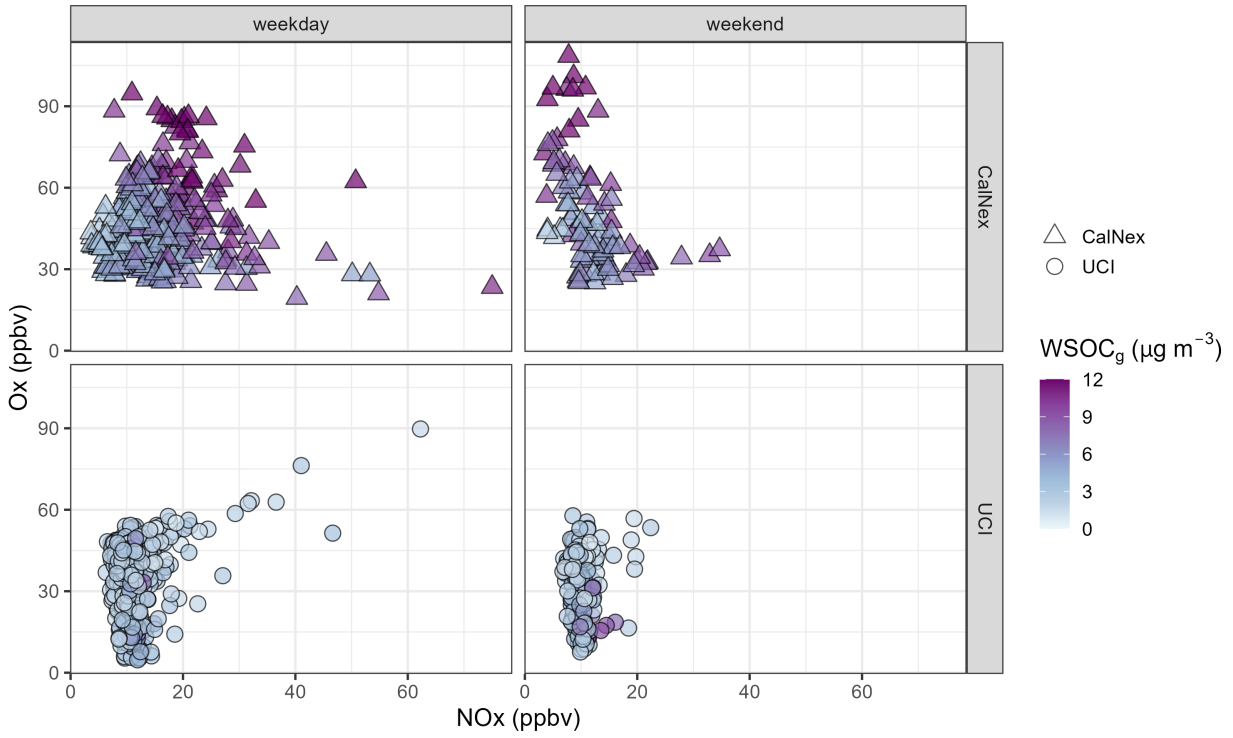


Figure C.10: Measured $O_x$, $NO_x$, and $WSOC_g$ relationships for each campaign during weekdays and weekends for each campaign. Pasadena data is in the top row (CalNex) and Irvine data is in the bottom row (UCI).

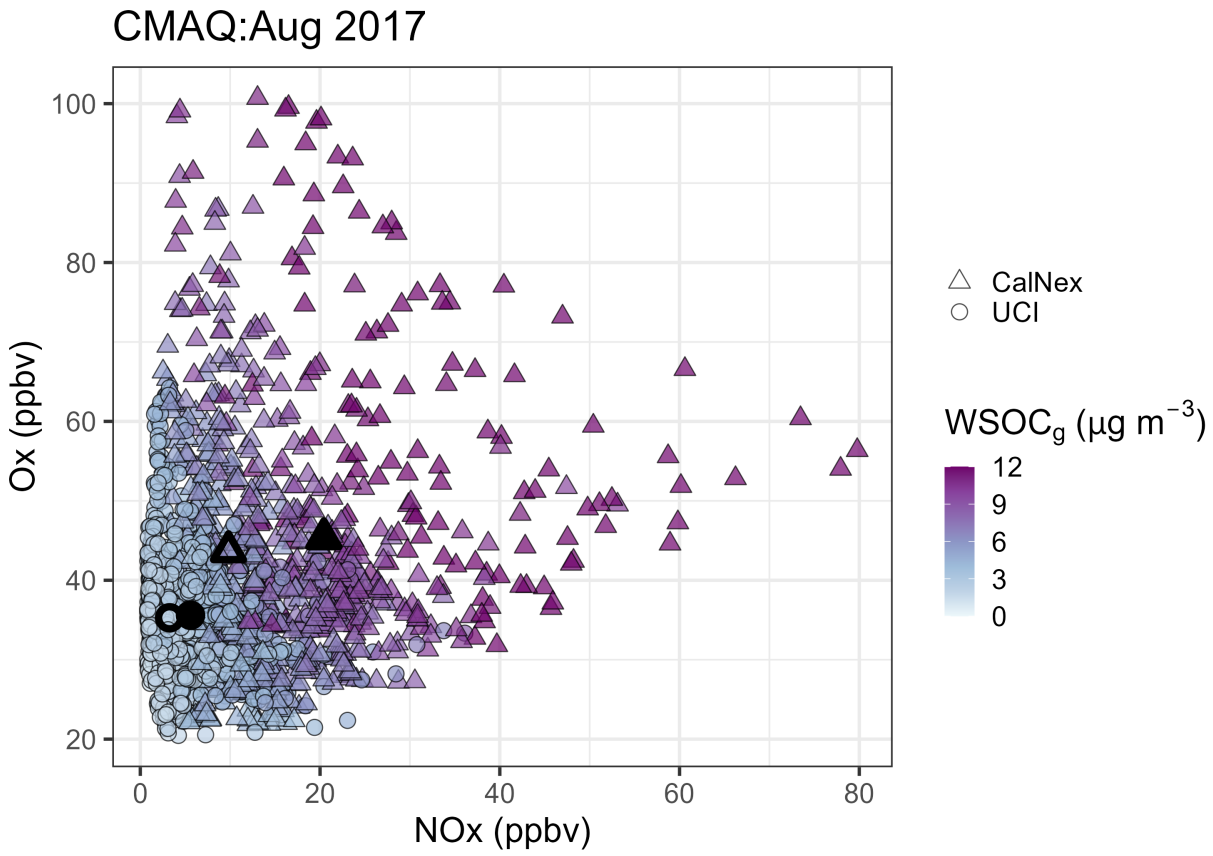


Figure C.11: Relationship of CMAQ-simulated $O_x$, $NO_x$ and $WSOC_g$ at Pasadena (CalNex, triangles) and Irvine (UCI, circles). The bold black points represent the overall average values of $O_x$ and $NO_x$ for weekdays (solid points) and weekends (open points).

Figure C.12: Correlation matrix of CMAQ-simulated $WSOC_g$ versus other chemical variables. Pearson's correlation coefficients are displayed in each cell, and are color-coded according to that value.

# Appendix D

# A Specifications-Graded, Spice-Themed, General Chemistry Laboratory Course Using an Argument-Driven Inquiry Approach

The contents in this Appendix are reproduced with permission from the following publication: Shannon J. Saluga*, Alyssa M. Burns*, Yong Li*, Melanie M. Nguyen, and Kimberly D. Edwards. Journal of Chemical Education. **2023**. 100 (10), 3903-3915. DOI: 10.1021/acs.jchemed.3c00433. Copyright © 2023 The Authors. Published by American Chemical Society and Division of Chemical Education, Inc. This publication is licensed under CC-BY 4.0. ** denotes equal contribution*

The Supporting Information includes the IRB Statement, Project Manual Links, Survey Questions, Posters, Sample Quiz and Exam Questions, Specifications Use and Letter Grade Requirements, and Modifications to Project 2, and is available at: https://pubs.acs.org/doi/10.1021/acs.jchemed.3c00433.

## D.1 Abstract

This paper describes the creation of a second quarter of a two-quarter sequence of argument-driven inquiry general chemistry laboratories. The course contains four projects investigating the chemistry of spices (vanilla, cinnamon, spearmint, and cloves) and incorporates a structured review and hands-on applications of fundamental concepts necessary to transition between general and organic chemistry (colligative properties, TLC, synthesis, characterization tests, and unknown determination). The inquiry-based curriculum was designed to give students increasing responsibility and freedom to develop experimental design skills. Specifications grading is used to increase concept iteration and encourage teamwork among students. Survey results for student learning style, feelings about chemistry, and perception of the course format are compared for the first and second quarter courses. Changes in survey responses show higher average positive responses in many categories for the second quarter course.

## D.2 Introduction

Herein, we describe the thematically connected curriculum for the second quarter of the general chemistry laboratory course (GCL-II) at the University of California, Irvine (UCI). We previously described the creation of the first quarter large-scale general chemistry laboratory course (GCL-I) using the same methodology.[1]

### D.2.1 Course Scale and Structure

UCI's nonchemistry-major two-course general chemistry laboratory sequence (GCL-I and GCL-II) spans two 10-week quarters. Weekly four hour laboratory sessions with 24 students are supervised by one graduate student teaching assistant (GTA). The first quarter of lab (GCL-I) is taken with the last quarter of general chemistry lecture (GC-III) and the second quarter of lab (GCL-II) is typically taken with the first quarter of organic chemistry lecture (OC-I) (Table D1). The high-enrollment (1300+ students) GCL-I course offering occurs each spring, followed by a high-enrollment (1000+ students) GCL-II course offering each fall. Summer session and alternate quarter course offerings for both courses typically have enrollments of approximately 200 students who either did not initially pass prerequisite lecture courses or completed the course sequence off track. On-sequence high-enrollment GCL-I and GCL-II courses typically require 50 lab sessions and 25 GTAs. Off-sequence low-enrollment courses require 8 lab sessions and 4 GTAs. (Online SI contains GCL-II student demographics).

UCI's offset of lower division lab from lecture, specifically the coupling of the large enrollment on-sequence GCL-II with OC-I, permits the incorporation of organic chemistry content in GCL-II, resulting in a transitional course bridging general and organic chemistry. Because GCL-II relies on theories connected to intermolecular forces introduced in GC-II, students in the off-sequence GCL-II can still connect conceptually with course content and benefit from the exposure to introductory organic techniques once enrolled in the organic chemistry laboratory.

Originally, the 8 weeks of traditional expository-type experiments in GCL-II addressed diverse topics derived from general chemistry lecture and the corequisite organic chemistry lecture course (e.g., solubility and miscibility, vapor pressure, analysis of a chelated iron salt, aspirin, and chlorophyll). During the laboratory, students worked in pairs to complete the

| Year | Fall Quarter | Winter Quarter | Spring Quarter |
|---|---|---|---|
| First-Year On-Sequence | General Chemistry Lecture I (GC-I) *(No Laboratory Course)* | General Chemistry Lecture II (GC-II) *(No Laboratory Course)* | General Chemistry Lecture III (GC-III) **General Chemistry Laboratory I (GCL-I)** |
| First-Year Off-Sequence | | General Chemistry Lecture I (GC-I) *(No Laboratory Course)* | General Chemistry Lecture II (GC-II) *(No Laboratory Course)* |
| Second-Year On-Sequence | Organic Chemistry Lecture I (OC-I) **General Chemistry Laboratory II (GCL-II)** | | |
| Second-Year Off-Sequence | General Chemistry Lecture III (GC-III) **General Chemistry Laboratory I (GCL-I)** | No Lecture Course **General Chemistry Laboratory II (GCL-II)** | Organic Chemistry Lecture I (OC-I) *(No Laboratory Course)* |

Table D.1: Structure of on-sequence and off-sequence general chemistry courses.

procedures outlined in the laboratory manual. After completing the experimentation, each student worked independently to answer postlaboratory questions including calculations with collected data or answering conceptual questions.

### D.2.2 Theme

Instead of a broad expository coverage of topics, the new GCL-II course still takes advantage of the corequisite organic lecture (OC-I), but is structured around four spice-themed projects following the argument-driven inquiry (ADI) format developed for GCL-I. Theme-based instruction in general chemistry laboratory courses has been used to contextualize course content for students.[2−8] Thematic connections between experiments provide students a conceptual framework,[9] make course content more relevant,[4,9] and increase student understanding[10,11] and engagement.[4,5,9,11,12] Because of this and the positive student response

to the Gatorade theme in GCL-I, we also adopted a theme for GCL-II.[1] Spices were chosen because their organic nature resonates with students concurrently enrolled in OC-I while still utilizing concepts from GC-II to remain accessible to off-sequence students. Furthermore, their benign nature eliminates most chemical hazards and waste.

In the first project of GCL-II, students use freezing point depression and melting point spectroscopy to determine the identity of an unknown spice compound. In the second project, students identify spice compounds in an essential oil through thin-layer chromatography (TLC). The final two projects require students to use techniques learned in GCL-I and the previous projects in GCL-II to synthesize and determine the product of vanillin oxidation and to synthesize and determine the better sunscreen product from ketone and cinnamaldehyde reactions.

### D.2.3 Argument-Driven Inquiry

The previous version of GCL-II used confirmation-type experiments which provided detailed procedures and postlaboratory questions. Such an approach encourages students to engage in basic science process skills: observation, measurement, and data interpretation. There is support in the education community for going beyond this type of confirmation style experiments.[13–16]

In comparison, Argument Driven Inquiry (ADI) experiments now used in GCL-II provide general procedural guidance and use the claim-evidence-justification framework.[11] Students engage both in the above skills and in additional science process skills: hypothesis (claim) formulation, experimentation, and communication (through argumentation).[15,17–20] The inquiry approach engages students more authentically in experimentation by requiring them to develop their own procedures.[14,21] Furthermore, argumentation requires students to defend their claims and critique those of others. By combining inquiry and argumentation,

| **Students will be able to . . .** |
|---|
| LO1: Broadly, engage in scientific inquiry and argumentation with a team of peers. |
| LO2: Develop fundamental laboratory skills and design experimental procedures. (Skills: recordkeeping, safety/waste disposal, UV-Vis spectroscopy, separations, chromatography, melting and freezing point, and synthesis). |
| LO3: Collect data, determine and perform data analysis on characterization test results. |
| LO4: Determine what data are evidence that can be used as justification to support a claim. Defend scientific reasoning to peers. |
| LO5: Produce an independent report defending their team's claim using scientific reasoning, experimental design, and data analysis. Utilize the revision process to correct misconceptions. |
| LO6: Demonstrate laboratory skill proficiency and argumentation abilities in the final practical exam. |
| LO7: Demonstrate a basic understanding of lab safety through safety moments, weekly quizzes, and the safety exam. |

Table D.2: GCL-II Learning Outcomes (LOs)

ADI has been shown to increase student ability to use evidence and reasoning, create a more positive student attitude toward chemistry, and improve performance on summative assessments.[17,20,22,23]

Additionally, the encouraging results of the Laboratory Course Assessment Survey (LCAS) given to GCL-I students led us to continue the ADI approach in GCL-II.[1] The LCAS measures student perception of peer collaboration, knowledge discovery, and iteration (revision and repetition) for course-based undergraduate research experiences (CUREs).[24] We incorporated the survey because it also probes student perception of relevant ADI activities and, hence our course learning outcomes (Table D2): planning and conducting investigations (LO2 and LO3), collecting and analyzing data (LO3 and LO4), working with others (LO1 and LO4), and presenting and revising work (LO5).

## D.3 Methods

GCL-II's ADI course structure like GCL-I[1] contains four 2-week projects. The learning outcomes (Table D2) are inseparable from the seven-step ADI process (Figure D1):

1. **Guiding Question (LO1):** To prepare for a project's first laboratory session (the fundamental skills (FS) session), students are given an initial guiding question (Table D3, second column) and provided general technique information. Before entering the lab, students independently complete a prelaboratory quiz and prepare their electronic laboratory notebook (ELN) with an objective, safety and chemical tables (LO7), and a draft of procedures to follow in lab.

2. **Fundamental Skills (LO2 and LO3):** During the FS session, a team of 3 to 4 students (randomly formed during the first course meeting) practice the general technique, collect data, and perform data analysis to answer the guiding question. The team then creates a procedural plan to approach a second guiding question (Table D3, third column) for the original investigation (OI) in the following laboratory session.

3. **Plan for Original Investigation (LO2):** To prepare for a project's second laboratory session (the OI session), students independently complete a prelaboratory quiz and prepare their ELN as they did for the first lab session.

4. **Original Investigation (LO3):** During the OI session, the team follows their procedural plan to collect more data, performs data analysis, then provides a justification of their claim (the second guiding question's answer).

5. **Argumentation (LO1 and LO4):** Using chalk paint on their benchtop, the team creates a poster with their claim, evidence, and justification. One team member stays with the poster to defend the team's argument to other teams, while the remaining team members travel to other posters and critique their claims.

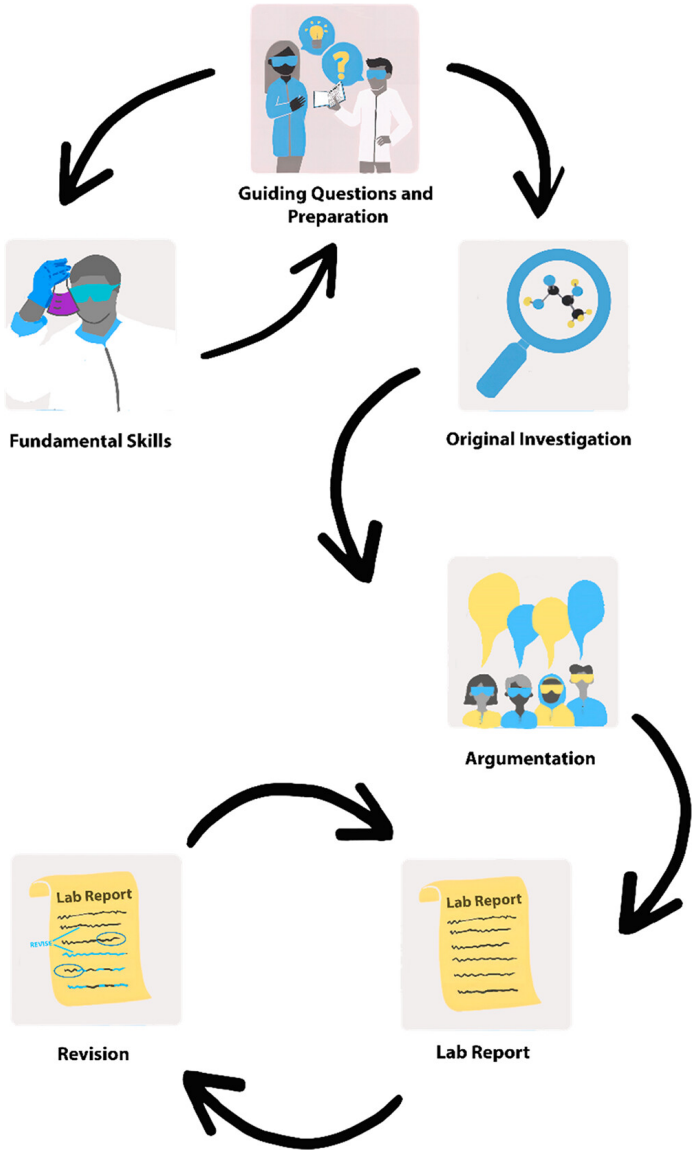


Figure D.1: ADI process.

6. **Laboratory Report (LO5):** After the OI lab session, students individually write a report based on their experimental work, data analysis, and feedback received during the argumentation session.

7. **Revise and Resubmit (LO5):** Students may revise work based on GTA feedback in exchange for tokens earned through the specifications grading system (see SI).

| **Project** | **Fundamental Skills (FS)** | **Original Investigation (OI)** |
|---|---|---|
| 1 | What is the average freezing point depression constant for menthol? What is the melting point of the solute? *Students measure the freezing point of pure menthol and a menthol solution to determine the freezing point depression constant. Students also measure the solute melting point.* | What is the identity of the unknown spice chemical? *Students measure the melting point of an unknown and the freezing point of a menthol solution containing a known amount of that unknown. The unknown's molecular mass is determined by freezing point depression.* |
| 2 | What are the Rf values of the spice compounds? Which heptane:acetone ratio is the best eluent? *Students run multiple TLCs of known compounds in various eluent mixtures.* | Which spice compounds are present in the essential oil? *Students run a TLC of an essential oil with an eluent mixture chosen from the previous work and compare the Rf values to the standards.* |
| 3 | What is the percent yield of the synthesis if the product is divanillin? If the product is vanillic acid? *Students perform an oxidation of vanillin and measure the product's yield.* | What is synthesized, divanillin or vanillic acid? Is the product pure? *Students use product solubility, melting point, TLC, and UV-Vis absorbance to characterize their product.* |
| 4 | What are the characteristics of the products observed so far make for a good sunblock? *Students synthesize, crystallize, and begin characterization tests.* | When combined with cinnamaldehyde, which reagent (acetophenone or acetone) makes the best sunblock? Why? *Students complete characterization tests on both products.* |

Table D.3: Guiding Questions for GCL-II.

Our seven ADI steps incorporate scientific inquiry processes: problem identification, making observations, posing questions, collecting data, using scientific concepts to analyze data, and

finally, summarizing and communicating results.[25] While most undergraduate laboratory curriculum contains the above steps, the amount students can control experimentation (the inquiry level) is on a continuum. Experiments can range from confirmation type experiments (in which all experimentation parts are dictated) to authentic inquiry (where the student is responsible for the entire process, from the problem investigated to the conclusion derived from the results). Structured, guided, and open inquiry span the difference between these two extremes (Figure D2).[21,36–29]

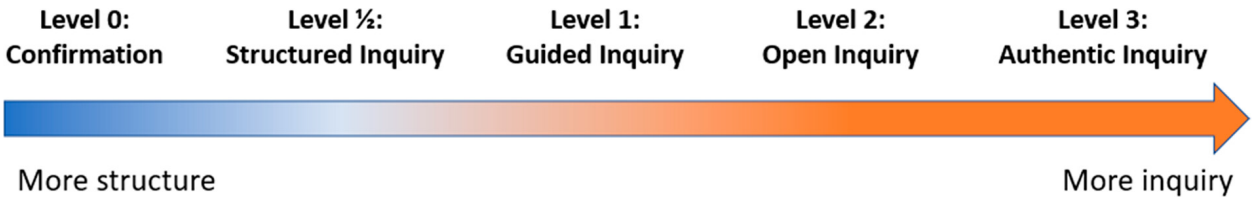


Figure D.2: Spectrum of inquiry instruction.[21]

An analysis of GCL-I and GCL-II experiments using Bruck et al.'s *Rubric to Guide Curriculum Development*[27] is shown in Table D.4. In the first week of each GCL-I project (the FS session), the questions, background, procedures, and data analysis are provided. Therefore, the inquiry level for the FS sessions is structured. The second week of each GCL-I project (the OI session) provides:

- A new guiding question (Table D3)
- General instructions about poster creation for argumentation including claim, evidence, and justification.
- Lab report content questions regarding concepts investigated, procedures used, and claim justification. Students have access to a rubric, which is specific to each project and provides the student some direction as they prepare their report (Rubric examples, SI Section II).

| Characteristic | GCL-I FS 1-4 | GCL-I OI 1-4 | GCL-II FS 1 & 2 | GCL-II OI 1 & 2 | GCL-II FS 3 & 4 | GCL-II OI 3 & 4 |
|---|---|---|---|---|---|---|
| Problem /Question | P[a] | P | P | P | P | P |
| Theory /Background | P | P | P | P | P | P |
| Procedures /Design | P | P | P | P | P | NP |
| Results Analysis | P | NP | P | NP | NP | NP |
| Results Communication | NP[b] | NP | NP | NP | NP | NP |
| Conclusion | NP | NP | NP | NP | NP | NP |
| Level of Inquiry | Structured (0.5) | Guided (1) | Structured (0.5) | Guided (1) | Guided (1) | Open (2) |

Table D.4: Level of Inquiry by a Laboratory Session. [a]P = provided, [b]NP = not provided.

Because results analysis/interpretation are not provided in the OI sessions, the inquiry level is guided.

Like GCL-I, the first two projects of GCL-II start with structured inquiry FS sessions, followed by guided inquiry OI sessions. The third and fourth projects of GCL-II rely on the techniques learned in GCL-I and the first two projects of GCL-II to characterize products. Students are reminded of the techniques learned thus far and a few experimental directions (potential solvents, dilution factors, and synthesis procedures). This reduces cognitive load and ensures lab work can be completed during the 4 h time block. Therefore, the inquiry level in the FS sessions has increased to guided inquiry in the last two projects of GCL-II. While the question, background and procedures are given, no indication of how to analyze the data is provided. The OI sessions for these two projects increase inquiry further toward open inquiry by not providing procedures/design. By Project #4, the only information available to provide guidance in answering the OI guiding question is a list of the characterization tests learned during the course sequence with a few experimental details so that students can accomplish the work within the allotted laboratory time.

For an ADI course, content that predictability results in naturally occurring variability is often chosen. (Note: this is the opposite of confirmation-type curriculum which relies on the students finding one correct answer.)[13,32] Therefore, an experiment that does not consistently provide good data for novices may work well for ADI. Another important aspect of ADI experiment design is the type of guiding question. Choosing a guiding question focusing on distinguishing (or identifying) instead of obtaining mathematical values supports variation in experimental design and data interpretation.[19]

While GCL-II's FS guiding questions often ask students to obtain specific mathematical values (such as melting points, retention factors, and percent yields), the guiding questions of the OI (which are central to the argumentation process) do not (Table D3). Furthermore, while the OI guiding questions of GCL-II's first three projects do have correct, scientifically sound answers, flaws in student extrapolation of FS procedure and data analysis in the OI sessions lead to varied data and result in differing claims between student teams. Finally, the last GCL-II project (#4) starts with a guiding question with only conditional answers. One team's product might be better because it is pure, while another team's product has a higher yield, and so on. Another benefit of this variability is that small experimental details are interchangeable in a way that does not affect project structure or documentation (learning outcomes, the manual, the answer key).

### D.3.1 Projects

GCL-II is a transitional course bridging general and organic chemistry with a mixture of concepts and techniques from the two subdisciplines. The course is designed so major concepts and techniques, such as TLC, reoccur throughout projects. Projects also have enough variability to increase the level of inquiry and foster discussion. TLC eluent, for example, is not dictated, and students can choose characterization tests when determining product

identity. Furthermore, some conclusions depend on techniques learned (Projects #1 and #2) while others allow students to choose techniques they wish to perform (Projects #3 and #4).

#### D.3.1.1 Project #1: Menthol and Freezing Point Depression

Project #1 focuses on determining an unknown's identity with freezing and melting points. Many freezing-point depression experiments are known;[29,33–37] herein, we use menthol as a solvent and spice compounds as the solute. In the FS session, student teams measure menthol and cinnamic acid melting points using a melting point apparatus. Students also set up, measure, and analyze the cooling curves for menthol and cinnamic acid-menthol solutions to determine freezing points and calculate their team's $K_f$ and average $K_f$ values of menthol for the lab section.

For the OI, students are provided an unknown: cinnamic acid, 4-hydroxybenzaldehyde or vanillin. Students identify the unknown by measuring the melting point and finding the molar mass using freezing point depression. Because the collection of the cooling curve requires proper technique (vigorous mixing), freezing point depression data are more varied compared to melting point data (Figure D3). As seen in Figure D3, the ability to determine the freezing point (based off of the graph's inflection point, or the plateau that follows) is more difficult with an incorrect technique.

As part of argumentation, students must decide if they would use freezing point depression or melting point to characterize an unknown. A majority of students decided that freezing point depression is less useful. For future projects, most students choose the melting point over freezing point depression.

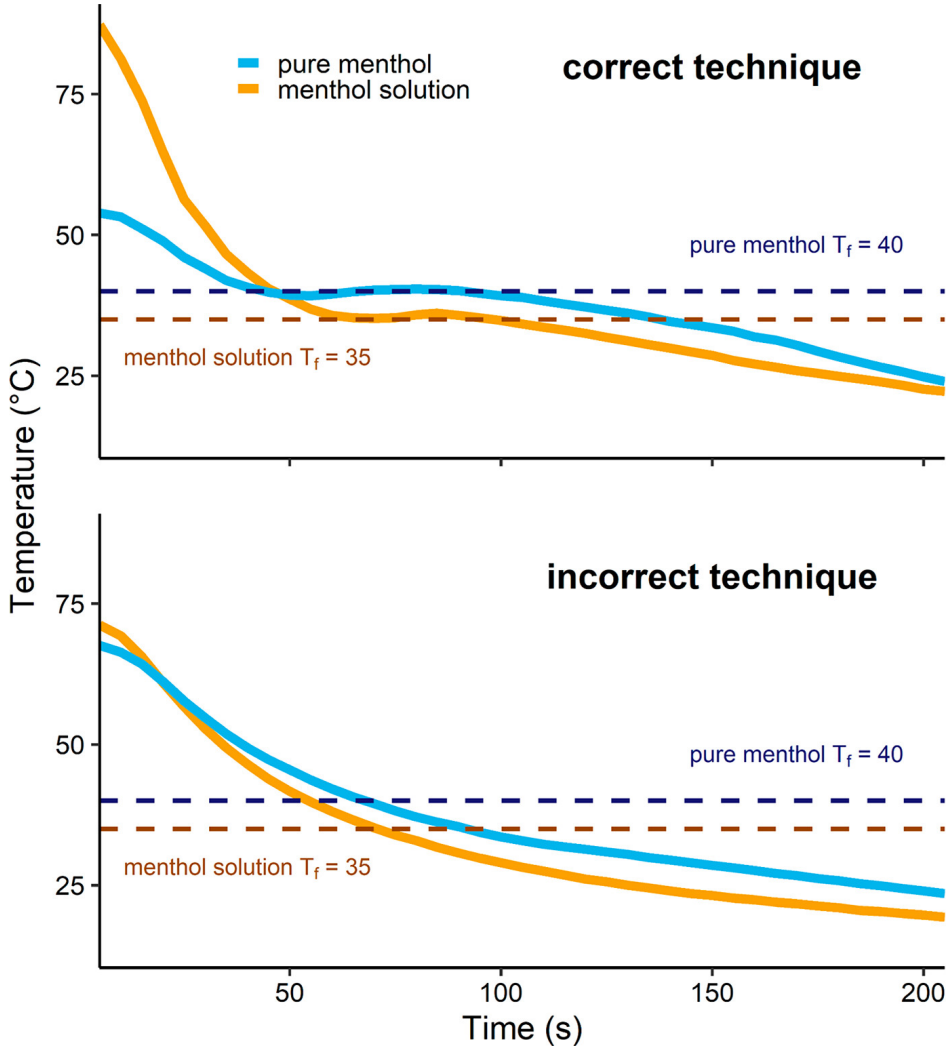


Figure D.3: Cooling curves of pure menthol and menthol solution acquired by using the correct (top) and incorrect (bottom) technique.

#### D.3.1.2 Project #2: Essential Oils and TLC

Project #2 focuses on thin-layer chromatography (TLC) and serves as a building block for later experiments. TLC is a separation technique widely employed in industry and laboratory courses.[38–40] Food-based analytes such as essential oils have been used for undergraduate TLC experiments since they are common, inexpensive, and often contain a mixture of organics for separation.[41,42] Inquiry-based TLC experiments have also been utilized, though these experiments are generally limited to factors modulating TLC performance.[38,43,44]

In the FS session, students are tasked to determine the best eluent to achieve good TLC separation of the provided standards: carvone, cinnamaldehyde, dihydrocarveol, eugenol, limonene, and vanillin. The eluents are of variable polarity, consisting of 1:1, 1:2, 2:3, or 3:2 heptane:acetone. (This procedure has since been improved; see SI). Students work within a team with each student developing TLC plates of all standards for a particular eluent ratio. All standards appear colorless, so UV light and permanganate dip techniques are employed to visualize aromatics/conjugated systems and oxidizable groups respectively. While the various eluent ratios produce varied separation between standards, results are also affected by the student technique. Once all plates are developed, teammates compare $R_f$ values to determine the best eluent ratio. (The eluent ratio with the most distinct standard $R_f$ values is 3:2 heptane:acetone, Figure D4.) These $R_f$ values are also used in the OI.

In the OI, teammates work together to determine the chemicals present in an unknown essential oil. Ideally, students select the best eluent ratio from the FS session to run TLC on their unknown and then compare Rf values between standard and unknown plates to determine the unknown components. Other approaches may include running multiple plates with different eluent ratios, and/or rerunning standard plates from the FS session. The unknown sample is the same for all students (spearmint oil), and contains only carvone, limonene, and dihydrocarveol. One of the unknown components (carvone) is UV-active,

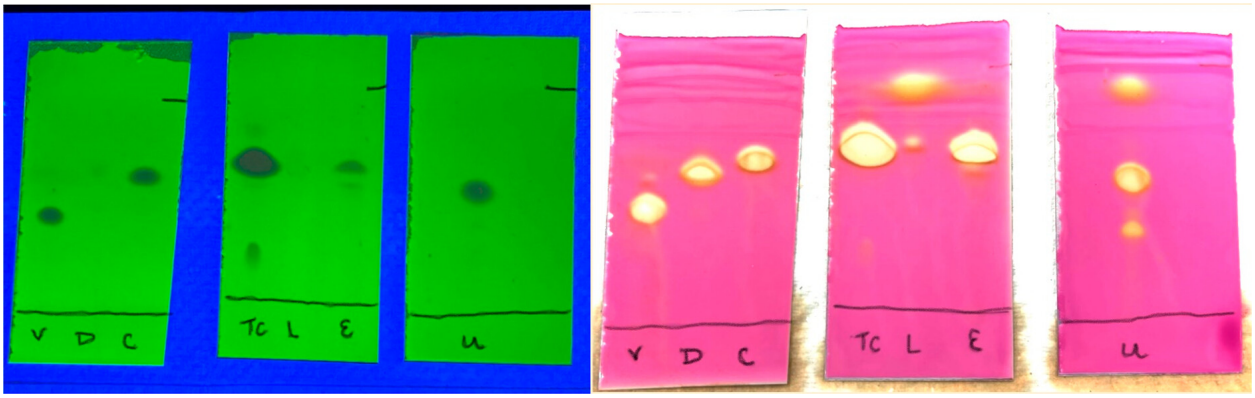


Figure D.4: TLCs of essential oil standards under UV light and after a permanganate dip (left to right: vanillin (V), dihydrocarveol (D), carvone (C), trans-cinnamaldehyde (TC), limonene (L), eugenol (E)) and the unknown spearmint oil (U) (rightmost) in a 3:2 heptane:acetone eluent mixture.

| **Claim: Which essential oils are present in the unknown?** | **Eluent Ratio (heptane:acetone)** |
|---|---|
| Carvone and Limonene | 2:3 |
| Carvone and Eugenol | 2:3 |
| Carvone | 3:2 |
| Carvone, dihydrocarveol, and limonene | 3:2 |

Table D.5: Representative Sample of Project #2 Student Claims and the Eluent Ratios used.

while the other two are visible after the permanganate dip. During argumentation, student results tend to vary both in eluent ratio selected and in the unknown components determined. For example, student claims vary from one to three unknown chemicals. Sample student responses (Table D5) and an argumentation poster example (Figure D5) are provided, and 39% of students sampled (n = 157) found 2 of the 3 right unknown compounds, and 56% of students used the best ratio (3:2 heptane:acetone).

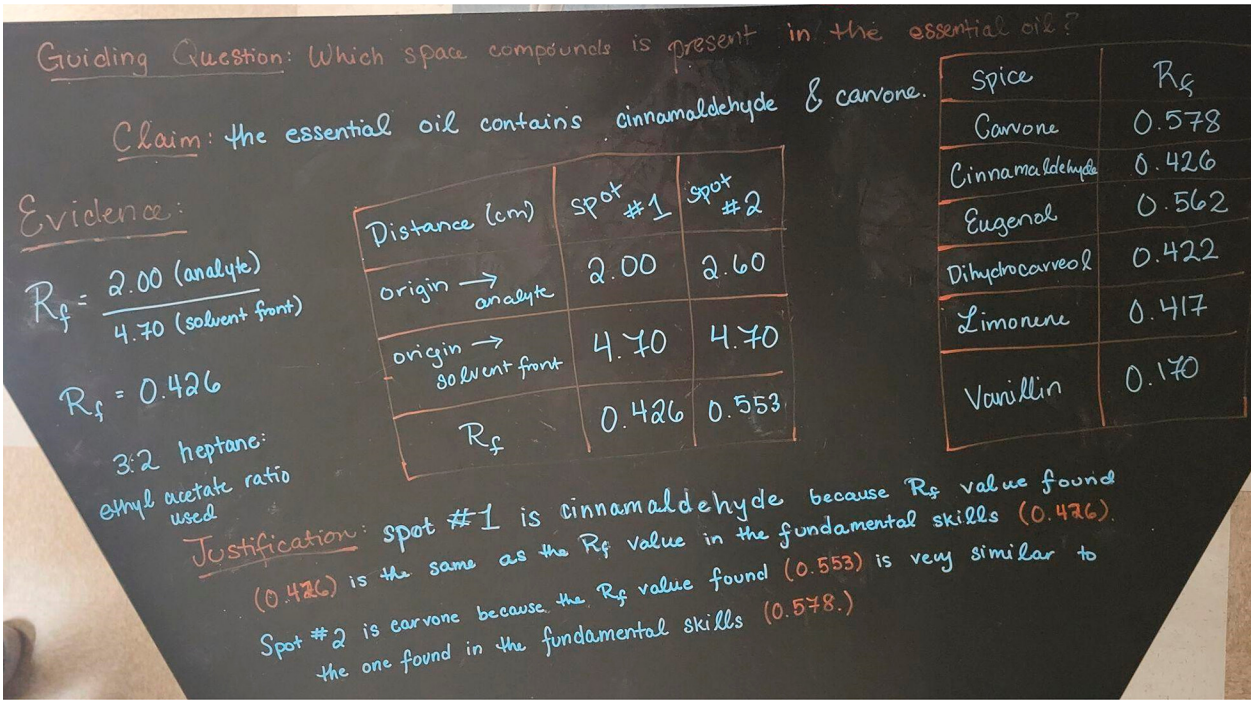


Figure D.5: Example of a Project #2 argumentation poster. Poster has been rewritten from a student poster by the authors for increased legibility.

#### D.3.1.3 Project #3: Vanillin Oxidation and Melting Point

Projects #3 and #4 are adapted from the literature[45–47] and focus on performing a synthesis during the FS session and then using characterization techniques of the student's choice during the OI session.

In Project #3, vanillin is reacted with hydrogen peroxide in the presence of horseradish peroxidase. The procedure is adapted from Vosburg,[45] with one modification: students are instructed to cool the reaction to room temperature before adding acetic acid and horseradish peroxidase solution (0.05 mg/mL). The FS session is the students' first exposure to organic synthesis and vacuum filtration. During the OI session, students are expected to determine the major product after the synthesis: vanillic acid, divanillin, or recovery of the vanillin starting material. While students can choose from characterization techniques they have used before, melting point analysis between the product and the provided standards of vanillin and

| | **Vanillin** | **Vanillic Acid** | **Divanillin** |
|---|---|---|---|
| Yield | n/a | n/a | 57.8%[a] |
| Solubility | EtOAc, EtOH, Water | EtOH, Water | EtOH |
| Melting Point (C) | 81-83 | 210 | 315 |
| $R_f$ (in 7:3 ethyl acetate:heptane | 0.64 | 0.46 | 0.15 |

Table D.6: Representative Sample of Student Data for Project #3 Chemicals. [a]Averaged from student data, *n = 102*, after excluding students who calculated over 100% recovery.

vanillic acid allows for conclusive determination that divanillin is the synthesized product. Other techniques used to determine the identity of the product include solubility, UV–visible spectroscopy (which students used in GCL-I) and TLC (sample data, Table D6). Because students successively build upon concepts learned in the course, no explicit procedure is provided for TLC or UV–vis spectroscopy.

#### D.3.1.4 Project #4: Cinnamon Sunscreen and UV-Vis Spectroscopy

Project #4 focuses on the synthesis of two aldol products from cinnamaldehyde and either acetone or acetophenone. At this point in OC-I (typically taken with GCL-II), the students have not learned aldol condensation and do not know the mechanism; therefore, the experimental focus is product characterization (sample data, Table D7).

| | **Acetophenone Aldol** | **Acetone Aldol** |
|---|---|---|
| Yield | 30-70% | 40-50% |
| Solubility | EtOAc (partial), EtOH (partial) | EtOH, EtOAc |
| Melting Point (C) | 100-102 | 142-143 |
| $R_f$ (in 3:2 ethyl acetate:heptane) | 0.57 | 0.46 |

Table D.7: Representative Sample of Student Data for Project #4 Chemicals.

The procedure was adapted from Jaworek-Lopez and Dicks, but with only acetone or acetophenone as the ketone partner to cinnamaldehyde.[46,47] The FS session focuses on the synthesis of either the cinnamaldehyde–acetone or cinnamaldehyde–acetophenone product; students work in teams of four with each pair performing one synthesis. During the procedure, students are introduced to recrystallization to purify products. The OI session focuses on the student's choice of three previously used characterization techniques to determine which product is the more effective sunscreen. The main technique for determination is designed to be UV–vis spectroscopy (Figure D6), but this characterization test is not required and is performed only at the student's prerogative. A conclusion can be made using whatever characterization tests are performed.

Both products could be argued to be the most effective based on a myriad of factors, from the respective absorbances in the UV region to the color of each purified product (Table D8).

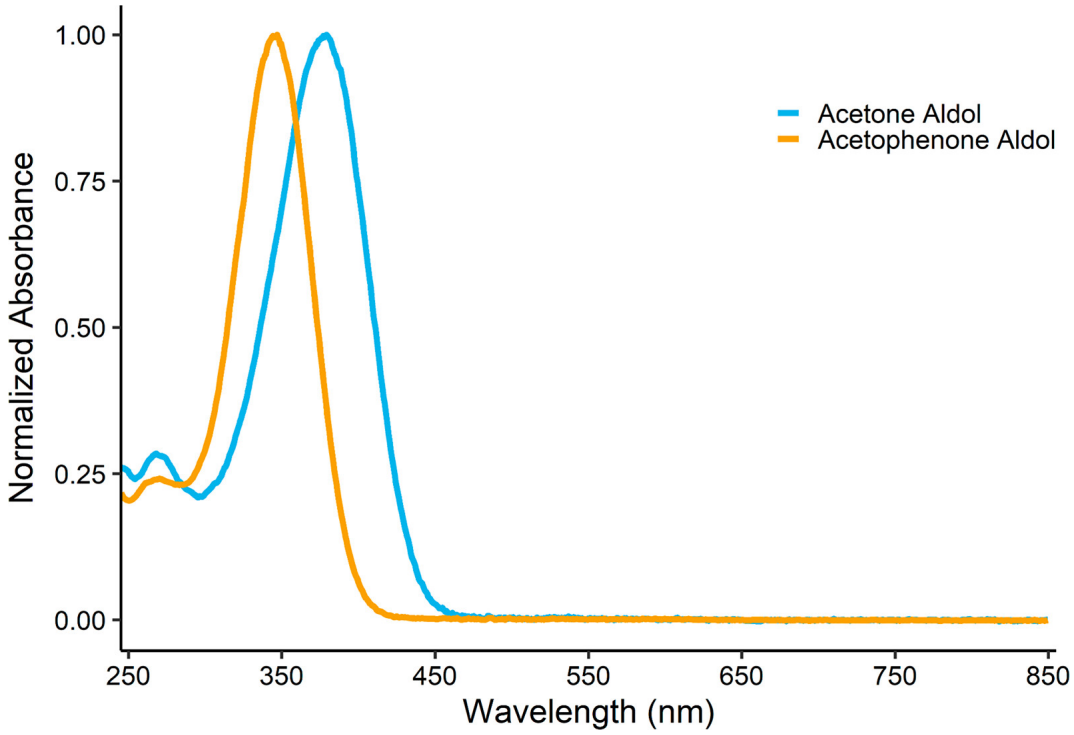


Figure D.6: UV–vis spectra of acetophenone and acetone aldol.

| **Claim: Which product is the better sunscreen?** | **Sample Justification** |
|---|---|
| Acetophenone Aldol Product | "It is insoluble in water... so it will be effective as a water resistant sunscreen. In addition, it had a higher yield, and will therefore be more cost-effective." |
| Acetone Aldol Product | "[The] acetone [product] is a better sunscreen ingredient because it had a higher melting point than the [acetophenone product]... and we want a sunscreen that will only melt at high temperatures." |
| Acetone Aldol Product | "[The acetone product] makes a better sunscreen... proven by the broader peak and the higher absorbance [relative to the acetophenone product] of the UV–vis spectra." |
| Acetophenone Aldol Product | "The amount of UV light that the [acetophenone aldol product] absorbed was the determining factor. The peak is larger and broader than that for the [acetone aldol product]. From this, we can conclude that the acetophenone product absorbs a larger amount of UV light." |

Table D.8: Sample Project #4 student claims and justifications

### D.3.2 Hazards

While many chemicals used (vanillin, cinnamaldehyde, eugenol, carvone, etc.) are flammable and skin and/or eye irritants/sensitizers in concentrated or pure form, all chemicals are used in either small quantities or are provided in dilute forms. The organic solvents used (acetone, heptane, ethanol, and ethyl acetate) have the same hazards, with the addition of central nervous system toxicity. Heptane is used in place of hexane because of its lower volatility. Horseradish peroxidase (Project #3) is a respiratory and skin sensitizer. Sodium hydroxide (3M, Project #4) is corrosive to the skin and can cause eye damage.

If required, waste is neutralized with citric acid and sodium bicarbonate. Glass TLC spotters are collected and disposed of by the GTAs to minimize contamination and injury.

Required laboratory attire for GCL-II includes safety goggles, lab coats, long thick pants covering ankles, sturdy water-resistant closed toed shoes, and nitrile gloves. These steps protect against exposure (to irritants, sensitizers, and corrosives) and cuts from broken glassware. All heating is done with hot plates and water baths to reduce the risk of ignition of flammable substances. Volatile organic solvents are used in the fume hood. No open flame is present in the laboratory.

### D.3.3 Student Assessment and Specifications Grading

In specifications grading, assignments or rubric items are combined into bundles, and the level to pass each bundle for a particular grade is specified. Each rubric item and bundled assignment are assessed as satisfactory or unsatisfactory. This grading method was first introduced by Linda Nilson in 2014.[48] Examples of specifications grading have been reported for general chemistry, biochemistry, biology, math, anatomy and physiology, engineering, and physics lectures, as well as scientific writing courses, general, and organic chemistry

| General Rubric Items | Fundamental Skills (FS) | Original Investigation (OI) | Lab Reports (LR) | Final Exam |
|---|---|---|---|---|
| Safety | × | × | | × |
| Objective/Purpose | × | × | × | |
| Concepts | × | | × | |
| Procedure | × | × | × | × |
| Observations | × | × | | × |
| Data Analysis | × | × | × | × |
| Argumentation | × | × | × | × |

Table D.9: General Rubric Items by Assignment Type.

laboratory.[1,49–62]

The specifications grading structure of GCL-II is the same as GCL-I. (1) For each project, three types (or grading bundles) of assignments are due: (1) the in-laboratory work done during the FS session; (2) the in-laboratory work done during the OI session; and, (3) the lab report completed after the OI session. All assignments have student facing rubrics, with each assignment type (bundle) containing the same general rubric item categories (Table D9). A final assignment bundle is the laboratory practical consisting of safety, technique, and argumentation. The practical contains all but two of the same general categories: (1) the safety part of the practical includes the safety rubric item; (2) the technique part includes procedure, observations, and data analysis rubric items; and (3) the argumentation part includes data analysis, but focuses on argumentation rubric items (claim, justification, and evidence).

The goal of specifications grading is to focus students on the specific skills/knowledge needed to meet course learning outcomes.[48,50,54,63,64] The repetition of the general rubric items throughout the courses is central to this effort. To ensure this repetition is obvious to students, rubric items are titled with a general rubric item name and then have a description specific to each assignment (SI Section II). Each rubric item is pass or no pass; no partial credit is given. To further encourage students to meet course learning outcomes,[58] students can revise and resubmit graded work in exchange for tokens earned by completing introduc-

tory course assignments, educational study surveys (described below), and midquarter GTA student evaluations (SI Section VII). (Note: Completion rate for token earning opportunities (including educational surveys) typically exceeded 98% of course enrollment.)

For a given course grade, students must pass a given number of assignments (Fundamental Skills, Original Investigation, Laboratory Reports) and practical exam sections. Performance on the prelaboratory quizzes dictates the assignment of + or – to the letter grade. This requirement is the same as published for GCL-I (1) (SI Section VII).

Because specifications grading is a noncompetitive grading process, teams work together in a collaborative manner, supporting the ADI process.[50,54,65] Furthermore, token earning and exchange permits revision on 5 of the 12 assignments (4 FS + 4 OI + 4 LR = 12). Token exchange for revision replaces the peer-review step often present in ADI.

## D.4 Results

### D.4.1 Attitude toward the Subject of Chemistry Inventory

Because the Attitude toward the Subject of Chemistry Inventory (ASCI (V2)) has shown the impact of a curriculum change, we choose to use the survey to measure students' attitude toward chemistry midway through each quarter of GCL-I and GCL-II.[66–69] In general, students indicate that the general chemistry laboratory is hard, tense, and challenging work that is beneficial and somewhat interesting and worthwhile regardless of their enrollment in GCL-I or GCL-II. (Figure D7).

Going from GCL-I to GCL-II, a statistically positive shift occurred in 9 of 20 items surveyed (demonstrated by bold green average shift values, Figure D7). While on the negative side of the center value (4), GCL-II is more relaxed, more organized, more secure, and clearer

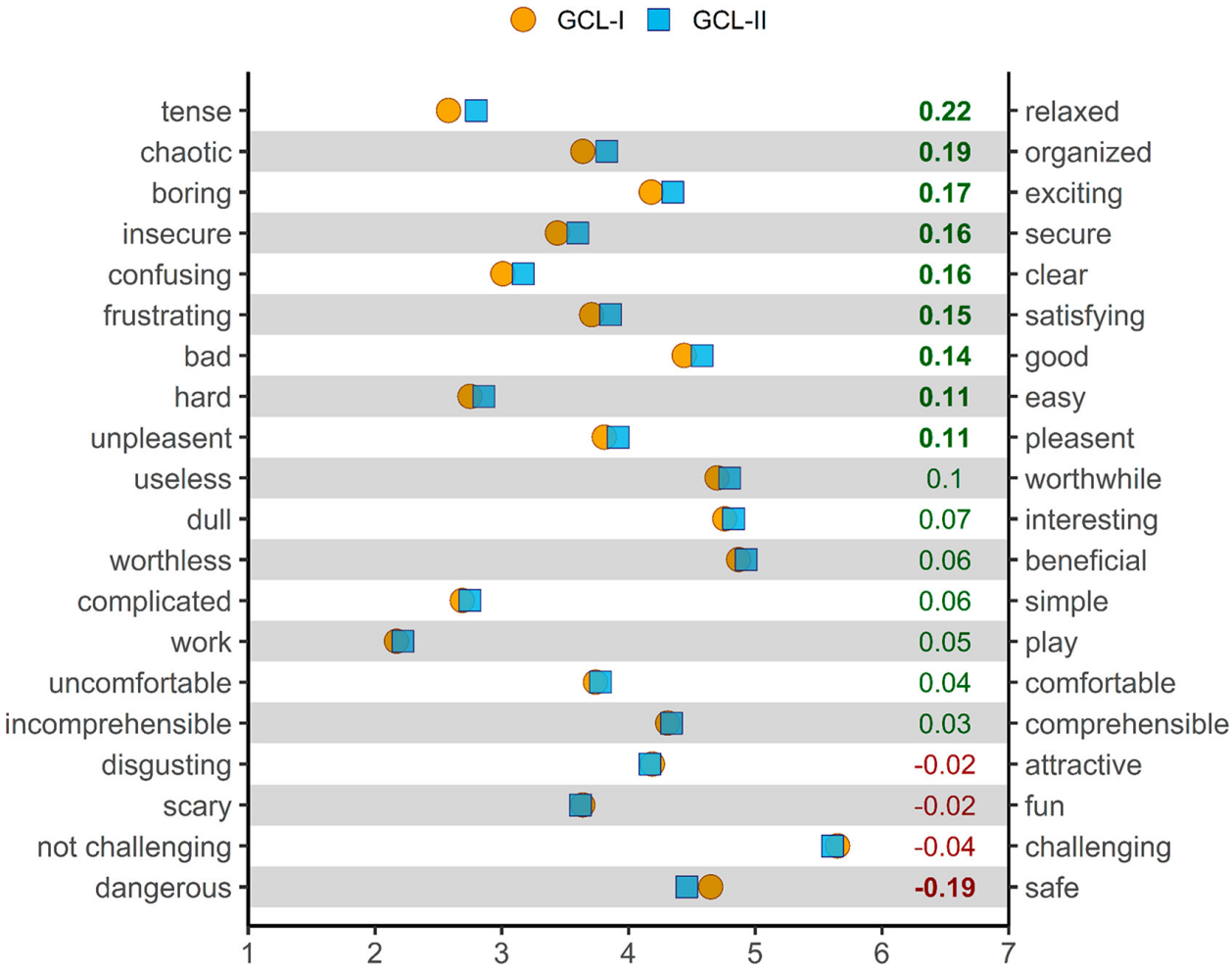


Figure D.7: Attitude toward the Subject of Chemistry Inventory (ASCI (V2)) results for GCL-I and GCL-II, large on-sequence courses. Positive adjectives are shown on the right, and their corresponding negative values on the left, reported as a continuum from 1 to 7. Average responses for GCL-I are shown in orange and GCL-II in blue . Changes that are statistically significant ($p < 0.05$ with Mann–Whitney U test) are denoted in bolded text. Numerical data can be found in the SI.

than GCL-I. Furthermore, GCL-II is more exciting, with an increase of 0.17. It cannot be discounted that with increased time in the lab, students will become more comfortable, which may influence the positive trends seen.

The only significant negative attitude shift is that students perceive GCL-II as less safe than GCL-I, with an average shift of -0.19. The increase in hazards between the GCL-I and GCL-II courses is a potential source. The hazards in the Gatorade themed GCL-I are limited to dilute solutions of acids, bases, and bleach. No chemical reactions require heating, and no vacuum is used. However, in GCL-II, the organic nature of many of the chemicals requires the use of volatile organic solvents (and, therefore, fume hood use), oxidizers, reaction heating, etc. in combination with safety curriculum covering these hazards.

### D.4.2 Laboratory Course Assessment Survey

A modified version of the Laboratory Course Assessment Survey (LCAS) was given to GCL-I and GCL-II while students were engaged in the fourth and final project. LCAS, a 17-item survey designed to measure the effectiveness of course-based undergraduate research experiences (CUREs),[24] contains three sections: assessing student perception of peer collaboration, generation of new knowledge, and work revision and repetition. In addition to the activities mentioned above, the LCAS tool measures student perception of course activities central to ADI: experimental design, data collection/analysis, and argumentation. Conclusions from survey data are offered with the caveat that no control group was used for comparison.

Collaboration was measured on a four point scale: weekly (4), monthly (3), 1 or 2 times (2), and never (1). Both Discovery/Relevance and Iteration were modified from the six point scale in the earlier work to a five point scale: (5) strongly agree, (4) somewhat agree, (3) neither, (2) somewhat disagree, and (1) strongly disagree. The sum of the averages for each of the three categories is reported in the gray box in the average (Avg) column.

The responses in the Collaboration (C1–C6) section are consistently high (Table D10). On average most activities occur almost weekly for both GCL-I and GCL-II. This consistent response indicates the ADI team structure results in the perception of collaboration (C1–C6).

The Discovery/Relevance (D1–D5) section contains survey items closely connected with the inquiry processes of the course: designing experimentation, forming a hypothesis, creating an argument, and communicating work. Overall, the averaged response shows small increases in agreement strength from GCL-I to GCL-II, indicating students perceive these inquiry processes are occurring repeatedly throughout the course sequence (Table D10). The agreement with the item about new argument creation based on data (D4) is the highest agreement level of all of the survey items. Furthermore, the agreement with this item increases slightly from GCL-I to GCL-II, suggesting the argumentation sessions (which occur with each project) play a prominent role in the students' perception of the curriculum. Conversely, the "generate novel results... of interest to the community" item (D1) garnered a neutral response in both GCL-I and GCL-II. The theme-based nature of the courses could explain this response. GCL-II's spice theme (like GCL-I's Gatorade theme) was used to provide students with a familiar connection to the course content but also reduces the "novelty" of the subject matter.

Multiple survey items showed significant increases in agreement in the Iteration section (I1–I6), specifically in items related to revision (I1 and I2, Table D10). Rather than the period-long techniques in GCL-I, GCL-II provides students with multiple small characterization tests that can be repeated. The time barrier that restricted multiple attempts of a single technique is not as prevalent in GCL-II, which is likely tied to the increase in agreement with I1 and I2. This can also be seen in the previously presented ASCI (V2) survey results, which indicate that students in GCL-II felt more organized and more relaxed than in GCL-I.

The effect of iteration is shown in the students' mastery of TLC. TLC is repeated throughout

| Course (Enrollment) | GCL-I Avg | (1224) SD | GCL-II Avg | (927) SD |
|---|---|---|---|---|
| Collaboration | 22.1 | 0.6 | 22.2 | 0.7 |
| C1. Discuss elements of my investigation with classmates and instructors | 3.8 | 0.8 | 3.8 | 0.6 |
| C2. Reflect on what I was learning | 3.6 | 0.8 | 3.7 | 0.7 |
| C3. Contribute my ideas and suggestions during class discussions | 3.6 | 0.7 | 3.6 | 0.8 |
| C4. Help other students collect or analyze data | 3.7 | 0.7 | 3.7 | 0.7 |
| C5. Provide constructive criticism and challenge each other's interpretations | 3.7 | 0.6 | 3.6 | 0.7 |
| C6. Share the problems and seek input on how to address them | 3.7 | 0.7 | 3.7 | 0.7 |
| Discovery/Relevance | 18.4 | 0.9 | 19.0 | 1.1 |
| D1. Generate novel results that could be of interest the community | 3.0 | 1.2 | 3.2 | 1.2 |
| D2. Conduct an investigation to find something previously unknown | 3.6 | 1.1 | 3.7 | 1.19 |
| D3. Formulate my own research question or hypothesis to guide an investigation | 4.0 | 1.0 | 4.0 | 1.07 |
| D4. Develop new arguments based on data | 4.1 | 1.0 | 4.2 | 0.91 |
| D5. Explain how my work has resulted in new scientific knowledge | 3.8 | 0.9 | 3.9 | 1.14 |
| Iteration | 20.9 | 1.0 | 22.7 | 1.1 |
| I1. Revise and repeat work to account for errors or fix problems | 3.2 | 1.3 | 3.6 | 1.2 |
| I2. Change methods of investigation if it was not unfolding as predicted | 3.1 | 0.9 | 3.5 | 1.2 |
| I3. Share and compare data with other students | 4.0 | 1.0 | 4.3 | 0.9 |
| I4. Collect and analyze additional data to address new questions | 4.1 | 1.0 | 3.8 | 1.2 |
| I5. Revise and repeat analyses based on feedback | 4.1 | 1.0 | 3.8 | 1.2 |
| I6. Revise drafts of papers or presentations based on feedback | 3.5 | 1.0 | 3.8 | 1.1 |

Table D.10: Modified LCAS Results Comparisons between GCL-I and GCL-II.

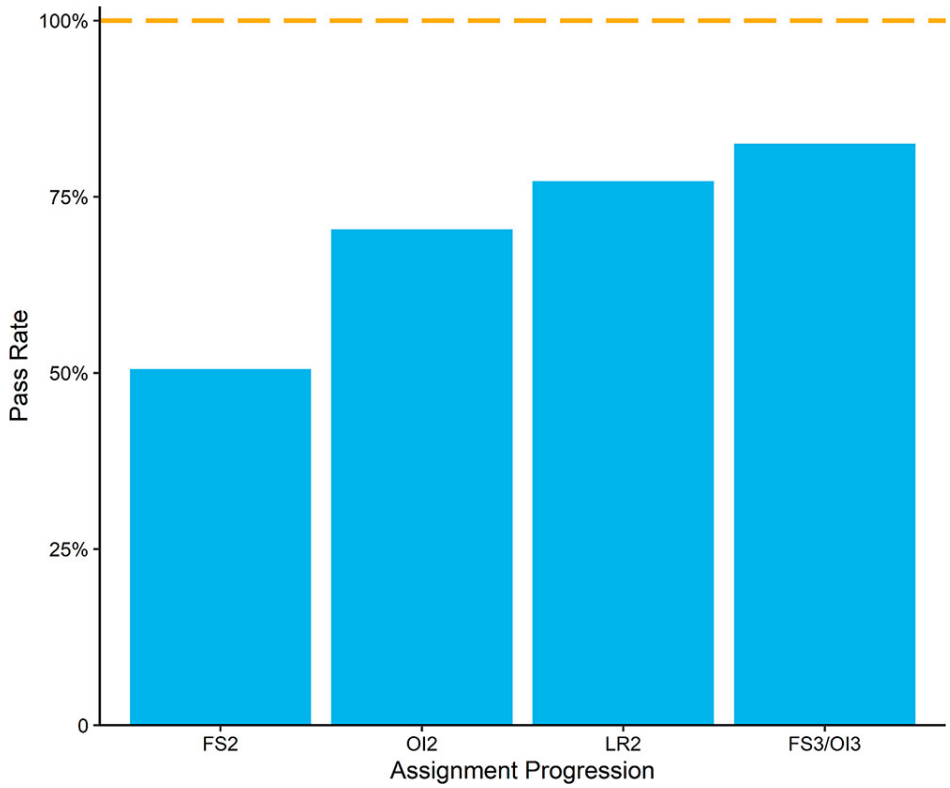


Figure D.8: Student pass rates on rubric items concerning the TLC technique throughout GCL-II.

GCL-II: in the FS of Project #2, then in the OI and LR of Project #2, and finally in Project #3 with only basic eluent information provided. The pass rate for TLC (Figure D8) increases from an initial 50.5% pass rate to a 77.2% pass rate within Project #2, and increases again to a 82.5% pass rate during Project #3, indicating increasing retention of TLC techniques and concepts.

## D.5 Summary and Future Work

Herein, we have presented a theme-based, specifications-graded, ADI-focused lab for GCL-II. The thematic connection was well-received in GCL-I and was continued to connect projects and increase the relevance of the content.[1] Furthermore, the iterative application of methods and skills from previous projects gives student teams an increasing responsibility and freedom

to collaboratively develop experimental design skills.

The modified LCAS results indicate that the GCL-II course results in varying student engagement compared to GCL-I, mostly showing small to significant increases, especially for iteration. The designed repetition of fundamental concepts and techniques results in increased comprehension, as shown in an increasing pass rate on related rubric items as the course proceeds. From GCL-I to GCL-II, the ASCI (V2) results show a positive attitude shift, notably with students considering GCL-II to be more relaxed, more organized, and more exciting than GCL-I.

Since the results presented here, adjustments have been made to Project #2 (detailed in the SI). Future adjustments are being made to the specifications grading tools such as switching to general rubric items from assignment bundles to ensure a passing score reflects proficiency for course objectives. Technique videos are also being developed and implemented to enhance retention and iteration.

## D.6 References


[1] Howitz, W. J.; Frey, T.; Saluga, S. J.; Nguyen, M.; Denaro, K.; Edwards, K. D. A Specifications-Graded, Sports Drink-Themed General Chemistry Laboratory Course Using an Argument-Driven Inquiry Approach. J. Chem. Educ. 2023, 100 (2), 672–680.

[2] Bell, P. Design of a Food Chemistry-Themed Course for Nonscience Majors. J. Chem. Educ. 2014, 91 (10), 1631–1636.

[3] Byrd, H.; Donnell, S. E. O. A General Chemistry Laboratory Theme: Spectroscopic Analysis of Aspirin. J. Chem. Educ. 2003, 80 (2), 174.

[4] Shultz, M. J.; Kelly, M.; Paritsky, L.; Wagner, J. A Theme-Based Course: Hydrogen as the Fuel of the Future. J. Chem. Educ. 2009, 86 (9), 1051.

[5] Logan, J. L.; Rumbaugh, C. E. The Chemistry of Perfume: A Laboratory Course for Nonscience Majors. J. Chem. Educ. 2012, 89 (5), 613–619.

[6] Nivens, D. A.; Padgett, C. W.; Chase, J. M.; Verges, K. J.; Jamieson, D. S. Art, Meet Chemistry; Chemistry, Meet Art: Case Studies, Current Literature, and Instrumental Methods Combined To Create a Hands-On Experience for Nonmajors and Instrumental Analysis Students. J. Chem. Educ. 2010, 87 (10), 1089–1093.

[7] Hopkins, T. A.; Samide, M. Using a Thematic Laboratory-Centered Curriculum To Teach General Chemistry. J. Chem. Educ. 2013, 90 (9), 1162–1166.

[8] Leber, P. A.; Szczerbicki, S. K. Theme-Based Bidisciplinary Chemistry Laboratory Modules. J. Chem. Educ. 1996, 73 (12), 1130.

[9] Chaplin, S. B.; Manske, J. M. A Theme-Based Approach to Teaching Nonmajors Biology: Helping Students Connect Biology to Their Lives. J. Coll. Sci. Teach. 2005, 35 (1), 47.

[10] Tessier, L.; Tessier, J. Theme-Based Courses Foster Student Learning and Promote Comfort with Learning New Material. J. Learn. Arts 2015, 11 (1).

[11] Wingert, J. R.; Wasileski, S. A.; Peterson, K.; Mathews, L. G.; Joy, A.; Clarke, D. Enhancing Integrative Experiences: Evidence of Student Perceptions of Learning Gains from Cross-Course Interactions. Journal of the Scholarship of Teaching and Learning, 2011, 11 (3), 34-57.

[12] Mangan, K.'Fear and Horror'-Themed Courses Help Keep Texas System's Students Engaged. The Chronicle of Higher Education, 4 March, 2014. https://www.chronicle.com/article/fear-and-horror-themed-courses-help-keep-texas-systems-students-engaged/ (accessed 2023-08-22).

[13] Domin, D. S. A Review of Laboratory Instruction Styles. J. Chem. Educ. 1999, 76 (4), 543.

[14] Abraham, M. R. What Can Be Learned from Laboratory Activities? Revisiting 32 Years of Research. J. Chem. Educ. 2011, 88 (8), 1020–1025.

[15] Hosbein, K. N.; Alvarez-Bell, R.; Callis-Duehl, K. L.; Sampson, V.; Wolf, S. F.; Walker, J. P. Development of the Investigation Design, Explanation, and Argument Assessment for General Chemistry I Laboratory. J. Chem. Educ. 2021, 98 (2), 293–306.

[16] Clark, T. M.; Ricciardo, R.; Weaver, T. Transitioning from Expository Laboratory Experiments to Course-Based Undergraduate Research in General Chemistry. J. Chem. Educ. 2016, 93 (1), 56–63.

[17] Walker, J. P.; Sampson, V. Learning to Argue and Arguing to Learn: Argument-Driven Inquiry as a Way to Help Undergraduate Chemistry Students Learn How to Construct Arguments and Engage in Argumentation During a Laboratory Course. J. Res. Sci. Teach. 2013, 50 (5), 561–596.

[18] Grooms, J.; Enderle, P.; Sampson, V. Coordinating Scientific Argumentation and the Next Generation Science Standards through Argument Driven Inquiry. 2015, 24 (1).

[19] Walker, J. P.; Wolf, S. F. Getting the Argument Started: A Variation on the Density Investigation. J. Chem. Educ. 2017, 94 (5), 632–635.

[20] Walker, J. P.; Sampson, V.; Southerland, S.; Enderle, P. J. Using the Laboratory to Engage All Students in Science Practices. Chem. Educ. Res. Pract. 2016, 17 (4), 1098–1113.

[21] Bruck, L. B.; Bretz, S. L.; Towns, M. H. Characterizing the Level of Inquiry in the Undergraduate Laboratory. Journal of College Science Teaching, 2008, 38 (1), 52-58.

[22] Seda Cetin, P.; Eymur, G.; Southerland, S. A.; Walker, J.; Whittington, K. Exploring the Effectiveness of Engagement in a Broad Range of Disciplinary Practices on Learning of Turkish High-School Chemistry Students. Int. J. Sci. Educ. 2018, 40 (5), 473–497.

[23] Walker, J. P.; Sampson, V.; Grooms, J.; Anderson, B.; Zimmerman, C. O. Argument-Driven Inquiry in Undergraduate Chemistry Labs: The Impact on Students' Conceptual Understanding, Argument Skills, and Attitudes Toward Science. J. Coll. Sci. Teach. 2012, 41 (4), 74–81.

[24] Corwin, L. A.; Runyon, C.; Robinson, A.; Dolan, E. L. The Laboratory Course Assessment Survey: A Tool to Measure Three Dimensions of Research-Course Design. CBE—Life Sci. Educ. 2015, 14 (4), ar37.

[25] Walker, J. P.; Sampson, V.; Zimmerman, C. O. Argument-Driven Inquiry: An Introduction to a New Instructional Model for Use in Undergraduate Chemistry Labs. J. Chem. Educ. 2011, 88 (8), 1048–1056.

[26] Bruck, L. B.; Bretz, S. L.; Towns, M. H. A Rubric to Guide Curriculum Development of Undergraduate Chemistry Laboratory: Focus on Inquiry. In Chemistry Education in the ICT Age; Gupta-Bhowon, M., Jhaumeer-Laulloo, S., Li Kam Wah, H., Ramasami, P., Eds.; Springer Netherlands: Dordrecht, 2009; pp 75–83.

[27] Banchi, H.; Bell, R. The Many Levels of Inquiry. Sci. Child. 2008, 46 (2), 26–29.

[28] Fay, M. E.; Grove, N. P.; Towns, M. H.; Bretz, S. L. A Rubric to Characterize Inquiry in the Undergraduate Chemistry Laboratory. Chem. Educ. Res. Pract. 2007, 8 (2), 212–219.

[29] Allen, J. B.; Barker, L. N.; Ramsden, J. H. Guided Inquiry Laboratory. J. Chem. Educ. 1986, 63 (6), 533.

[30] Driver, R.; Newton, P.; Osborne, J. Establishing the Norms of Scientific Argumentation in Classrooms. Sci. Educ. 2000, 84 (3), 287–312.

[31] NGSS Lead States. Next Generation Science Standards: For States, By States; The National Academies Press: Washington, DC, 2013.

[32] Katchevich, D.; Hofstein, A.; Mamlok-Naaman, R. Argumentation in the Chemistry Laboratory: Inquiry and Confirmatory Experiments. Res. Sci. Educ. 2013, 43 (1), 317–345.

[33] D'Amelia, R. P.; Franks, T.; Nirode, W. F. Introduction of Differential Scanning Calorimetry in a General Chemistry Laboratory Course: Determination of Molar Mass by Freezing Point Depression. J. Chem. Educ. 2006, 83 (10), 1537.

[34] Johnson, T. R.; Shaffer, T. A.; Holland, L. A.; Veltri, L. M.; Lucas, J. A.; Elshamy, Y. S.; Rutto, P. K. A Low-Cost and Simple Demonstration of Freezing Point Depression and Colligative Properties with Common Salts and Ice Cream. J. Chem. Educ. 2022, 99 (10), 3590–3594.

[35] Novo, M.; Reija, B.; Al-Soufi, W. Freezing Point of Milk: A Natural Way To Understand Colligative Properties. J. Chem. Educ. 2007, 84 (10), 1673.

[36] Parker, R. C. Molecular Weight of Volatile Liquids by Freezing Point Depression. J. Chem. Educ. 1974, 51 (7), 492.

[37] McCarthy, S. M.; Gordon-Wylie, S. W. A Greener Approach for Measuring Colligative Properties. J. Chem. Educ. 2005, 82 (1), 116.

[38] Dickson, H.; Kittredge, K. W.; Sarquis, A. M. Thin-Layer Chromatography: The "Eyes" of the Organic Chemist. J. Chem. Educ. 2004, 81 (7), 1023.

[39] Silver, J. Let Us Teach Proper Thin Layer Chromatography Technique! J. Chem. Educ. 2020, 97 (12), 4217–4219.

[40] Brinkman, U. A. Th.; de Vries, G. Chemically Bonded Stationary Phases in (HP)TLC. In Drug Determination in Therapeutic and Forensic Contexts; Reid, E., Wilson, I. D., Eds.; Methodological Surveys in Biochemistry and Analysis; Springer US: Boston, MA, 1984; pp 99–100.

[41] Davies, D. R.; Johnson, T. M. Isolation of Three Components from Spearmint Oil: An Exercise in Column and Thin-Layer Chromatography. J. Chem. Educ. 2007, 84 (2), 318.

[42] Pelter, L. S. W.; Amico, A.; Gordon, N.; Martin, C.; Sandifer, D.; Pelter, M. W. Analysis of Peppermint Leaf and Spearmint Leaf Extracts by Thin-Layer Chromatography. J. Chem. Educ. 2008, 85 (1), 133.

[43] Thomson, P. I. T.; Lamie, P. Introducing Elements of Inquiry and Experimental Design in the First Year of an Undergraduate Laboratory Program. J. Chem. Educ. 2022, 99 (12), 4118–4123.

[44] Nash, J. J.; Meyer, J. A.; Everson, B. What Factors Affect the Separation of Substances Using Thin-Layer Chromatography? An Undergraduate Experiment. J. Chem. Educ. 2001, 78 (3), 364.

[45] Nishimura, R. T.; Giammanco, C. H.; Vosburg, D. A. Green, Enzymatic Syntheses of Divanillin and Diapocynin for the Organic, Biochemistry, or Advanced General Chemistry Laboratory. J. Chem. Educ. 2010, 87 (5), 526–527.

[46] Ter Meer Guardia, L. K.; Belli, A. J.; Molta, G. J.; Gordon, P.; Jaworek-Lopes, C. H. Green Crossed Aldol Condensation Reactions Using Trans- Cinnamaldehyde. Chem. Educ. 2011, 16, 23–25.

[47] Stabile, R. G.; Dicks, A. P. Two-Step Semi-Microscale Preparation of a Cinnamate Ester Sunscreen Analog. J. Chem. Educ. 2004, 81 (10), 1488.

[48] Nilson, L. B. Specifications Grading: Restoring Rigor, Motivating Students, and Saving Faculty Time; Stylus Publishing, LLC, 2015.

[49] Noell, S. L.; Rios Buza, M.; Roth, E. B.; Young, J. L.; Drummond, M. J. A Bridge to Specifications Grading in Second Semester General Chemistry. J. Chem. Educ. 2023, 100 (6), 2159–2165.

[50] Donato, J. J.; Marsh, T. C. Specifications Grading Is an Effective Approach to Teaching Biochemistry. J. Microbiol. Biol. Educ. 2023, 0 (0), e00236-22.

[51] Katzman, S. D.; Hurst-Kennedy, J.; Barrera, A.; Talley, J.; Javazon, E.; Diaz, M.; Anzovino, M. E. The Effect of Specifications Grading on Students' Learning and Attitudes in an Undergraduate-Level Cell Biology Course. J. Microbiol. Biol. Educ. 2021, 22 (3), e00200-21.

[52] Evensen, H. Specifications Grading in General Physics and Engineering Physics Courses; Presented at American Society for Engineering Education, 2022.

[53] McKnelly, K. J.; Morris, M. A.; Mang, S. A. Redesigning a "Writing for Chemists" Course Using Specifications Grading. J. Chem. Educ. 2021, 98 (4), 1201–1207.

[54] Howitz, W. J.; McKnelly, K. J.; Link, R. D. Developing and Implementing a Specifications Grading System in an Organic Chemistry Laboratory Course. J. Chem. Educ. 2021, 98 (2), 385–394.

[55] Prasad, P. V. Using Revision and Specifications Grading to Develop Students' Mathematical Habits of Mind. PRIMUS 2020, 30 (8–10), 908–925.

[56] Tsoi, M. Y.; Anzovino, M. E.; Erickson, A. H. L.; Forringer, E. R.; Henary, E.; Lively, A.; Morton, M. S.; Perell-Gerson, K.; Perrine, S.; Villanueva, O.; Whitney, M.; Woodbridge, C. M. Variations in Implementation of Specifications Grading in STEM Courses. 2019.

[57] Ring, J. ConfChem Conference on Select 2016 BCCE Presentations: Specifications Grading in the Flipped Organic Classroom. J. Chem. Educ. 2017, 94 (12), 2005–2006.

[58] Boesdorfer, S. B.; Baldwin, E.; Lieberum, K. A. Emphasizing Learning: Using Standards-Based Grading in a Large Nonmajors' General Chemistry Survey Course. J. Chem. Educ. 2018, 95 (8), 1291–1300.

[59] Martin, L. J. Introducing Components of Specifications Grading to a General Chemistry I Course. In ACS Symposium Series; Kradtap Hartwell, S., Gupta, T., Eds.; American Chemical Society: Washington, DC, 2019; Vol. 1330, pp 105–119.

[60] Mendez, J. Standards-Based Specifications Grading in Thermodynamics. Presented at the 2018 ASEE Annual Conference & Exposition; 2018.

[61] Mendez, J. Standards-Based Specifications Grading in a Hybrid Course. Presented at the 2018 ASEE Annual Conference & Exposition; 2018.

[62] Carlisle, S. Simple Specifications Grading. PRIMUS 2020, 30 (8–10), 926–951.

[63] Blackstone, B.; Oldmixon, E. Specifications Grading in Political Science. J. Polit. Sci. Educ. 2019, 15 (2), 191–205.

[64] Toledo, S.; Dubas, J. M. A Learner-Centered Grading Method Focused on Reaching Proficiency with Course Learning Outcomes. J. Chem. Educ. 2017, 94 (8), 1043–1050.

[65] McKnelly, K. J.; Howitz, W. J.; Thane, T. A.; Link, R. D. Specifications Grading at Scale: Improved Letter Grades and Grading-Related Interactions in a Course with over 1,000 Students. ChemRxiv August 18, 2022.

[66] Bauer, C. F. Attitude toward Chemistry: A Semantic Differential Instrument for Assessing Curriculum Impacts. J. Chem. Educ. 2008, 85 (10), 1440.

[67] Mooring, S. R.; Mitchell, C. E.; Burrows, N. L. Evaluation of a Flipped, Large-Enrollment Organic Chemistry Course on Student Attitude and Achievement. J. Chem. Educ. 2016, 93 (12), 1972–1983.

[68] Xu, X.; Lewis, J. E. Refinement of a Chemistry Attitude Measure for College Students. J. Chem. Educ. 2011, 88 (5), 561–568.

[69] Brandriet, A. R.; Xu, X.; Bretz, S. L.; Lewis, J. E. Diagnosing Changes in Attitude in First-Year College Chemistry Students with a Shortened Version of Bauer's Semantic Differential. Chem. Educ. Res. Pract. 2011, 12 (2), 271–278.